Tree Branch Geometry:
Efficiency and Design Optimisation in Sitka Spruce

Keith Douglas Farnsworth

Doctor of Philosophy

University of Edinburgh

1994

CONTENTS

Appendix

References

Symbols used in the text

a	The ageing factor (how length changes with link age in a shoot).
A_p'	The sum of total areas of foliage projected onto horizontal and 45° planes.
A_p	The sum of total areas of foliage projected onto horizontal and 45° planes, then weighted by shading functions $F_1...F_4$.
B	Bending moment.
B_{in}	The bending moment at the basal end of a shoot.
B_s	The moment about the base of a shoot's centre of gravity, assuming the shoot is straight.
B_{tip}	The bending moment at the distal end of a shoot.
W_B	The total mass of the branch including foliage.
W_{Bt}	The mass of all the branch's foliage with surface water.
C	Tree clone (in ANOVA)
d_1	The average diameter of the first shoot (the branch leader).
F_D	The distortion factor: the difference between total length of shoots projected onto a horizontal plane before and after the action of gravity.
d_{fl}	Deflection from relaxed position of shoot tip resulting from gravitational strain.
c_{lr}	The rank length ratio (how length changes with shoot rank).
c_{lr}	The generation length ratio (how length changes with shoot generation).
c_{dr}	The rank diameter ratio (how diameter changes with shoot rank).
c_{dg}	The generation diameter ratio (how diameter changes with shoot generation).
d_j	The diameter step (or jump) factor (how diameter changes at link boundaries within a shoot).
E	Young's modulus - modulus of elasticity.
$F_1...F_4$	Shading functions representing the light regime within a tree crown.

g	Generation of shoot in model branch.
$\boldsymbol{G}$	Hessian matrix for a multivariate quadratic function.
$\mathfrak{G}$	Generation of shoot or link in canonical variate analysis.
$\boldsymbol{H}$	Hessian Matrix (matrix of second order partial derivatives of a function in n variables).
I	Second moment of area about the neutral axis of a member.
l_1	The length of the first link of the rank 1 shoot in the branch.
$(l_i\text{-}l_j)$	Difference in lengths between order i and order j branches.
k	Light extinction coefficient (from Beer's law).
K	Curvature of bending (reciprocal of radius of bending).
L_p	Niklas's Load factor [Niklas, 1990].
m	Order of a branch (number of morphogenic units)
M_T	Sum of all bending moments in a structure (as defined by Niklas & Kerchner [1984])
M	The bending moment needed to keep the whole branch at a specified angle.
$O(\underline{p})$	Objective function for optimisation.
$\underline{p}$	Vector representation of driving variables to the branch form model.
P	Tree provenance (C: Cordova; SI: Sitka Island; SK: Skidegate; NB: Northbend).
P_n	Specific rate of photosynthesis.
Q	Point moment applied to a parent shoot by its lateral.
r	Radius of shoot.
r	Rank of model shoot.
$\mathfrak{R}$	Rank of shoot or link in canonical variates analysis.
t	The mean taper factor for all links within the branch (d/l).
$\underline{\boldsymbol{T}}$	Transport matrix.
y	Height in the crown of a tree.
y_k	Year of growth of a link with respect to current year.

$(w_i\text{-}w_j)$	Difference in branch weights between order *i* and order *j* branches.
W	Total weight of a branch.
α	The angle of incidence of light on the branch.
δ	Deflection of a shoot element in local co-ordinates.
ε	Shear strain due to bending.
η_a	The efficiency defined by the total projected area (*AP*) divided the total branch mass.
η_m	The efficiency of the Branch defined as the total foliage mass divided by the total mass of branch wood used to support it.
η_w	The efficiency defined by the foliage fresh weight divided by the branch wood fresh weight (*BW* - *BfW*).
λ	The path length from branch base to a shoot tip.
φ_i	Horizontal component of angle of emergence of lateral shoots in a branch (with respect to axis of parent)
Φ ordinates	φ_i transformed into global Cartesian co- where the direction of action of gravity is 180°.
Φ_m	Molar photon flux density.
θ	Vertical component of branch angle.
Θ	θ_i transformed into global Cartesian co-ordinates where the direction of action of gravity is 180°.
θ_k	Vertical component of *k*th branch angle (k = 1...4 designates 1st to 4th order branch of a tree).
θ_i	Vertical component of angle of emergence of lateral shoots in a branch (with respect to axis of parent).
$(\theta_i\text{-}\theta_j)$	Difference in vertical branch angles between order *i* and order *j* branches.
ψ	Angle subtended between axes of parent and lateral shoots in local co-ordinates.

$\underline{\Psi}$	Vector representing input or output to transport matrix.
Ω	Angle in the plane perpendicular to a parent shoot axis defining the sector of the circle occupied by a lateral branch system. If there are n laterals in the whorl, $\Omega = 2\pi/n$..
Σ_{dfl}	The sum of vertical displacements of shoot tips from there original positions .
Σ_l	Sum of all shoot lengths within a branch.
ζ	Measure of distance from the neutral axis in the perpendicular direction in a member.

TABLE OF FIGURES

ACKNOWLEDGEMENTS

SUPERVISORS: Dr. J. Morgan (Edinburgh University)
Dr. M.G.R. Cannell (Institute of Terrestrial Ecology, Edinburgh)

Special thanks are due as follows:

For assisting in supervision:

Dr. P. Van Gardingen

For stimulating discussions and encouragement:

Prof. J. Grace (Edinburgh University)
Prof. P.G. Jarvis (Edinburgh University)
Prof K.J. Niklas (Cornell University, U.S.A.)
Dr. K. McKinnon (Edinburgh University)
Dr. C. Legg (Edinburgh University)

For technical advise:

Edinburgh University Computer Services, Life Sciences User Support.
Scottish Agricultural Statistics Service.

This work was supported by a CASE grant award from the Natural Environment Research Council in conjunction with the Institute of Terrestrial Ecology, Edinburgh.

ABSTRACT

The branches of trees serve to advantageously distribute their foliage in space in a heterogeneous light environment. It is likely that the performance of this function is an important component of fitness and that as a consequence geometric form will closely relate to function.

This study set up the hypothesis that branches are shaped so as to maximise total photosynthetically active radiation interception per unit of assimilate expended in branch structural material. Measurements of branch geometry, combined with computer modelling were used to develop a deeper understanding of form-function relations. The thesis seeks to discover whether light interception (as a measure of benefit) per unit invested material (as a cost) is maximised in natural branches by the optimisation of allocation of structural material among the shoots of branches. Thus a cost-benefit analysis paradigm is applied to the problem of structural carbon allocation among shoots. Topology of branches has been regarded as an invariant property of branch age, so providing an appropriate constraint.

A topological classification scheme was devised for branch elements (links and shoots) so that form-function relations could be resolved.

Geometric attributes of 125 individual branches from trees of *Picea sitchensis* Bong. (Carr.) were analysed to find evidence for form-function relationships. Multivariate differences in geometric design among genotypes were not considered sufficient to motivate form optimisation through a breading program. Within branch shoot length distribution was related to position in the topology which may be a reflection of light interception potential. Diameters of branch elements were proportional to lengths, but proportionality constants varied with topological position. An allocation model based on mechanical design of shoots was more successful in explaining shoot allometry than one based on the pipe model. The mechanical load safety factor varied among branch elements according to their expected potential for light interception. Hydraulic (pipe model) design of branches reinforced the pattern of distribution in mechanical safety factors. This provides possible support for the theory of shoot autonomy.

A mathematical model was constructed which simulated the complex interactions between bending moments and attachment angles among sets of hierarchically connected shoots within spruce-like branches in predicting the distortion of shoots due to gravitational stress. Branch efficiency, defined as projected area per unit

branch mass, was shown to be most sensitive to the vertical component of branch angle from amongst 15 design variables by multivariate stochastic sensitivity analysis. Deflections per unit length of shoot were linearly co-variant with branch efficiency. The model was found to suffer from a mode of failure which limited its use in practice.

Mathematical optimisation of branch design was attempted using the branch model, but no satisfactory algorithm was found because of the difficulties brought about by the model failure and the ill-conditioning of objective functions resulting from the varying calculation paths taken during their computation.

Proposals for simplifications of the model based on the sensitivity analysis results are made and new directions of research are discussed, especially the extension of light regime modelling, the inclusion of hydraulic design and the development of a growth model based on the principles of dynamic optimisation of carbon allocation within the branch.

It is concluded that tree branches are likely to be a result of competing optimisation goals acting within genetic and ontogenic constraints and that shoot size may be related to the potential for competition for light interception, with shoots that show greater potential taking a disproportionate share of resources within the branch.

chapter 1

INTRODUCTION

• 1.1 Yield Improvement - The role of branch design

• 1.1.1 Why is branch design important to forestry ?

• 1.1.1.1 The overall goal in commercial forestry

In commercial forestry, capital, labour and raw materials are combined to generate a net income from the land by producing a saleable commodity : wood. The primary aim of the forester is to maximise the income from the wood products sold. This is achieved by economic means, by the planing and control of production and by the optimisation of trees as crop plants. The harvested portion of a tree - the stem - represents a percentage of the total mass assimilated by net photosynthesis during the life time of the tree (the harvest index). Clearly any method of increasing this proportion would be of interest to commercial foresters. Likewise, maximising the dry matter assimilation rate achieved by trees will lead to a greater return on investments for foresters.

• 1.1.1.2 Why branches ?

Different branch designs require different amounts of branch wood to construct: minimising the wood mass used would improve the harvest index. Additionally, branch design can influence the relative growth rate of a tree via its effect on the light extinction coefficient (k) and on the spatial distribution function for the foliage [Cannell, 1989]. Provenance studies of Sitka spruce have shown the potential for a wide variation in branch design [Cahalan, 1981 ; Cannell 1974], although detailed studies of branches have not been carried out per-sé. It is believed likely that there will be sufficient heritable variation in design to select forms which offer the advantages of harvest index improvement and increased light interception per unit leaf area. With Sitka spruce specifically, improvements in light interception are not likely to be dramatic because they already achieve leaf area indices of 8-12 [Norman & Jarvis, 1974], intercepting almost all incoming radiation. However, if this can be achieved with less

investment in shoot building, then an improvement would be gained. Understanding the relationship between branch morphology and light interception in Sitka spruce has significant implications for improvement of other species (for example *Pinus sylvestris* Ait., which intercepts 70-85% of non-reflected solar radiation).

• 1.1.2 Why concentrate on Sitka Spruce ?

Although Sitka spruce (*Picea sitchensis* (Bong.) Carr.) is an evergreen conifer native to North-West America which was introduced in Scotland in 1831 [Fletcher & Faulkner, 1972] it now plays a dominant role in Scottish forestry. In 1980 48% of the total high forest area of Scotland had been planted with Sitka spruce [Low, 1987], in 1984 68% of planting in Britain was with Sitka spruce. The wood from this tree is used principally for pulping in Britain [Cahalan, 1987] and for particle and fibre board [Brazier, 1987]. Sitka spruce has shown very great advantages as a forest tree for upland Scottish sites which have led to this popularity. Stands of Sitka spruce consistently produce higher mean stem volume increments than any other tree grown in Scotland after crown closure even on poor soils [Malcolm, 1987].

The natural range of Sitka spruce extends along the Western coast of North America in a narrow strip from Mendocino County, California (39°N) to the Kenai peninsula, Alaska (61°N) [Burley, 1965]. Differences in phenotypic expression of morphological traits are observable among both individuals and whole populations. Over many generations local conditions have favoured certain genotypes so that where gene interchange is limited, populations have become progressively adapted to their local environment. Distinct morphological variants of Sitka spruce are often identified according to their provenance: the native seed source. Genetic selection is essential to the success of forestry and improvements in harvest yield can be achieved by selecting genotypes which show the most desirable morphological traits . A tree breeding program needs a goal so that those forms which most closely coincide with some target optimum can be positively selected.

Clearly, Sitka Spruce is a tree with considerable commercial importance in Scotland and offers the possibility of sufficient heritable genetic variation in form. Furthermore, the considerable mass of information which has arisen from the study of this species, because of its importance, places it in a favourable position for the work of this thesis.

• 1.1.3 What is the design goal ?

We need to unambiguously define the goal of the tree branch at the outset. This definition will be a fixed reference point throughout the work: something to maintain a well defined direction and purpose to the study. What is being asked is: what are branches for and what would make one branch better than another ? What will be stated is strictly speaking an hypothesis, but it is not intended to be tested here, its purpose in this study is an assumption.

Tree branches have a number of different functions [Tomlinson, 1987], but for this work, their function is taken to be that indicated by the following hypothesis.

Tree branches set the foliage in a spatial distribution so as to maximise the total photosynthetically active radiation (PAR) intercepted.

This defines a task and suggests a means of comparing the merit of different branch designs, but it is not complete without also describing the cost associated with any design. The cost of tree branches is defined here as: the total of assimilate investment and respiration loss in the branch, excluding the foliage.

Implicit in the above definition of cost (which declares an other assumption) is the assumption of carbon as the basic currency for resource allocation in the tree.

Taking the task and cost definitions together, a design goal can be defined for tree branches: to maximise the achievement of the task per unit cost.

The design goal is: To maximise total PAR interception per unit of assimilate expended in branch material.

This final definition, resting on the declared assumptions serves both as a hypothesis to be tested in this work: do branches appear to follow this goal? and as a goal for a simulation program: to design branches which fulfil this goal.

• 1.2 The Biological Background

• 1.2.1 Photosynthesis and light interception

The rate of assimilate gain is limited by:

a) the availability and distribution of PAR
b) the interception of radiation
c) the efficiency of photosynthesis (conversion and fixation)
d) respiratory losses from the tree

These limitations will be dealt with in turn.

First, the availability and distribution of PAR which can fall on a photosynthetically active surface is determined by i) the light regime above the crown (affected by latitude, season and time, weather conditions, atmospheric conditions and local topography) and ii) the shading effect of other structures within the crown. Above crown factors can not be changed by branch design and so are not considered further here except to note that the angular variation of photosynthetically active photon flux is an important factor for branch design. Shading of other structures may come from separate individuals which may even be from unrelated species and so not subject to the manipulation of branch design to be considered here. Alternatively it may come from branches and their foliage belonging to the same individual as the surface they are shading and therefore, presumably, subject to the same design principles, so that their distribution should be considered a factor of branch design. The consideration of within organism shading is included in the discussion of limitation (b) and includes the effect of branch geometry on the leaf area index (total leaf area/projected ground area) of the tree. Respiration loss from the tree as a whole obviously depends only partially on the branches. For a given foliage area, branch design can only affect foliage respiration indirectly through the rate of photosynthesis by means of varying the light regime (shading). Respiration losses from the branchwood are the only losses directly affected by branch design. In this work, it has been assumed that these losses are sufficiently small that their effect can be ignored (see discussion in 4.2.2).

This section will now deal with limitations (b) and (c) in more detail.

Photosynthesis in Sitka spruce follows the C3 pathway, but the maximum rate of CO_2 assimilation by needles is less than half that of many other C3 trees [Jarvis, 1981]. This is a result of four reasons identified by Cannell [1987] as:

i) mutual shading of needles on the shoot
ii) attenuation of PAR within the needle's thickness
iii) lower biochemical activity rates in photosynthesis
iv) limited stomatal conductance of CO_2.

Reasons (iii) and (iv) result in an overall lower light saturation point for Sitka spruce than in typical C3 plants. However, this turns out not to be a handicap over the whole tree because most needles in the crown are in diffuse light at low intensity relative to direct daylight. Because foliage persists for several years on the branches, it is advantageous to have good photosynthetic efficiency at low light levels. This is yet more of an advantage if photosynthesis can be made profitable through the winter when light levels and temperatures are reduced.

Most needles are neither light saturated nor light limited to the point below light compensation, but operate on the linear part of the photosynthesis/light curve (fig 1.1) This means that most foliage is operating at a high quantum efficiency (moles of carbon fixed per mole of light quanta) [Edwards & Walker, 1987] because, here the curve is at its steepest.

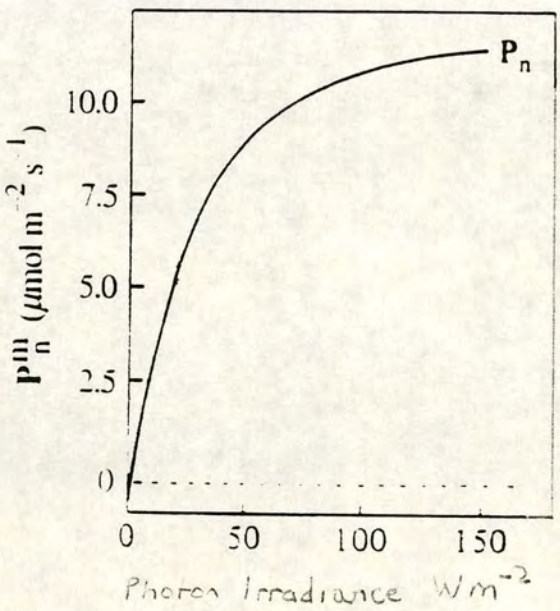

fig 1.1 Light response curve for Sitka spruce needles taken from Larcher [1983] (fig 7.14) using data from Ludlow & Jarvis [1971].

Sitka spruce foliage is adapted anatomically and physiologically to make use of low light levels, but the arrangement is not simple. Many needle properties vary with needle and main-stem node age and shoots are divided into 'sun' and 'shade' shoots with different anatomical adaptations to their light regimes [Leverenz & Jarvis, 1980]. Shade shoots have a low light compensation point and especially high quantum efficiency in the region of the light compensation point [Leverenz & Jarvis, 1979]. With quantum efficiencies of the order of 4.6μmol CO_2/μmol, the sensitivity of net photosynthesis to light flux within the shaded crown is very high indeed.

The photosynthetic activity of needles decreases rapidly with age (typically 1 year old needles have half the maximum photosynthetic rate of current needles) [Chandler, 1989] and it has been shown that most of the canopy photosynthesis of Sitka spruce is contributed by current year and one year old needles [Jarvis & Standford, 1986]. However, it is the maximum rate, usually the level of light saturation which varies most. As a result, older needles in the shaded crown perform only marginally worse than younger needles when placed deep in this position. It is therefore highly advantageous to arrange new needle growth at the top and outer edge of the upper crown.

More than 90% of the PAR incident on a Sitka spruce canopy is absorbed [Landsberg et.al., 1973]. The variation of absorption with distance of penetration in the crown, of course, depends on the arrangement of foliage, which depends in turn on the branching geometry. If a typical Sitka spruce canopy's leaf area was placed at random throughout space, then Beer's Law of exponential decay [Jones, 1992 p31] would predict total light extinction in the canopy well above ground level (in Beer's law the light extinction coefficient k = 0.5/sin(solar incidence angle)). However, in practice the canopy has an extinction coefficient far lower than this because of the clumping of foliage resulting from the branch geometry. This has enabled Sitka spruce to maintain a leaf area index of at least 15 [Cannell, 1989]. , According to Beer's Law, for 95% interception, if the leaf area index is 15, then the extinction coefficient must be 0.2. (since the product of leaf area index and light extinction coefficient = 3). The more clumped the foliage distribution, the lower k is.

This study considers the geometric design of branches. Thus the respiratory losses in organs such as foliage and roots, although very important to the carbon economics of the tree are not considered here. The respiratory losses in living shoots (branch elements) are typically one tenth as great as those of the foliage

it supports [Jones, 1986]. The respiratory losses of shoots is proportional to their surface area, so shoot respiration costs rise in proportion to diameter times length. Material investment costs rise in proportion to diameter squared times length, so the ratio of respiration to material investment costs in shoots is inversely proportional to shoot diameter.

Respiratory losses of carbon from shoots are not considered as of sufficient magnitude to be included in the model which will be discussed in chapter three.

It can be concluded that the distribution and degree of shading within the crown of the tree is of considerable importance in determining the photosynthetic efficiency of foliage because:

a) most needles operate just above light compensation and
b) photosynthetic properties of foliage vary with foliage position.

• 1.2.2 Carbon allocation

In each year of growth, what photosynthetic product remains after respiration losses, is allocated according to the carbon budget of the tree. Only a fraction of this increment of photosynthate goes into producing wood (it also goes into foliage, roots and storage materials). Of that some is used for structural roots, some for the stem and some for the branches: thus to a forester, the wood invested in branches is an overhead. If branches can be grown so that they adequately serve their purpose of fixing the foliage in space and providing the necessary water pathways to serve the foliage, using a minimum of wood mass then harvest index would be improved.

Once carbon is laid down as wood, it is permanently lost to the tree, but over a long time period, the height gain and shading ability which the tree gains from this strategy enables it to occupy a niche where it can compete with other forms in most circumstances. As long as the tree is able to capture as much nutrients as are necessary for growth and maintenance, it will survive, for the form to persist, a sufficient surplus for reproduction must also be collected. For this to have occurred, we can assume that during evolution, by natural selection, there has been a drive for optimal adaptation in wood allocation. This is likely to apply equally well to the distribution of resources within the structure of the branches i.e. to branch design. This is called the hypothesis of adequate design [Rosen, 1962]. According to the biological hypothesis the ultimate goal of an

individual in nature is to maximise the number of descendants left carrying its genes. This might lead to an optimisation which is very different to that intended by the forester which is oriented towards maximising harvest index. Every year, within the branch, a carbon allocation strategy apportions the relative effort expended on shoot length growth, ramification and thickening. This strategy may be genetically determined or, because the plant is partially genetically plastic, it may be environmentally determined. Efforts to understand the basis on which the allocations are made and to interpret natural branch forms would be a very valuable contribution to the science of form - function relations.

• 1.2.3 Branching architecture in plants

Most woody plants are modular organisms: during growth, a unit of morphogenesis is reiterated to produce a repetitive branching pattern (in plants which express a branching habit).

The description of branching architecture in trees is primarily associated with Hallé and Oldeman who defined a set of architectural classifications based on relatively few easily observed features [Hallé & Oldeman, 1970]. These classifications appear too general to be useful (yet) in seeking the underlying principles of branching function. They do, however highlight the strong dependency of form on growth and demonstrate the wide variation of possible forms. In fact all 23 identified classes can be observed in the same ecosystem in the tropics: often occupying very similar niches. Yet, widely differing forms can occur among taxonomically closely related species [Tomlinson, 1983]. Many people have asked the question 'how can the variety of forms be explained'. The answer must ultimately lie in the relationship between form and fitness as any tree which fails to compete with other forms will not survive. Küppers has stated that "*Understanding the ecological significance of above ground architectural patterns is a question of plant economy, i.e. of cost-benefit relationships.*" [1989] .

Attempts made so far to identify these relationships have concentrated on the specific; usually where some convenient simple mathematical analogy can be drawn on to help.

Fisher and Honda [1977] took values of direct measurements from *Terminalia catappa* L. and simulated its very regular branching morphology using a computer program which relied on the repeated application of simple branching

rules. This model has been used to demonstrate the optimum bifurcation angles for minimising foliage mutual shading [Honda & Fisher, 1978] and the effect on bifurcation length ratios on the distribution of foliage clusters in *Terminalia* species [Honda & Fisher, 1979] . Rules which restrict branching and growth in progressively higher orders of binary tree models are applied in subsequent simulations [Honda et.al., 1981 ; Borchert & Honda, 1984]. Honda and Fisher's studies are concerned with the basic geometry of binary trees as it relates to the foliage distribution of certain botanical tree species. Their methods could form the basis of a study of the task function of tree branches (as defined earlier), but does not address itself to the costs of branch structure building and maintenance and it takes no account of the mechanical limitations imposed upon the structures.

A more empirical approach was taken by Renshaw in the development of spatial branching models for the canopy growth and root structure of Sitka spruce using computer simulations [Renshaw, 1985]. He used stochastic rules for tree branching which had been derived through analysis of canopy measurements [Cochrane & Ford, 1978]. The work has led to a realistic mimicking of Sitka spruce branching: fig 2 of Renshaw [1985] is strikingly convincing. However, the method depends on a detailed description of the underlying topology of the tree and is inherently complicated by the statistical basis of the simulation: Renshaw made it clear that he was opening up new areas of research and asking more questions than he was answering, however, Cochrane and Ford's statistical conception of tree branches would not necessarily be the best starting point for this piece of work because of the complexity of a statistical treatment.

• 1.2.4 Mechanical constraints

Considerable interest has been shown in the mechanical aspects of botanical trees, recognising that the structure has to withstand the forces of gravity, snow load and dynamic wind loading. Engineering principles have been applied, both to the stem and the branches in a number of studies. Some workers were interested in finding the optimum taper law (relation between radius and distance from the base) for tree stems [Dean & Long, 1986 ; King, 1986 ; West et al., 1989]. Taper laws and more generally, allometry of shoots within branch complexes of trees have also been studied. For systems of branching where self similarity (fractal geometry) has been assumed: broad principles of support cost especially relating to optimum taper in shoots [McMahon & Kronauer, 1976] [King & Louks, 1978] have been demonstrated. Elastic similarity, in

which stresses are maintained at constant levels throughout the structure by adjusting the diameters, has become a standard hypothesis in the literature. Using elastic similarity and geometric similarity as reference points, detailed allometric analysis has extended the evidence for mechanical design [Bertram, 1989 ; King, 1990].

A detailed study of the stress distributions brought about by the bearing of weight in branches either for single or relatively simple order 2 systems of shoots (leader and first generation of laterals) has led to conclusions about support costs under those conditions. The structural theory of cantilever beams has formed the basis of work carried out by Morgan and Cannell [1987] who used it to look at support costs of different branch designs. They predicted the diameter of single shoots needed to maintain a given static deflection, with Young's modulus, wood density, branch angle and taper specified [Cannell et al., 1988]. They measured deflections of shoots in four species and concluded that Sitka spruce was particularly 'heavily' engineered, i.e. considerable investments were being made to maintain very low static deflections. Later, they simulated the effects of different numbers of lateral (order 2) branches at different positions, with various angles of attachment and required deflections [Morgan & Cannell, 1988]. Further simulation was performed for a growing shoot where length extension was shared between leader and laterals [Cannell & Morgan, 1989]. An important conclusion they reached was that after a certain length is reached, it is more mechanically efficient to grow laterals than extending the leader.

Only rudimentary studies of the dynamic behaviour of trees in the wind have been possible to date in which the stem alone is considered e.g.[Milne, 1991 ; Baker & Bell 1992]. The complexity of the dynamic behaviour of ramiform structures is formidable, but not necessarily intractable.

• 1.2.5 Mechanical and photosynthetic constraints together

Finding a way to combine mechanical and photosynthetic (light interception) constraints is vital to the advancement of our understanding of form and function in tree branches. However, it has proved extremely difficult and few conclusions have yet been drawn. It seems obvious that as a branch grows outwards from the stem, increased length will increase the light interception, but at the same time the deflection would also increase and so some of its effective length extension would be lost [McMahon, 1975]. This could be compensated

for by increasing the structural strength of the branch, but at a cost. Current plant shape has evolved from surface bound and water bound forms finding ways of achieving height gain to maximise light interception in a competitive situation. Niklas and Kerchner [1984] defined photosynthetic efficiency (*I*) as the ratio between projected surface area and total surface area of plants taking a full range of illumination angles into account. They simulated various symmetric binary trees (leaders always splitting into two equal shoots) and measured the total of bending moments (*M*) in the system to represent the cost. They found that *I/M* favoured sparse branching, whilst *I* alone favoured dense branching. Self shading was reduced by setting branches in horizontal planes, but this increased *M* substantially. Support costs and photosynthetic yield have been included in a branch growth simulation [Ford & Ford, 1990] where deflection of branches was maintained at a fixed value. The branches were grown, adding a finite biomass increment each year set by the productivity of foliage times the total foliage mass. The effect of differing light regimes was not explicitly catered for. Partitioning between length extension, shoot thickening and foliage increment was fixed by the requirement for constant deflections. The model was used to simulate the growth of trees with varying branching criteria: apical control and dominance, or criteria based on the proximity of neighbouring shoots representing competition [Ford et al., 1990]. The effect of bending moments from lateral shoots on leaders was not included in their analysis, but ramification of arbitrary order was. Tree designs were assessed according to the return of photosynthate to the stem and showed that optimisation was clearly possible in future work.

• 1.2.6 Hydraulic constraints

The functional relationship between the sapwood area of a tree and its corresponding leaf area has long been the subject of research. As a shoot increases in length, or a branch in complexity, new vessels, or tracheids need to be formed to supply water to an increased area of foliage. According to the pipe model [Shinozaki et. al., 1964] the minimum increase in branch cross section area to accommodate the increased foliage can be calculated in terms of the hydraulic function of sapwood. The pipe model is based on an application of Poiseuille's law to model xylem transport. This law states that conduction resistance of tracheids is inversely proportional to the fourth power of their radius. According to the analogy with Ohm's law, the resistance of a parallel network of tracheids is proportional to the reciprocal of the sum of reciprocals of individual resistances. The relation between water potential gradient (specific

energy difference (Pa) from soil to air) and flow rate, first described by Huber [1924] has been modified by Richter [1973] to include the effect of network branching. To this has been added a capacitance representing water storage in the xylem [Waring et al.,1980] which can be detected as a hysteresis in the response of water potential to transpiration. Water storage sets an other requirement for stem design and possibly branch design too. Cannell et. al. [1988] have rightly pointed out that the hydraulic conductivity of a section of branch wood is not necessarily closely related to its cross-sectional area. Certainly, the slope of the relation between sap- wood and leaf area has been shown to vary within a species with growing conditions and tree condition [Margolis et al.,1988]. These differences have, however, been interpreted in terms of tree nutrition and Whitehead et al. [1984] showed that relationships between cumulative foliage area in the crown and the product of sapwood area and xylem permeability were different with species and nutrition, but similar within species-nutrition classes. It would be most interesting to discover if the relationship between cumulative foliage area in the crown and the product of sapwood area and xylem permeability for a given species and nutritional treatment is related to the water regime (microclimate rainfall and humidity) in a predictable way.

Abrupt increases in hydraulic resistance have been found in several tree species at branching junctions [Tyree et al.1983] especially when small branches lead off larger ones: these usually have little impact on overall resistance [Tyree & Ewers, 1991], but may be involved in the prioritising of survival in the case of water stress leading to catastrophic embolisms [Zimmermann 1983; Tyree & Sperry 1988]. The hydraulic architecture of gymnosperms seems generally to be such that the frictional losses are concentrated at the distal ends of shoots which may confine loss of living parts due to water stress to the small, expendable terminal shoots rather than more important organs. More severe water stress in a branch segment would retard its growth and may produce a characteristic branch-wood distribution as a result.

In summary, branching pattern directly affects light capture, water transport, mechanical support, wind resistance and ultimately, the competitive advantage of trees.

• 1.3 Mathematical Background

• 1.3.1 Mathematical modelling

There are broadly two types of model and both are used in the work of this thesis. Empirical models take sets of observed data and represent them with mathematical simplifications, usually analytic equations. The main limitation of empirical modelling is that mechanisms are not specified, so that no underlying test of functionality is found from the relationships revealed. Conversely, the strength of empirical models is precisely that they do not require a theoretical relation to be proposed in order to reveal a relation. Theoretical modelling consists of forming relations between variables based on a functional hypothesis which is expressed mathematically. Data, either simulated or taken from measurements, are supplied as inputs to theoretical models to make predictions or to examine the behaviour of the hypothetical system. This approach is limited by its dependence on a theoretical description of the system under study, and it does not necessarily confirm the theory. All models are limited by the bounds of their parameters, beyond which model predictions will be at least uncertain, but may be irrelevant. Never the less, theoretical modelling can be valuable just for the experience of rigorously specifying the relationships between variables in the system. It is often used to assess the applicability of theories and is useful in simplifying complex systems by a process of sensitivity testing and model reduction. Empirical modelling will form a large part of the work presented in chapter 2 and theoretical modelling, likewise in chapter 3.

• 1.3.2 Functional optimisation for biology

Natural variation offers a multitude of potential solutions to the problem of passing on the genes to successive generations. The pressure of competition provides a driving function, or design incentive, by favouring those designs which have the highest ecological 'fitness'. Fig 1.2 shows diagramatically how an optimisation cycle results from natural selection. When the sensitivity of fitness to design parameters is great, one could expect the optimisation to be both quick and decisive: there would probably be only one solution surviving and all surviving systems (individuals, strategies organs or whatever) would have converged to that solution. A good example is the converged design for the shape of fish and sea mammals. It is likely that the optimisation of many

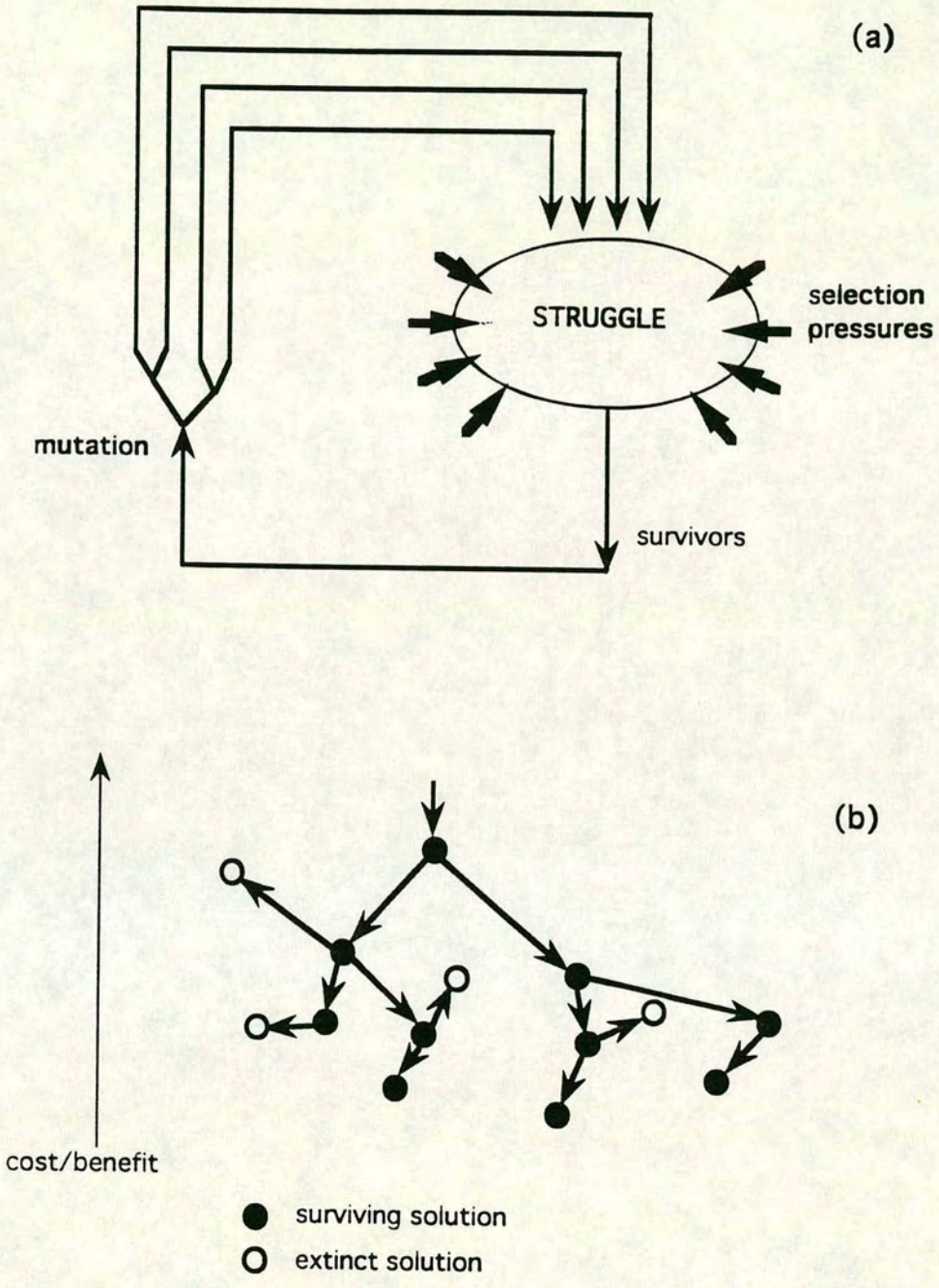

fig 1.2 The process of evolution and natural selection can be regarded as a natural optimiser. (a): A cycle of inovation followed by testing and selection of the best design guarantees convergence to an optimum design, because as diagram (b) shows solutions which have a higher cost to benefit ratio associated with them are eliminated.

branched structure designs in nature is highly advanced [Lefévre, 1983], although there exists, strikingly in botanical trees, a wide variety of surviving solutions. Maybe this is because there are a variety of different objective functions being optimised. Alternatively it might be because there is a weak gradient in the objective function giving rise to polymorphism through 'adaptive radiation'.

Natural optimisation can be simulated by mathematical optimisation: a procedure used widely in engineering applications. Indeed the theory has now turned full circle as biological concepts are being applied to engineering design [Mattheck, 1990]. Examples of simple mathematical optimisations applied to biological systems are given in a book by Rosen [1967] which is an excellent introduction to the subject. A more complex example, which was taken as an inspiration for the work presented here, concerns the optimum form of the pulmonary artery tree Lefevre, 1983]. The pulmonary artery tree is a branched structure and it has generally been assumed that strong selection pressure has resulted in a high degree of convergence and natural optimisation. This work is typical in that a cost function is defined to express the expenditure of metabolic energy in building and maintaining the structure and a task function is defined to measure the value of the structure to the 'client system'. Some procedure based on the calculus of variation (multivariate calculus) is used to minimise cost/benefit and hence find the optimum form. This approach is being used succesfully in medical science, for example in the lung [McNamee, 1991] and the kidney [Gilgarcia, 1992], but has not yet been applied in the study of botanical trees.

- 1.3.3 Mathematical description of ramiform structures.

Tree structures of all kinds are studied by mathematicians who classify them according to their topology as distinct from their geometry. The topological features of the tree can be treated purely by abstract mathematical concepts, irrespective of geometrical features such as lengths and angles - the topology only deals with the interconnectivity of elements or 'links' in the tree. This study is only concerned with what is called a rooted tree: in the mathematical definition, this is a graph with no cycles in which all termini are linked to one particular terminus (the root) [MacDonald, 1983]. More simply, this means a branching system with only one possible pathway between any two points where all points are joined to one unique point - the root. Examples of rooted trees are given in fig 1.3.

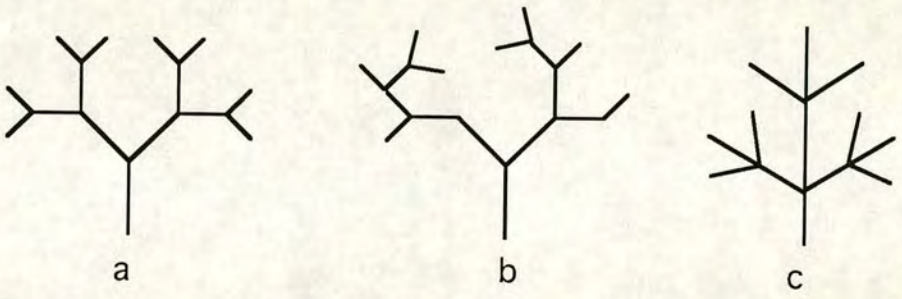

fig 1.3 Examples of rooted trees as topological forms. the regular binary tree (a), the stochastic binary tree (b) and the trifurcating tree (c).

Non stochastic trees usually follow a recognisable symmetry whose topology can be stated concisely by the Papentin form [Papentin, 1980]. Trees are by no means exclusive to botany, but are studied in fields such as geography (river systems), physiology (neural networks, vascular structures) and computer science (data structures) as well as mathematics. Several systems of ordering or labelling of links within trees have been devised which prove very useful in the mathematical analysis of trees: these are explained well in MacDonald's book [1983] and their application to botanical trees is discussed by McMahon and Kronauer [1976].

• 1.4 The task ahead

Tree branch geometry is likely to be of importance in determining the effectiveness of many of the functions that branches are required to perform. A base of knowledge has grown up, which covers aspects of mechanical and hydraulic design and light interception. This can be drawn upon to form a full description of the impact of branch geometry on branch function. This study seeks to answer some of the questions which need to be addressed in building that description.

• 1.4.1 What questions will be addressed in this work ?

An attempt is made at answering the following questions.

1) How can branches of Sitka spruce be parameterised for modelling the behaviour of different geometric designs ?

A topological description for Sitka spruce branches can be chosen and a set of geometric characters specified such that they can be constructed out of a small number of simple geometric measurements taken from real branches.

2) What are the geometric design features of Sitka spruce branches ?

Statistical analysis of measured branches will be carried out to determine relationships between geometric characters and to identify the nature of any dependence of mechanical deflections on these characters.

3) To what extent do branches of Sitka spruce conform to an optimum design in terms of foliage display per unit branch wood investment ?

Optimality can be defined in terms of an objective function (for example light interception). A model of Sitka spruce branch geometry will be constructed to predict the behaviour of the objective function for differing geometries. The measured branches will be assessed by simulation in the model. The branch modelling will be developed into a design optimisation procedure using multivariate mathematical optimisation algorithms.

4) What are the sensitivities of design goals to variation in the parameters which describe Sitka spruce branch geometry ?

Sensitivity testing of the model is capable of specifying the relative importance of the geometric characters in determining the value of objective functions.

chapter 2

THE ANALYSIS OF NATURAL BRANCHES

• 2.1 INTRODUCTION

The detailed nature of the geometry of tree branches can have a considerable effect on their efficiency in terms of net carbon export from the branch per unit carbon investment in the structure [Cannell & Morgan, 1990]. The geometry of tree branches determines the distribution of their foliage which is of fundamental importance in determining carbon gain. Carbon invested in the structure of the branch and lost in respiration represent costs that are dependent on the geometry of the branch. A cost-benefit analysis approach is, then, the basis of our understanding of branch architectural form. One regards tree branches as structures which perform certain functions and attempt to relate these to the observed form. Despite this, though, there have been few attempts to describe in full detail the geometry of tree branches, their relation to genetic and environmental factors and the underlying strategy in their design. Details of the wood distribution within a branch warrants close study because it is a prerequisite for these descriptions. Eventually, if this study is carried out, principles of efficient branch design (and a scheme enabling the recognition of different designs) may be put forward to breeders of forest trees.

• 2.1.1 A review of related work

Cannell studied the production of foliage and branches in immature Lodgepole pine (*Pinus contorta* Dougl.) and Sitka spruce, looking at provenance differences [Cannell, 1974]. He measured and simulated the total number and lengths of shoots in each whorl, classified by rank, considering apical control and 'ageing' (or invigoration) effects. Significant differences in total branch and foliage mass were found among the trees and this had implications for wood yield. Cannell stated that '*there seems to be a common rigid pattern of control over the distribution of growth for a wide range of genotypes*', which suggests that an underlying design scheme may be present.

Cahalan studied certain characteristics of four clones of five different provenances of Sitka spruce by nested analysis of variance, but characters of branch design were not included. The provenances were chosen to reflect the range in latitude of natural Sitka spruce habitats to interpret any differences in terms of environmental adaptation [Cahalan, 1981]. He found that there were significant differences between and within provenances in branch number and branch angle with the southerly provenances usually producing more branches each year, but large differences between clones caused large population overlaps.

Cannell et. al. [1983] measured total branch and needle dry weights and foliage areas of seven clones as well as other tree characteristics to describe the dry matter distribution and foliage 'efficiency', but the details of the branch geometry were not included in their investigation.

Bertram [1989] carried out whole tree allometric analysis of *Acer saccharinum* L, measuring lengths and mean diameters of branch links (interlateral segments of shoot). He found that the links scaled differently either side of a certain critical size and attributed this to a difference in function, with mechanical load resistance dominating over hydraulic requirements above the critical size. Bertram did not, though, concern himself with the distribution and allometric relations among links classified according to their rank or generation and only measured one individual tree.

Castéra and Morlier [1992] measured the length, fresh weight and basal diameter of links in order 3 branches of maritime pine (*Pinus pinaster* Ait.). They showed linear relationships between link diameter and link length and between unit weight (*w/l*) and basal diameter squared. However, they did not look at the distribution of allometric relations among the links or shoots in the branches they studied.

• 2.1.2 The purpose of this chapter

In chapter 3 of this thesis, a simulation model for Sitka spruce branch design will be developed and used to test theories of branch design. It is therefore necessary to have detailed, accurate and specifically organised measurements of branches taken from living trees. As the motivation for this work is ultimately to provide a goal for tree breeders, the range of opportunity for selecting appropriate branch designs should be assessed now. For modelling purposes, the measurements made on branches have to be organised into a well defined structure which relates to the underlying topology of the branch. The simulation exercise related in chapter 3 needs to have a fixed point

of reference. Experimental evidence shedding light on those theories addressed in the modelling must be provided.

This chapter sets out to answer the following questions using analysis of field gathered data:

a) Do the different provenances give rise to different branch geometries ?

b) What allometric relations exist between geometric characters within branches ?

c) Does a relationship exists between branch geometry and shoot tip deflections ?

d) Is an argument based solely on mechanical statics able to explain the distribution of thickening of shoots as load bearing elements ?

e) If not, what evidence is there for other design criteria (for example hydraulic design in the geometry of branch elements?

• 2.1.3 Definition of special terms

Ramiform structure is used here to mean an array of interconnected lengths of material in which there is always one and only one path leading from all termini to a unique terminus (the root). The **topology** of a ramiform structure defines the spatial relationships of connectivity of the component axes making up the structure. For ramiform structures, the topology is described by several ordering methods which are useful in identifying shoots and links. In this study, a **branch** is defined as the continuous ramiform structure connected to the tree stem of a botanical tree, a **shoot** is a length of branch wood resulting from the progress, over the years, of a single apical meristem (an axis) and a **link** is a length of the shoot between the points where annual whorls of lateral shoots emanate. (fig. 2.1). The **order** of a branch is the number of generations of repeated application of a growth rule which have resulted in its form (fig. 2.1). The **rank** of a shoot is taken from the Horton order [Horton, 1945] of its links: shoots of the same rank began their growth in the same year. (fig. 2.1). The **topological generation** of a shoot is taken from the Gravelius order [Gravelius, 1914] of its links: all shoots which emanate from a given parent shoot share the same topological generation (fig. 2.1). Individual links comprising a shoot are given a sequence number which is their Horsefield order [Horsefield et. al., 1971] (fig. 2.1). The symmetry of branches having the topology shown in fig. 2.1

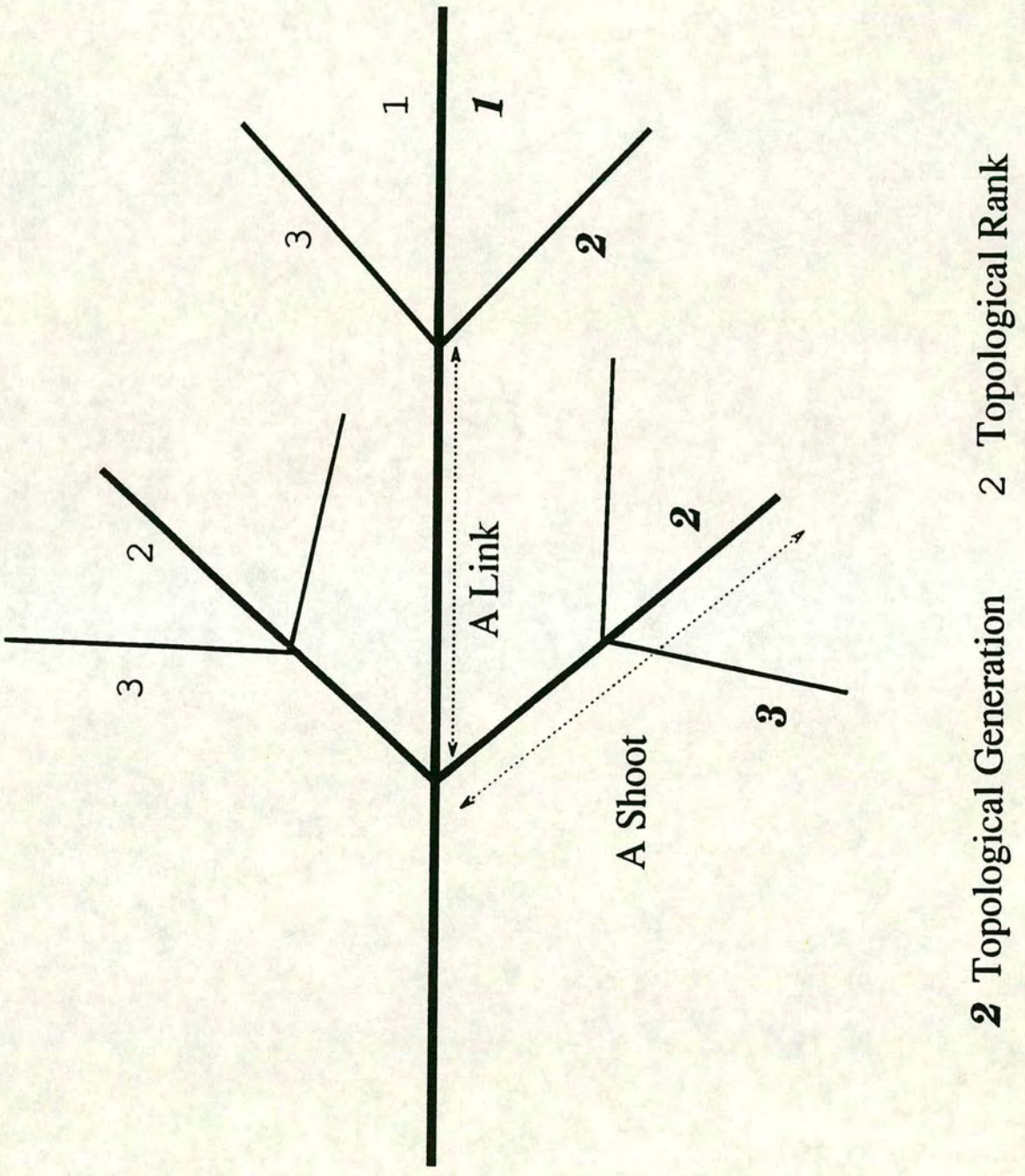

Fig 2.1. Definitions of branch parts referred to in the text: a branch can be divided into component parts -shoots which are the result of the growth of a single apical meristem and links which are lengths of shoots between lateral attatchments. The shoots and links can be indexed by referring to their topological rank: the Horton order [Horton 1945], or their topological generation: the Gravelius order [Gravelius 1914].

allows measures of certain links and shoots to be aggregated, because they are topologically similar. for example shoots 16-19 in fig. 2.2 are aggregated and any one from this set is referred to as shoot type 16. A convention has been adopted throughout the text for naming branch parts as follows (refer to fig. 2.2). Whole branches are described simply by their branch order. Shoots are given a label consisting of the branch order and the shoot type, for example shoot 3.4 refers to shoot type 4 of an order 3 branch (fig. 2.2) (which includes shoot numbers 4 and 5). Links are given a label which specifies the shoot to which they belong and the link number, for example link 4.6.3 refers to the terminal link of shoot number 6 or 7 in a branch of order 4 (fig. 2.2).

Because the topology of the Sitka spruce branch allows branch elements to be categorised according to topological indices, it is possible to consider the significance of differences in scaling (length-diameter relations) amongst them in an attempt to gain further insights into the relations between form and function.

• 2.2 Materials And Methods

• 2.2.1 Measurements

Branches were taken from the top of the crown of (18 year old) trees of Sitka spruce on a lowland plantation at the outside edge of a closed stand in June 1990.
Measurements of shoot tip deflection under gravity were made in the way described by Morgan and Cannell [1987]. The branches were cut into branch elements (topological links) and the following measurements were taken from the fresh material:

a) The length of the links.
b) The over bark-diameter at each end of the link.
c) The fresh weight of the link including its interlateral shoots with foliage intact.
d) The deflection under self weight of shoot tips.
e) The number of interlateral shoots and the sum of their lengths on each link.

The geometry of natural branches does not exactly follow any simple mathematical description, but, the Sitka spruce branches in this study were found to be sufficiently regular to allow the links to be classified and the data organised in a way that facilitated statistical analysis of geometry. Links and shoots that were identified as members of the topology defined in fig. 2.1 were included for data analysis, with all

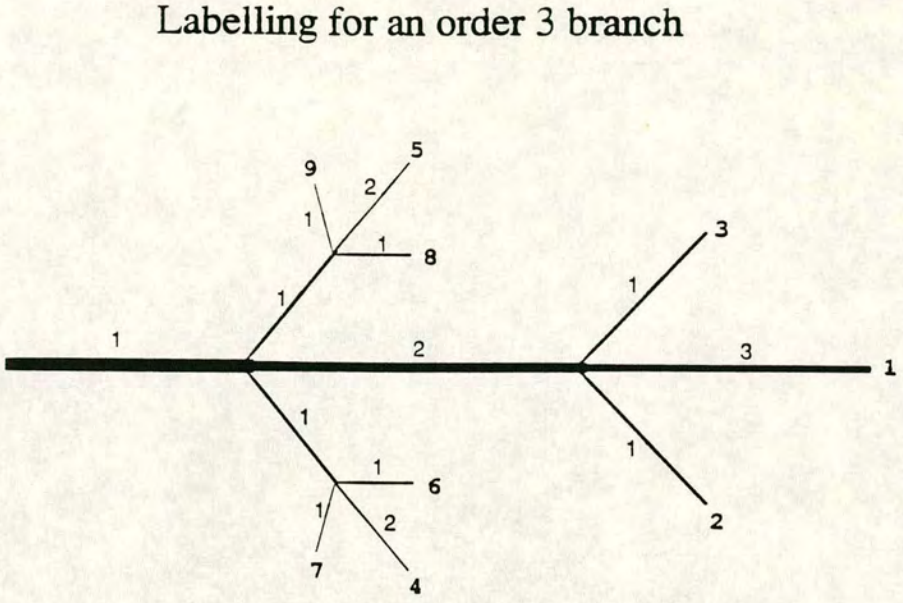

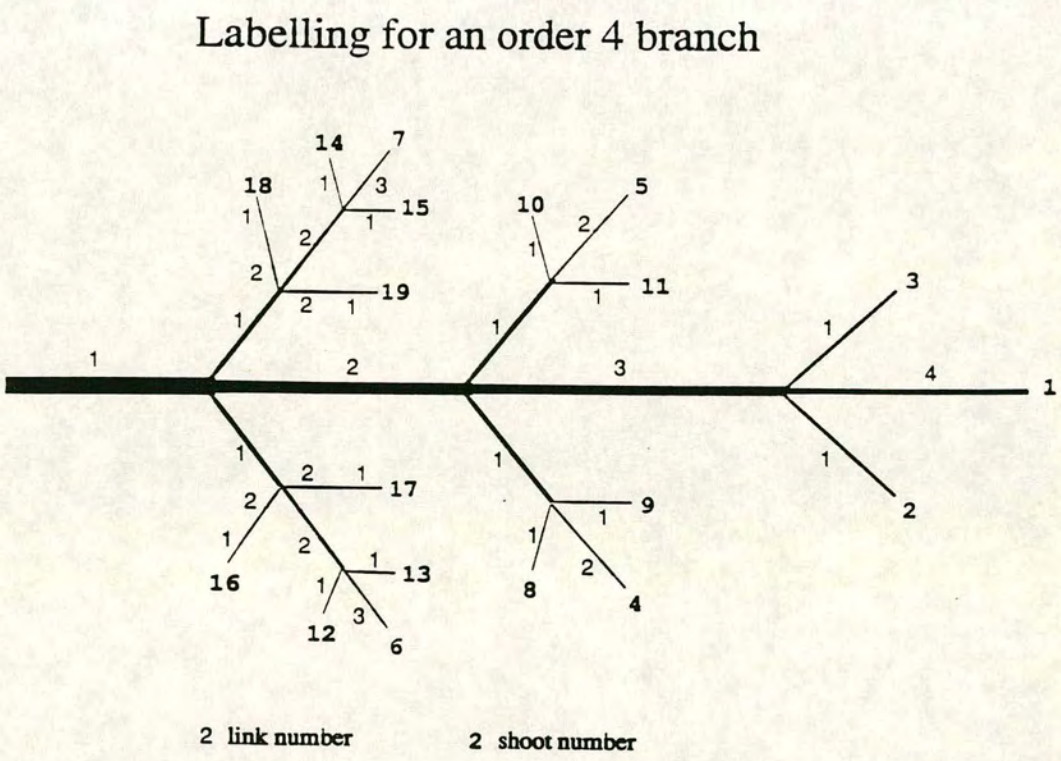

Fig 2.2. The labelling schemes used to specify branch shoots: those occupying equivalent positions in the branch (e.g. shoots 2 and 3) share the same designation

as the data taken from these shoots is pooled. Shoot designations consist of the branch order, followed by the contracted shoot designation.

others ignored. Where whorls have more than 2 members, the pair which projected most closely to the horizontal plane in the branch were chosen to be included in the analysis.
Measurements were taken from 125 branches (112 included in analysis - the others were incomplete) giving data for 1150 links from branches of order 1 through 4 and 832 shoot tip deflections.

In the measurement of deflection, the branches were clamped rigidly at their base in a horizontal position and the vertical displacement of the tip of each shoot from the horizontal projection of the base was recorded using a ruler to a resolution of 1mm. The branches were then rotated through 180° and the measurement was repeated (see fig. 2.3). The deflections due to gravity are given as

$$d_{fl} = h - (d_1 + d_2) / 2 \qquad (2.1)$$

where h = height of the suspended branch above the origin and d_1, d_2 are the heights to the tips of shoots in the branch in the two measurement orientations.

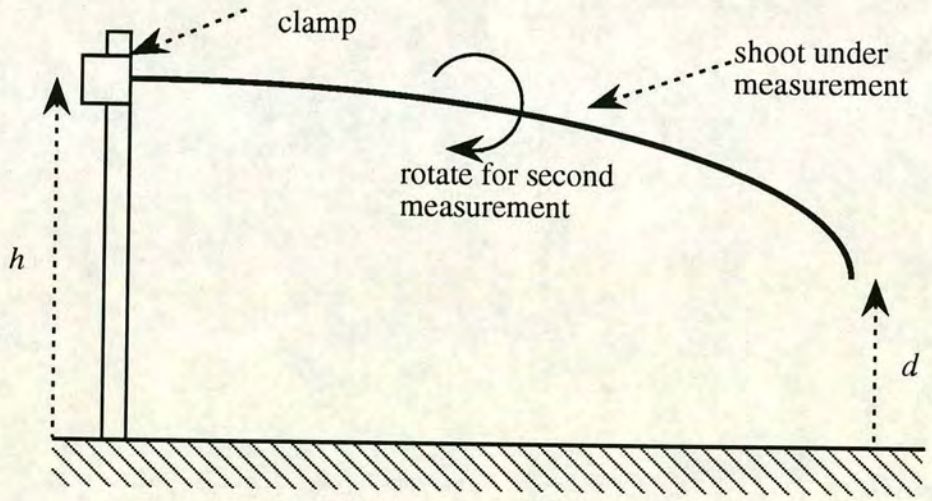

fig 2.3 showing the method used to measure shoot tip deflections. Branches were rotated between measurements to reverse the direction of loading.

- 2.2.2 A description of Sitka spruce branches

Natual branches do not exactly follow any simple mathematical description, but, to a considerable extent, those of Sitka spruce were found to lend themselves to such a description because of their regularity. This is useful for two reasons. 1) The links

can be classified and the data organised in a way which allows detailed morphological analysis. 2) A non-stochastic mathematical model can be built to accurately simulate various aspects of the behaviour of the branches. The topological definition of Sitka branches which is used in the model (see chapter 3) is used to classify the data in this study. It is defined by the Papentin form [Papentin, 1980]:

$$3n(ieee) \qquad n=1,2,3...$$

where n defines the order of the branch, i represents interior links (which end in another link) and e represents external (terminal) links (this is a standard notation used in graph theory of which the topology of ramiform structures is a branch [MacDonald, 1983]). This topology is defined in fig 2.5.

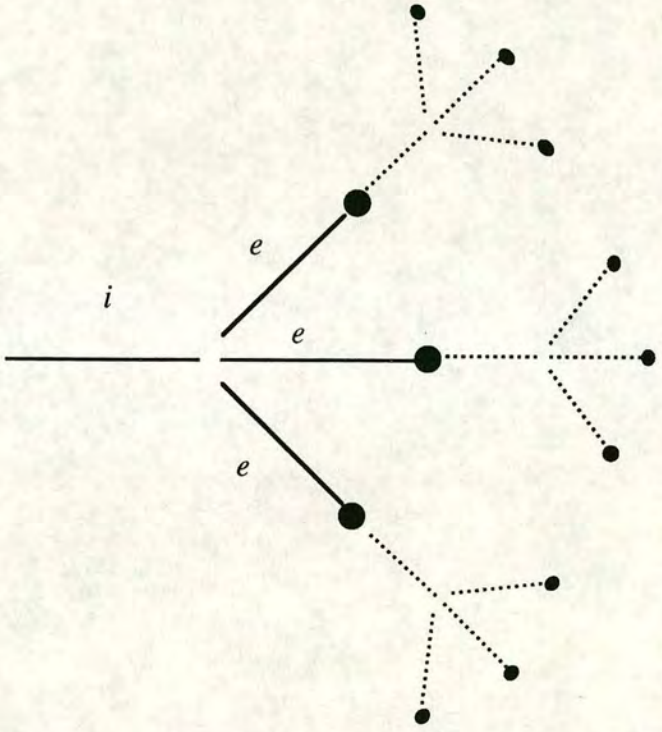

Fig 2.5 illustrates the *ieee* topology for Sitka spruce.
(*note: Fig 2.4 has been deleted due to redundancy*)

Links and shoots which are identified as members of the topology are included as data for analysis, whilst all others are ignored. Those which are ignored come from either interlateral shoots, where they are counted as a character of a link, or from whorls with more than 2 members. Where whorls have more than 2 members, the pair which project most closely to the horizontal plane in the branch have been chosen as members of the topology. Using this topology, links and shoots have been labelled with indices based on the hierarchical nature of the topology. This

hierarchical data organisation has been carried on upwards to organise branches on trees and trees into genetic groupings as follows:

Provenance
Genet number
Ramet number
Branch order
shoot index
link index.

• 2.2.3 Calculating branch characters from measured data

Some of the characters are made up of combinations of those taken from direct measurements. A FORTRAN program was written to calculate these. This was done using a program because of the large number of data involved and also to allow for future additions to the dataset. The program was also used to find outlying results due to errors in data entry and to sort and categorise the data. The whole process was quite complicated and the resulting program is not small. This confirms the choice of using a flexible programming language to do the job: this part of the analysis could have been carried out with a spreadsheet program, but there would have resulted a loss of portability. The FORTRAN program is able to deal with data input in a more flexible way, whereas a spreadsheet would require a fixed input scheme with a definite order for entry etc. *

• 2.2.4 Statistical Techniques

Reduced major axis regression [Seim & Saether, 1983] was used in allometric analysis of the branches, regressions were calculated and displayed with the computer package *Mathematica* [Wolfram, 1992]. Multivariate data was analysed by canonical variate analysis [Digby & Kempton, 1987] and Procrustes rotation analysis [Digby & Kempton, 1987] using the GENSTAT 5 software package [Genstat 5 Committee, 1988]. Analysis of variance was used to test for differences in

* this was written before sophisticated spreadsheats such as *Excell* and *WINGS* were available to the author.

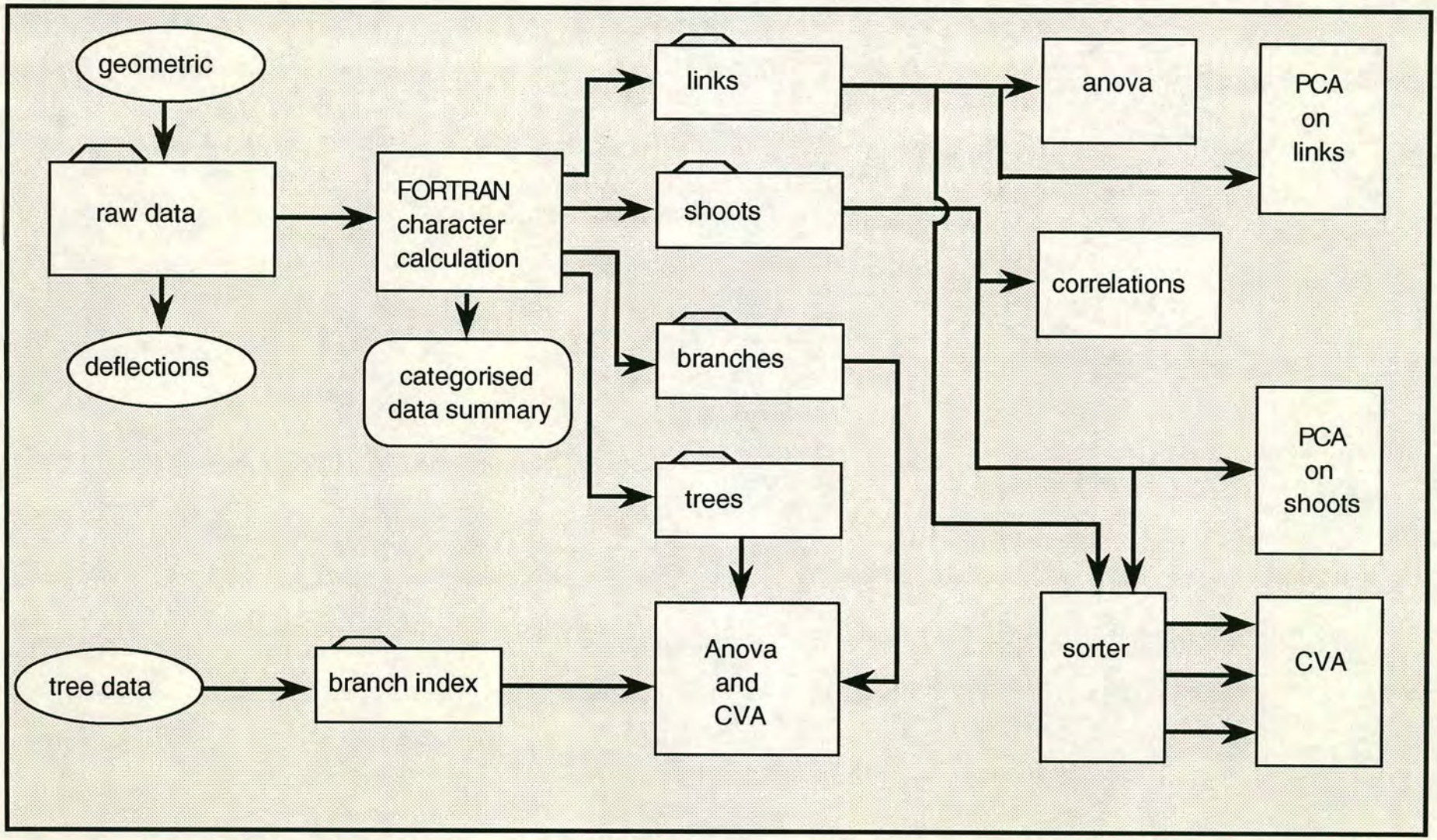

Fig 2.6. Diagram showing the stages in the analysis of the data collected from the branches.

morphometric properties among branches and branch parts. This was augmented by pair-wise comparisons of classes using Bonferoni t-tests [Schlotzhauer & Littell, 1987]: a multiple comparison procedure which controls the experiment-wise error rate. Procrustes rotations [Digby & Kempton, 1987] is a technique which compares the pattern of variables in one data matrix to that in an other (dependent) data matrix, with the purpose of measuring the extent to which they might reflect a common underlying pattern in the data.

Fig 2.6 gives an over-view of the treatment of the data which is discussed in this chapter. Appendix 1.1 gives a fuller account of the multivariate methods used in this work.

• 2.3 Discrimination between genotypes

• 2.3.1 Method

Two methods of discrimination analysis have been used. First a nested analysis of variance (ANOVA) [Sokal & Rolf, 1969] was used for each individual variate in turn with the tree level data. In this, the data strata were, from top down, provenance (P), genotype (C) and replicate (I). The Genstat 5 suplementary procedure HANOVA [NAG, 1990] was used to perform this analysis. A break down of individual strata ANOVA has been made available by using 2 way ANOVA and Bonferroni t-tests [Schlotzhauer & Littell, 1987] with the SAS procedure ANOVA [Schlotzhauer & Littell, 1987]. Secondly, the multivariate method of canonical variates analysis was used to show the optimal separation of provenances with tree level data using Genstat 5. The first two canonical variate axes have been used to provide graphical representations of the CVA results with 95% confidence intervals calculated from the Chi-squared distribution [Genstat 5 Committee, 1988].

• 2.3.2 Nested Anova

Each variable for each branch can be regarded as made up of components as follows:

$$Y_{ijkl} = \mu + P_i + C_{ij} + I_{ijk} \qquad (2.2)$$

where μ is the global population parametric mean, P_i is the contribution for the ith provenance, C_{ij} is the contribution for the jth genet of the ith provenance and I_{ijk} is

the contribution of the kth ramet of that genet. The contributions from different levels have means μ_P, μ_C and μ_I which are all assumed to be zero and the variances are σ_P^2, σ_C^2 σ_I^2, respectively.

The null hypothesis is that variability between individuals has no genetic basis : phenotipic plasticity would then explain all the variability. For each trait derived from the geometric features, a test of 'broad sense' heritability [Cahlan, 1981] is made. The model has 23 degrees of freedom distributed as shown in table 2.1.

ANOVA of differences among provenances shows 95% significance for variates (l_4-l_3) and (w_3-w_2) and 99% for variatesθ_0 and (θ_4-θ_3). t- tests applied to all combinations of pairs of provenances for these variates however shows poor separation : in all cases, no provenance was completely separate from the group. (fig 2.7). For differences among clones, pooling provenances, 95% significance was found with variates (l_4-l_3) and (l_3-l_2) and 99% with (w_3-w_2), (θ_2-θ_1), (θ_2-θ_3) and (θ_3-θ_4). Again there were no full separations of groups. It is possible that the significant results for provenances and clones were simply type 1 errors, so all the variates have been treated equally in the nested ANOVA.

Table 2.1 The distribution of degrees of freedom among classification levels for nested ANOVA calculations.

LEVEL				
P	C	SI	SK	NB
C	1 2 3	1 2 3	1 2 3	1 2 3
I	1 2	1 2	1 2	1 2

Number of provenances (*P*) = 4	Degrees of freedom (*P*) = 3
Number of genets per provenance (*C*) = 3	Degrees of freedom (*C*) = 8
Number of ramets per genet = 2	Degrees of freedom (*I*) = 12
	TOTAL = 23

Number of branch orders from each tree (*O*) = 4

Total number of branches = 96

Variation among provenances	$\sigma_i^2 + 2\sigma_c^2 + 6\sigma_p^2$
Variation among genotypes within provenances	$\sigma_i^2 + 2\sigma_c^2$
Variation among clonal replicates	σ_i^2

- 2.3.3 Canonical Variates Analysis

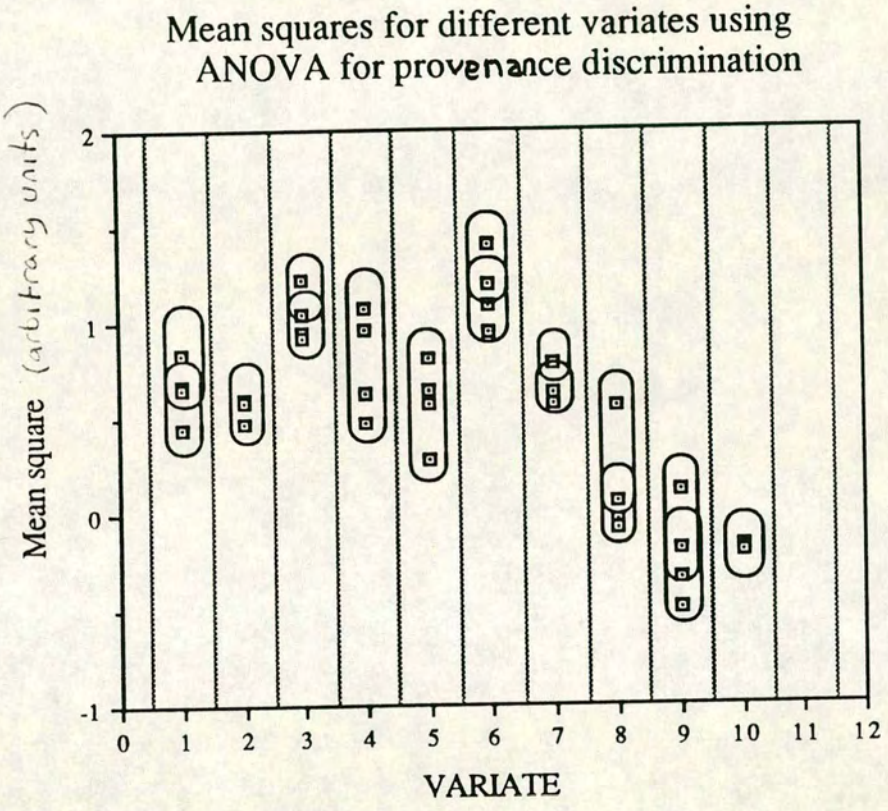

Fig 2.7. Univariate ANOVA of branch data classified into four provenances. Variate class means are shown to scale against the global means. Classes which are not separated are shown encompassed by a line.

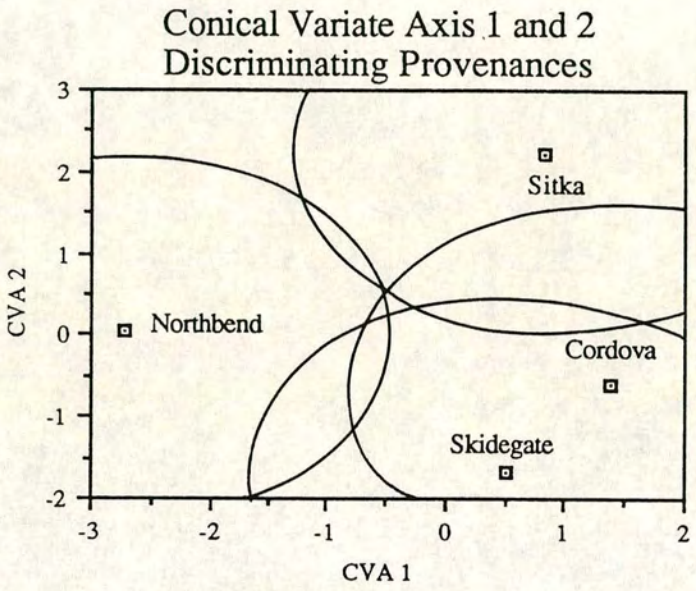

Fig 2.8. Canonical variates analysis of branches from four provenances showing population means in the first and second canonical variates. Elipses show the 95% confidence intervals. All pairs of provenances are separated with 95% confidence except Cordova-Skidegate.

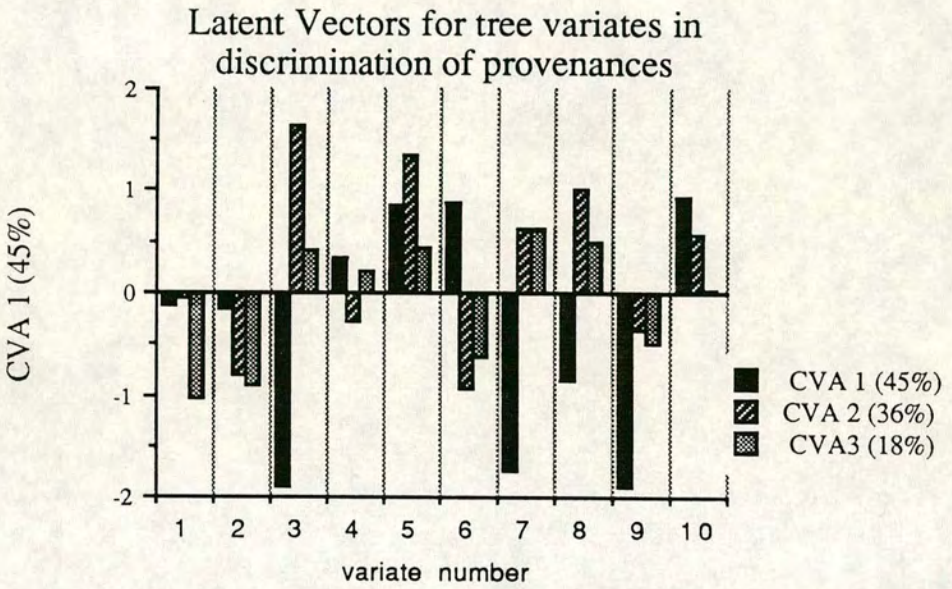

Fig 2.9. Latent vectors of the canonical variates used to separate provenances by branch design. The latent vectors reveal the relative contributions made by the different branch variates to the discriminating axes.
(variate number as in fig 2.7)

Canonical variates analysis is generally a much more powerful discriminator than univariate ANOVA. Fig. 2.8 shows the first and second canonical variates plotted together demonstrating the separation of all provenance pairs with 95% confidence (except Cordva-Skidegate). 81.7% of the variation separating the provenances was represented by these two canonical variate axes. The make-up of the first three axes from a linear combination of the measured variates is given in fig 2.9. The variates dominating in the first canonical axis, which accounts for 45% of the discrimination, are $(l_4\text{-}l_3)$, θ_0 and $(\theta_3\text{-}\theta_2)$. Variates $(l_4\text{-}l_3)$, $(w_3\text{-}w_2)$ and $(\theta_1\text{-}\theta_2)$ dominate the second axis which accounts for 36% of the discrimination.

There was then, very little to distinguish between the provenances on the basis of those traits of branch geometry which were chosen. However, it has been possible using canonical variates analysis to discriminate between all but one pairing of the four provenances. If shoot measurements were explicitly included among the branch characters, it might have been possible to find a more decisive measure for discrimination. This finding does not contradict the belief that there is sufficient heritable variation in branch design to enable a breeding program for design goals, but it may be seen to undermine its value. The discriminating axes are made up of seemingly unrelated variates. It could not be claimed that any consistent pattern has emerged from the characters treated in this analysis.

• 2.4 The distribution of geometric characters among branch links

• 2.4.1 The distribution of link lengths

Table 2.2 gives the means of link lengths averaged over 26 branches in each branch order, fig. 2.10 shows order 3 and 4 branches labelled with shoot and link numbers with mean link lengths and mean diameters drawn to scale.

There is a striking similarity between the mean lengths of links of the same topological generation even though these links have not grown in the same year, for example compare 4.6.1, 4.4.1 and 4.2.1, in contrast with 4.4.1, 4.1.3, 4.16.1 which grew in the same annual increment, or 3.2.1, 3.6.1 and 4.6.2, 4.1.3, 4.16.1 which belong to the same topological rank. Lengths of link 1 from leader shoots in

table 2.2

link o.s.k*	average length	average weight	average diameter	sd length	sd weight	sd diameter
1.1.1	319	27	6.4	91	23	1.7
2.1.1	329	72	9.5	97	58	2.2
2.1.2	333	23	5.8	66	15	1.2
2.2.1	165	6.5	3.4	37	3.4	1.0
3.1.1	236	61	10.1	49	34	2.3
3.1.2	307	43	7.2	71	18	1.3
3.1.3	270	14	4.7	65	6	1.0
3.2.1	158	5	3.1	27	1.7	0.6
3.4.1	137	5	3.4	35	3	0.8
3.4.2	96	2	2.1	36	1.4	0.7
3.6.1	57	1	1.4	32	1.4	1.0
4.1.1	260	108	12.6	75	81	2.8
4.1.2	279	67	9.4	56	41	1.9
4.1.3	294	35	6.8	61	23	1.6
4.1.4	240	11	4.1	77	6	1.3
4.2.1	153	4	2.9	30	2.1	0.8
4.4.1	153	6	3.6	28	3.3	0.8
4.4.2	118	3	2.4	42	1.7	1.9
4.6.1	130	6	3.6	35	3.4	1.3
4.6.2	120	4	2.5	41	3.5	1.0
4.6.3	80	1.4	1.5	52	1.3	1.0
4.16.1	79	2	1.8	143	0.9	0.5
4.16.2	23	0.2	0.4	31	0.4	0.5
4.20.1	0	0	0	0	0	0

* link index is given as :- o: branch order, s: shoot number (fig.1), k: link number

all measurements in mm.
weight given in g mass.

Lengths and diameters of links in order 3 branches

Average of 26 branches

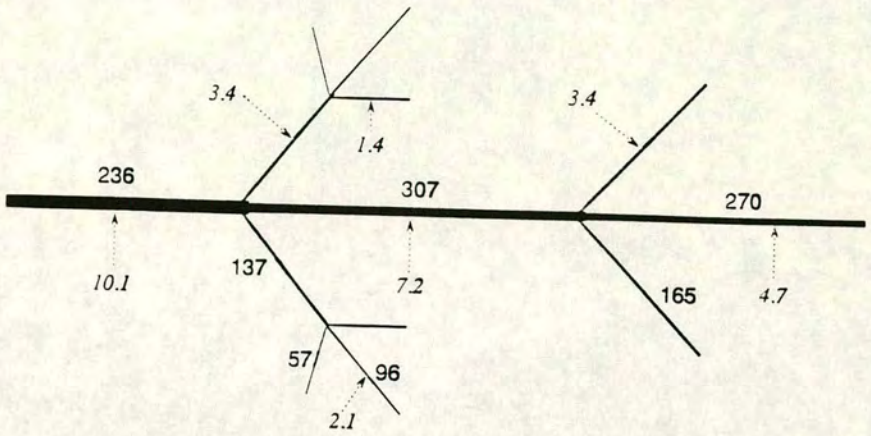

Lengths and diameters of links in order 4 branches

Average of 26 branches

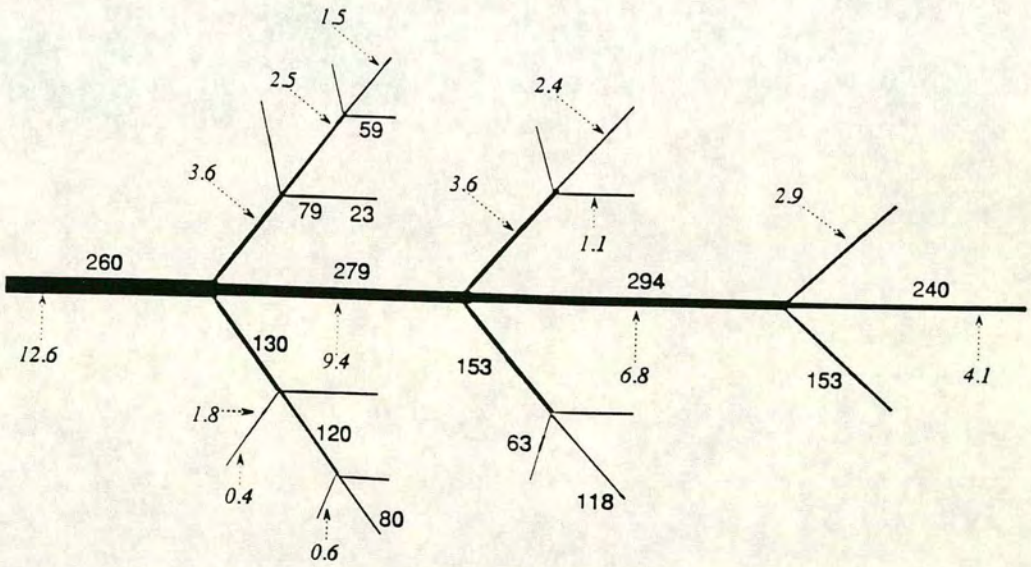

Fig 2.10. 26 branches were measured to give mean link lengths and diameters for both order 3 and order 4 branches. Mean link lengths are given in bold type and diameters in italic type. The branches are drawn approximately to scale representing these measurements. All measurements in mm

branches are believed to be slight underestimates because the location of their base was obscured by their anchorage in the tree stem. Except in the leader shoot, there is a definite decline in link length as the shoot extension progresses: older links are longer. However, the most noticeable variation in lengths comes from contrasting links belonging to shoots of different topological generation, e.g. 4.1.3, 4.6.2, or 3.1.1, 3.4.1, 3.6.1 where a trend of decreasing length, diameter and mass is clearly demonstrated indicating a decrease in investment. Analysis of variance of all the link lengths classified by topological generation, growth year and topological rank show that significant ($p < 0.0001$) differences exist among classes. There is considerable overlap in these classifications however, for example all links in order two branches share rank and generation classification: thus the different classification schemes are not fully resolved. Bonferoni t-tests [Schlotzhauer & Littell, 1987] of paired classes showed significant separation of class means within all classifications for link lengths.

The combination of aging effects (reduction of length increment with age of a shoot) and apical control (reduction of length with topological generation) has led to a branch form which gives the overall impression of outreach rather than spread of foliage: strong growth of the leader and a bias towards extension of more the acropetally situated laterals.

• 2.4.2 The distribution of link diameters

The diameters of branch links are usually regarded as a secondary character, being related to length through the need for hydraulic conduction and mechanical support. Taking all branch links together from all branch orders, a linear relation is found between their length and mean diameter (fig. 2.11). This is consistent with that found by Castera and Morlier [1992] for young branches of *Pinus pinaster* Ait.. A more detailed analysis of the relationship between lengths and diameters will now be presented which will demonstrate that this initial result is rather misleading.

The main aim here was to find whether the diameters conform primarily to a hydraulic demand model or a mechanical support model, or to some simple rule such as a constant allometric relation. First consideration was given to the make up of the allometric relation revealed in fig. 2.11. Analysis of variance was carried out on link diameter/length ratios classified by their topological rank, generation and growth year respectively. In each case, class means were significantly different ($p < 0.0001$). Bonferoni t-tests of all pairs of classes showed all pairs separated with >95%

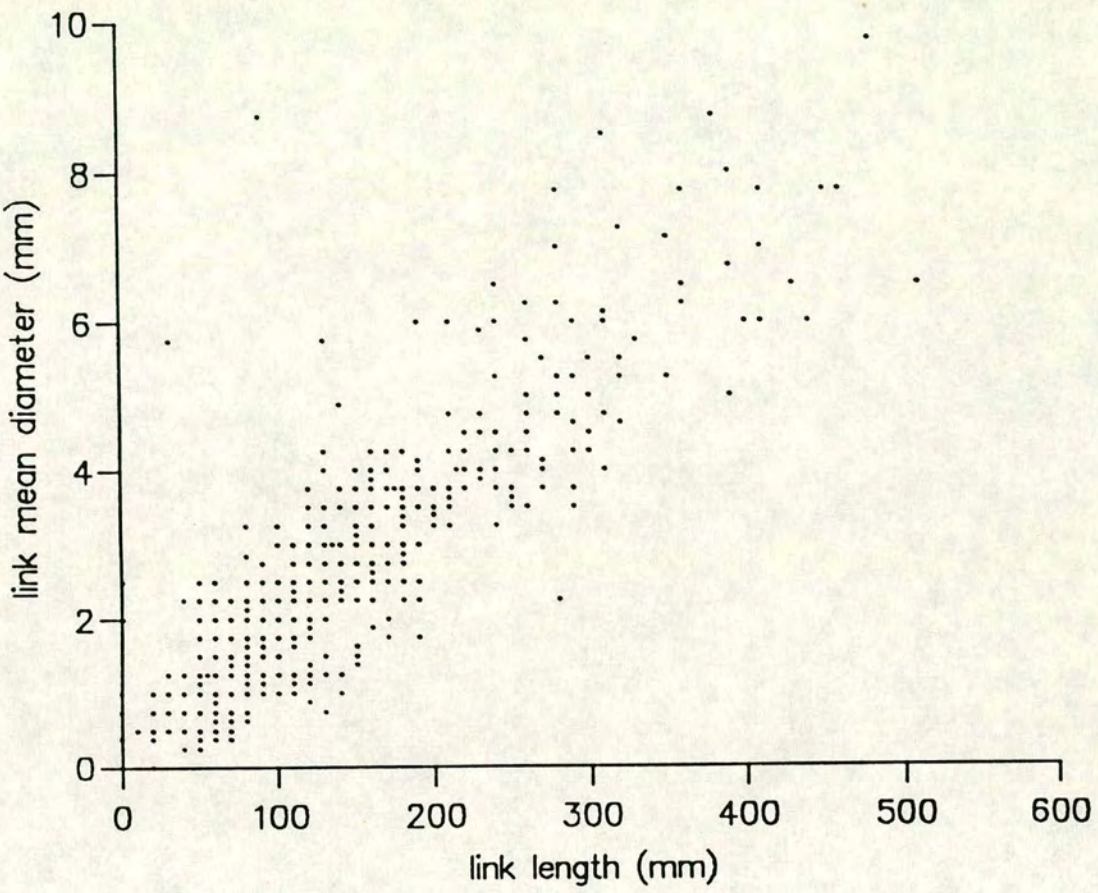

Fig 2.11. Length/diameter allometry for all shoots pooled. When all links from all branch orders (1-4) are included in the same population, link diameters are shown to be proportional to link length.

confidence except 3.4.1, 2.1.1 in topological rank and 4.1.3, 4.2.1 in generation classifications (statistically, even these can not be assumed to be of similar diameter/length). Thus the allometric constants are significantly different among links in all classifications of rank, generation and growth year. Table 2.3 lists these constants taken from the slope of the linear regression of link diameter on link length.

Table 2.3 Average length and diameter of link number 1 averaged over shoot ranks and generations (in mm)

link classification	length	diameter	regression slope	R^2
all links	136	3.4	0.030	0.65*
order=1, rank = 1	319	6.4	0.002	0.08
order=2, rank = 1	329	9.5	0.017	0.57*
order=2, rank = 2	165	3.4	0.013	0.09
order=3, rank = 1	236	10.1	0.006	0.51*
rank = 2	137	3.4	0.013	0.31
rank = 3	111	2.4	0.015	0.52*
generation = 1	236	10.1	0.006	0.51
generation = 2	151	3.4	0.009	0.17
generation = 3	57	1.4	0.013	0.10
order= 4, rank= 1	260	12.6	0.024	0.41
rank = 2	130	3.6	0.022	0.31
rank = 3	116	1.5	0.021	0.58*
rank = 4	92	1.5	0.017	0.67*
generation = 1	260	12.6	0.024	0.41
generation = 2	145	3.4	0.013	0.16
generation = 3	67	1.2	0.007	0.14
generation = 4	10	0.2	0.008	0.44

At branching nodes there are abrupt changes in the diameter of the parent shoot: in this study, these have been termed "diameter steps". As the shoot grows, successive annual increments of diameter alter the diameter steps which initially result from differences in link length and diameter/length ratios of contiguous links in the shoot.

Links in one order of branch can be identified with links in the next higher order by considering the incremental branch development. Fig. 2.12 shows four branch orders and explains how links from one order grow to become new links in the next order: each connection is termed a "growth stage". In table 2.4, the differences between the mean diameter of links related to a growth stage are shown.

Table 2.4 Average diameter increments of links (in mm)

Shoot	Mean Diameter	S.D.	Diameter Difference	Growth stage
1.1.1	6.38	1.66		
		3.08	(1)	
2.1.1	9.46	2.21		
2.1.2	5.82	1.20		
		1.36	(2)	
3.1.2	7.18	1.31		
2.1.1	9.46	2.21		
		0.67	(3)	
3.1.1	10.13	2.28		
3.1.3	4.73	1.02		
		2.04	(4)	
4.1.3	6.77	1.57		
3.1.2	7.18	1.31		
		2.25	(5)	
4.1.2	9.43	1.89		
3.1.1	10.13	2.28		
		2.46	(6)	
4.1.1	12.59	2.84		
2.2.1	3.43	0.90		
		-0.04	(7)	
3.4.1	3.39	0.76		

3.4.1	3.39	0.76	
		0.27	(8)
4.6.1	3.66	1.23	
3.4.2	2.13	0.55	
		0.39	(9)
4.6.2	2.52	0.97	
3.2.1	3.16	0.65	
		0.41	(10)
4.4.1	3.57	0.85	
3.6.1	1.35	0.67	
		-0.04	(11)
4.16.1	1.31	0.68	

There is clearly a substantial variation in diameter growth increment among the growth stages, thus it can not be concluded that a very simple rule is being followed in branch growth which adds a fixed thickness to all branch axes. It should be noted that a climate signal in growth will complicate comparison between years. The comparisons assume that branches of different orders simultaneously removed from the trees represent the growth which would be expected for any one branch as it extends from one order to the next in annual growth increments. Possibly, the branch has a fixed percentage of thickness added to its axes in the annual growth increment. Table 2.5 shows the percent increment relative to original link diameters in two groups: leader increments and those of links not in the leader. Again a large spread is noticeable, but the leader's links seem to receive a consistently larger relative increment than the others. A two sample t-test comparing these two groups confirms that impression ($p=0.035$).

The main reason for the low value measure in growth stages 2, 3 and 7 is likely to be that all growth in the year before these growth stages was greater that that to which they belong : in other words a climate effect.

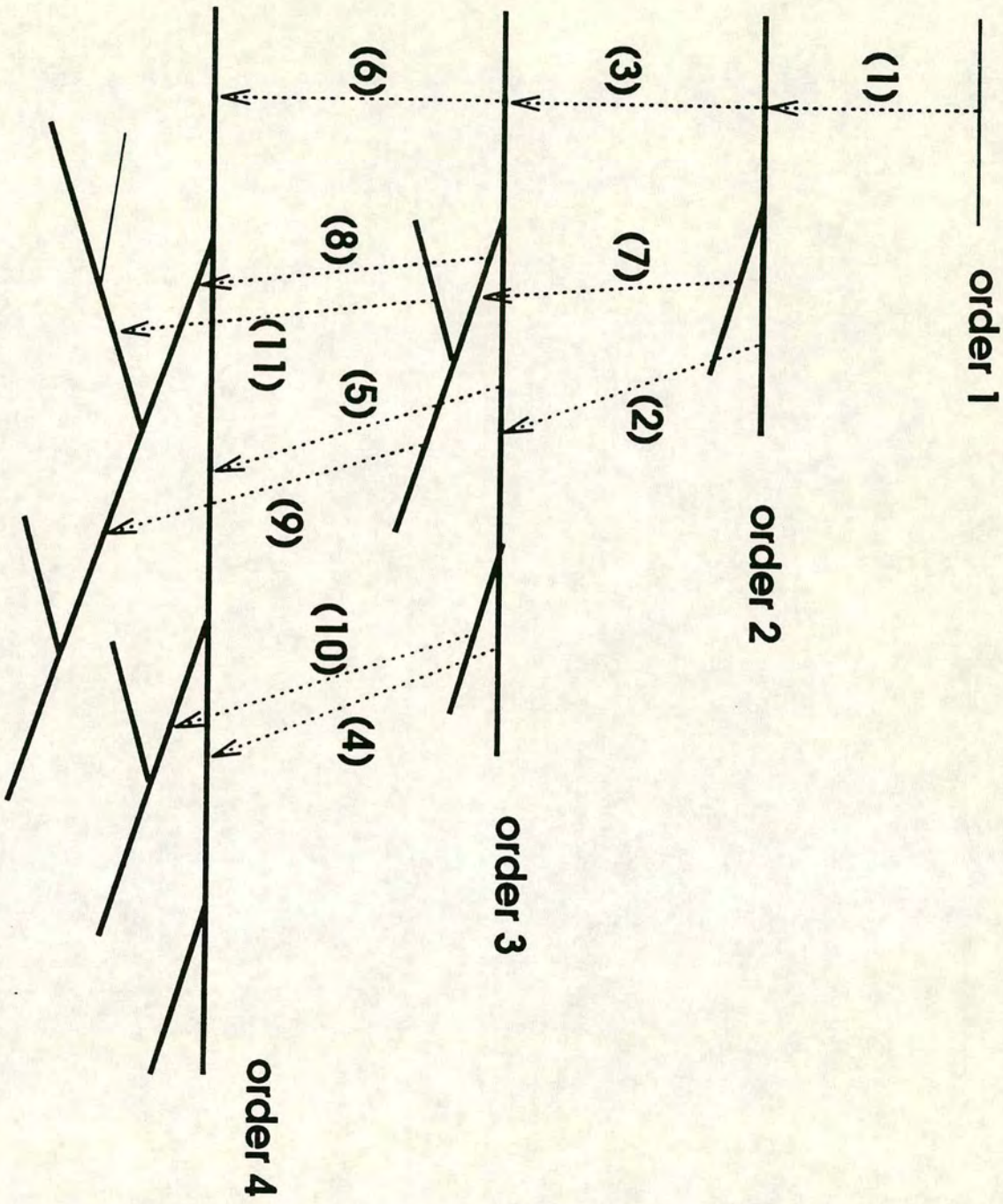

Fig 2.12. Diagramatic representation of the growth stages leading from one branch order to the next on the tree. The order 2 branch (second from the top of the crown) developed via growth stage (gs1) from an order 1 branch the previous year. Each year everyshoot increases in topological rank by 1 and each branch increases in order by 1. The set of branches from order 1 to 4 represent 11 growth stages in total. Each of these growth stages is associated with an annual increment in diameter of the link which has been estimated from the data and is presented in table 3.

Table 2.5 Percentage relative differences between average diameters for each growth
(refer to fig. 2.12)

Leader Growths

(gs1)	(gs2)	(gs3)	(gs4)	(gs5)	(gs6)
48	23	7	43	31	24

Non-Leader Growths

(gs7)	(gs8)	(gs9)	(gs10)	(gs11)
-1	13	15	13	-3

Leader links have larger diameters and receive larger annual diameter increments relative to their diameters than the others. Further variation in growth increments does not form into any recognisable pattern, but could be climatic (overall tree growth variation due to climate may, for example, explain some of the difference between (gs1), (gs3) and (gs6).

Analysis of variance of link diameters classified by rank, topological generation and growth year shows significant differences for all classes in each classification ($p < 0.0001$) and Bonferoni t-tests show all pairs of classes separated with a confidence >95%.

- ## 2.4.3 Contrasting models of diameter distribution among links.

Having established that link diameters are not simply a constant multiple of link lengths throughout the branch, a more sophisticated test of form-function hypothesis shall now be undertaken using the hydraulic function 'pipe model' [Shinozaki *et al.*, 1964] prediction of diameters and also a model based on the mechanics of cantilever beams [Morgan & Cannell, 1987].

In an attempt to assess the relative importance of static mechanical loading and hydraulic conduction demands on the secondary growth of branch links, two load

factors were described from the measurements. Good mechanical design of branches would result in strain being fairly evenly distributed among the links. Risk averse design would perhaps see a steady reduction in strain in the basepetal direction because sub-branch units representing more resource investment for the tree would be protected by a greater margin of safety. To investigate branch design in these terms, a mechanical load parameter was defined following Niklas [1990]

$$L_p = \frac{Wl_i^2}{EI_i} \qquad (2.3)$$

where W is the total weight supported by the link plus the weight of the link, I_i is the second moment of area of cross-section of the link about the neutral axis defined using the average radius (instead of diameter) as

$$I_i = \pi r^4/4 \qquad (2.4)$$

E is the elastic modulus, here given a value of $3.6 .10^9$N m^{-2} [Cannell & Morgan, 1987]. The subscript i denotes the property of the ith link.

Hence:

$$L_p \propto r^4 \qquad (2.5)$$

Secondly, according to the pipe model of hydraulic demand, shoot cross-section area should be proportional to the total foliage area distal from the point of measurement. Foliage was assumed to be distributed at approximately a constant number of needles per unit shoot length, thus the hydraulic demand model predicts that the diameter of the ith link d_i is

$$d_i \propto (\Sigma l)^{0.5} \qquad (2.6)$$

where Σl is the sum of lengths of all shoots connected distally to and including the *ith*..

Table 2.6 gives mean values for d_l and load parameter for all the link classes.

(figures are taken from 24 separate branches of each order).

Table 2.6 Load parameters of links classified by topological type.

link (o.s.k)	Σl mean	s.d	L_p mean
	s.d		
1.1.1	319	91	1.73
	0.92		
2.1.1	992	203	1.42
	0.64		
2.1.2	333	66	2.31
	1.13		
3.1.1	1612	279	1.23
	2.56		
3.1.2	894	151	2.61
	1.86		
3.1.3	270	65	2.98
	1.83		
4.1.1	3296	1096	0.77
	0.36		
4.1.2	1825	446	1.39
	0.59		
4.1.3	872	177	2.41
	0.96		
4.1.4	254	63	2.36
	1.16		
3.4.1	242	129	1.44
	0.98		
3.4.2	100	31	1.40
	0.74		
4.4.1	304	300	1.38
	1.34		
4.4.2	248	137	2.46
	2.06		
4.6.1	606	360	1.56
	1.09		

4.6.2	256	138	2.63
	2.10		
4.6.3	80	52	2.68
	2.39		

When all the links are taken together, regressions of $\log_{10}(r)$ with $\log_{10}(L_p)$ and with $\log_{10}(\Sigma l)$ show the following allometric relations:

$$L_p = 1.9\, r^{3.37} \qquad (2.7)$$

and

$$\Sigma l = 138\, r^{1.2} \qquad (2.8)$$

The $\log_{10}$ regressions are shown in fig. 2.15. Comparison of the regression models and the theoretical models in each case indicates whether the theoretical models may explain the primary form-function relationship for link diameters. The mechanical model prediction is within the 95% confidence limits of the regression, but the pipe model's prediction is not reconciled with the regression for $\log_{10}(\Sigma l)$. This represents evidence in favour of the precedence of the mechanical model. However, in regression for allometry, where there is no independent variable, reduced major axis regression should be used [Seim & Saether, 1983]. The reduced major axis regression slope is equal to the conventional regression slope divided by the regression coefficient (R^2), so the exponents in equations (2.4) and (2.5) become 3.89 and 1.68 respectively. Whilst the 95% regression confidence interval for the exponent in equation (2.5) does not include the theoretical exponent of 2.0 predicted by equation (2.3), if the reduced major axis value of value 1.68 is taken, then the theoretical value is within 95% of the that measured. In both conventional and reduced major axis regression the theoretical value of the exponent for load (equation (2.5)) is within 95% of the measured figure.

The fact that the power to which radius is raised may be slightly less than the predicted 4.0 shows that if anything the load declines with increasing r, this being indicative of a decrease in load basepetally within branches or with increasing branch size. The mean load parameter of all leader links of each branch order has been plotted against link number in fig. 2.13. The rise in load parameter with link number and its falling with increasing branch order suggest the kind of risk averse mechanical design mentioned earlier. Fig.2.13 also shows the load parameters for three classes of laterals in which a similar pattern is observed except the 3.4.2 links

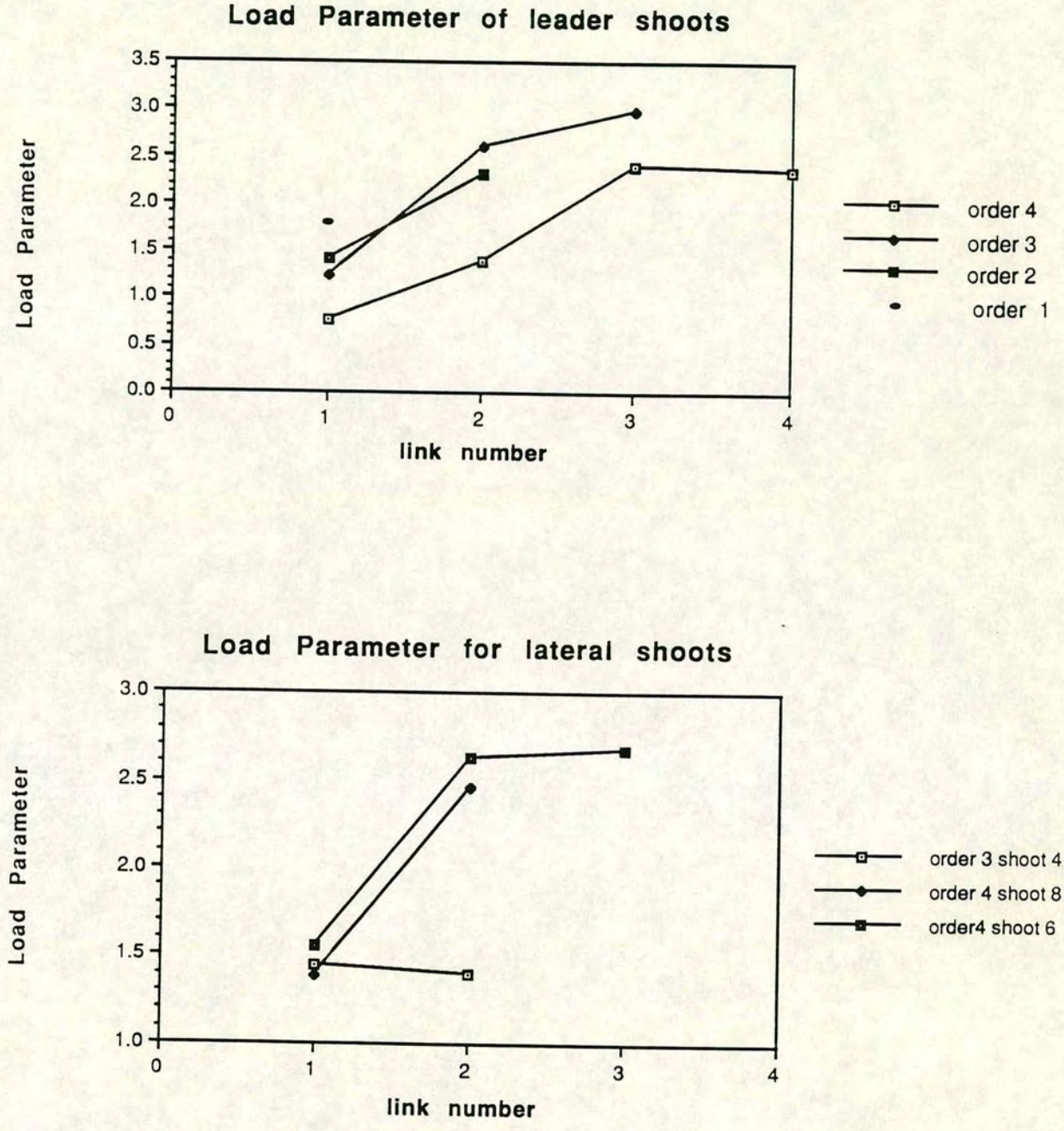

Fig 2.13. Mechanical load parameter (Wl^2/E) and link diameter predicted from the pipe model equation ($d = k(\Sigma l)^{0.5}$) are shown by labelling the links of order 3 (a) and order 4 branches (b) .Loads are expressed relative to the load applied to the apical link of the branch leader shoot. Loads are shown in bold text, predicted diameters in italics.

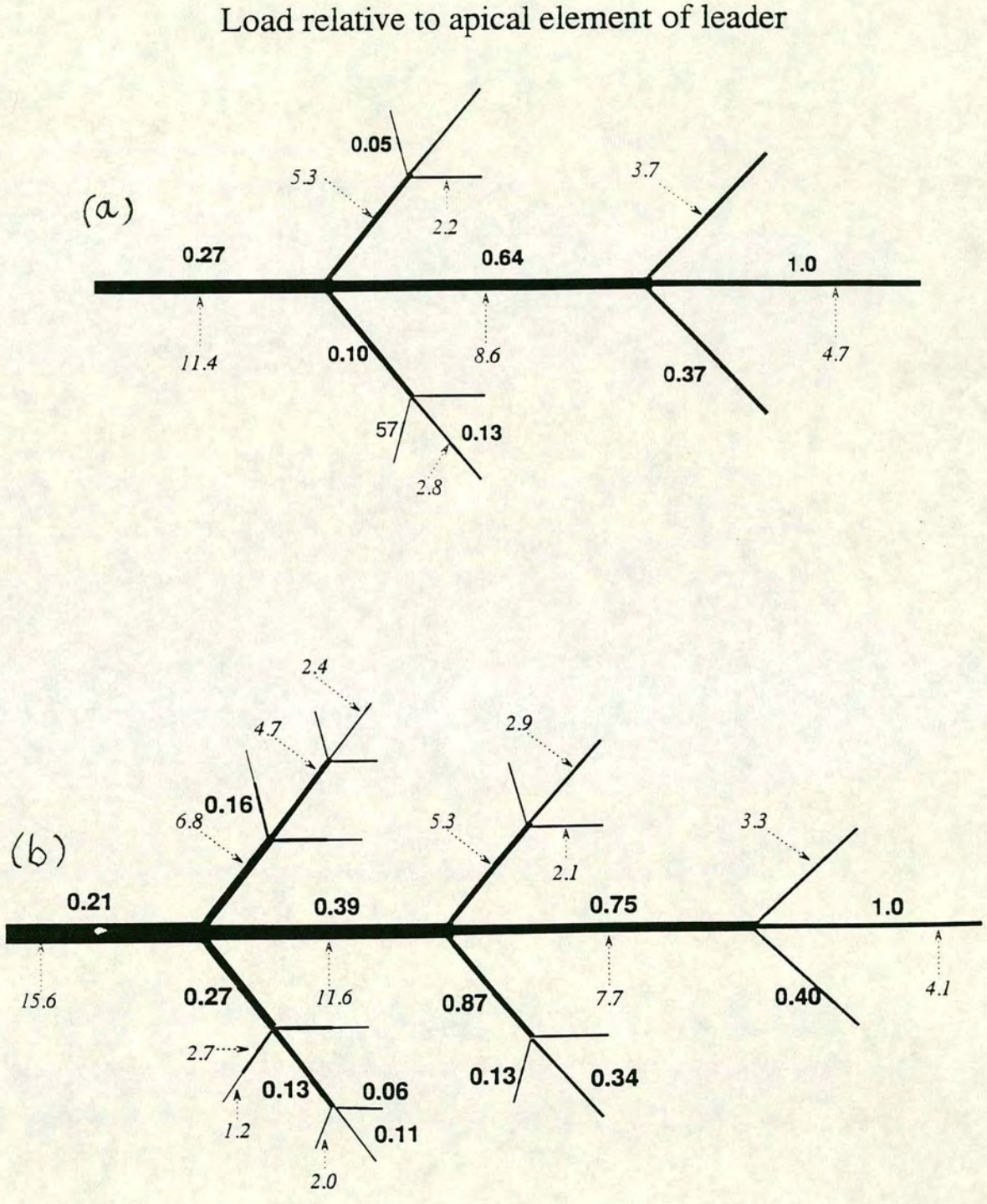

Fig 2.14. The variation of load parameter along the length of the leader shoots in branches of order 1-4 is plotted in (a). Load parameter is plotted for selected laterals of order 3 and 4 shoots in (b). The lower the load parameter is, the safer the design from a mechanical point of view.

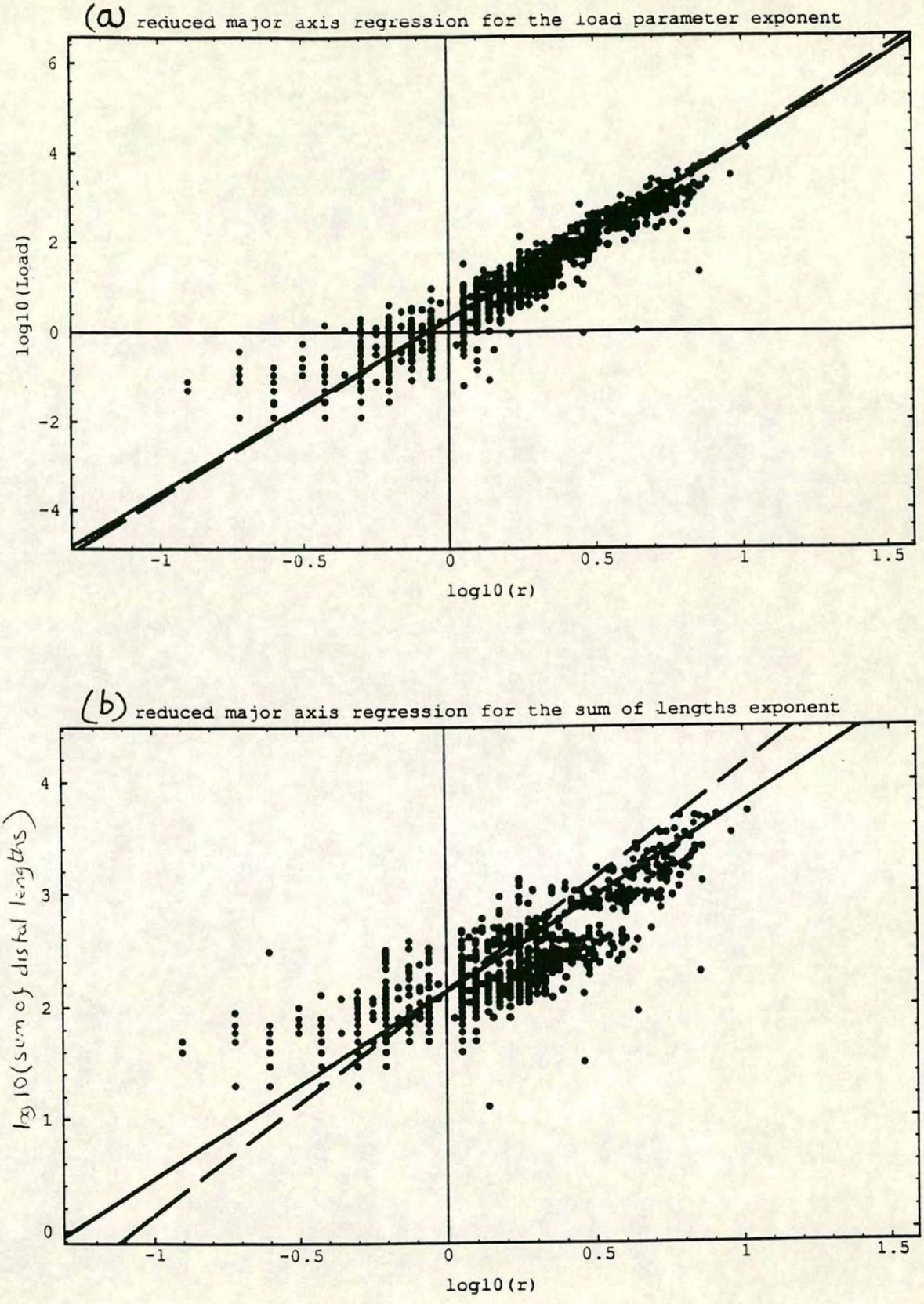

Fig 2.15. Log regression of link diameters with load parameter (a) and total length of distal shoots (b). Observed regression for load parameter ($r^{3.37}$) matches the r^4 law expected from theory, whilst the regression for distal lengths ($r^{1.2}$) does not match the r^2 law expected from theory.

have a slightly lower load parameter than 3.4.1. The lateral's load parameters are similar to those of the leaders in equivalent topological positions e.g. 4.6 laterals and 3.1 leaders.

It was revealed earlier that although the diameters of all links conformed to a linear regression model, when they were classified into ranks and topological generations, significant differences in allometric constants were present: it is possible that the log regressions of loads and total distal lengths with diameters similarly contain further structure. Links were classified according to rank and topological generation and the regressions of $\log_{10}(r)$ with $\log_{10}(L_p)$ and with $\log_{10}(\Sigma l)$ were repeated. Tables 2.7 and 2.8 lists the results. Much less variation in allometric constants is apparent with these measures. Analysis of variance has confirmed that there are not significant differences between the loads of different link classes, nor between their total distal lengths. This implies that the relationships given in equation (2.2) and equation (2.3) apply as whole branch design formulae.

Table 2.7. Scaling of link radius with total distal shoot length (Sl)

category	multiplier	power	R^2
	all branches		
link rank = 1	0.23	3.08	0.77
link rank > 1	0.23	3.49	0.91
shoot rank = 1	0.18	3.01	0.77
shoot rank = 2	0.28	3.23	0.84
shoot rank = 3	0.37	3.30	0.85
generation = 1	0.50	3.31	0.84
generation = 2	0.29	2.81	0.69
generation = 3 -	0.22	1.45	0.30
	order 3 branches only		
generation = 1	0.91	2.62	0.61
generation = 2	0.13	3.57	0.73
generation = 3 -	0.32	1.74	0.31
	order 4 branches only		

generation = 1	0.72	3.01	0.87
generation = 2	0.33	2.67	0.69
generation = 3	0.15	1.51	0.35

Table 2.8 scaling of link radius with load factor

category	multiplier	power	R^2
	all branches		
link rank = 1	2.04	0.74	0.66
link rank > 1	2.27	1.30	0.78
shoot rank = 1	2.03	0.71	0.65
shoot rank = 2	2.15	0.96	0.61
shoot rank = 3	2.25	1.21	0.70
generation = 1	1.87	1.81	0.75
generation = 2	2.14	1.01	0.39
generation = 3	1.99	0.45	0.1
	order 3 branches only		
generation = 1	1.96	1.67	0.63
generation = 2	2.03	1.01	0.38
generation = 3	1.89	0.60	0.35
	order 4 branches only		
generation = 1	1.88	1.97	0.83
generation = 2	2.02	1.06	0.44
generation = 3	2.04	0.51	0.19

Whether a mechanical or hydraulic model forms the basis for link length / diameter allometry, it will have implications for the effectiveness of the branch in terms of the other model. The effect of one model on branch performance with respect to the alternate is a function of the distribution of link lengths. The question now arises : if, hypothetically, a branch with link lengths as given by the mean values in fig. 2.10

which was designed according to the pipe model formula would result in a bad mechanical design, and if so, to what extent ? To answer this question, the link diameters which would result from the pipe model prediction and then the link load parameters of the resulting design were calculated. This was carried out for an order 3 and an order 4 branch for which the results are presented in fig.2.14. The proportionality constant between r and $\Sigma l^{0.5}$ was taken from the apical link of the leader shoots (3.1.3 and 4.1.4 in order 3 and order 4 branches respectively) and this same constant was applied through out the branch (different for the different orders). Then the load parameter of the apical link of the leaders was calculated and its reciprocal taken for scaling so that all the other link's load parameters could be calculated as relative values to the apical link of the leader. It is striking that the pipe model has given rise to a mechanical risk averse design of the leader shoot in both branch orders. However, the reverse is the case for the lateral shoots, although all calculated load parameters are less than that of the apical link of the leader. Thus this design would result in a mechanically stable, but highly conservative branch. The calculated diameters, especially of more basepetal high rank shoots are considerably greater than the means measured from real branches. The hydraulic design principle used here leads to an inefficient design (in terms of carbon investment), rather than an unstable one.

It is informative to calculate the effect on mechanical load of the link lengths relative to one another using the pipe model for design. Using the pipe model design, the load parameter of link a is given by

$$Ld_a = \frac{a_2(br_b + (ar_b^2 / b)(a+b+2c) + 2cr_c^2}{b(a+b+2c)^2 r_b^2} \qquad (2.9)$$

This function is plotted in terms of *a/b* and *c/b* in fig. 2.16.

Clearly, the most important parameter is *a/b* which is determined by the degree of 'ageing' in the shoot. This result which is intuitive, corroborates the findings of Cannell and Morgan [1990] when they showed with model branches that placing the laterals nearer to the base of the parent resulted in smaller diameters to maintain a given shoot tip deflection due to self weight.

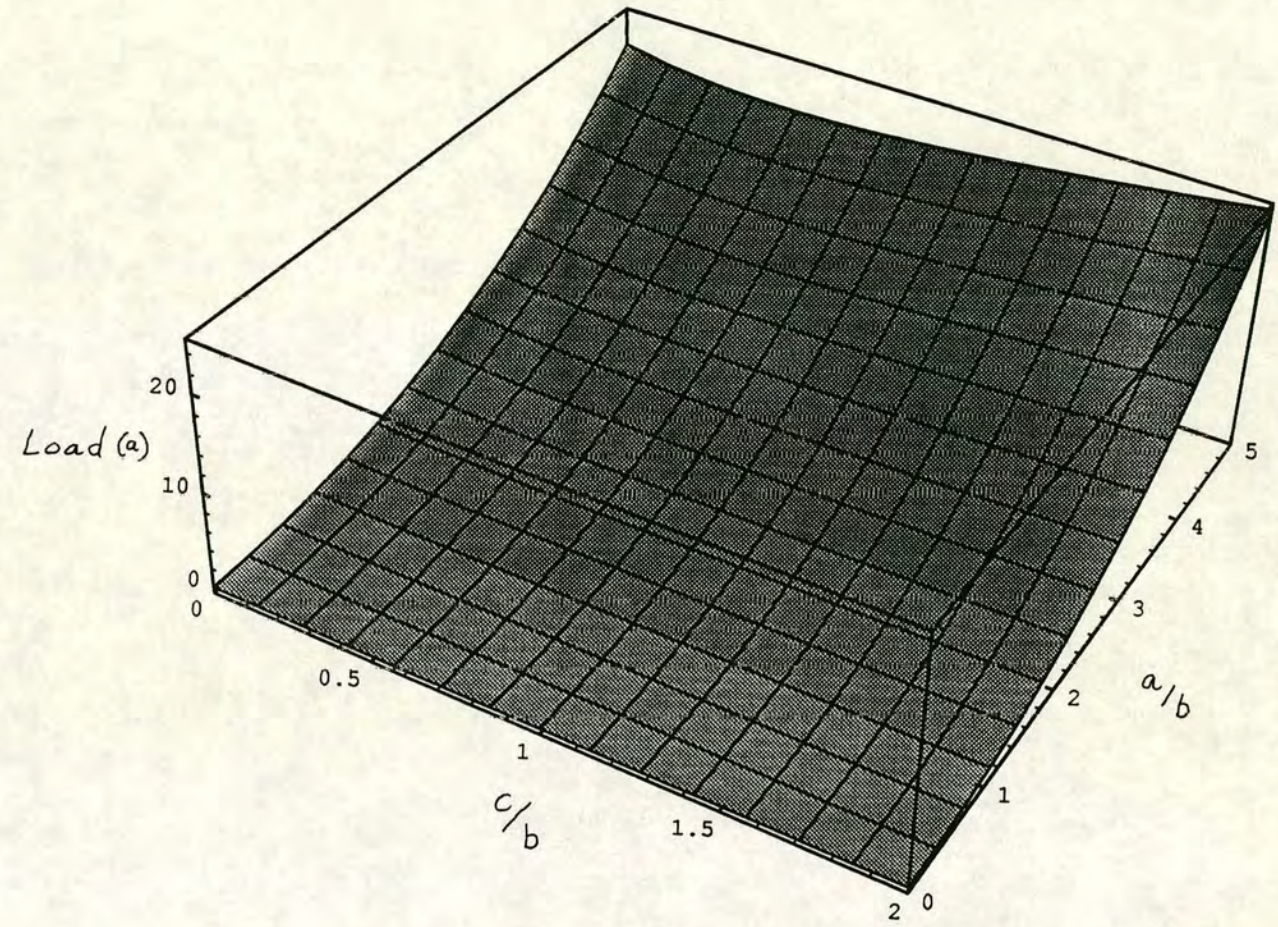

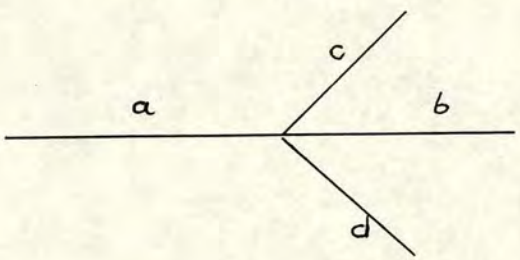

Fig 2.16. The Load applied to link (a) (see insert) varies as a function of the lengths of links (a), (b), (c) and (d) and their diameters. If the links (c) and (d) are made identical (represented by (c)) and the diameters are determined by using the pipe model theory ($d = k(\quad)^{0.5}$), then the load applied to (a) is the function of the length ratios c/a and a/b plotted

• 2.5 Geometric characters and deflections of shoots

• 2.5.1 deflection of shoot tips

The mechanical design of branches results in a particular distribution of strains among the links and shoots when the branch is mechanically loaded. A crude indicator of these strains can be derived from measurements of shoot apex deflections (δ) [Morgan & Cannell, 1987].

Deflection of shoot tips are simple to measure, but may not be the best measure of strain. A better measure might be the deflection per unit path length (λ) on a route from the branch base to shoot tip as defined in fig.2.17. This deflection per unit length (δ/λ) was found to be related to the tip deflection (δ) by the linear regression model

$$\delta/\lambda = 0.04 + 0.0013\ \delta \qquad (2.10)$$

with a correlation coefficient of $R^2 = 0.69$.

• 2.5.2 relations between shoot characters

Shoots are made up of a contiguous set of links, the number being equal to the shoot rank. Geometric relations among links are expected to result in geometric relations among shoots which can be measured. The distinction between links classified by topological rank and topological generation proved useful earlier in revealing aspects of resource allocation. When shoots are similarly classified, differences of allocation between the topological classes would show how this determines shoot size. Shoots sharing the same rank are topologically similar (they have the same number of links and lateral whorls) , but those of the same topological generation are not necessarily similar. Thus if topological rank is found to be a more discriminating classification of shoot geometries than topological generation (as it was for links), this would show that allocation was not simply determined on the basis of reiteration of a unit of morphogenesis [Kuppers, 1989]. The hypothesis that topologically similar branch parts are not geometrically, or functionally, similar was tested by comparing the maximum multivariate discrimination among shoots of the same topological rank with that of shoots of the same topological generation. This comparison was made using canonical variate analysis (CVA), which takes a set of characters and finds the

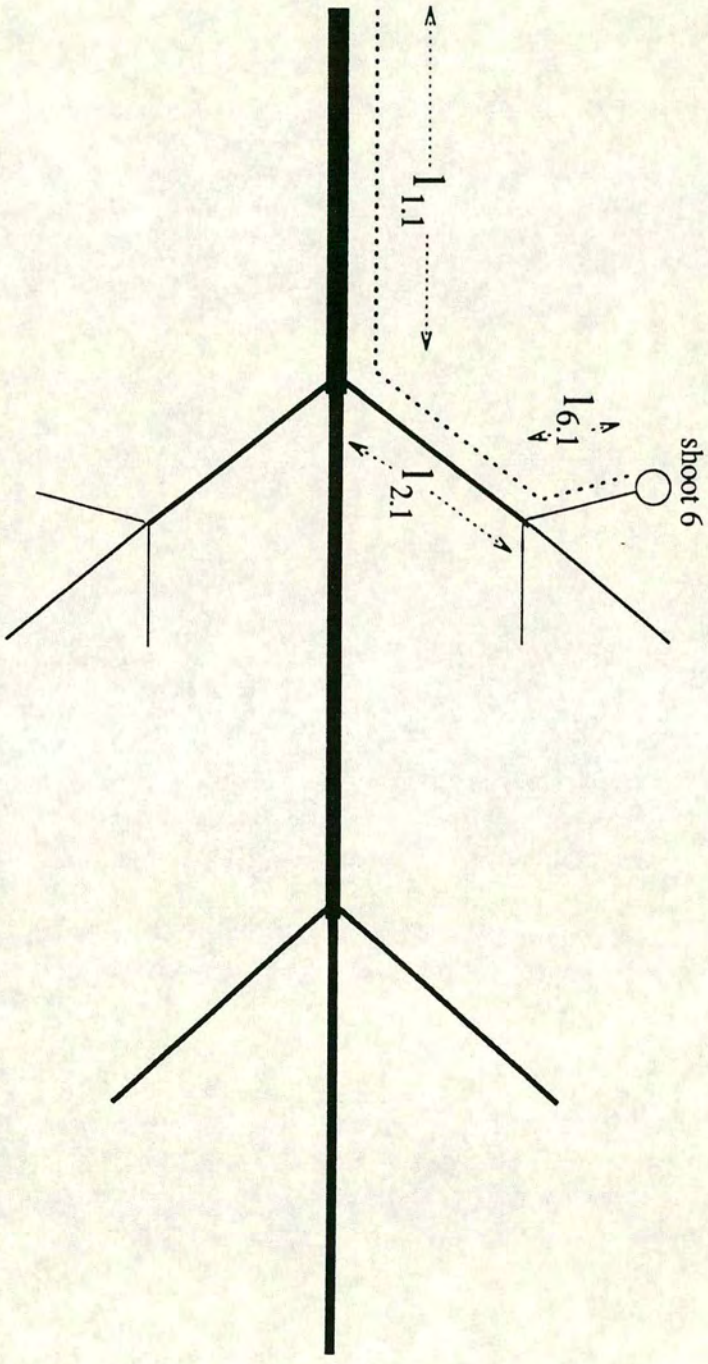

Fig 2.17. The relative deflection of a shoot apex is defined as the measured deflection divided by the path length to the apex from the base on the branch leader. For example in this order 3 branch, the path length for the shoot type 6 shown is the sum of the lengths of links 3.1.1, 3.4.1, 3.6.1.

linear combination of them which maximises the ratio: inter-group dispersion / intra-group dispersion. CVA was performed using shoots from order 3 and order 4 branches, classified by topological rank and topological generation separately and the intergroup distance (for maximum discrimination of classification groups) was taken as a measure of non-similarity.

24 branches of each order were characterised by the variates : shoot length (l_s), shoot mean diameter (d_s), total shoot weight (w_s) and relative tip deflection (δ/λ). The intergroup distances are summarised in fig. 2.18. In the cases where topological generations were equal and ranks differed (classification by rank) (ℜ), the mean inter-group distance was 2.3, where ranks were equal and topological generations differed (classification by topological generation) (𝔊), intergroup distance was 5.7. In all but one out of the five rank or generation classes, generation gave a higher inter-group distance than rank, thus generation was a stronger discriminator of shoot characters. The latent vectors show the relative contributions of variates to the canonical variate of maximum group separation (the importance of individual variates in discriminating shoots); these are presented as a percentage of the total discrimination in fig. 2.19. In all cases the shoot mean diameter was the major contributor to the canonical variate (however, recall that the diameters and lengths are highly correlated), so shoots differ most in their mean diameters .

Because topological rank dictates how many links together form the shoot, shoot lengths would be expected to be more dependent on rank than topological generation. Shoot rank would also be expected to be the stronger indicator of diameter and weight because high rank shoots contain links with greater thickening to support more laterals and a greater total shoot length. Thus shoot rank would be expected to be more discriminating of shoot geometry than topological generation. The contradictory result of CVA on shoot geometries described above provides strong evidence leading to the conclusion that there is a tendency for distributing material among shoots according to their topological generation. This supports the hypothesis that topologically similar branch parts are not geometrically, or functionally, similar.

• 2.5.3 Relations between deflections and geometric characters

The distribution of shoot apex deflections (δ) among shoots within the branch may provide more clues regarding the geometrical design of branches. The measured end point deflections of shoots within branches describe the distortion of the branch and indicate the strain distribution among the shoots resulting from the mechanical

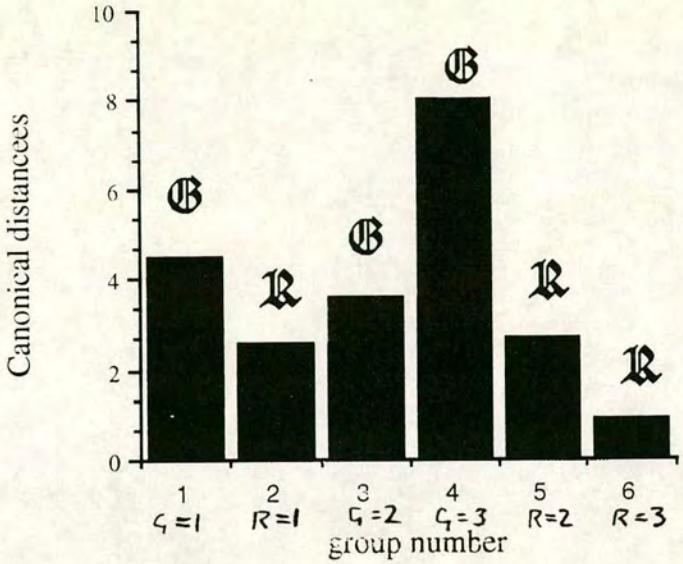

Fig 2.18. The canonical variate intergroup distances among shoots classified either by their topological rank (ℜ) or topological generation (𝔊) show whether topological rank or topological generation is a a better indicator of shoot design. In most cases topological generation discriminates shoot design better than rank: shoots of the same rank are more similar than shoots of the same topological generation.

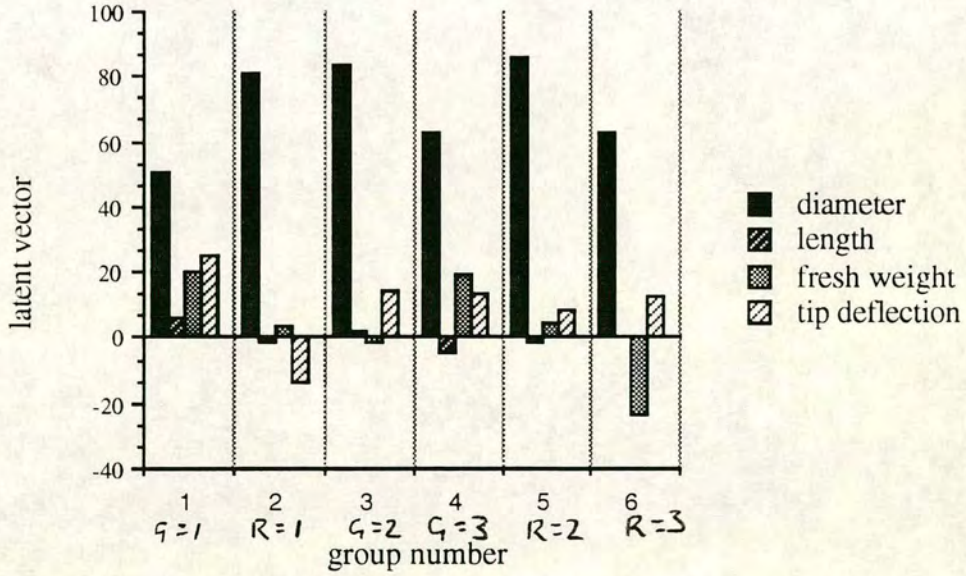

Fig 2.19. Latent vectors of the canonical variates which make up the maximum discrimination axis for shoot geometry. in every case, mean shoot diameters made the gratest contribution to the canonical variate which maximally discriminated shoots of different topological rank or topological generation.

loading of self weight. It is possible that there exists a relationship between the distribution of deflections and the branch geometry. Using statistical techniques, a pattern was sought in the distribution of deflections among shoots.

Deflection measurements of shoots where rank was equal to branch order and generation was greater than 2 (the most peripheral shoots) were not included in this examination. This was because these shoots were subject to intolerable measurement errors (error > data) because of small deflections and branch positions compromising the accuracy of the measurement.

Fig. 2.20 shows a scatter graph comparing the deflection per unit length to the fresh weights and the lengths of shoots respectively. The graph gives no reason to believe that a relation exists between the deflections and the geometric characters. Multiple regression of deflection with shoot length, weight and diameter shows that none of the characters are significantly correlated with tip deflections: the data represent only random scatter.

Procrustes Rotations (Digby & Kempton, 1987) is a multivariate technique for comparing two data matricies in a way that identifies common patterns in the distributions of values. This technique can be more sensitive to correlations within data because it takes account of correlations among groups of characters acting together. The data matrix of relative deflections of shoots was mapped by linear transformations onto the matrix of principle coordinates from both shoot length and shoot weight data by Procrustes rotation. The analysis has been carried out for branch order 3 and 4 in turn. In every case, the sum of residuals was substantially larger than the sum of fit (see table 2.9).

The sum of square of residuals results from the real data were compared with 100 others where the positions of shoots in the deflections matrix were randomised. This was intended to establish whether the residuals for the real data were significantly less than the expected value for random sets of points. Table 2.9 also shows the means of residuals from Procrustes rotations of 100 random permutations of the shoots. The table shows that the residuals from Procustes rotations of the data are more than 3 standard deviations less than mean random permutation residuals for all order 4 branch data - indicating that there is a significant relationship between deflection and geometry data sets in order 4 branches, but not for any of the order 3.

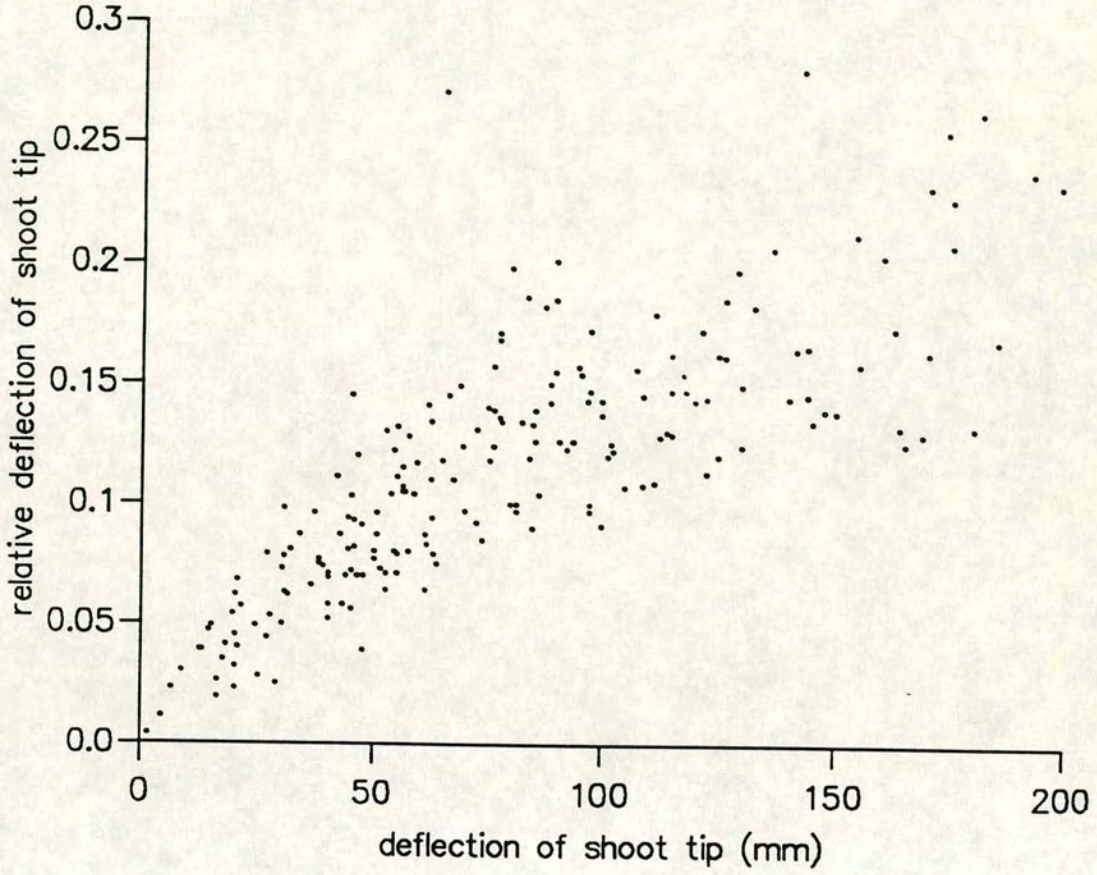

Fig 2.20. Deflection per path length (d/l) plotted with shoot length. There is no relationship between these variates. Similarly, there is no relationship between (d/l) and shoot mean diameter, or weight. This indicates that mechanical stresses are distributed among the shoots evenly compared to random scatter.

This implies that for order 4 branches there is some systematic relationship between the spatial distribution of morphological characters and shoot tip deflections. However, the measure of fitted configurations is so small (less than 0.3) that it is not possible to discern the nature of the spatial relationships.

Table 2.9 residuals from procrustes rotations showing significant differences from random permutations of shoots in order 4 branch characters. Larger variances in order 3 branch random permutations leave the order 3 data non-significant. Significance is taken to be : data residual more than 3 standard deviations from random residual.

	rotation from the data	mean of 100 random
l 3	.934	.937
l 4	.750 *	.885
d 3	.947	.923
d 4	.713 *	.859
w 3	.933	.925
w 4	.810 *	.864
l/d 3	.951	.919
l/d 4	.675 *	.854

* indicates data residual more than 3 standard deviations from random mean residual.

Shoot tip deflections will depend on factors other than those measured here. The fact that relationships between deflections and the geometric characters in order 3 branches were not significant may be due to the complexity of the real branches. Variation in foliage mass per unit length of shoot, mechanical properties of shoots and nodes and the signal-to-noise ratio of the data all conspired to obscure the geometric relations.

• 2.6 Discussion

Biomass is distributed among the shoot links of branches of Sitka spruce in a way that is closely related to their position in the branch topology. Material investment appears to be most closely related to the topological generation of shoots,

establishing a hierarchy among shoots of the same topological rank which counts shoots of low topological generation as more important than those of high topological generation. This has the effect of distributing resources among shoots in a way which is highly biased in favour of those offering the greatest opportunities for extension into new space as opposed to those filling in space within the crown. Priority is given to extension of the leader and the most distal of its laterals in each annual growth increment, while resources available for growth in shoots of increasingly high topological generation become so constrained that in the limit they cease to grow and subsequent laterals are entirely suppressed (self pruning). This pattern of resource allocation might be interpreted as being determined by the availability of light resources, but it seems to in some way anticipate future light availability and the relative opportunities for shoots to exploit resources in the future.

The relationship between the diameter of branch links and their length differs significantly among links classified by their topological position. The distribution of allometric relations was tested against two competing models: one based on a theory of hydraulic transport requirements (the pipe model), the other being based on the requirement of shoot axes to provide mechanical resistance to static loads. Static load resistance required link radius raised to the power 4 to be proportional to a load parameter ($W l_1^2 / E I_1$). This was shown to be true within 95% statistical confidence for the measured branches. On the other hand the pipe model required link radius squared to be proportional to total distal shoot length, but the measured branches did not conform to this model. This leads to the conclusion that diameters of branch links are related to mechanical load requirements rather than to hydraulic transport requirements (according to the pipe model).

No clear relationship was found between measured shoot tip deflections under static load and the geometric branch characters. Some obscure relationship may exist in a multivariate sense, but no conclusion could be drawn about what that might be because it was so weak and because no phenomenological interpertation was found. At first sight this result may appear puzzling, since it seems to imply that the geometry has no influence on the shoot tip deflections and therefore on the distribution of strain in the branch under static load. It is, though, precisely because of the arrangement of matter in the branch that no pattern is observed in the shoot tip deflections. The distribution of secondary growth amongst the branch links has equalised total shoot strains to the extent that all that has been possible to measure was a residual statistical variation in strain among the shoots. This result would be

the conclusion of assuming that load parameter is proportional to radius raised to the power 4 in all branch links.

The cost of following an hydraulic design principle (the pipe model) for diameter control, in terms of mechanical efficiency was estimated. By designing a branch using the average of measured link lengths and the pipe theory model, it was possible to calculate diameters and load parameters for such a hypothetical branch. Following the pipe model resulted in an increase in mechanical strength with increasing rank of shoot over that of the mechanically orientated design. Using the most distal of the leader shoots as a bench mark for design, the pipe model branch was not mechanically compromised, but was materially inefficient, using more wood than appears to be necessary. It is interesting that while significant differences among all rank and generation classes of links were observed in length-diameter allometric constants, no differences were found for load factors or modelled hydraulic demands. This is surely an indication of the presence of design principles at work to distribute structural resources according to the requirements.

• 2.7 Conclusions

• 2.7.1 How uniform is the geometry of Sitka spruce branches ?

A uniform underlying topology is adhered to in branches of Sitka spruce so that shoot indexing systems could repeatably identify the principle shoots of the branch, but this did not apply to the interlateral shoots.However, the physical characteristics of the branches, shoots and component links all varied to the degree that standard deviations were little less than the means. Biomass was found to be distributed among the shoot links of branches of Sitka spruce in a way that is closely related to their position in the branch topology. Material investment appears to be most closely related to the topological generation of shoots, establishing a hierarchy among shoots of the same topological rank which counts shoots of low topological generation as more important than those of high topological generation.

• 2.7.2 Are there genotypic differences in branch design ?

The four provenances: Cordova, Sitka Island, Skidegate and Northbend could not be separated with confidence on the basis of single characters of branch geometry alone. However, when branch geometry characters were combined into optimum discrimination functions by canonical variates analysis, then all combinations of pairs of provenances could be separated, except for Cordova-Skidegate. Branch angles made the highest contribution to the Northbend-Cordova axis of discrimination whilst the Sitka-Skidegate axis was made up of a wide variety of variates with no obvious concentration of variate type. The claim that the provenances were adequately separated by the analysis of these branches is made on a weak foundation, especially as no obvious pattern could be found in the latent vectors of the canonical variates analysis. This result is not a strong encouragement for breeders to embark on a program of selecting for improved branch design efficiency. However, there is room for hope, because the variates used in the analysis of tree differences were only the most gross combination of branch characters. This analysis should now be repeated to include shoot level and link level combinations and even single characters such as the lengths of leaders of order 4 branches etc. When this is done, more significant differences between the branch designs might be revealed. If that becomes the case, then the data presented in this work will not, after all, be in contradiction of the general view supported by Cannell [1974]: that different provenances give rise to significantly different branch characters.

- ### 2.7.3 What allometric relations exist between geometric characters within branches ?

Shoots show a linear relationship between total length and mean diameter which contrasts with the diameter-squared law for constant mechanical stress. Fresh weights of shoots bearing interlaterals are proportional to their length times mean diameter squared. These findings concur with those of Castéra and Morlier [1991]. Relative deflection is linearly related to deflection among all the shoots, thus longer shoots are less rigid than short ones. There are significant differences in allometric ratios among shoot types in branches.

The relationship between the diameter of branch links and their length differs significantly among links classified by their topological position. The distribution of allometric relations was tested against two competing models: one based on a theory of hydraulic transport requirements (the pipe model), the other being based on the requirement of shoot axes to provide mechanical resistance to static loads. Static load resistance required link radius raised to the power 4 to be proportional to a load parameter ($W l_1^2 / E I_1$). This was shown to be true within 95% statistical confidence

for the measured branches. On the other hand the pipe model required link radius squared to be proportional to total distal shoot length, but the measured branches did not conform to this model. This leads to the conclusion that diameters of branch links are related to mechanical load requirements rather than to hydraulic transport requirements (according to the pipe model).

- ### 2.7.4 Does a relationship exists between branch geometry and shoot tip deflections ?

Shoot tip deflections per unit length from branch base to shoot tip (relatived eflections) were found to be proportional to the shoot tip deflections.

A clear relationship between the shoot tip deflections and the geometric variates could, perhaps, be expected. No such relation was found for any individual geometric character although, some obscure relationship may exist in a multivariate sense. No conclusion could be drawn about what that relation might be because it was so weakly expressed and because no phenomenological interpertation was found. The lack of observable relation between branch geometry and shoot tip deflections has been taken as an indication that branches are designed in a way which distributes deflections evenly (on average) among the shoots.

- 2.7.5 Does static load bearing explain shoot thickness ?

The static load bearing model showed the distribution of thickening within the branches to be at least adequate for mechanical design. It was argued that risk averse design (greater margins of safety) could usefully apply for shoots which are more important to the tree's survival. Greater margins of safety were found amongst shoots which may be exposed to greater light flux and which may therefore be capable of greater photosynthetic production of fixed carbon.

- 2.7.6 The implications of this chapter for the next

The detailed pattern of resource allocation among structural branch links within the branch has been shown to be consistent with mechanical stability criteria and also to indicate the possibility of allocation on the basis of some other criterion differentiating shoot topological generations (for example potential light interception by the shoots).

The above conclusion provides a strong motivation for building a mathematical model to represent the behaviour of branches under mechanical loading which includes a description of the light regime under which they operate.

The branch model must be true to the observed branch topology so that the implications of the variation in allometric laws among shoots occupying different topological positions can be studied.

chapter 3

A Mathematical Model To Simulate The Effect Of Gravity On The Effectiveness Of A Branch From Sitka Spruce

• 3.1 The definition of the model

• 3.1.1 The purpose of the model

A mathematical model is developed to help to understand in detail the way in which the architectural design affects a branch's mechanical behaviour and thereby to study the relationship between the form and function of mechanical design. This could be an attempt to simulate the natural branch with as many ad hoc rules and modifications as are desired to create an acceptable resemblance. However, such an approach would be of limited value in further analysis and prediction. Frijters [1978] argued that if a concise expression can be used to simulate the form, then much more (and more general) information can be gained. The intention here is to develop a tool which will enable an understanding of how geometry determines the effectiveness of a Sitka spruce branch as a light collector. The modelling process itself should help to make sense of this rather vaguely expressed problem as the development will demand a rigorous description of the geometric and mechanical features: reducing the confusing complexity of the real world to an idealisation which is expressed in mathematical terms as an object with a definite topology and a set of geometric characters. Sensitivity testing of the model allows judgements to be made about the relative importance of the characters and some may be eliminated on the basis of this, bringing further simplification.

A model of this kind seeks to identify the underlying principles of design by investigating the behaviour of an analogous system. The model is intended to be useful when considering the hypothesis which states that biological form is close to an optimal form as a result of repeated redesign and natural selection. The

mathematical description of the branch and its behaviour presented here lends itself to a mathematical design optimisation procedure. Optimisation modelling is a strong test of the underlying assumptions concerning the relationship between form and function.

A mathematical model is being built to assess the effect and importance of various measurable geometric characters on the light interception-to- branch mass ratio.

- 3.1.2 Definition of further special terms

Some of the terms used in this chapter have already been defined in section 2.1.3. Those defined here are additional. Where two shoots which differ in generation by one are referred to, the shoot with the lower generation (more proximal)is called the **mother** and the other (more distal) is its **daughter**. Shoots which occupy symmetrically equivalent positions in the topology are referred to as **sisters** (see fig 3.1).

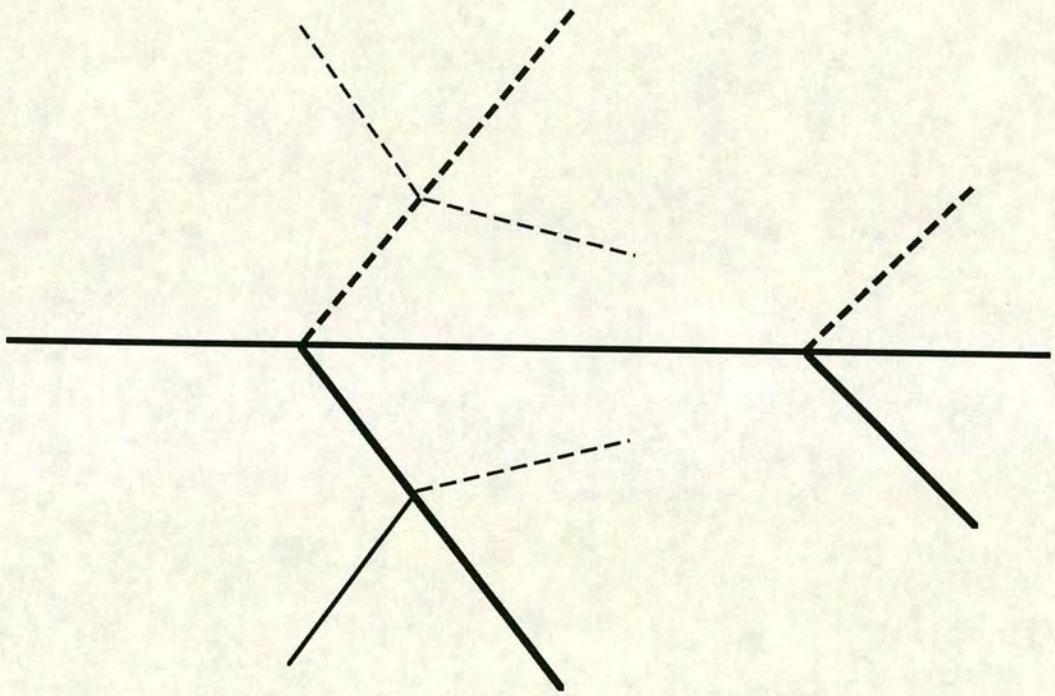

fig 3.1

Shoots shown by dashed lines are sisters of the corresponding shoots shown by solid lines. Only the shoots represented by solid lines are explicitly included in the calculations in the model - the rest are built into the description of the model branches by the application of symmetry rules.

Branch geometry has been described with reference to established botanical characters. The rate of change in length (and diameter) with generation is what is meant by **apical dominance** in this study. The change in link length with Horsefield order is described by an **ageing parameter** because the Horsefield order gives the link's age. The rates of change of length and diameter with rank are termed the rank

length and diameter ratios (c_{lr},c_{dr}) and the generation length and diameter ratios are similarly defined (c_{lg},c_{dg}). The abrupt changes in diameter of shoots at nodes where laterals are attached is called the diameter step (d_j). The mathematical definitions of these terms are explained later in section 3.3.1).

• 3.1.3 The limits of the model

The model is limited in three respects:

1) the degree of detail in representing reality
2) the range of parameter values which can be tolerated
3) the accuracy of the calculations.

It is not possible to run the model with any arbitrary set of input values: most combinations of values would result in failure. This is reasonable, since the majority of possible inputs describe branches which could not be found in nature. However, there are some combinations of values which could represent possible natural branches, but with which the model is unable cope. This is due to a lack of robustness in some of the calculations within the model: a problem which is discussed in section 3.4.3.

The calculations are subject to errors from a variety of sources. The finite precision of computation and number representation in the computer allows small truncation errors. These may become amplified to quite serious proportions in some kinds of iterative calculation, of which there are examples in the model. The calculations are approximate in theory as well as in practice. Many interim values in the model are calculated to within an accuracy threshold and consequently have a (predictable) error associated with them; this is further discussed in section 3.4.3.

• 3.2 Idealisation of the natural form

• 3.2.1 Topological grammar

In this type of study it is first necessary to define the 'grammar' of the branching: that is a set of discrete rules governing the number and directions of branch forming operations. Onto this mathematical construction is built a continuous geometric description using a set of parameters (or characters) which together describe the

whole three dimensional form of the model branch (e.g. thicknesses and lengths of shoots). An example of this kind of grammar is the L-system developed by Lindenmayer [1968] in which shoot axes branch according to simple rules. Although the concept underlying the specification of branch topology in this work is that growth produces increased topological complexity through repeated iteration of form, the specification does not represent growth explicitly. Rather, a set of growth stages are generated each representing the completion of an annual flush of shoot extension, each specifying a particular stage of development which is denoted by the branch order (defined in 2.1.3). This formulation is intended to allow the extension of the model to one in which growth is included explicitly.

3.2.2 Idealised Picea form

The grammatical rules chosen here to model a Sitka spruce-like branch are closely related to the GMT3 model Anno [1984] which is based on the L-system of Lindenmeyer [1968] with monopodial branching (leader does not change direction on branching) [Lindenmeyer, 1982] and ternary ramifications (two laterals only at each branching point), but always branching symmetrically. Such a description is only possible because of the periodic repetition of a unit of morphogenesis [Küppers, 1989] during growth in Sitka spruce. According to the Papentin [1980] method of describing the symmetry of trees the topology of the idealised Sitka spruce form is:

$$3m(ieee) \quad m = 1,2,3... \tag{3.1}$$

where m defines the order of the branch, i represents interior links which end in an other link and e represents exterior ones which end in 'leaves'; this topology was illustrated in fig 2.5. (see also section 2.2.2). From this kind of description, the growth of a branch can be simulated in a very simple way by incrementing m.. The computer program which implements the model generates these forms and labels the links using the arithmetic relations which equation (3.1) implies (see Appendix A2.2).

The geometry has been treated with the same kind of reductionism. Instead of describing each length, angle and diameter individually according to ad hoc

empirical rules, a small number of iterative relations are used to give values to geometric parameters throughout the branch, based on those of the leader.

Shoot lengths are set as follows. First, the length of the leader is given as part of the input parameter list. The leader is broken into m links of length l_1, where m is the branch order. This initial link length is given to the links of all the other shoots in the branch. The ageing parameter is applied to all the shoots such that the length of the ith link in a shoot is modified by the equation

$$l_i = l_1((i\text{-}1)a + 1) \tag{3.2}$$

where a is the ageing parameter.

The lengths of whole shoots are then modified by the rank and generation length ratio parameters c_{lr}, c_{lg} as follows

$$l_s = \sum l_i \, (c_{lr}{}^{r\text{-}1}) \tag{3.3}$$

$i = 1...m$

$$l'_s = l_s \, (c_{lg}{}^{g\text{-}1}) \tag{3.4}$$

where r and g are the shoot rank and generation respectively and the subscript 's' denotes a shoot property.

Calculations of the shoot diameters are made as follows. The mean diameter of the leader d_1 is given in the input parameter list. The diameters of all the other shoots in the branch are initially calculated by

$$d_s' = d_1 \, (r/m) \tag{3.5}$$

and then modified by the rank and generation ratio parameters c_{dr}. c_{dg} by

$$d_s'' = d_s'(c_{dr}{}^{r\text{-}1}) \tag{3.6}$$

and

$$d_s = d_s'' \, (c_{dg}{}^{g\text{-}1}) \tag{3.7}$$

Next the taper factor (t) is applied to add a taper to the shoots. Each shoot is divided along its length into n elements.

The diameter of the most proximal element d_1 is given by

$$d_1 = t\, l_s' \tag{3.8}$$

and that of the most distal is

$$d_n = d_s - (t\, l_s'/2) \tag{3.9}$$

then the *jth* element has the diameter:

$$d_j = d_1 - (j + 1/2)\ \{\ (d_1 - d_j)/\ j\text{-}1\ \}/2 \tag{3.10}$$

Finally, the mean diameters of the links of every shoot are modified to create the steps in diameter at interlateral junctions using the diameter step factor d_j . The diameter of the jth element in the kth link is then given by

$$dj_k' = dj_k\ (1 + d_j.(r\text{-}k)) \tag{3.11}$$

Angles within the branch are always referred to global Cartesian co-ordinates so that the interactions between shoots making up the branch are all calculated using a common co-ordinate system. However, the angles of attachment of laterals are initially specified simply as the angles between their axis and that of their parent shoot. The component of the attachment angle in the horizontal plane is initially set to a single value applying throughout the branch. Distortion of the branch by mechanical loading alters these angles and they become different from one-an-other during the calculation of this distortion. The orthogonal component of lateral attachment angles is treated similarly. The use of global Cartesian co-ordinates necessitates transformations from the local system during the course of calculation.

Local angles ϕ, θ, ψ are transformed to global angles Θ and Φ by the following equations (Morgan, 1990) *

$$\sin \Theta = (\cos \psi \cos \phi \sin \theta) + (\sin \psi \cos \theta) \tag{3.12}$$

* Private comm.

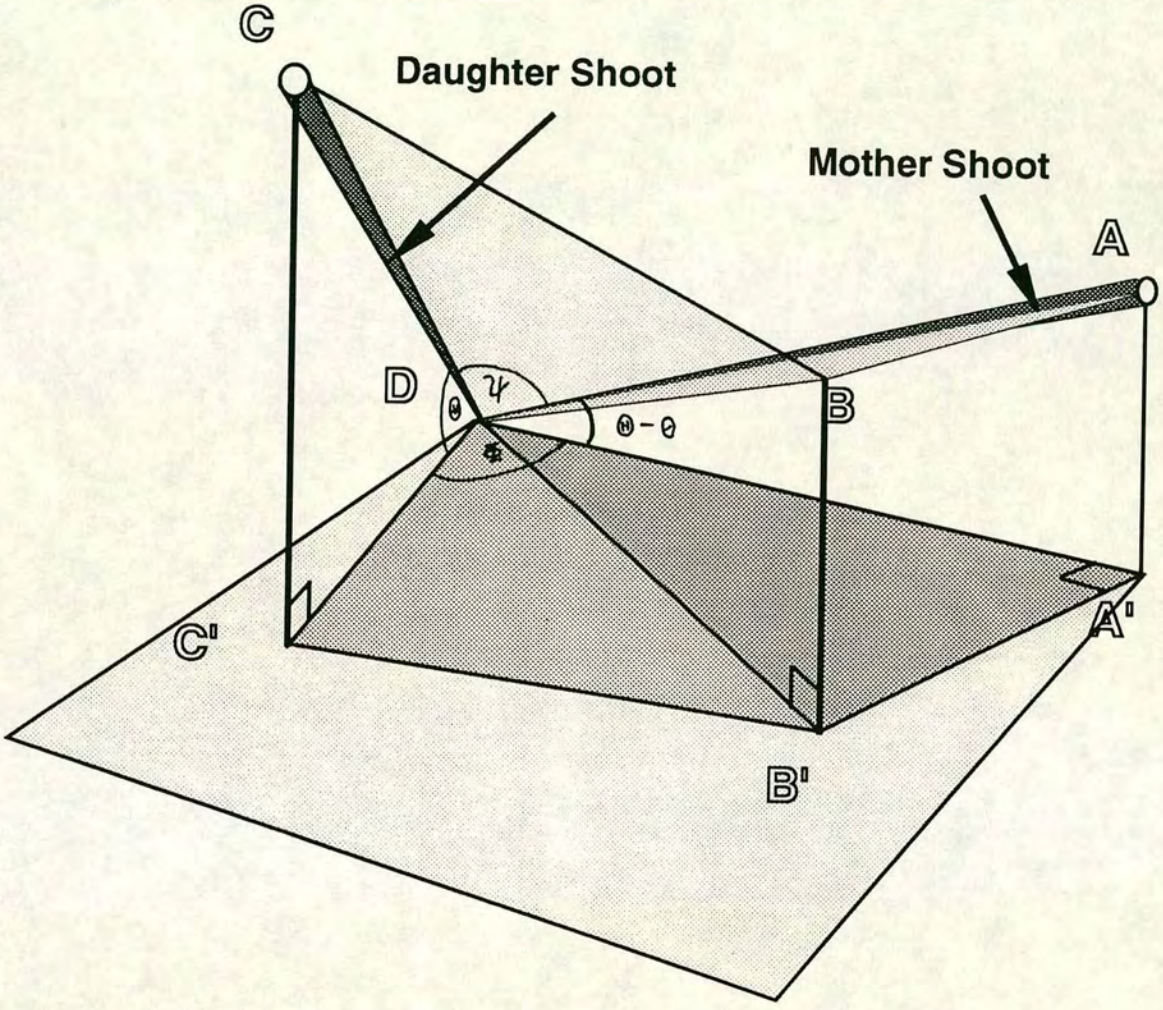

Fig 3.2. Geometry of the transformation of angles between parent and daughter shoots from local to global co-ordinate sets.

note θ is the vertical component of a shoot relative to the parent in local coordinates and φ is the horizontal component of that angle,

$$\tan \Phi = (\cos \psi \sin \theta) / (\cos \psi \cos \theta \cos \Theta - \sin \psi \cos \Theta) \qquad (3.13)$$

These transformations are illustrated in fig 3.2.

The branch has a single value of elasticity and density throughout. These values are taken from Cannell and Morgan (1987) who measured Young's modulus and dry and fresh weights of branch wood and foliage and wood density for Sitka spruce. The foliage parameters used in this model (fresh weight per unit length and foliage area per unit length) are also taken to be constant through the branch, though this is obviously a simplification (see section 4.3.1) and values are again taken from Cannell and Morgan [1987].

Together with the branch topology (section 3.2.3), the above relations define the branch's geometry.

• 3.3 The Branch Form Model

• 3.3.1 The input variables

The model branch can be of any order from 1 (a single shoot) to 5 . All the shoots in the branch start straight (before the action of gravity). Laterals occur in pairs i.e. there is 'decussate' branching only [Küppers, 1989]. There are no inter-lateral shoots Chochrane & Ford [1978]. The angle at which the branch is held can take any value relative to the vertical. The angle of growth of lateral shoots can be varied in both the vertical and the horizontal plane, but all the laterals of any shoot are given the same initial angles. The branch can be of any size; the inter lateral lengths and average shoot diameters are used to define it. Parameters are chosen to represent apical control, ageing (change in length extension with shoot age), differences of shoot dimensions with rank and generation and abrupt changes in shoot diameter at lateral attachments. The taper is linear and can take only one value throughout the branch. Foliage is represented simply as a mass and a projected area per unit length of shoot, but the projected area is a function of illumination angle and shading which is related to position in the tree crown. Stiffness of shoots given by the bending elasticity and density take a single value throughout the branch, this value was taken

from results published in Morgan and Cannell [1987]. The input variables to the model are listed in table 3.1.

TABLE 3.1 The input variables to the model

1) The branch order (m)
2) The modulus of elasticity (E)
3) The length of the first link of the rank 1 shoot (l_1)
4) The average diameter of the first shoot (d_1)
5) The taper factor for all links within the branch (t)
6) The rank length ratio (c_{lr})
7) The generation length ratio (c_{dg})
8) The rank diameter ratio (c_{lr})
9) The generation diameter ratio (c_{dr})
10) The diameter step factor (d_j)
11) The ageing factor (a)
12) The angle of the branch in the vertical plane (θ_0)
13) The relative angles of laterals in the vertical plane (θ_i)
14) The relative angles of laterals in the horizontal plane (ϕ_i)
15) The incidence angle of the second light beam (α)

• 3.3.2 Light interception

The simplest description of light interception is the horizontal projection defined by

$$\Sigma l_s' \, . \, s \tag{3.13}$$

where 's' is a constant representing the foliage silhouette area per unit length of shoot for light projected at normal incidence onto a horizontal plane. The constant is found by multiplying the average needle length by the normal incidence shoot needle fraction which is the average needle-to-gap ratio with a value of approximately 0.7 for Sitka spruce [Norman and Jarvis 1974]. In order to provide a more realistic goal for the branch's growth, a first approximation towards the effect of the presence of other branches in the same tree is made. The region of space over which the horizontally projected area is effective is limited, first by branches which are members of the same whorl so that the lateral extent is defined by an angle Ω in the

horizontal plane equal to $2\pi/j$ if there are j members of the whorl. If a part of the branch grows outside its allotted sector, a 'penalty filter' comes into operation - defined as follows:

$$F_1 = 2^{(\cos \delta)} \tag{3.14}$$

(Ω as defined previously), where $\delta = 10\{ \tan^{-1}(y/x) - \Omega \}$

and $\tan^{-1}(y/x)$ is the azimuth of the shoot element. This function is chosen arbitrarily since there are no known precedents for its modelling. Second, branches overhead cause shading and indeed, if the tree is a part of the crown structure in a stand, then shading from neighbouring trees will be important. Most of the detailed work on this shading has concentrated on the vertical distribution of light intensity [Wang, 1989]. Modelling the light environment on a sub-branch scale has not been dealt with in detail up to now : most work considers more or less random foliage distributions in the crown [Wang, 1989]. The light interception properties of needles and shoots has however been considered in detail [Wang,1990 ; Oker-Blom et al., 1983 ; Norman & Jarvis, 1974 ; Leverenz & Jarvis, 1980] and some of the simpler ideas of those studies, particularly Norman & Jarvis [1974] have been used to represent the shoots here. Fig 3.3 explains why the projected area of a shoot varies with its azimuth relative to that of the shoot held in the horizontal plane (A_p/A).

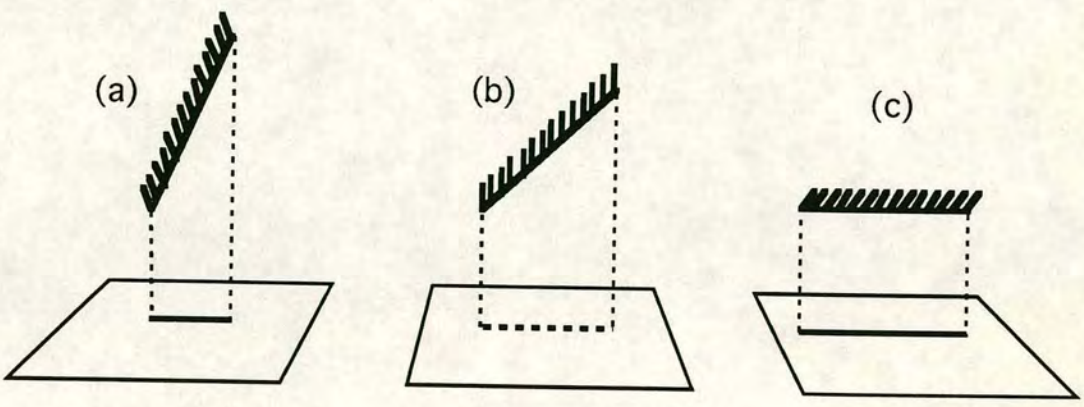

fig 3.3 shoots held at different angles to the vertical show different silhouette areas, but the total foliage sillhouette area also depends on the angle of attachment of the foliage: this is a minimum in example (b).

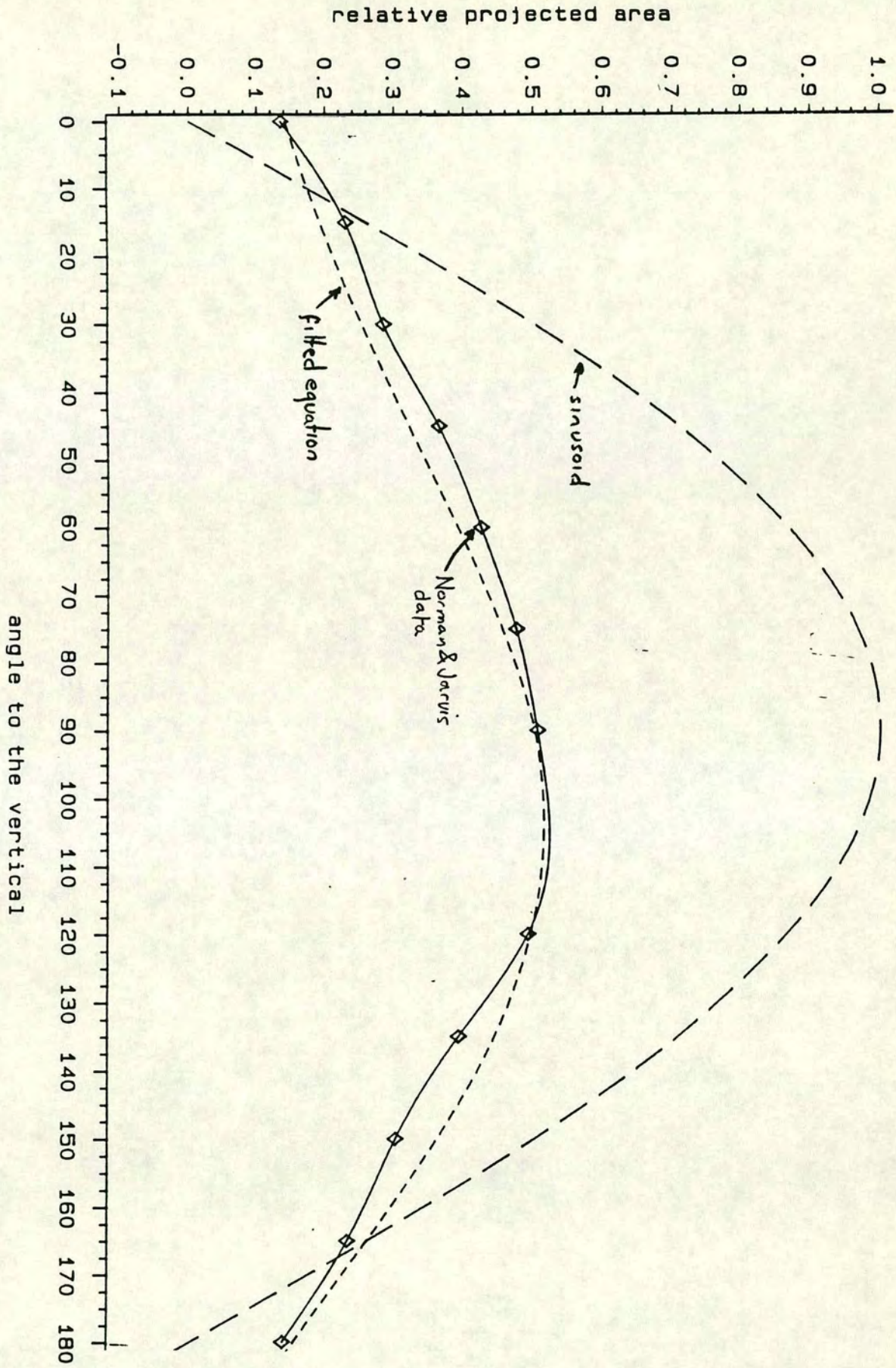

Fig 3.4. Variation of projected area per unit area of foliage (specific leaf area) with light projection angle. Data based on Norman & Jarvis [1975]. Also shown is a simple sinusoidal variation for comparison and the model of the Norman & Jarvis data which is used in the light interception model here.

If the foliage distribution was represented as a band of needles projecting at right angles from the shoot parallel to the horizontal the sine curve would give the variation of projected area relative to the normal incidence case. However because the needles are set at an angle of approximately 30° to the shoot axis, and distributed spirally around the shoot (described by Norman and Jarvis [1974]), the variation of A_p/A follows a more complex function. The data taken from Norman and Jarvis [1974] have been used to empirically model the relation between realised projected area and projection angle by manually fitting an analytic function. This empirical function serves as an approximation in the branch light interception model, it is as follows:

$$F_2 = 0.535 + 0.3b + d.e + f \qquad (3.15)$$

where $b = \sin\{\ \theta - \pi/9 \sin(\theta)\ \}$

$d = 0.1 \sin\{\ 3/2\theta - \pi/3.5\ \}$

$e = 0.85 - \{\ |\ \theta - \pi/2\ |\ /\ \pi/2\ \}$

$f = -0.4 \sin\{\ \theta/3 + \pi/3\ \}$

where the angle between the shoot and the vertical is θ. This function, together with Norman and Jarvis's data and the sine curve are shown in fig 3.4.

The vertical distribution of light intensity in the crown is important and likely to play a role in determining the value of height gain for branches. The model, *Maestro* [Wang and Jarvis 1989] uses beta- functions to represent within crown light distributions, but these cover a large distance of crown compared to the scale studied here, where a simple linear variation is used:

$$F_3 = 0.2\ \{\ y + (5 - m/2)\ \} \qquad (3.16)$$

in which m is the order of the branch and y is the vertical position of a branch element relative to its base in a 5m high tree. Finally the horizontal distribution of

light (also given as a beta- function in Maestro) is described here by a function in two parts. If the shoot length l_s extends beyond a limit ζ in space where

$$\zeta = l_1\{ m/(m\text{-}1)\} \tag{3.17}$$

where l_1 is the length of the leader shoot of the branch and m is the order of the branch, the shoot is considered to be in daylight, so

$$F_4 = 1.0 \quad \text{if} \quad l_s > \zeta \tag{3.18}$$

If a shoot element is at a radial distance (r) less than ζ, an exponential shading function is used:

$$F_4 = 2 - 2(\zeta\text{-}r)/\zeta \quad \text{if} \quad l_s \leq \zeta \tag{3.19}$$

which has the values F_4=0 at r=0 and F_4=1 at r=ζ. This is a crude representation of horizontal shading which increases with horizontal depth in the crown.

Finally, account has to be taken of the angular distribution of daylight available to the tree. This is a function of the distribution above the atmosphere which is a matter of astronomical geometry and of scattering by the atmosphere in both clear sky and overcast conditions. Typically, the mix of direct to overcast light components in Scotland is in a ratio of about 1:1 in which case the beam fraction is 1/2. For overcast sky the standard overcast sky function [Steven and Unsworth 1980] (eqn 3.20) was used to represent the light conditions above the canopy

$$I_d = (1 + 1.23 \cos(\theta)) / 2.23 \tag{3.20}$$

where θ is the azimuth

It is clear that relying on a simple horizontal projection to describe the light regime could lead to very misleading results. As a compromise between model fidelity and complexity, light has been taken in two representative beams: from vertically above and from an angle of 45° and projected areas are taken as the average with respect to the two beam angles. Axial symmetry is assumed and the effect of varying azimuth between the shoot axes and solar beams has been ignored. It would be a simple matter to extend this model to a weighted sum of light beams from all possible solar zenith angles.

- 3.3.3 Distortion analysis

The computer simulation regards the shoots of the branch as a system of connected cantilever beams. They are allowed to distort in response to gravity (loading by self weight). Dynamic forces including wind-load are not considered here, although the wind loading has been estimated to be an order of magnitude greater and in random directions of action (see section 4.2.1). The bending stiffness of Sitka spruce shoots as measured by Morgan and Cannell [1987] has been used in the distortion calculations. No account has been taken of torsional stress or strain (but the branches are assumed to be axi-symmetric).

For each shoot (cantilever), the deflection profile is calculated using a transport matrix technique in which the length of the shoot is divided into small elements and forces are balanced at each end of each contiguous element, whilst the deflection gradually accrues. This method correctly predicts deflections even when they are large enough for the elementary theory to fail and is very flexible in allowing point loads and changes in cross section to be incorporated [Morgan & Cannell, 1987].

The calculation of distortion can be considered as a function operating on a shoot with the geometric description of the shoot, including its angle relative to gravity, as the input (independent variable). The outputs of the function (dependent variables) are the deflection profile (the new geometry) and the bending moment at the base of the shoot which would be required to hold it in equilibrium at the angle specified. This bending moment is used as an input parameter for the function when the shoot's parent is analysed. The shoot, thus evaluated, may be a lateral extension (daughter shoot) of a parent shoot and as such, it exerts a point load and point moment on the parent. When the deflection profile of the parent is calculated, these point loads are taken into account.

Clearly, the new geometry of a shoot depends on the point loads and moments which are applied by its laterals and so, therefore, do the angles at which these laterals are held. However, the geometry of the laterals depends on these angles and in turn, the point bending moments applied to the parent are again modified.

In this way, there is then, a mutual dependence relationship between the deflection of laterals and the deflection of the parent, via the angle of attachment. As a result, some sort of iterative scheme of successive recalculation of the deflections involving multiple use of the bending function is necessary.

In the case of order 2 branching, this is not really a problem, because a solution is found simply by recalculating iteratively, after about four cycles. However, for 3, 4, or general order branching, the mutual dependency will 'ripple through' the structure and the number of iterations will escalate very rapidly, incurring considerable cost in computation time and potentially magnifying rounding errors.

An efficient strategy to control the flow of calculations has been developed which relies on breaking the problem into a series of order 2 problems, each with only one pair of shoots involved - the mother and one daughter. It is a relatively simple matter to find a solution to the mutual dependence in bending response between these two shoots. This is a calculation which applies generally throughout the structure, so can be made self contained. Thus the operation which finds an equilibrium between a mother and a daughter is repeatedly called upon in the analysis of a whole branch. A set of rules (which is different for each branch order) is required to select for this analysis the shoot pairs in the correct order. These rules are generated by the program as part of the initialisation procedures. The rules also include instructions controlling loop-back decisions made during the analysis of a whole branch. All this is described in detail in Appendix 2.

- ### 3.3.4 Objective functions and model output

The output of the model is a set of function predictions each of which is defined in the space made up of driving variables (model input) and parameters (values which are fixed in the model): the functions which the model output predicts are the objective functions described in section 1.1.3.

The model is designed to be flexible and can be used in a number of different ways : as a stand alone, interactive design investigation tool, as part of a surface plotting investigation of branch characteristics or as part of a design optimisation or dynamic growth program. The concept is modular and different tasks will require different kinds of results (output), so a number of options are available from option specifiers passed to the main program. It is possible to plot the shape of the distorted branch in

3 orthogonal projections and to plot the initial and distorted shapes of any individual shoot together, or their difference. The diameter-with-length variation can also be shown for any shoot within a branch and all the vertical displacements of shoot tips resulting from gravitational distortion can be made available as output. Each branch design is characterised by a vector describing properties of interest to optimising geometric design: the branch characters. These characters are listed in table 3.2

Table 3.2 Output - Branch Characters :

1) The total mass of the branch including foliage (W_B).

2) The mass of all the branch's foliage with surface water (W_{fB}).

3) The efficiency of the branch defined as the total foliage mass divided by the total mass of branch wood used to support it. (η_m)

4) The bending moment needed to keep the branch at a specified angle. (M)

5) The sum of vertical displacements of shoot tips from their original positions (Σ_{dfl}).

6) The distortion factor defined as the difference between total length of shoots projected onto a horizontal plane before and after the action of gravity (Δ).

7) The sum of total area of foliage projected onto horizontal and 45° planes. (A_p).

8) The total area of foliage projected onto horizontal and 45° planes, which is weighted by shading functions (A_p).

9) The efficiency defined by the total projected area (7) and also the shaded area (8) divided the total mass (1) (η_a).

10) The efficiency defined by the foliage fresh weight divided by the branch wood fresh weight (η_{fw})

- 3.3.5 Description of the computer program

A FORTRAN 77 computer program has been written to run under VAX VMS to perform the numerical simulation of branch behaviour under gravity. The results from the modelling are presented using the UNIRAS computer graphics package. The program consists of three distinct phases :

1) setting up the morphological description of the branch (initial conditions).

2) simulating the distortion under gravity.

3) reconstructing the branch and evaluating its distorted form and its light interception properties.

The overall structure of the program is shown in fig 3.5. The model takes 15 input values and returns 6 single value results, the set of tip shoot deflections and the Cartesian co-ordinates which define the shape of the entire branch in three dimensional space, which is plotted in three orthogonal projections using UNIRAS procedures.

Fig 3.6 shows the program flow during the initialisation phase. In addition to building the topology and geometry of the branch, given its order, this part of the program builds a set of rules for feed-back loops. These loops are used in the simulation to structure the iteration at the shoot interaction level. This structure is called the FOD sequence, meaning fixed order differencing, since decisions made within its loops are based on difference calculations of test parameters.

The total mass of the branch and the diameters and lengths of shoots are evaluated in the initialisation phase. In addition, a representation of the completed branch before bending is built up in Cartesian space (for reference in later calculations). A more detailed description of the initialisation phase is provided in Appendix A2. (Note that information flowing into the procedures SETUP2, SPECIES, sequence generator and WEIGHT sum fills arrays providing data used in the simulation and evaluation phases of the program).

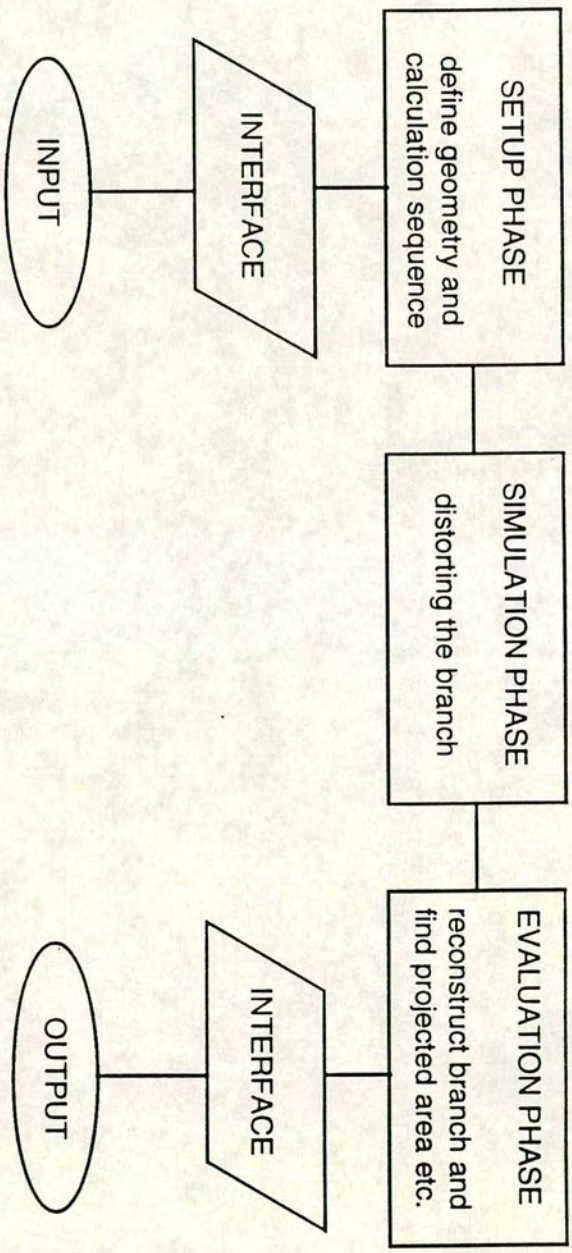

Fig 3.5. Flow diagram of the overall structure of the branch efficiency model.

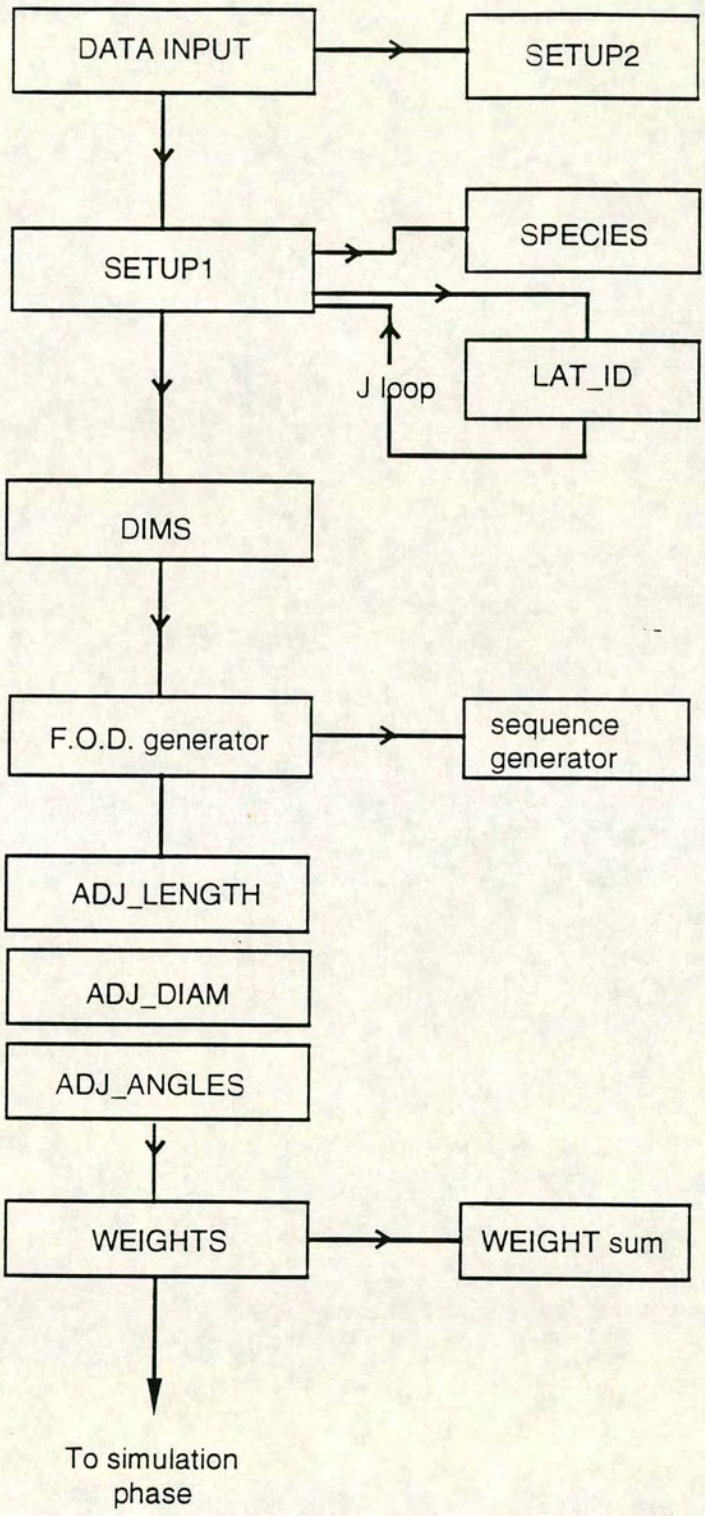

Fig 3.6. Flow diagram of the initialisation phase of the branch efficiency model. (Note SETUP2, SPECIES, etc fill arrays with data for later processing)

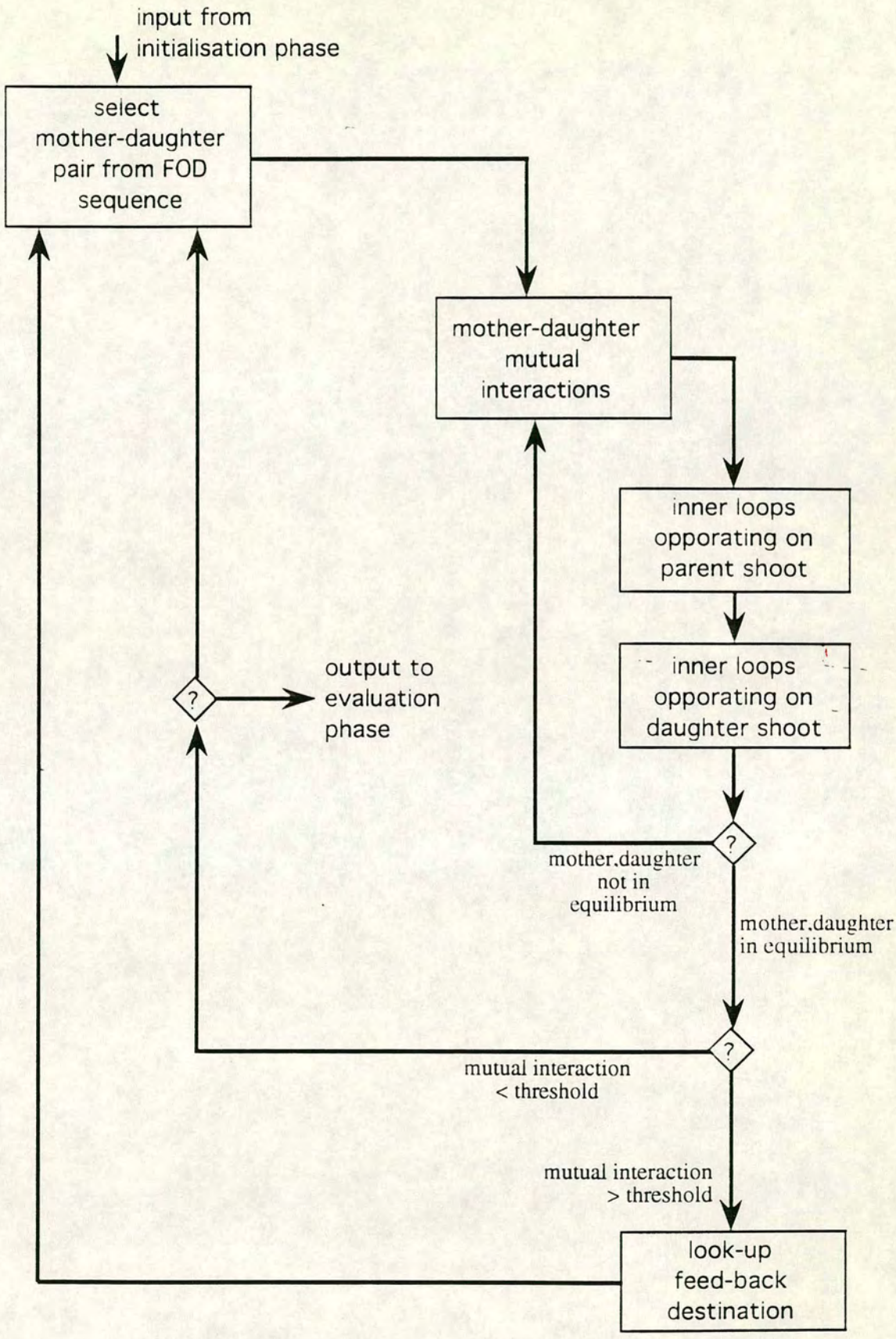

fig 3.7 Flow diagram of the outer loops of the simulation phase, showing FOD sequence feedback loop.

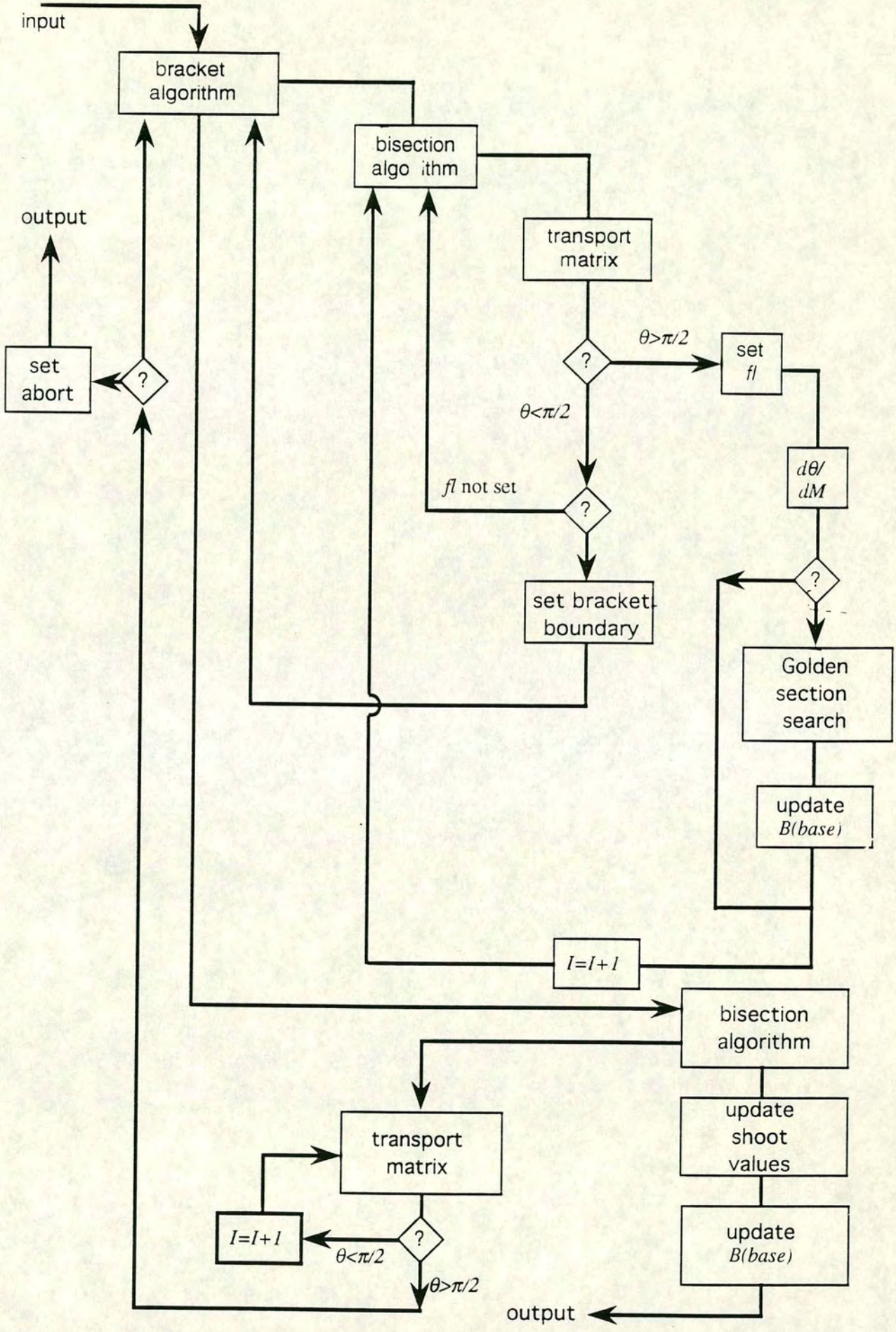

Fig 3.8. Flow diagram of the inner loops of the simulation phase of the branch efficiency model.

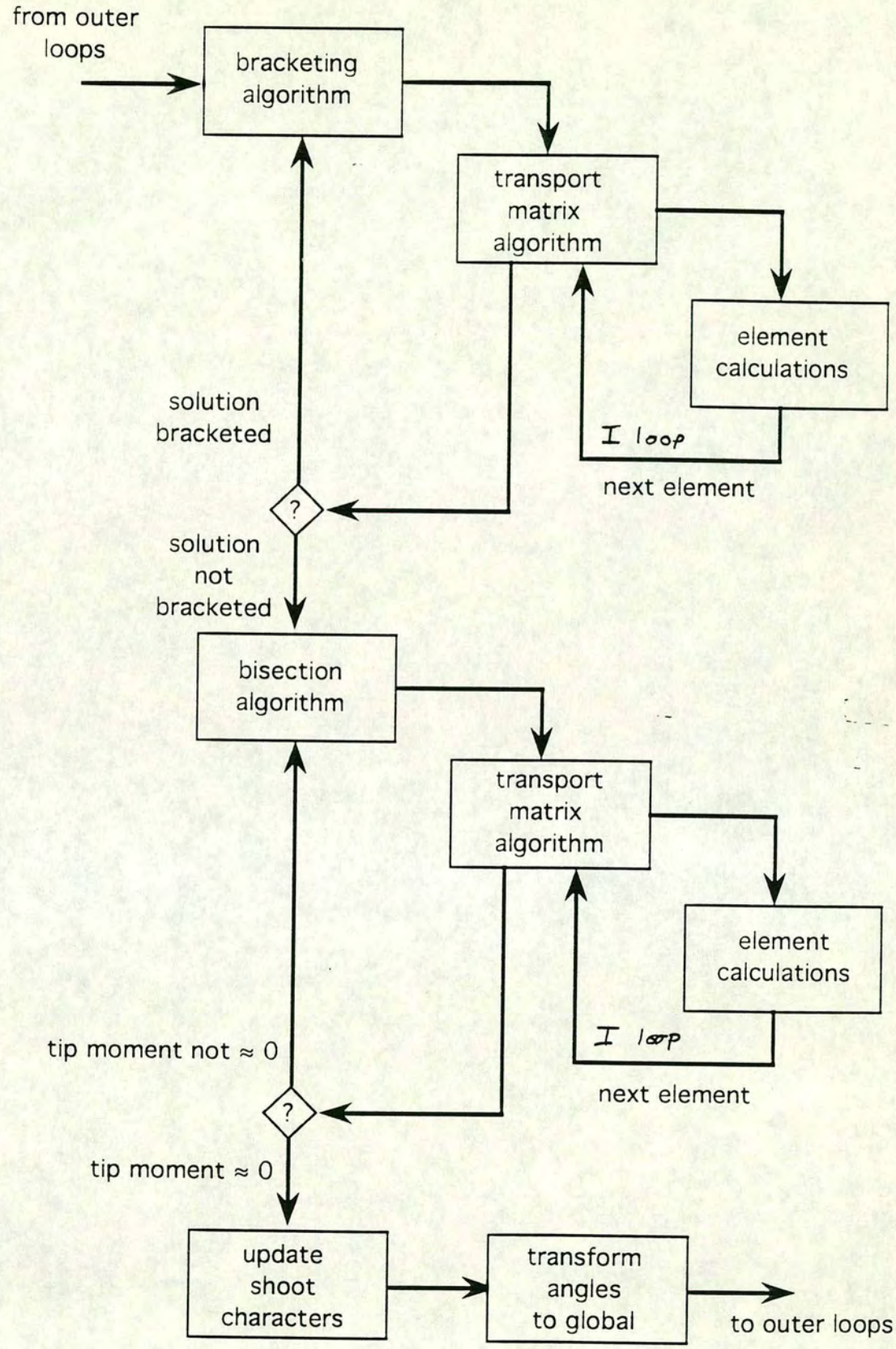

Fig 3.9. Simplified flow diagram of the whole simulation phase of the branch efficiency model.

Figs 3.7 and 3.8 show the program flow during the simulation phase (inner and outer loops). The inner loops are complicated by various measures which were taken to try to ensure successful termination of the calculation within the subroutine STEM2 which finds an equilibrium distortion for a single shoot. The program flow shown in fig 3.9 which is a simplified version of that in fig 3.8 will be described here and the action of the more complex realisation of the algorithm will be discussed later in section 3.4.3.

To make effective use of space and economise computation time and complexity, the branches are generally treated as a number of individual shoots each of which is representative of a set of 'sister' shoots (see fig. 3.1) which can at any time be constructed using geometric reflection operations in Cartesian space (i.e. sister shoots are identical and represented by one shoot only in the calculations).

The branch's shoots are divided into a number of contiguous elements for calculation of shoot distortion by a transport matrix method [Morgan and Cannell, 1987] .In this implementation of their method the number of elements depends on the shoot's rank in a way which ensures adequate spatial resolution without excessive computation costs. The transport calculation is carried out in the I loop shown in fig 3.9. This inner-most loop runs the transport matrix down a shoot from the proximal to distal end, evaluating the transport relations one element at a time. The elements are related to one-an-other by input output relations which maintain mechanical equilibrium between adjacent elements. At each end of the element, distortion angle θ, deflection δ, shear force F and turning moment B are matched. A much fuller description of this calculation process and the computer program used to implement it is given in Appendix 2.

The residual moment on the last element B_{tip} is passed back as a calculation result to the next higher shell of calculation following the completion of the transport matrix calculation. Here, a bisection algorithm [Press et. al. 1988] and its associated bracketing algorithm solve an equation in B_{tip}. This process attempts to find the shoot input moment B_{in} (B_{in} is the moment applied to the shoot's parent to hold it in position) which results in B_{tip} being zero (within a pre-determined accuracy range). When B_{in} is found such that $B_{tip}=0$, the shoot is in mechanical equilibrium. When this has been achieved, each element making up the shoot will be in equilibrium with its neighbours because all the forces and moments will have been balanced by the distortion of the shoot.

Once the equilibrium distortion of a shoot has been found by this algorithm, its new shape, bending moment and insertion angle are passed up to the next higher nested level in the program (fig 3.7). Here the shoot is united with its parent (mother). In the loop at this level (*k* loop), the calculation of shoot distortion is repeated for the mother and daughter shoots alternately until the effects of one's distortion on that of the other diminishes to below a pre-determined threshold value. When this stage has been completed, the mutual effects of these two shoots in the branch will have been predicted. Mutual effects are explained by fig 3.11.

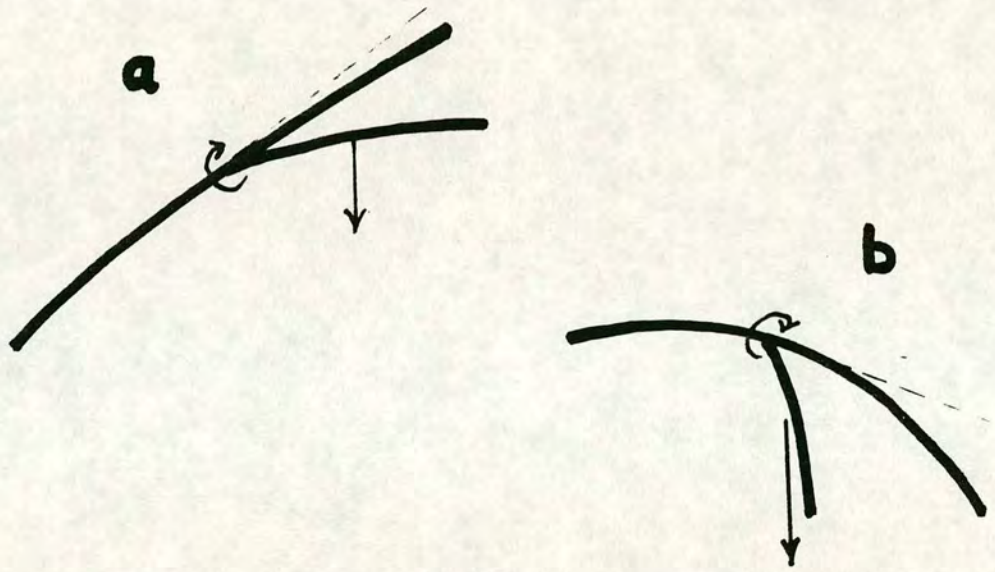

fig 3.11 The angle of attachment of the daughter shoot determines the bending moment that it exerts on its parent. This in turn affects the angle of attachment so that there is a mutual effect between the parent and daughter shoots. In example (a), the parent is bent little so that the laterals are projected out further and therefore exert a larger bending moment than in example (b) where the parent is bent more.

However for branch orders greater than 2, there are further mutual interactions: between pairs of shoots. These effects are dealt with in the top level loop of the simulation phase (the *J* loop). This loop is constructed as a set of feedback rules which cause the recalculation of mother-daughter pair interactions. The criteria for feedback are based on an assessment of the predicted effect of the most recently evaluated shoot pair on all the others. The *J* loop implements the *FOD* sequence

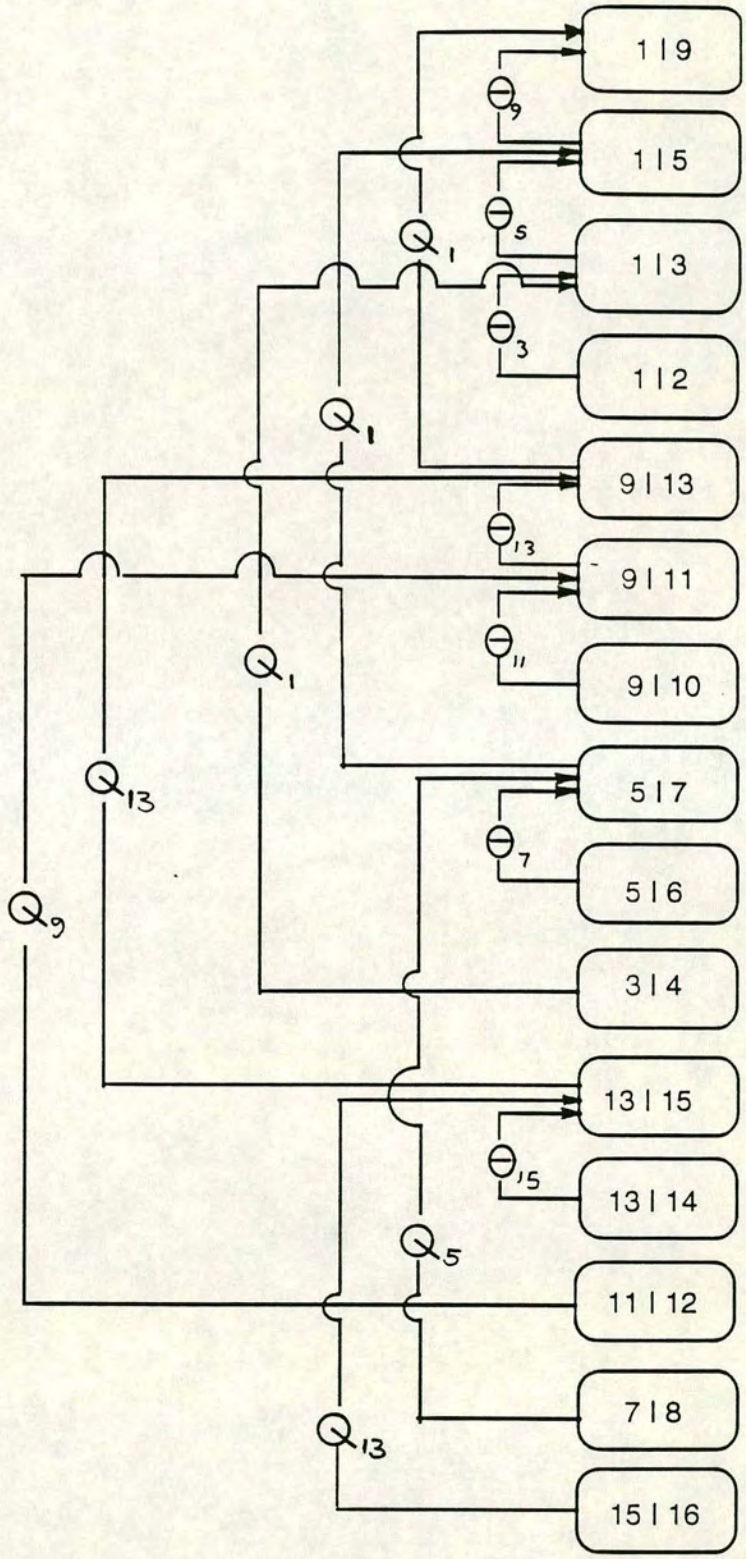

Fig 3.12. The Fixed Order and Difference sequence (FOD) showing the sequence in which shoot pairs are taken through the simulation phase and the feedback rules to be applied for an order 5 branch.

established during the set-up phase. An example of an *FOD* sequence (for order 5 branches) is given in fig 3.12. If the feedback looping is too slow to converge, the tolerance of the calculations is increased steadily by slackening the rules for feedback. Eventually, all the shoots will have been allowed to interact in an ordered way such that the branch system has attained an internal equilibrium (within the set tolerance). At this point the description of the distorted branch is complete and the new geometry is passed on for evaluation.

Fig 3.13 shows the program flow during the evaluation phase. The calculations so far have made use of the symmetry of the defined topology and so have only described a subset of the total number of shoots in the branch. The entire branch is now re-constructed in three dimensional Cartesian space by a series of geometric operations. The whole branch is subjected to a specified light regime and the total light interception capability of the branch given its light regime is calculated using the shading functions described in section 3.3.2. Summary results giving the total degree of distortion, the total light interception and branch efficiency measures are then calculated and passed out as model results.

• 3.4 Modelling results

• 3.4.1 Validation of the model

Variability in natural branches and the fact that it is not possible to hold 12 parameters constant and vary a 13th as a controlled experiment cause problems for model validation. This could be overcome by the use of plastic physical models [Morgan and Cannell, 1987] designed to vary certain parameters at a time in isolation, but this would be completely impractical because of the number of models needed and their complexity. An other problem is encountered with natural branches because of the variability of their geometry from link to link. Where the model branches relate link dimensions through simple geometric rules (e.g. link length declining by a constant proportion with rank), natural branches may have random variations in link dimensions which are greater than the differences required by the geometric rules. Finally, the measurements of tip deflection (distortion of shoots) have small values compared to the statistical noise. As a result, statistical similarity between model results and those measured from natural branches can be found without there being a genuine correspondence between the assumptions of the model

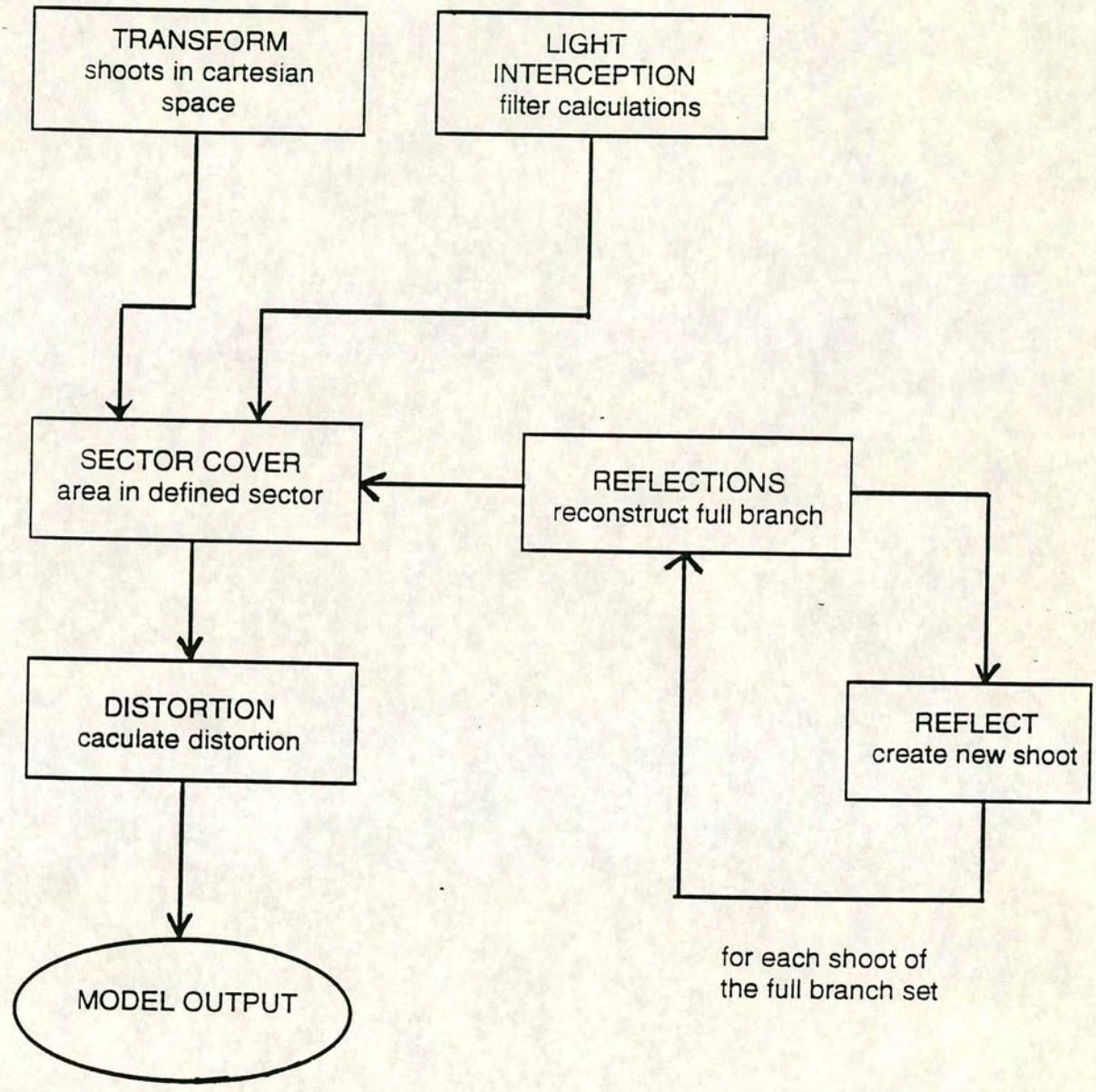

Fig 3.13. Flow diagram of the evaluation phase of the branch efficiency model.

and the real influences which give rise to the natural branch forms. Thus, validation of a model (particularly one with a large multi-dimensional state space) against data subject to large statistical variation should not be taken as complete or convincing, merely supportive. It has often been noted (e.g. Jeffers, 1988) that it is not possible to fully validate a mathematical model and that it should always remain under critical assessment. This is particularly the case when the model describes a function of many variables, as here.

Firstly a visual check of predicted branch shapes was carried out by graphing the positions of elements in three orthogonal projections: x-y, y-z and x-z, following distortion modelling. Fig 3.14 shows the result of distortion calculations on the shape of an order 4 branch - only the set of unique shoots are shown for clarity (the sister shoots could otherwise be included, but are identical and symmetrically positioned with respect to the representative set shown). The y-z projection shows the branch 'head on' looking towards the base of the leader. This in combination with the x-z projection (the side view) shows the complexity of relations among shoot angles and distortion in three dimensional space. Fig 3.15 shows the distortion of two order 2 branches differing in shoot taper factor - effectively the less tapered branch has dropped to near horizontal under the excess weight of distal elements, while the more tapered branch shows more distal distortion. Fig 3.16 shows an order 3 branch held at two different angles to demonstrate the effect of whole branch vertical angle on the angle of attachment of laterals after distortion (due to changes in bending moments). In the last example, fig 3.17 shows two branches with different rank length and diameter ratios (c_{lr} and c_{dr}) . From visual inspection of various model branches, it appears that the model may be valid. (Unless shoots are specified at too small a stiffness, in which case distortion errors compound and the model soon fails due to a cumulative error which affects branching angles and shoot distortions. This failure of the model is discussed at length in section 3.4.3.)

The 96 branches of orders 1 to 4 which were taken from the field were simulated by modelling and their relative shoot tip deflections were predicted by the model. These predictions were compared statistically using the paired-difference t-test which assumes that both populations are sampled from normal distributions. The two distributions are shown in fig. 3.18. Table 3.3 shows the results of comparing field measured and simulated branch relative deflections.

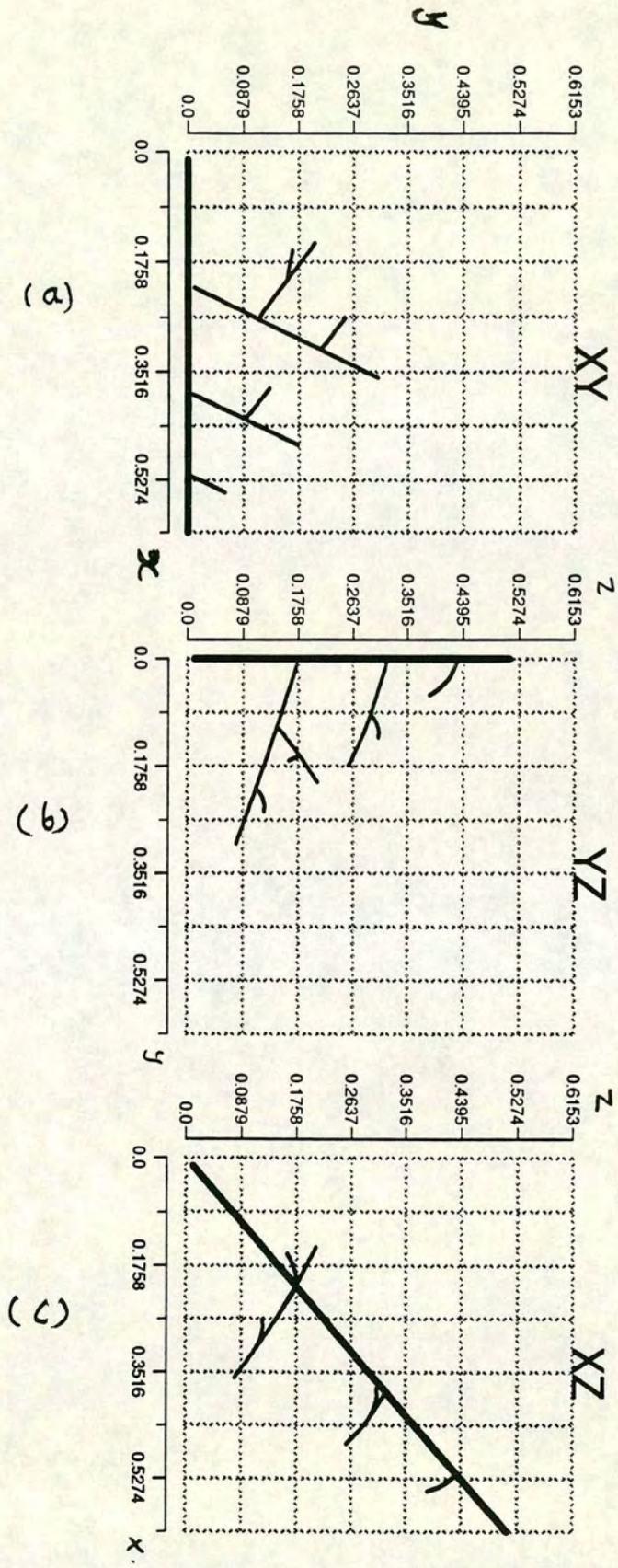

Fig 3.14. An example of an order 4 branch after calculation of distortion. Only a representative set of shoots are shown for clarity. The three dimensional branch is shown in three orthogonal projections: plan, end-on and side-view.

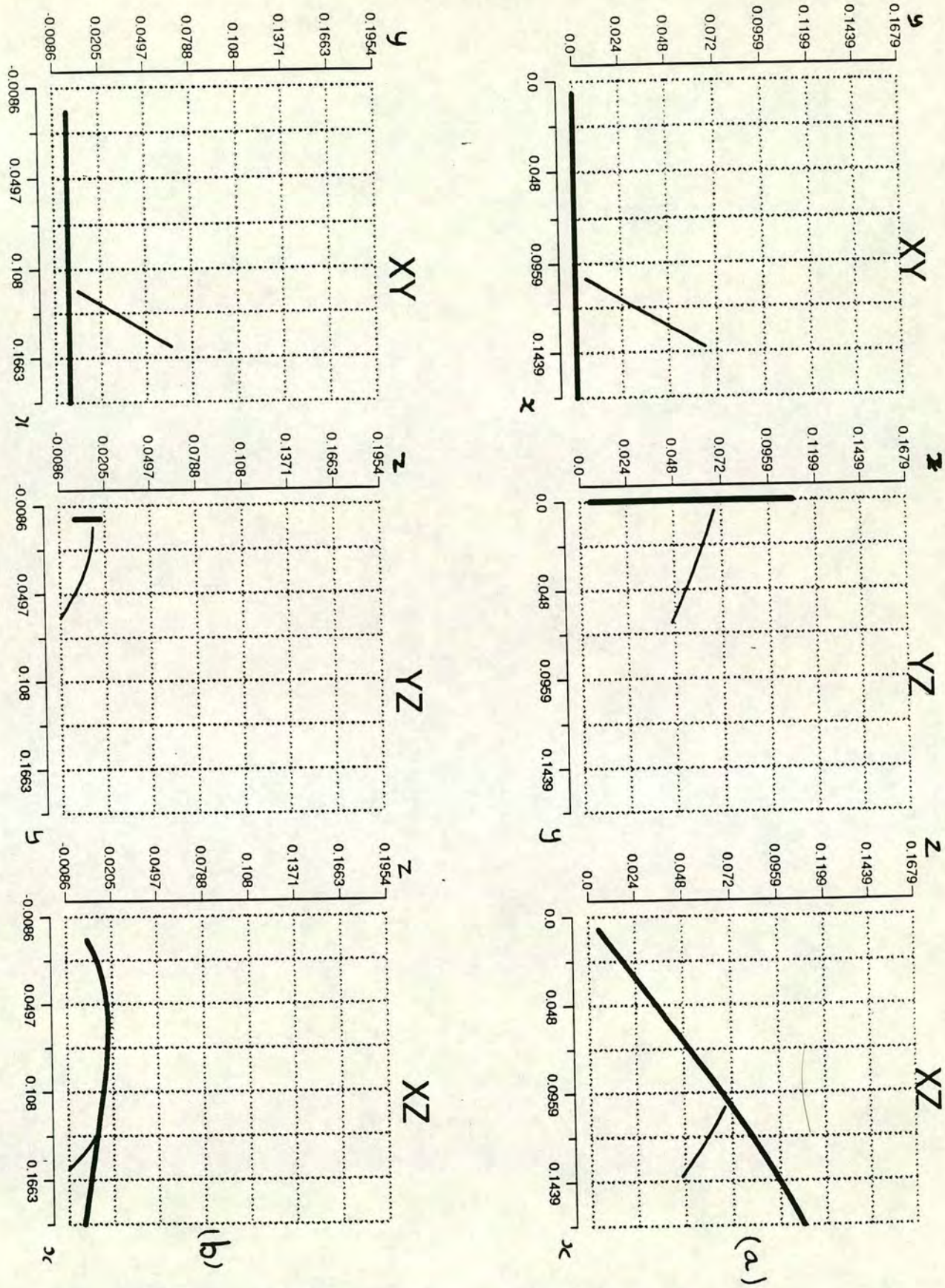

Fig 3.15. Example showing the effect of taper factor on the distorted shape of an order 2 branch. In (a) the taper (d/l) is 0.005, whilst in (b) it is 0.003. The smaller taper in (b) results in an excess of distal weight increasing the distortion of the branch.

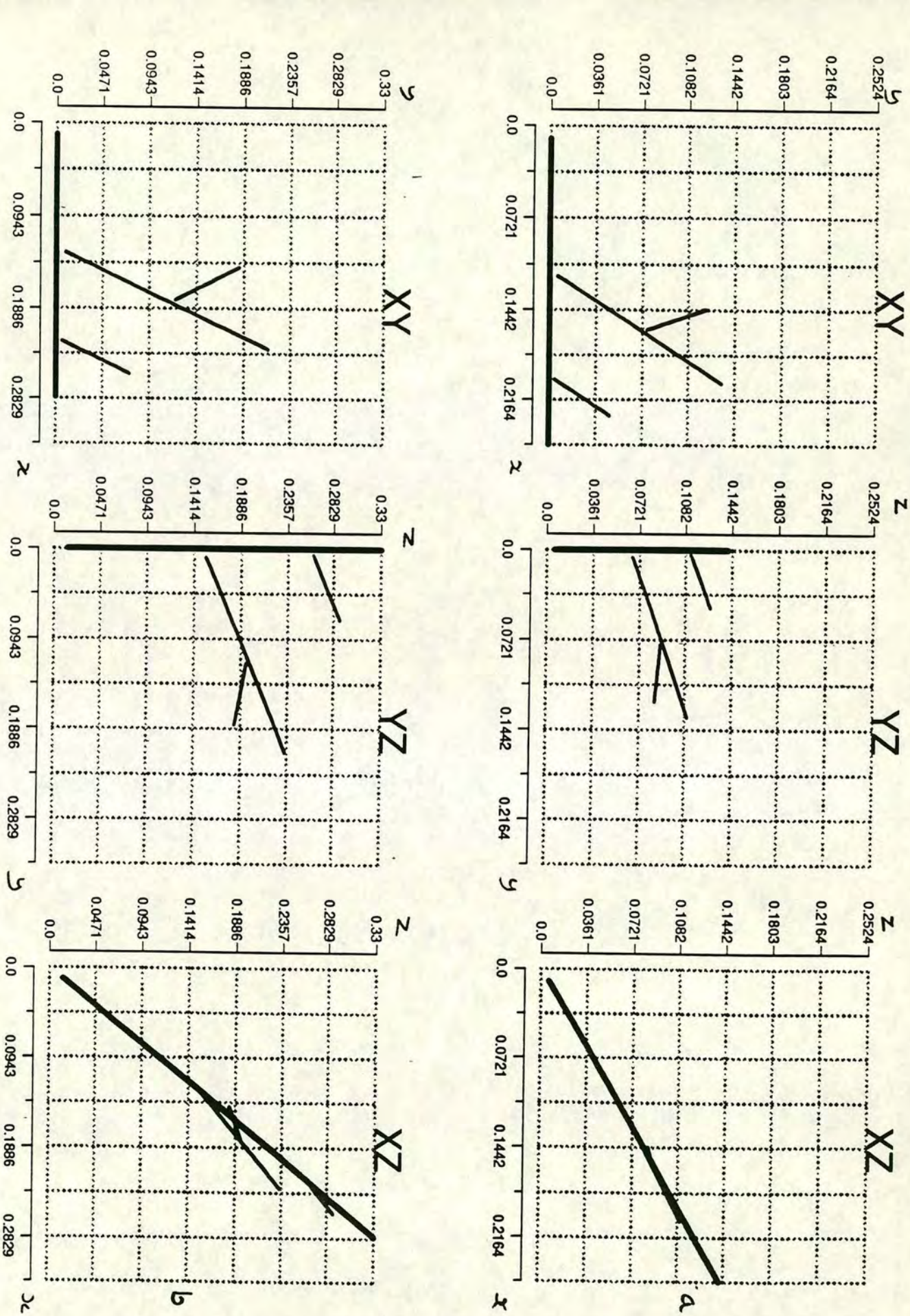

Fig 3.16. Example of an order 3 branch held at a vertical angle of 30° (a) and 50° (b) to show the effect whole branch angle has on the angles of laterals via changes in moment which is difficult to predict intuatively).

Fig 3.17. Example showing he effect of varying rank length and diameter ratios in an order 2 branch. In (a), the rank length ratio is 0.8 and the rank diameter ratio is 1.0. In (b) the ratios are 1.0 and 0.8 respectively (i.e. reversed). The parent shoot is thinner relative to its lateral in (b) and the weight of the lateral distorts the parent much more than when in (a) the lateral is relatively long, but thin.

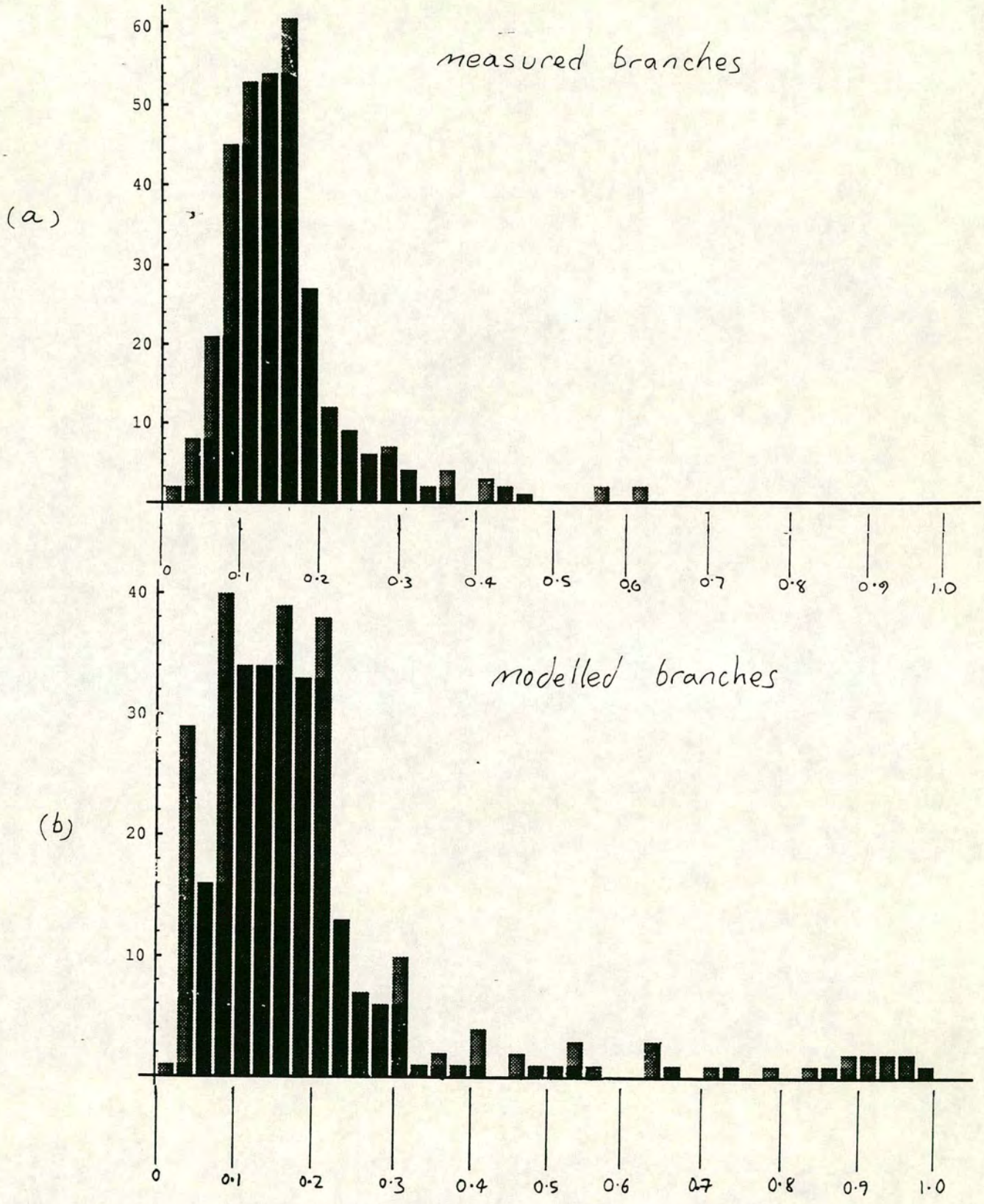

Fig 3.18. Statisical distribution of shoot tip deflecions (a) among measured branches and (b) among modelled branches. Small frequencies of high tip deflections in the modelled branches relate to the failure of the model.

Table 3.3 Comparison of deflection per unit length in field measured and simulated branches, broken down into individual shoot type categories. There were 24 cases for each shoot type. Model predictions differ significantly from field data at the 5% level when P<0.005. (P is the standard symbol for confidence intervals).

shoot	field mean	model mean	field sd	model sd	t test	P
1.1	0.084	0.069	0.038	0.040	0.68	0.510
2.1	0.135	0.178	0.061	0.041	2.35	0.030
2.2	0.105	0.061	0.061	0.048	3.68	0.0009
3.1	0.133	0.132	0.055	0.036	0.10	0.920
3.2	0.116	0.196	0.067	0.093	3.77	0.0006
3.4	0.125	0.153	0.059	0.044	2.13	0.038
3.6	0.214	0.713	0.042	0.095	4.47	0.012
4.1	0.160	0.143	0.076	0.035	0.80	0.430
4.2	0.171	0.115	0.124	0.130	2.47	0.019
4.4	0.148	0.110	0.069	0.045	1.95	0.063
4.6	0.168	0.063	0.092	0.150	3.00	0.005
4.8	0.231	0.234	0.256	0.475	0.55	0.960
4.16	0.305	0.261	0.508	0.909	0.39	0.770

Means of field measured and model predicted relative deflections were significantly different among shoot types : 2.2, 3.2 and 4.6. In 2.2 and 4.2, the model underestimated relative deflection and in 3.2 it was overestimated. It is very difficult to explain this kind of non-systematic deviation. The estimates of relative deflection variance (described by standard deviation) give more insight into the validity of the model predictions. For shoot types 3.6, 4.6, 4.8 and 4.16, the standard deviation of model predictions was much greater than that of the field measured data. These shoot types have the highest recorded mean relative deflections and certain individuals within the model prediction population have very large deflections (for example shoot type 6 in two order 3 branches had a predicted relative deflection greater than 1.0, whilst the measured values for these shoots were 0.242.) In the case of other shoots, the standard deviation of predicted relative deflections is more frequently similar or less than that of the field measured data. It is concluded from

the standard deviations that where relative deflections are expected to be large, the model increasingly overestimates them, eventually leading to a break down in prediction (perhaps due to a failure of the calculation within the model). There is not a particularly strong relationship between the field measured relative deflections and their model predictions. Most of the deviations from measured results are non-systematic and it is suggested that they can be attributed to the differences in link characters (length, diameter, elasticity etc.) among links of real branches, which are not allowed for in their model counterparts. The fact that standard deviations of model results were less than measured results for most shoot types supports such an assertion.

Because no measurements were made of light interception by the branches collected in the field, validation of the predictions of light interception made by the model are not possible here. This further precludes any validation of predictions of branch efficiency made by the model, since that involves the estimation of light interception. Measurements of light interception, or at least branch silhouette areas are clearly needed before any real confidence can be put into the predictions of the model.

• 3.4.2 Sensitivity testing

The relative importance of the different input parameters in determining the values of the output is assessed by sensitivity testing.

The sensitivity of any measure of branch performance to a single character, or variate, is itself a function of the other characters and will vary throughout the function space. In order to take this into account in a reliable prediction of function sensitivity, a statistical method was used.
Techniques for analysing sensitivities of multivariate models are described by Elston [1992] who lists them in order of increasing reliability (and, by implication complexity). In order to reveal the cross term effects (variation of a variable's sensitivity with changes in other variables), a technique which perturbs all the driving variables simultaneously has been followed in this work. The analysis was further improved by making the magnitudes of perturbations for each variable proportional to their likelihood as Elston [1992] suggested, so that the multivariate perturbation is unbiased.

Fig 3.19. Projections through the 15-dimensional multivariate sensitivity test results in the five most significant variate directions. Each projection gives an indication of the proportion of total variation in model outomes due to changes in the variate direction shown.

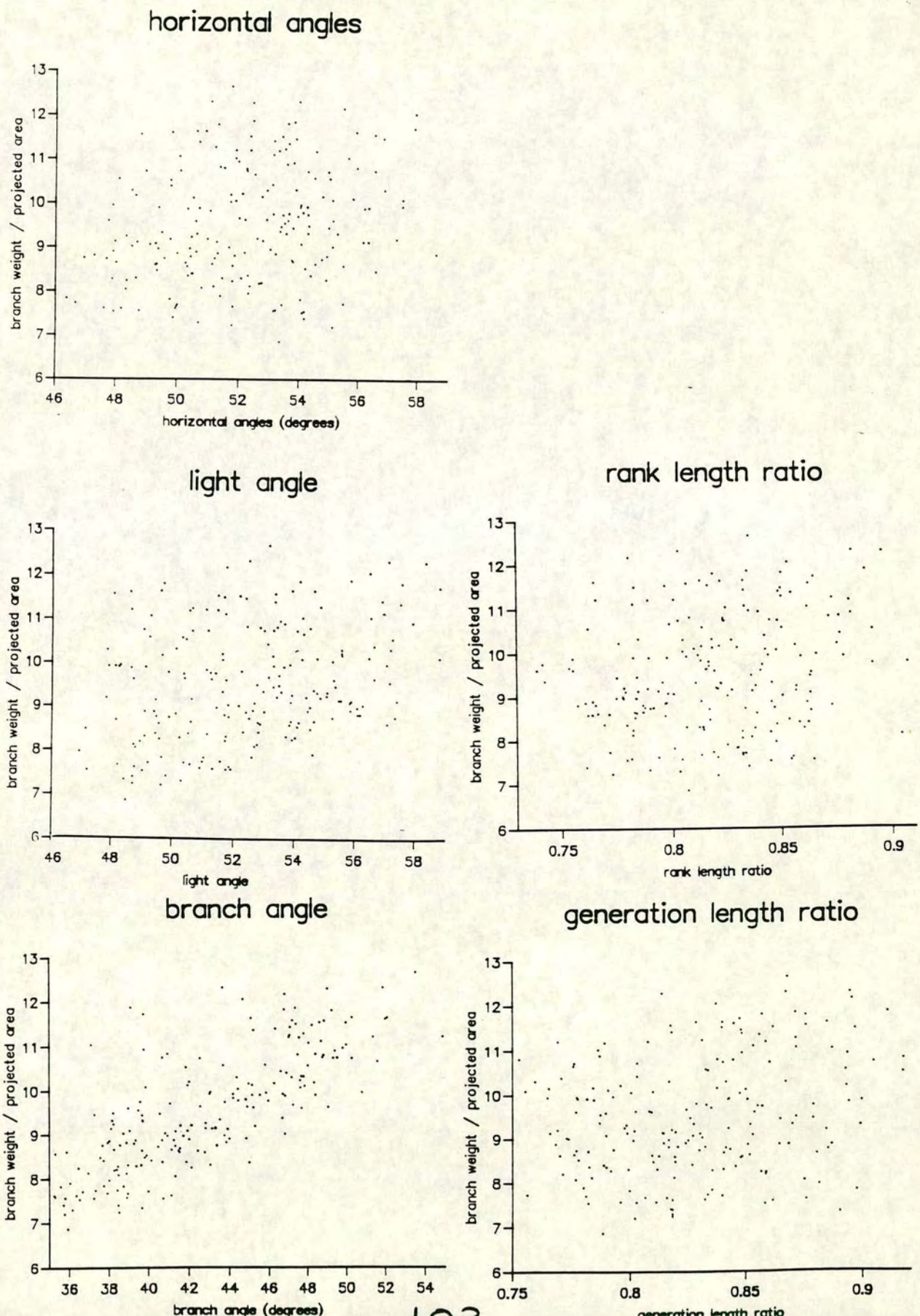

The input variables were all set to a central starting value which represented the mean for measured branch values. They were then simultaneously varied randomly according to a normal distribution with zero mean and standard deviation equal to 10% of the parameter's natural range. 10% was used to avoid model failure due to out-of-bounds conditions, but also to have large enough perturbation that fine grain errors do not affect the results (e.g. errors from internal estimates of derivative from difference equations). 200 repetitions were carried out giving 185 degrees of freedom. Two parameters with assumed values (as opposed to variables) were included in the sensitivity analysis to test the importance of their assumed values. These were: Young's modulus for the shoots and the angle of incidence of light illuminating the branch (which, in the model, comes in two beams: one at 0°, the other at 45°).

Multiple regression analysis was used to measure the relative importance of the input parameters in determining the model output, the objective function describing branch efficiency: whole branch weight divided by foliage area projected to daylight at the specified angle of incidence with the shading loss calculated within the model. A backwards elimination procedure was employed to further refine the regression result. Results are presented in table 3.4. On the basis of t-statistics branch vertical angle was the most influential parameter, followed some way behind by daylight angle and generation length ratio. These parameters together explained 91% of the variation in objective function results. Lengths, taper factor, diameter step factor and Young's modulus were all eliminated without loss of information. The sensitivities are well illustrated by scatter plots showing cross sections through the 16 dimensional cloud of 200 points, or to put it an other way, by projections of the points onto the branch efficiency - individual variate plane. Fig 3.19 shows such projections for each variate in turn. Only vertical whole branch angle shows any visual correlation with the objective function: the other variates all seem to have no influence on it according to these univariate scatter plots. Such a conclusion is misleading, though as the variation in objective function shown in each of the plots is entirely a result of the combined effect of the variation in the individual variates. When the scatter plot appears to show no correlation, this does not necessarily mean that a variate does not influence objective function values, rather that its contribution to the variation is small compared to the total of all contributions from all other variates.

Table 3.4. Results of multiple regression and backward elmination procedure fitting model parameters to branch efficiency (model output) to show sensitivity of efficiency to individual parameters.

DATA:

Identifier	Minimum	Mean	Maximum	Values
efficiency	6.859	9.521	12.653	200
length (l)	0.1886	0.2063	0.2246	200
diameter (ad)	0.003858	0.003996	0.004124	200
age factor	0.923	1.048	1.155	200
taper	0.003994	0.005170	0.006216	200
rank length (dlr)	0.7389	0.8188	0.9066	200
rank diameter (ddr)	0.933	1.027	1.100	200
gen length (dlg)	0.7527	0.8281	0.9168	200
gen diameter (ddg)	0.914	1.005	1.110	200
branch angle (th0)	35.25	42.89	54.92	200
lateral angle (thi)	8.33	10.50	12.98	200
horizonal angle (phi)	46.01	52.17	58.60	200
diameter jump (jmp)	0.1788	0.2496	0.2999	200
Young's modulus (e)	3.140E+09	3.848E+09	4.532E+09	200
light angle (alpha)	0.2263	0.2642	0.3084	200

***** Regression Analysis *****

Response variate: efficiency
Fitted terms:
Constant, l, ad, age, taper, dlr, ddr, dlg, ddg,
th0, thi, phi, jmp, e, alpha

	d.f.	s.s.	m.s.	v.r.
Regression	14	330.70	23.62131	301.80
Residual	185	14.48	0.07827	
Total	199	345.18	1.73456	
Change	-14	-330.70	23.62131	301.80

Percentage variance accounted for 95.5

*** Estimates of regression coefficients ***

	estimate	s.e.	t
Constant	-38.62	2.11	-18.26
l	-0.02	2.88	-0.01
ad	1012.	402.	2.52
age	-1.035	0.406	-2.55
taper	-15.8	43.5	-0.36
dlr	6.805	0.589	11.55
ddr	3.050	0.600	5.08
dlg	11.255	0.530	21.23
ddg	2.662	0.461	5.78
th0	0.22822	0.00455	50.16
thi	0.2253	0.0197	11.45
phi	0.11838	0.00782	15.14
jmp	0.648	0.787	0.82
e	-0.88E-10	0.73E-10	-1.21
alpha	24.31	1.07	22.71

BACKWARDS ELIMINATION RESULT

dropped : length, taper, diameter jump, Young's modulus

***** Regression Analysis *****

Response variate: efficiency
Fitted terms: Constant, ad, age, dlr, ddr, dlg, ddg, th0, thi, phi, alpha

	d.f.	s.s.	m.s.	v.r.
Regression	10	330.51	33.05117	425.92
Residual	189	14.67	0.07760	
Total	199	345.18	1.73456	
Change	0	0.00	*	

Percentage variance accounted for 95.5

*** Estimates of regression coefficients ***

	estimate	s.e.	t
Constant	-38.84	1.98	-19.65
ad	972.	394.	2.47
age	-1.000	0.401	-2.49
dlr	6.802	0.581	11.70
ddr	3.138	0.593	5.29
dlg	11.230	0.525	21.41
ddg	2.636	0.452	5.83
th0	0.22851	0.00449	50.89
thi	0.2268	0.0195	11.62
phi	0.11844	0.00767	15.45
alpha	24.33	1.05	23.12

- 3.4.3 Failure of the model

Validation showed that there is some problem with the model which causes errors in predictions of strain distortions in branches above order 2 when predicted strains are large. Sensitivity testing further helped to isolate two factors which are likely to be responsible for this problem. The first was that the angle of attachment of laterals can be changed during the calculations by a degree far greater than expected. The second was that for large strains, distal elements of shoots showed very great displacements; far greater than expected. Following this discovery, it became necessary to investigate the reasons for such a failure in model predictions and to rectify it.

Recall that the distortion of shoots by gravitational forces is calculated from a transport relation which propagates from one element to the next towards the distal element (see Appendix 2.2). An unknown bending moment, B_{in} has to be applied to the proximal element of the shoot (i=1) such that the residual moment at the tip (B_{tip}) is zero. This amounts to finding the solution to:

$$B_{tip} = f(B_{in}) \tag{3.20}$$

by an iterative process. First, a trial value of B_{in} is used: because bending will always tend to lower the moment of the shoot, the trial value chosen is

$$B_{in}' = 0.8\, B_S \tag{3.21}$$

where B_S is the moment about its base of the shoot's centre of gravity, assuming the shoot is straight (fig 3.20).

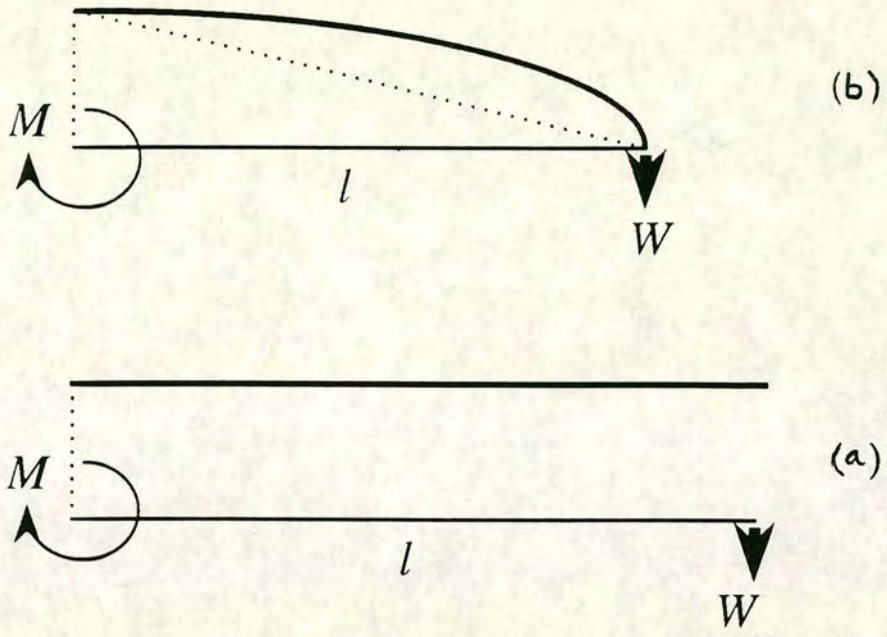

fig 3.20 The moment about the base of the straight shoot (a) is greater than that about the base of the distorted shoot (b).

Unfortunately, the transport relation calculation can be very sensitive to the value of B_{in} so that it becomes unstable and grossly miscalculates the distortion. The calculation propagates the angle θ (fig 3.21). If B_{in}' is outside of certain boundaries, then $|\theta|$ will exceed $\pm \pi$ so that the shoot will coil up within the space of a single element. From that point on, all subsequent values in the transport relation become meaningless.

The iteration which attempts to solve equation 3.20 is implemented as a bisection algorithm [Press, 1986]. This first requires that the solution be bracketed by a bracketing algorithm. In an attempt to solve the problem of the coiling shoot, the bracketing algorithm has been modified so that if the fail condition is encountered, it will stop on the 'safe' side. (The algorithm is included in fig 3.8). If the solution still lies between the two brackets after this process, then the problem is over, but it is possible that the solution itself appears to be in the unstable region beyond the point the bracket algorithm was prepared to go. In this case, the calculation will break down. In reality, the solution could not be in that region, but the bracketing algorithm may not be able to get beyond a value which causes the breakdown, even though the solution is just short of the barrier. Alternatively, the solution could lie beyond a prohibited band which the bracketing algorithm encounters. Both these circumstances have been considered, but no working solution to the problem has yet been found. Alternatives to the bracketing algorithm have been considered, but

nothing has yet been found which offers a significantly more reliable behaviour. The modifications to the model are described further in Appendix 2.

A reduction in model complexity, which removed a number of the iteration loops has reduced the sensitivity of the model to this problem and hence increased reliability. The effects of this change have been evaluated and are discussed in section 3.7.2.

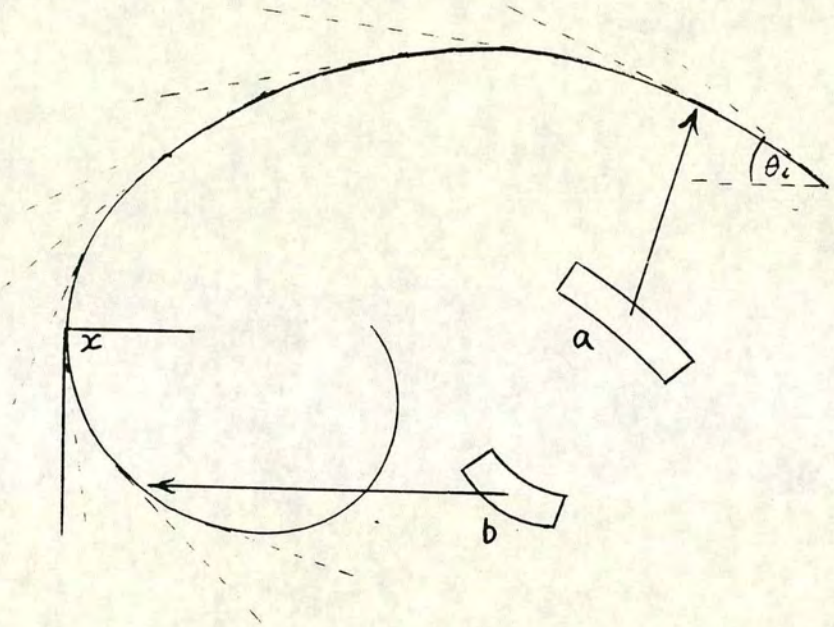

Fig 3.21. The angle each element axis makes with the horizontal θ_i is the accumulation of all others before it, working acropetally ($\Sigma\theta_i$.). If the bending of elements increases (for example element (a) to element (b) in the diagram), then it is possible for the accumulated angle to exceed π /2 (at the point x in the diagram). This then causes the calculation of tip moment to be unstable and gross errors result.

- 3.4.4 Properties of branch designs

There are twelve design parameters which can be varied for any given order of branch (1 to 4) and so each of the 6 branch description functions (of which two are objective functions) is represented in a 13 dimensional space. Mapping this space for each function over a range which at least encompasses the observed natural values of parameters would involve a prohibitively large number of modelling experiments. In the same way as it was for the sensitivity testing, a stochastic approach has been taken to examine the space i.e. the space is sampled. Using this method, the probability of any point (set of parameter values) being sampled can be controlled and the probability density function over the space can be defined.

Simulations using the model have been carried out to study the effect of shoot deflections on the light interception and objective function value. Morgan and Cannell [1990] showed that very small tip deflections are maintained (at the expense of carbon invested in the structure) in Sitka spruce. The advantage (if any) of maintaining very small deflections of shoots was sought here using simulations of model branches. The relationship between the objective function - shaded projected foliage area per unit branch weight - and the mean deflection per unit length of the tips of shoots in a branch was used to reveal aspects of design strategy regarding static load bearing. 200 branch designs were simulated using randomised geometric parameter values and the following measurements were recorded:

1) the projected area relative to vertical light
2) the projected area relative to light from the vertical mixed with light from 45°
3) the total branch mass
4) the mean of shoot tip deflections per unit length of shoot

Fig 3.22(a) shows the variation of the projected area A_p per unit mass to the mean deflection per unit length of shoots $<d_f/l>$ in the case of vertical illumination only. This relationship is clearly linear over the range given by the randomised trial designs. The least squares line fitted is represented by the equation

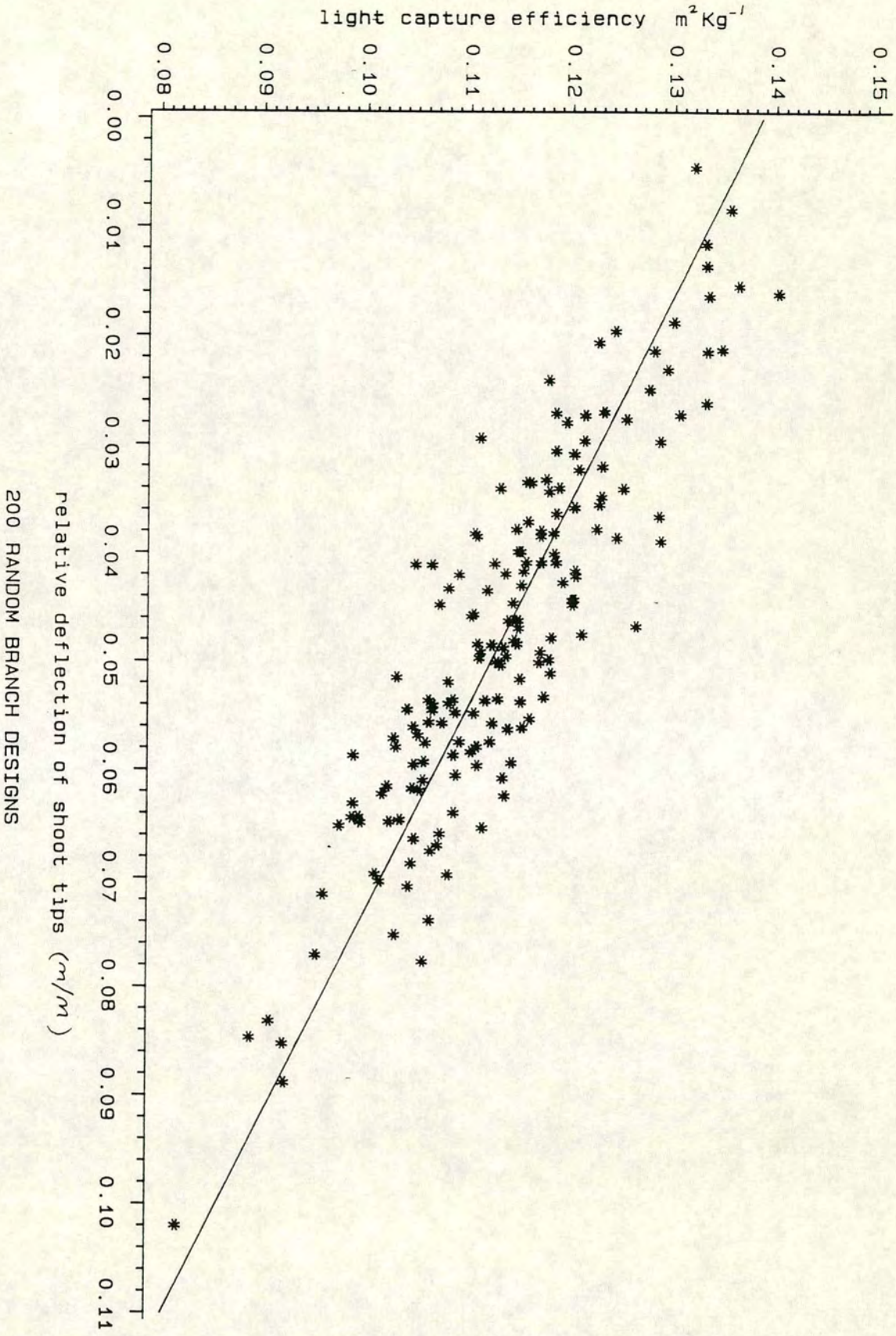

Fig 3.22. (a) The covariation of vertically projected area of modelled branch foliage with the shoot tip deflections per unit length of shoot.

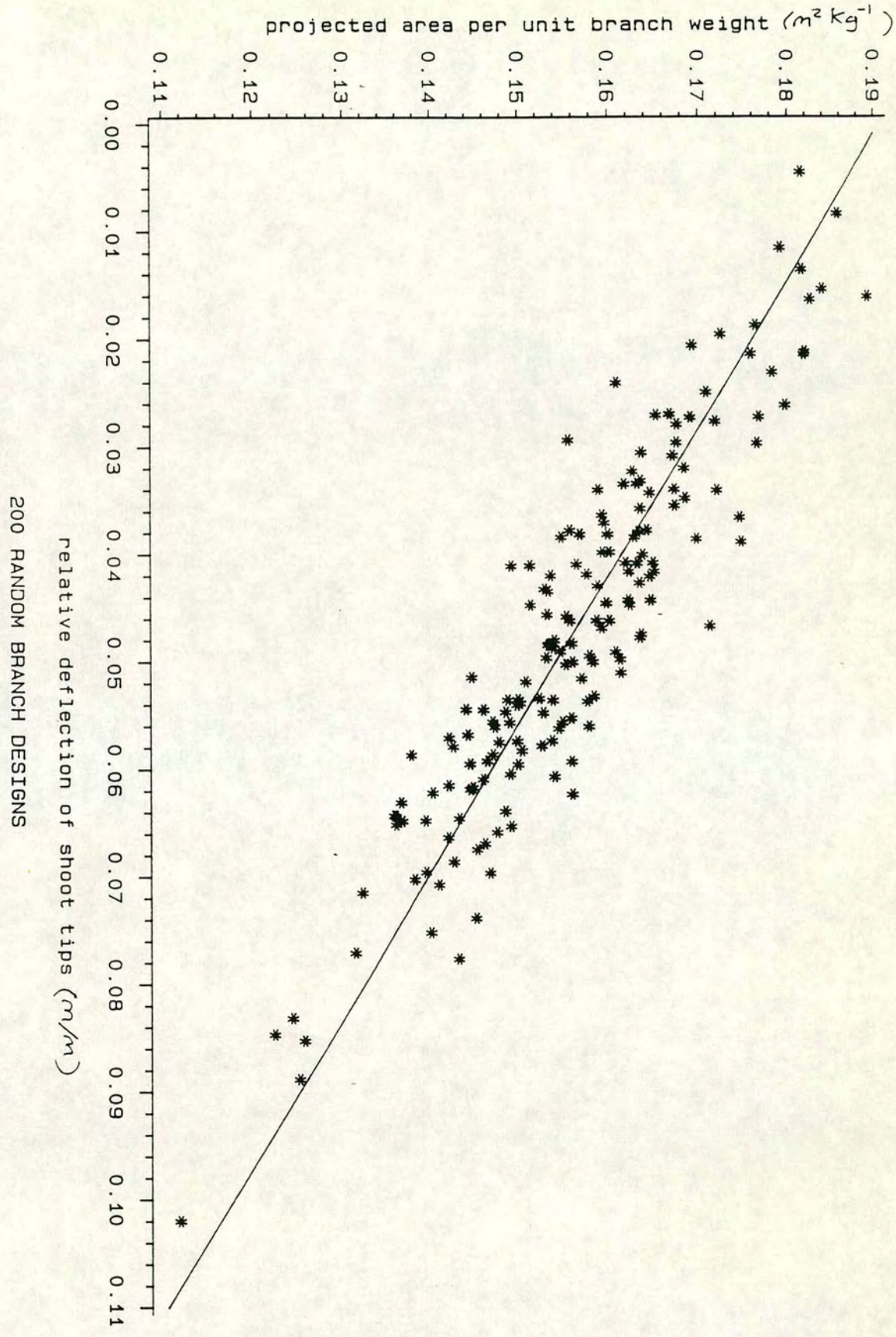

Fig 3.22. (b) The covariation of mixed light angle projected area of modelled branch foliage with the shoot tip deflections per unit length of shoot.

$$A_p\,(0°)/\text{ unit mass} = 0.19 - 0.73 \langle d_{fl}/l \rangle \qquad (3.22)$$

for which the associated R^2 correlation coefficient was 0.79 and highly significant.

A similar linear relation was found between projected area per unit branch mass and mean relative deflection for a mixture of light beams from the vertical and a 45° angle.

$$A_p(45°) / \text{ unit mass} = 0.14 - 0.55 \langle d_{fl}/l \rangle \qquad (3.23)$$

for which R^2 was 0.78 and also highly significant and this is plotted in fig 3.22(b).

There was no real evidence of a relationship between the mean deflection per unit length of shoot and the branch mass (see fig 3.23) since the correlation coefficient here was only 0.1. Thus the clear linear dependence of branch efficiency (projected area per unit mass) on deflections is a result of changes in the projected area of branches : deflection causes a loss of extension of shoots in the plane perpendicular to the incident light. The branch efficiency was less for light from 45° because the orientation of needles on the shoots is disadvantageous with respect to light at this angle. This effect is included in the model by the function F_2 (equation 3.14). The sensitivity of branch efficiency to deflections was also reduced when the 45° light beam was introduced because although extension of shoots is lost due to distortion, the angle of the shoots (particularly at the distal ends) becomes more opportune for catching light at 45°. If photosynthesis were directly proportional to light capture and this was proportional to projected area, then, the relations between branch efficiency and total deflection might indicate a productivity advantage for branches maintaining very small deflections. Section 4.3.1 points out that such assumptions would be far from the truth. If, though, the improvement in projected area can be achieved at little or no cost (in carbon), then it seems plausible that design would tend in that direction within the constraints of other design factors. One possible advantage of this strategy may be found in the theory of the competitive use of branch foliage shading - as a weapon against competitor plants by subjecting them to shade [Grime, 1977].

The sensitivity of branch efficiency to deflection, measured here, might not be enough to account for excess secondary thickening. However in this examination, the deflections were not strongly dependent on branch mass: the variation in

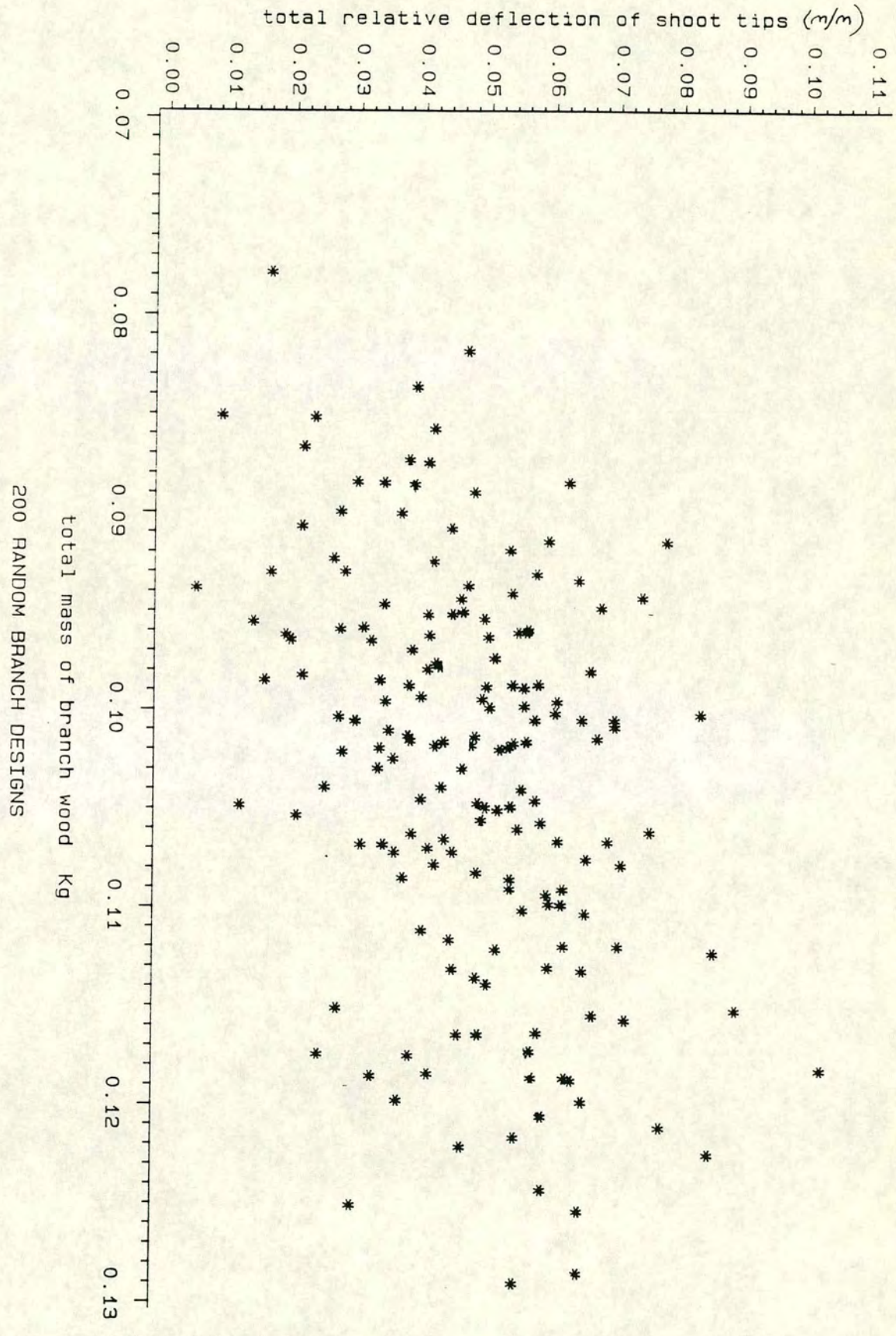

Fig 3.23. The covariation of shoot tip deflections per unit length of shoot with branch mass - there is no evidence here of a relationship.

deflections were produced by changing the distribution of matter in the branch, not the total amount. This seems to show that there is a considerable opportunity to so arrange the distribution of matter in the branch that the light interception potential is maximised.

A substantial range of branch efficiencies can be produced from different arrangements of matter distribution within branches. There is likely to be an incentive for optimal design based on this.

The univariate relations between geometric parameters (branch characters) and branch efficiency (or its inverse) were examined by simply evaluating branches of a fixed design where one parameter at a time was allowed to vary. The results of these examinations are given in fig 3.24. Most of the relationships appear to be near linear because variations in parameter values were restricted to small ranges by the limitation set by model failure. Considerable differences in sensitivity are apparent from the plots. Branch vertical angle θ_0 has the most profound effect on branch efficiency. Light angle α , leader diameter, the rank and generation length and diameter ratios c_{lr}, c_{dr}, c_{lg} c_{dg} and the lateral vertical angles θ_i come next with similar sensitivities, lateral horizontal angles φ a little less. Taper factor t, diameter step factor d_j, and age factor a have very small effects on branch efficiency as does the Young's modulus of the branch wood E. It must be emphasised that these results relate to a single point in objective space and may be quite misleading. The multivariate stochastic measures of sensitivity are regarded as more reliable. The univariate examinations do reveal the nature of the variation, at least at some point in space, which the stochastic test can not. discontinuities in the slope of relations, especially seen in the age factor relation are a result of the finite calculations and different computational pathways followed in the model. Thus, these charts reveal some of the sensitivity of model results to the computation method. Discontinuities in relations, or their derivatives, mark points where a threshold was reached for some indicator within the program, either side of which a different calculation path has been taken (see Appendix 2). These effects are artefacts and therefore constitute an error in model predictions.

Fig 3.24. (a) - (n) Results of univariate sensitivity analysis showing the variation in objective function with individual variates. Initially the range of values over which each variate was varied was a constant proportion of the mean of that variate in the measured branches (described in chapter 2), but this range caused moedel failure until some variates were constrained. The plots here are for the range of stable values in the neighbourhood of the varite means.

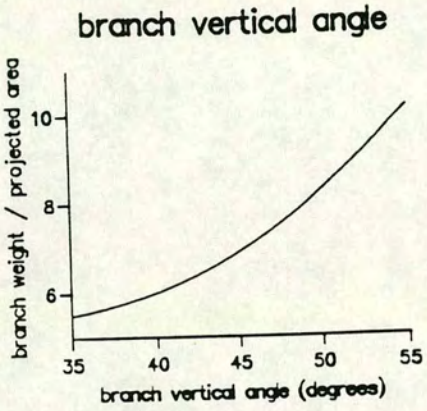

(a)

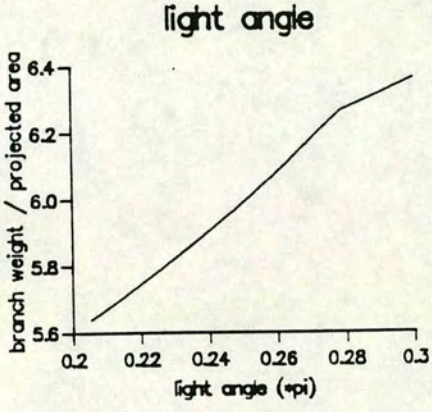

(b)

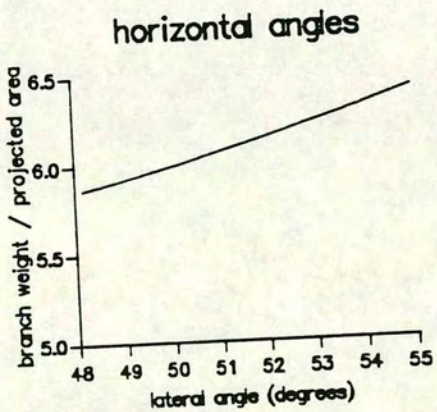

(c)

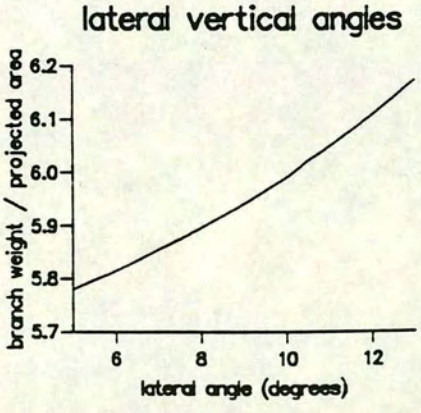

(d)

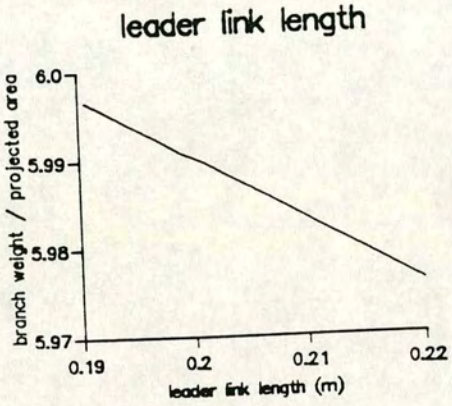
leader link length
branch weight / projected area
6.0
5.99
5.98
5.97
0.19
0.2
0.21
0.22
leader link length (m)

(e)

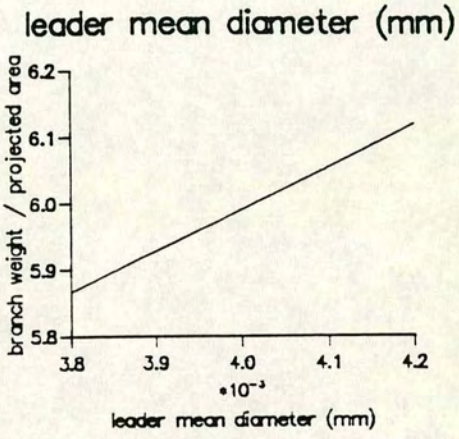
leader mean diameter (mm)
branch weight / projected area
6.2
6.1
6.0
5.9
5.8
3.8
3.9
4.0
4.1
4.2
*10⁻³
leader mean diameter (mm)

(f)

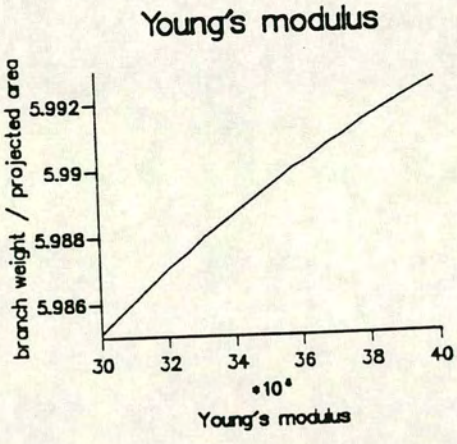
Young's modulus
branch weight / projected area
5.992
5.99
5.988
5.986
30
32
34
36
38
40
*10⁶
Young's modulus

(g)

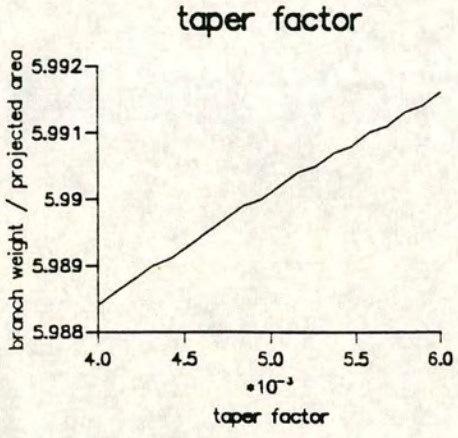
taper factor
branch weight / projected area
5.992
5.991
5.99
5.989
5.988
4.0
4.5
5.0
5.5
6.0
•10⁻³
taper factor

(h)

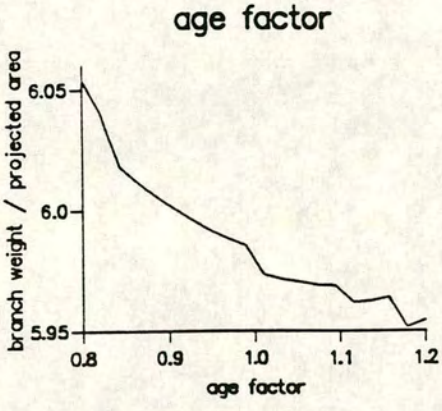
age factor
branch weight / projected area
6.05
6.0
5.95
0.8
0.9
1.0
1.1
1.2
age factor

(i)

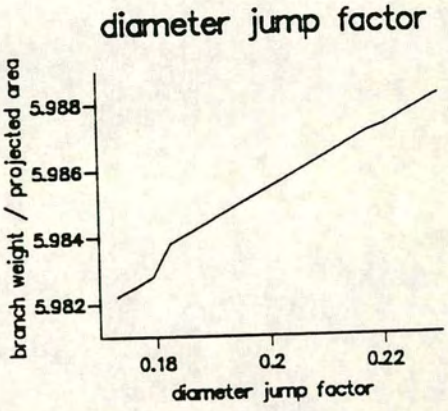
diameter jump factor
branch weight / projected area
5.988
5.986
5.984
5.982
0.18
0.2
0.22
diameter jump factor

(j)

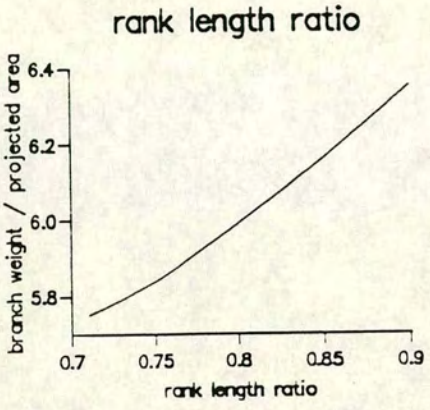
rank length ratio
branch weight / projected area
6.4
6.2
6.0
5.8
0.7
0.75
0.8
0.85
0.9
rank length ratio

(k)

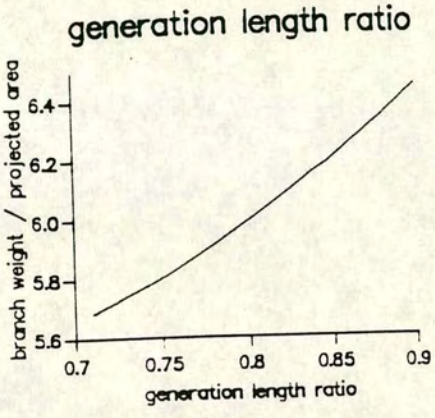
generation length ratio
branch weight / projected area
6.4
6.2
6.0
5.8
5.6
0.7
0.75
0.8
0.85
0.9
generation length ratio

(l)

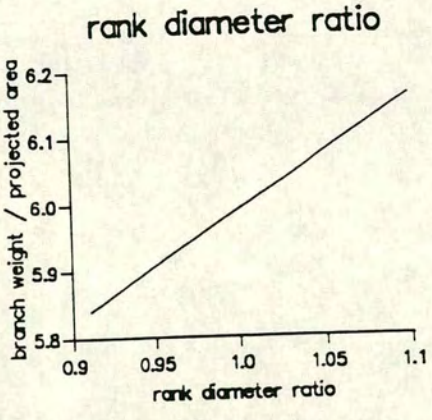
rank diameter ratio
branch weight / projected area
6.2
6.1
6.0
5.9
5.8
0.9
0.95
1.0
1.05
1.1
rank diameter ratio

(m)

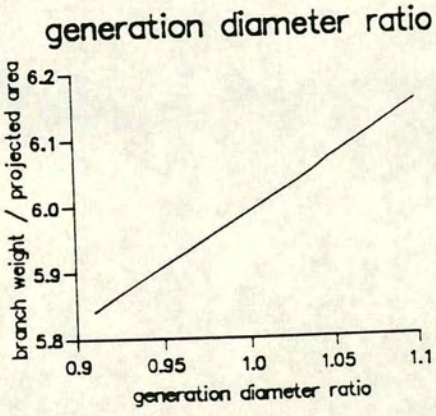
generation diameter ratio
branch weight / projected area
6.2
6.1
6.0
5.9
5.8
0.9
0.95
1.0
1.05
1.1
generation diameter ratio

(n)

• 3.5 Optimisation of branch design

• 3.5.1 The scope of optimisation

With as many as 15 characters to optimise an objective function, it can rarely be certain that a true global optimum has been reached. In this case no certainty can be attained and so we have to accept optima as local, however, they may be unique within the parameter boundaries of what is natural or physically possible. It is possible that an objective function is monotonic with respect to some parameters, for example the minimum weight is not reached until the shoots are vanishingly thin. To state this may seem unnecessary, but it can be an important consideration when designing the optimisation procedure. Because of the limitations of the branch model, which were discussed in section 3.4.3, the optimisation has to be limited in its range to those parameter value combinations which give 'sensible' results. Even if that were not the case, the optimisation would be limited in that it only attempts to find the best value of a single objective function as it is defined. In reality, it is possible that several objectives have to be met and some kind of composite objective function, which appropriately weights the objectives may be required.

For the reasons outlined above, the optimisation attempted here is necessarily limited in scope to less than that which might be expected to operate in nature.

• 3.5.2 Mathematical optimisation for tree branch design

The design goal for branches can be expressed as finding the minimum point in the inverse objective function $O(\underline{p})$ which is defined in the state space of the geometric variables ($\underline{p}$). $O(\underline{p})$ is given as the total branch mass $M(\underline{p})$ (representing costs) divided by total light interception capability $\eta(\underline{p})$ representing productivity. This productivity function depends on the branch's distorted geometry which is a function of the variables that define the original branch geometry ($\underline{p}$) and so control the mass. For a given incident radiation and description of shading, a calculation of $O(\underline{p})$ can be made for any set of values $\underline{p}$ by calculating the mass and the shape of the branch after distorting with self weight and finding the total of projected area weighted by the shading functions ($F_1 ... F_4$) to give a light interception value.

However the objective function has to be calculated by a complex iterative procedure which is very time consuming and no notion of its analytic expression exists. The first and higher derivatives, if needed would have to be estimated from function evaluations, thus an efficient minimisation of $O(\underline{p})$ would require a technique which offers superior convergence with the least number of function evaluations without any knowledge of the function's analytic derivatives.

The calculation of $O(\underline{p})$ is not exact, but results from the completion to within set limits of a number of sub-calculations. Although, in each single parameter, or dimension of the objective space, $O(\underline{p})$ is likely to be a smooth, well behaved function, its estimate $O'(\underline{p})$ will be less simple. This is important as it affects optimisation greatly.

First, the estimate function can be un-differentiable at certain points due to abrupt changes in function value. This makes the use of the most efficient optimisation algorithms: those based in the Newtonian method, unsuitable for the problem.

Second, because the path of program control taken in the calculation can vary depending on the data vector $\underline{p}$, the result in a small neighbourhood may increase or decrease unpredictably giving rise to highly misleading estimates of gradient and higher derivatives. The fine structure of $O'(\underline{p})$ is ill-conditioned (that is a small change in $\underline{p}$ can give rise to a very large change in O') - a situation which compromises the reliability of any optimisation algorithm chosen.

Third, it has been stated that the model which calculates $O'(\underline{p})$ breaks down given $\underline{p}$ outside a certain range, such that shoots will appear to coil up on themselves or bending moments grow out of control in an effort to prevent the coiling. As a result, there are (unknown) boundaries in $O'(\underline{p})$ over which the function becomes highly ill-conditioned and once an optimisation program has strayed into this region, it is unlikely to recover so the possibility of just one model failure within the optimisation process leads to a high likelihood of optimisation failure.

Fourth, the Hessian matrix $\boldsymbol{H}$ (the array of second partial derivatives) of the function can be estimated by forward difference approximations. If the Hessian is found to be approximately constant over a neighbourhood of the state space (see below), then $O'(\underline{p})$ can reasonably be approximated as a multivariate quadratic and the vector direction towards the minimum point will be simply estimated: this forms the basis

Fig 3.25. Variation of the objective function hessian matrix norm and eigenvalues along the hyper-diagonal of all variates.

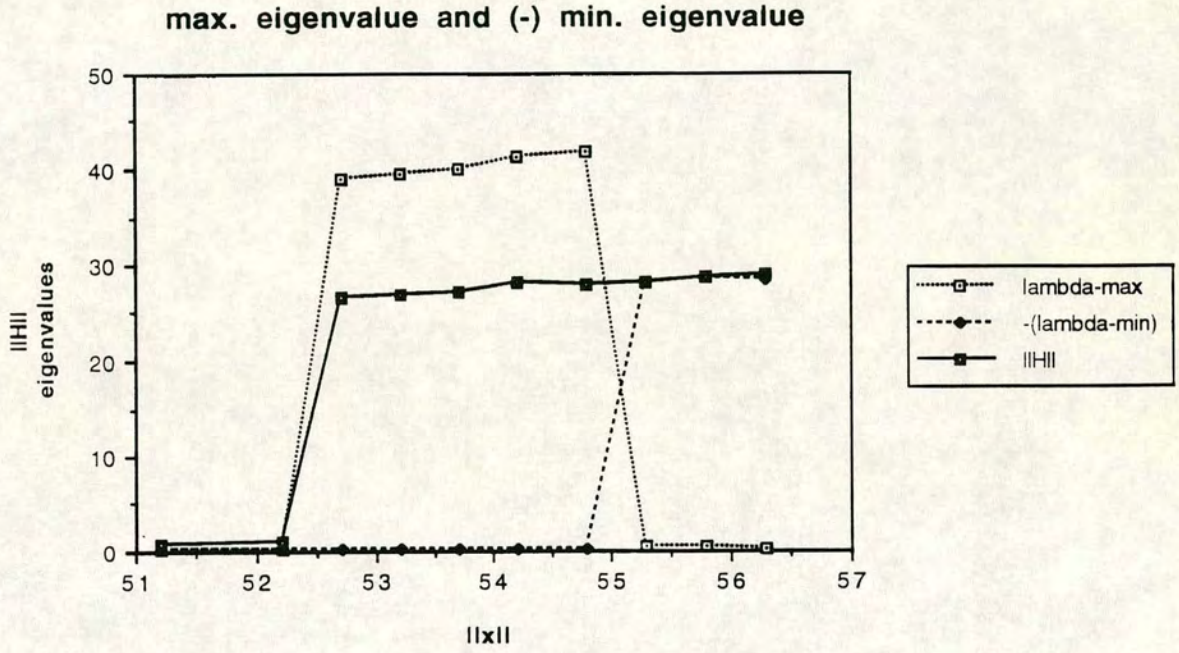

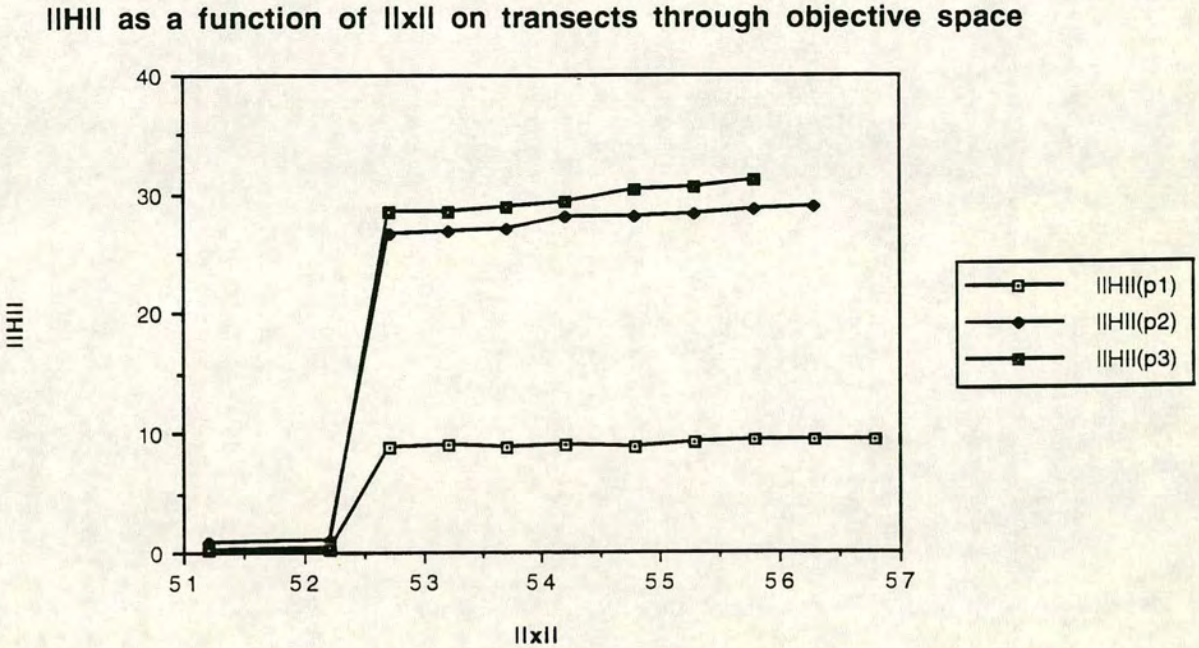

of Newtonian methods if the Hessian is definite (the estimating quadratic is bounded below so that the direction to a minimum is unambiguous) and quasi-Newtonian methods if it is not.

To examine the properties of the Hessian of $O'(\underline{p})$, the following experiment was carried out. From a central point $\underline{p}$, sample points were defined at $\underline{p} \pm \alpha p_i$ (i = 1...n) where α is a small fraction (< 0.01). This defines a line, i.e. a transect in objective space centred on $\underline{p}$, oriented along the hyper-diagonal of all dimensions. For each sample along this line, the following two characters of the objective function were calculated: a) λ_{max}, λ_{min} (the extreme eigenvalues of the Hessian) which indicate the steepest gradients and b) $\|\boldsymbol{H}\|$ the Hessian's norm, which describes its magnitude. The variation of these characters over the objective space gives an estimate of the variation in $\boldsymbol{H}$ and therefore, an indication of the degree of difficulty of the optimisation problem. Fig. 3.25 gives the results for the objective function : total projected area / total branch mass in order 3 branches.

Fig. 3.25 shows that there is a wide range in hessian norm and eigenvalues along the transects in objective space, indicating that the second derivative of the object function is far from simple. Where a sudden change in $\|\boldsymbol{H}\|$ occurs, it is likely to be associated with a sudden change in the curvature of$O'(\underline{p})$. These abrupt changes in $\|\boldsymbol{H}\|$ can be associated with a particular eigenvector becoming either very large or very small (fig 3.25b) which causes a large change in objective function sensitivity: at certain points in objective space, $O'(\underline{p})$ becomes highly sensitive to certain geometric parameters. This behaviour is attributed to the effect of changes of integer variables (e.g. the number of elements representing a shoot, or the number of iterations in a feedback loop) in response to changes in continuous variables. At a finer resolution (fig.3.25b), the hessian norm appears irregular (probably due to finite calculation errors) and this will prevent optimisation convergence when an algorithm is sensitive to changes at this resolution. In conclusion, it has been demonstrated that the estimated objective function presents serious difficulties for optimisation algorithms. The role of the Hessian in optimisation is developed further in Appendix 2.

• 3.5.3 The choice of optimisation algorithm

A very large number of algorithms have been developed for the solution of the unconstrained optimisation problem, each with a different balance of desirable features. In the case here the important features are as follows.

a) The algorithm needs to be robust against possible discontinuities in $O(\underline{p})$ and its first and second derivatives which result from finite difference calculations within the procedure evaluating $O(\underline{p})$.

b) The algorithm must make efficient use of function evaluations as these will dominate the total computation time.

c) There is a surface in objective space which forms a boundary between acceptable results from the successful working of the model and unacceptable results from its failure. The algorithm must be able to take this as a boundary constraint.

The NAG subroutine library [NAG, 1977] provides examples of most of the practical techniques which could be used. Other algorithms are discussed in [R.P. Brent 1973]. Many of these discussions include a decision tree for choosing algorithms.

i) Quasi-Newtonian

Following the decision trees, the most appropriate choice in this case seemed to be the Quasi-Newtonian type of algorithm. This dose not use explicit calculations of the first or second (or higher) derivatives although the theory is based on the behaviour of the Hessian. Quasi- Newtonian methods are reasonably economical in function evaluations and fairly robust. The one chosen was the NAG routine E04JAF [NAG, 1977]. Unfortunately, after spending time adjusting scaling and step length (algorithm parameters), without any successful convergence, the quasi-Newtonian method was abandoned. It appeared that the algorithm was being misled by the complexity of the fine structure in the estimated objective function. The estimated objective function is not a smooth function because decisions taken in its calculation during run time can be very sensitive to certain intermediate results and so generate

so generate different estimates in $O'(\underline{p})$ which are very hard to predict. It also frequently occurred that the algorithm drove the model beyond the bounds within which it can give plausible results and this led to failure as well.

ii) Newtonian

Strict application of Newtonian methods requires the availability of first and second derivatives, but these can be reasonably approximated by forward difference calculations. The step size for forward difference calculations is important because there is a trade off between precision (requiring small steps) and robustness (requiring larger steps because of the problems with $O'(\underline{p})$'s fine structure. Because the objective function was not expected to vary very rapidly in objective space, a value of 1% of the typical magnitude of each parameter (p_i) was chosen. The typical magnitude means the approximate magnitude of some typical value for example the typical magnitude for vertical angle is 45° and for shoot diameter is 5mm (typical magnitudes have usually been used for parameter scaling in optimisation to effect approximate normalisation of the problem and prevent relative weightings of parameters from distorting the optimisations [Brent, 1973]). So the Hessian matrix and gradients were calculated and supplied to a Newtonian algorithm supplied in the NAG FORTRAN procedure called E04LAF [NAG, 1977]. This method failed in a similar way to the quasi-Newtonian. It is thought that it was failing because the underlying quadratic model which it uses as a parametric model of the function was not a good approximation of $O'(\underline{p})$, although, ironically, it may be a good model of $O(\underline{p})$.

iii) Powell's Algorithm

In Powell's method, one dimensional line searches which minimise in the univariate case are combined in 'conjugate directions' (meaning directions which do not interfere with one an other. A FORTRAN listing of an algorithm using Powell's method is given in Press et al. [1986]. This was tried next because it is regarded as more robust at the expense of efficient convergence [Brent, 1973]. No success was achieved with Powell's algorithm because every line search it initiated resulted in the branch model being sent out of bounds and failing.

iv) Simplex Method.

A simplex is a geometric figure in n dimensions with n+1 vertices. If n+1 points in objective space are defined, this represents a starting position. An algorithm taken from Press et al. [1986, page 292] called *Amoeba* was used to try the simplex method which deliberately assumes nothing about the objective function or any of its derivatives. The vertices of the simplex are moved in test directions repeatedly so as to move towards the objective optimum. This process is very slow and costly in terms of number of function evaluations, but is very robust. However, once again, optimisation resulted in failure due to the breakdown of the branch simulation.

Clearly, something had to be found which could either avoid the boundaries over which the branch model breaks down, or which can recover from failure. The simplest way of doing this seemed to be to allow a human user to make decisions during the optimisation process and this became the basis of the final implementation.

• 3.5.4 The implementation and where it breaks down

Eventually, the simple rule of evaluating the Hessian and conducting a line search along the direction given by the most negative eigenvector was chosen as the basis of the algorithm. This, however had to be supplemented with alternative options and strategies to cope with model breakdown. The method is a hybrid combining a form of steepest descents algorithm with a simplex method which makes no assumptions about derivatives or any other property of the objective function. Fig 3.26 shows the structure of the optimisation program which was written specially for this work. Because none of the established techniques for automated optimisation were found to succeed, this program combines a number of optimisation tools into a flexible package and, most importantly, an independent record of the current best estimate of the optimum is constantly updated. This 'best so far' is incorruptible by other calculations in the program: it is automatically saved to an external file at various points in the program flow so that it is even immune to complete system 'crash'. Any time the optimisation goes wrong or breaks down, the option of relocating in objective space at the current best point is available, so the system works as a ratchet: allowing only the desired direction of movement in the outer loop. Giving

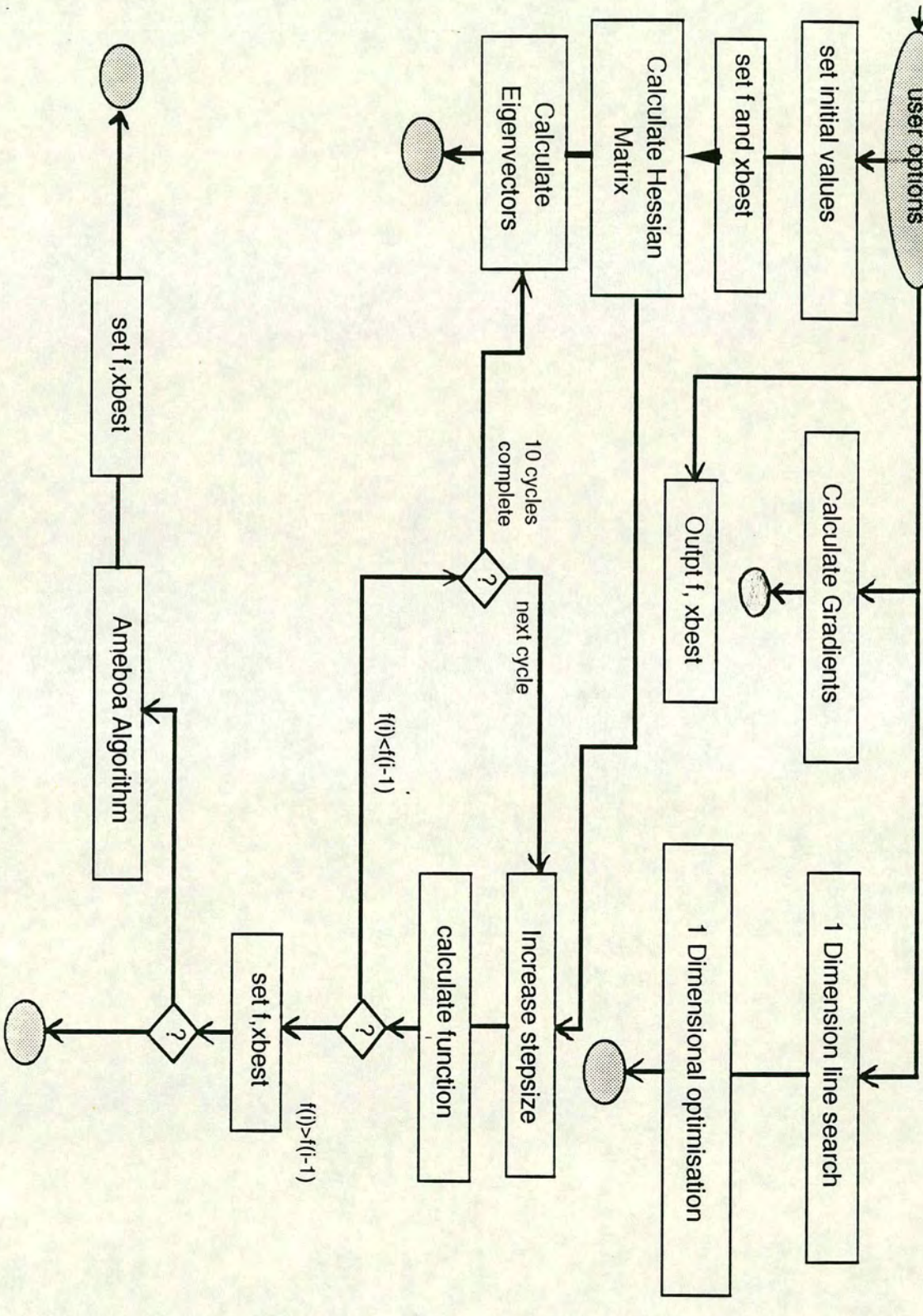

Fig 3.26. Flow diagram shoing the optimsation program.

command to a human operator has had advantages too, since intelligent decisions can often be made based on information concerning the state of the objective function in a neighbourhood, which are not at all easy to simulate automatically.

The main path taken during optimisation is as follows. Initial values are set to locate $O(\underline{p})$ in objective space. Then the Hessian matrix and the gradients in the directions $\underline{p}$ are calculated. Next the eigensystem of the Hessian is evaluated. These functions provide valuable information to the user as well as for the algorithm. Fig 3.27 is an illustration of the fact that in a multivariable space, moving down the steepest univariate gradient p_1(where $\underline{p}_i$ are here ordered in size of gradient) to a univariate optimum and then switching to the next p_2 will not, in general, find the multivariate optimum. However, the eigenvectors of the Hessian matrix form an orthogonal set of directions $\underline{v}$ which are oriented perpendicular to the multivariate gradients and so can find the multivariate optimum. For this reason, the program next takes the eigenvectors in turn (in order of the magnitude of their eigenvalues) and carries out a series of objective function evaluations along the eigenvector direction (with increasing stepsize). This process is carried on until a turning point in $O(\underline{p})$ is found at which point $O(\underline{p}_{best})$ is set and the Hessian is recalculated to start the loop again. Optionally, a simplex based method *Amoeba* [Press et al., 1986] is fed the eigenvectors as initial directions and allowed to progress until the operator wishes to try another line search. Another line search with in a direction specified by the operator can be selected and a dimensional optimisation based on the 'Golden Section Search [Press et al., 1986, page 282] can be applied in this direction. At any time the operator can call for a recalculation of the Hessian as well.

• 3.5.5 Optimisation results

Most of the experiments carried out with the optimisation algorithm ended in failure of one sort or an other. Calculations never reached a satisfactory conclusion, so it has to be said that no optimal designs have yet been found. Given the extensive contingencies described in the section above, this is indeed a surprising finding. The model of branch distortion was apparently so badly behaved that an optimisation procedure that finds an optimum in $O(\underline{p})$ still remains to be found. At this point, it is wise to reassess the branch model rather than to stretch optimisation any further.

However, often the direction of approach of a supposed optimum was revealing, even without actually reaching the goal. One very important function of optimisation

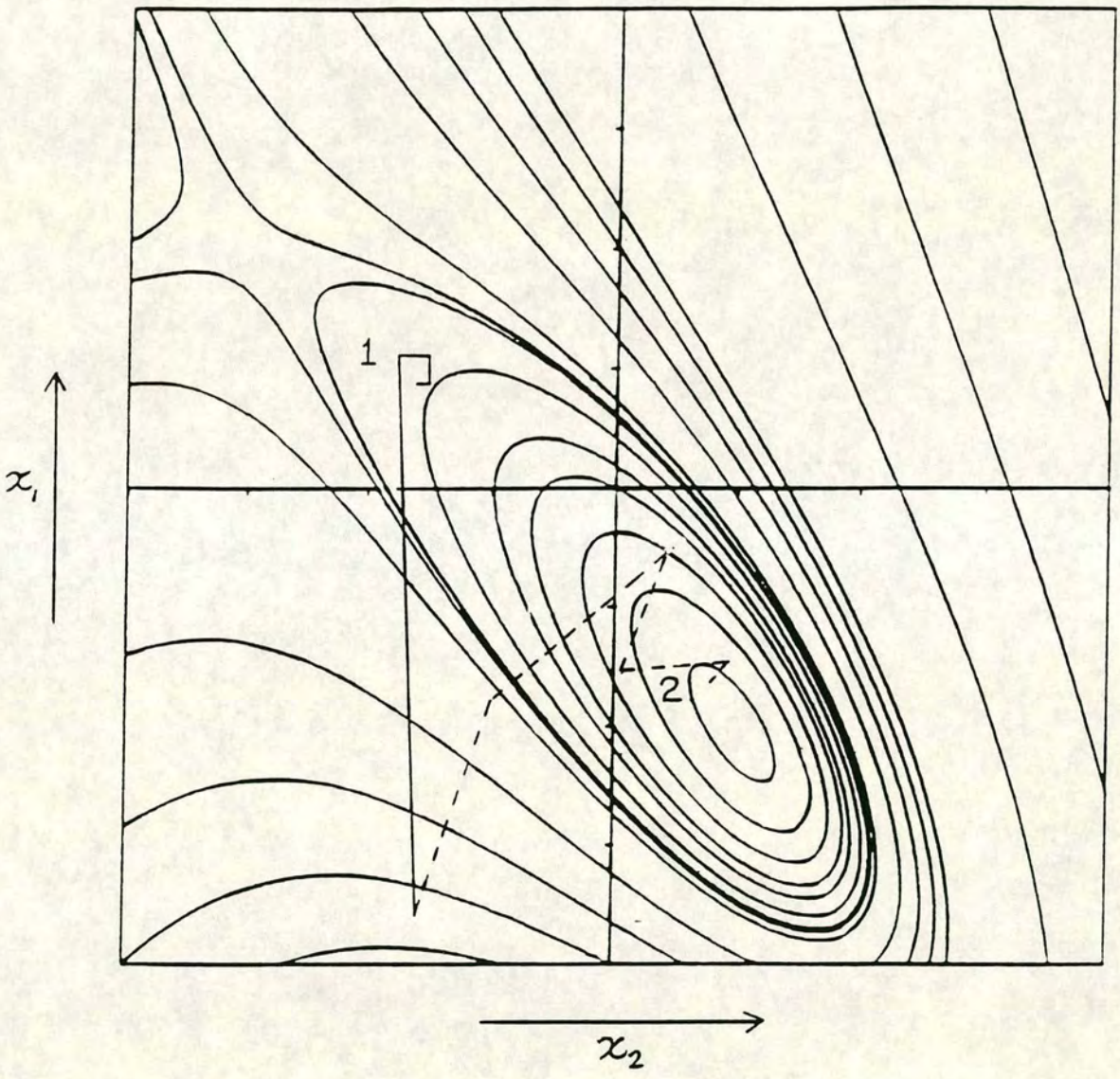

Fig 3.27. A demonstration showing how univariate optimisation algorithms (e.g. trajectory 1) can easily fail to find a minimum in a multivariate function with a feature (ridge or valley) aligned along a diagonal. The multivariate algorithm (trajectiry 2) moves along the steepest gradient and is more likely to succeed.

is to test the model being driven by the optimisation algorithm. Optimisation drives models extremely hard and can probe a very large area of the state space: much more than might be achieved with more straight forward testing. In practical terms, it was discovered that the most important results arising from attempts to optimise branch design were those which revealed flaws in the design model or which caused the calculations within the model to break down. For example unconstrained optimisation of a branch always led to the diminishing of all laterals as far as the algorithm could go, leaving insignificant stumps on the leader (see for example fig 3.28). This is a contradiction of Morgan and Cannell's work [Morgan, 1988] where they show that as branch increases in size it becomes more efficient to distribute new growth through laterals. A search for the cause of this discrepancy has proved unfruitful to date. An other feature of the model revealed in this way is that the optimisation of branch angle and stiffness always directed the design to produce a branch which was as nearly horizontal as possible near the base and rather pendulous at the distal end of the leader (for example fig 3.29). This is more explicable and interesting: the effect depends on the shading functions described in section 3.3.2. F_3 (equation 3.15) describes an incentive to grow upwards (phototropic response) and was based on results given by Wang [1990].

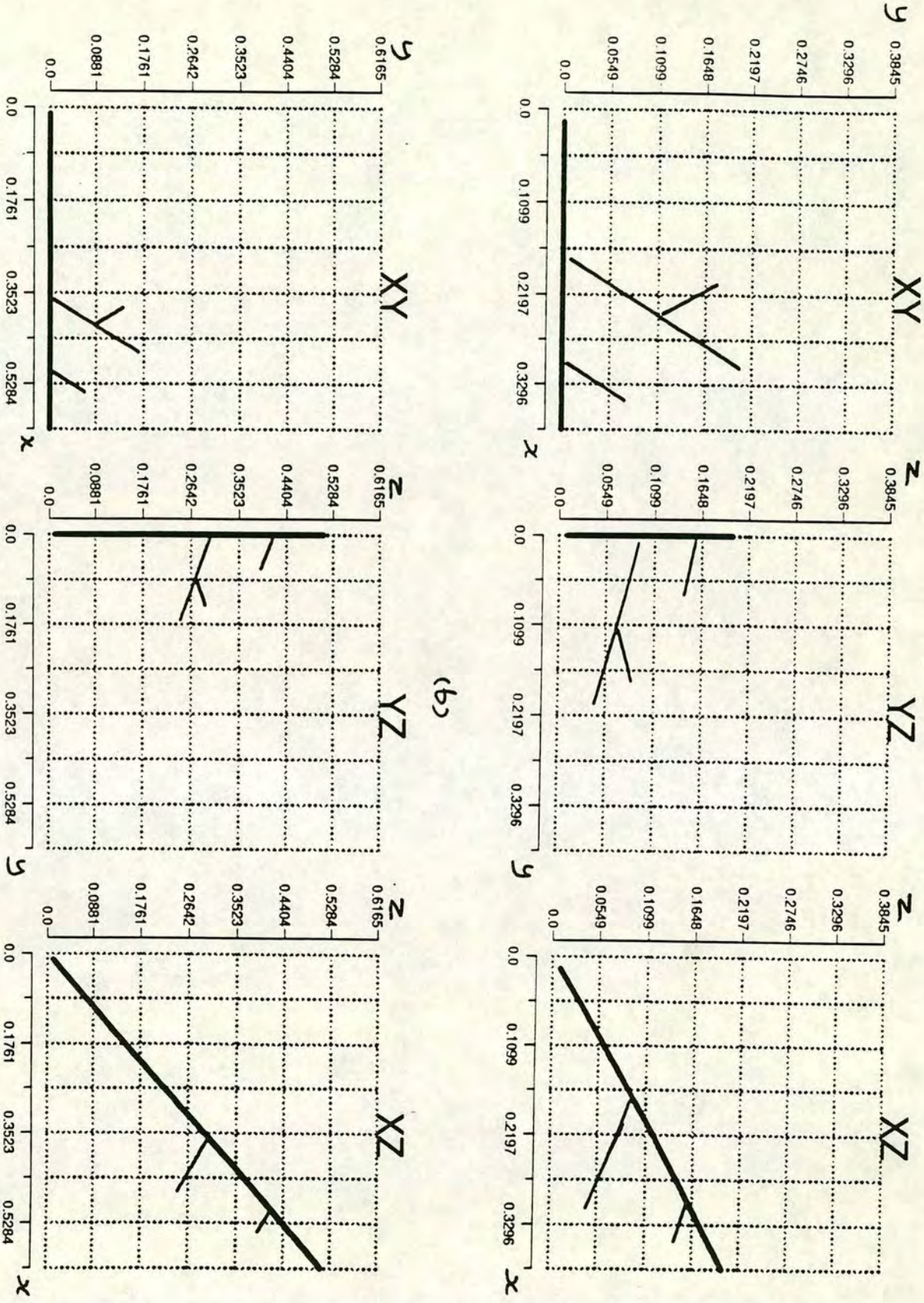

Fig 3.28. Example showing an order 3 branch in the progress of optimisation to illustrate the reduction in length of laterals which the optimisation algorithm causes. This occurs because, in the light regime specified, the laterals' mass to area ratio is always less than the parent shoot's.

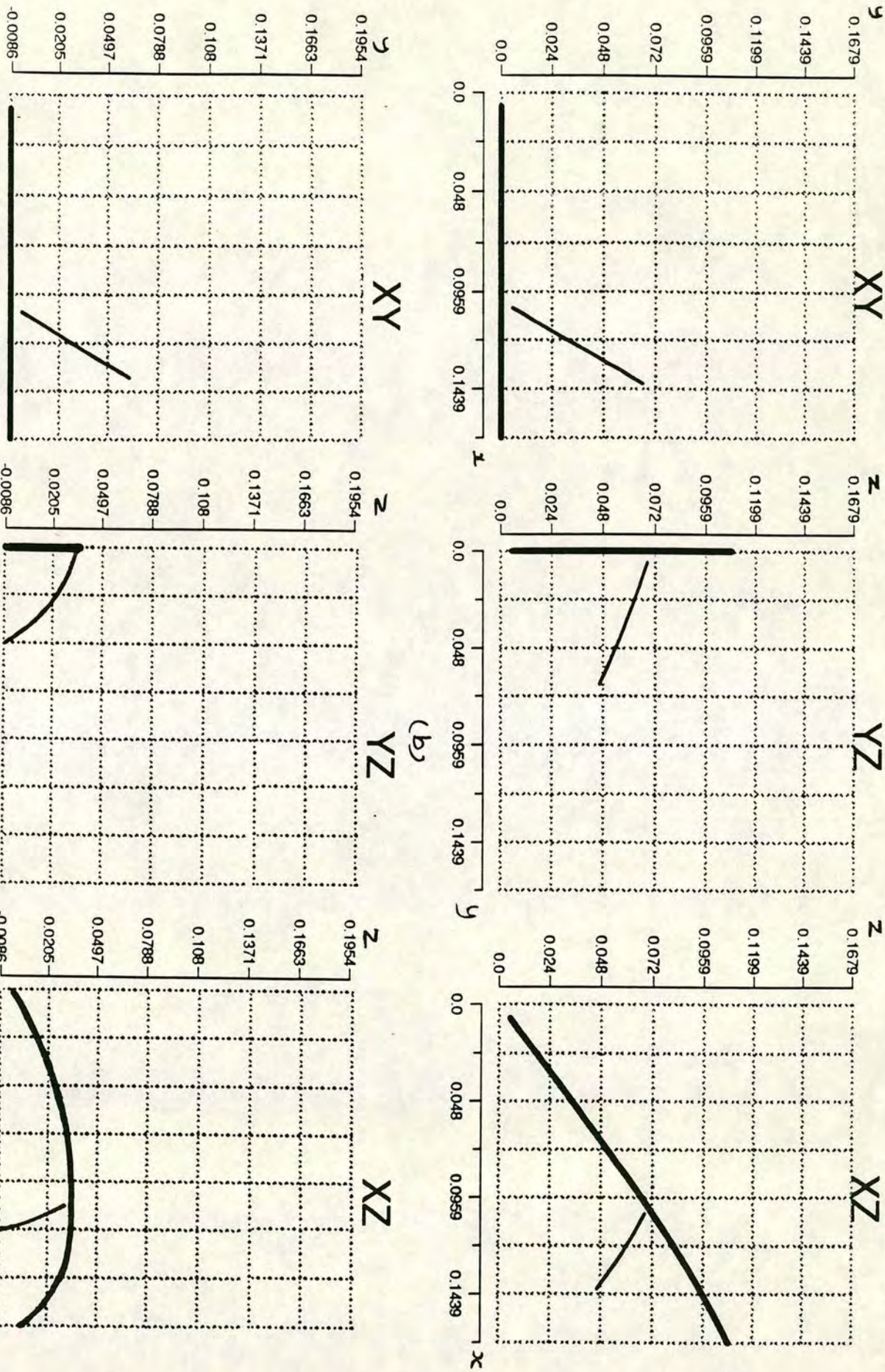

Fig 3.29. Example showing the reduction in branch angle θ as a result of optimisation (partial) for an order 2 branch. Note the increse in distortion giving pendulous tips to the shoots.

• 3.6 Conclusions from the modelling exercise

• 3.6.1 Is the model relevant ?

The original aim of the model was to identify the underlying principles of branch geometric design by investigating the behaviour of an analogous system. The model is relevant if the analogy is correct. Validation using real data is a pointer to the relevance. Validation was only possible with respect to one part of the model's predictions: that of shoot deflections under static gravitational load. It was possible to conclude from the validation analysis that the model is valid in this respect, so long as the total deflections are not allowed to become large. This condition arose because of a failure in model calculation for larger deflections accumulated over a number of hierarchically connected shoots.

Even if the model is valid, it has to simulate the behaviour of the branch which is salient to branch design. The model considers the response of designs to static loading brought about by self weight under the action of gravity. The conclusion reached from the analysis of natural branches in chapter 2 may be used to help support the notion that this simple view of mechanical design is the salient one. The model considers the branch in terms of its performance, under loaded conditions, as a light interceptor: this being presumed to be the primary function of branches. The modelling has shown that measures of branch efficiency in terms of light intercepted per unit mass invested in the structure are relatively insensitive to the design parameters considered (see table 3.1). The greatest sensitivity was simply to the relationship between branch angle and the angle of incidence of incoming light. It appears, then that more emphasis should be placed on the geometry of light interception in future. To this extent the model has not addressed one of the crucial constraints operating to achieve near optimal design, though without the modelling, it is difficult to see how such a conclusion could be drawn with confidence.

So far, as it is defined, the model is not entirely relevant to the issue of natural branch design optimisation, but it has been able to point to the factors which, if developed in further detail are likely to make it more so.

Chapter 4 offers suggestions for changes in the subject of the model which may prove to be more relevant.

• 3.6.2 Can the model be simplified ?

There are two ways to simplify the model. One is to reduce the number of input parameters used to describe the situation. A cut-off point is set, so that if the sensitivity to a given parameter is less than this cut- off, that parameter is set to a constant and removed from the design problem. The second way is to simplify the method of calculation. To investigate the effect of simplifying the calculations, parts of the model's internal complexity have been removed and sensitivity analysis has been used to compare the original with the stripped down versions. Two new versions of the model were produced. In the first, the interaction between a mother and daughter shoot was simplified to one iteration, so that the daughter was not allowed to cause a recalculation of the mother's shoot profile (see section 3.3.3). In the second, the interaction between mother-daughter pairs in the *FOD* network (see section 3.3.3) was disabled so that the *FOD* network was reduced to a single sequence to connect all the shoots in the branch with one an other once. The rival versions of the model were all given a set of 200 different randomly selected input value sets and run. The success or failure of the outcome was recorded (failure being ascribed to runs terminating in the abort route (see fig 3.7). The percent change in calculated objective function value from comparing the modified with the original model was also recorded in each trial. If the values given by the original model are regarded as a standard, then these percentages give a measure of the loss in accuracy due to the simplifications made. Fig 3.30 shows the results as a bar graph. The simplifications of the model both gave rise to small improvement in success, the greater simplification being slightly better than the other. This was achieved at a relatively small cost in accuracy. As a result, it would be recommended that the sophistications introduced into the model to take account of the interactions between shoots (described in section 3.3.3) should be left out: they are not justified by this sensitivity analysis of the technique.

• 3.6.3 What does the model tell us ?

The model demostrates that branches show only slight sensitivity to the geometric parameters described, over their natural ranges. On the other hand, it predicts great sensitivity to the altitudinal angle of attachment of branches on the tree.

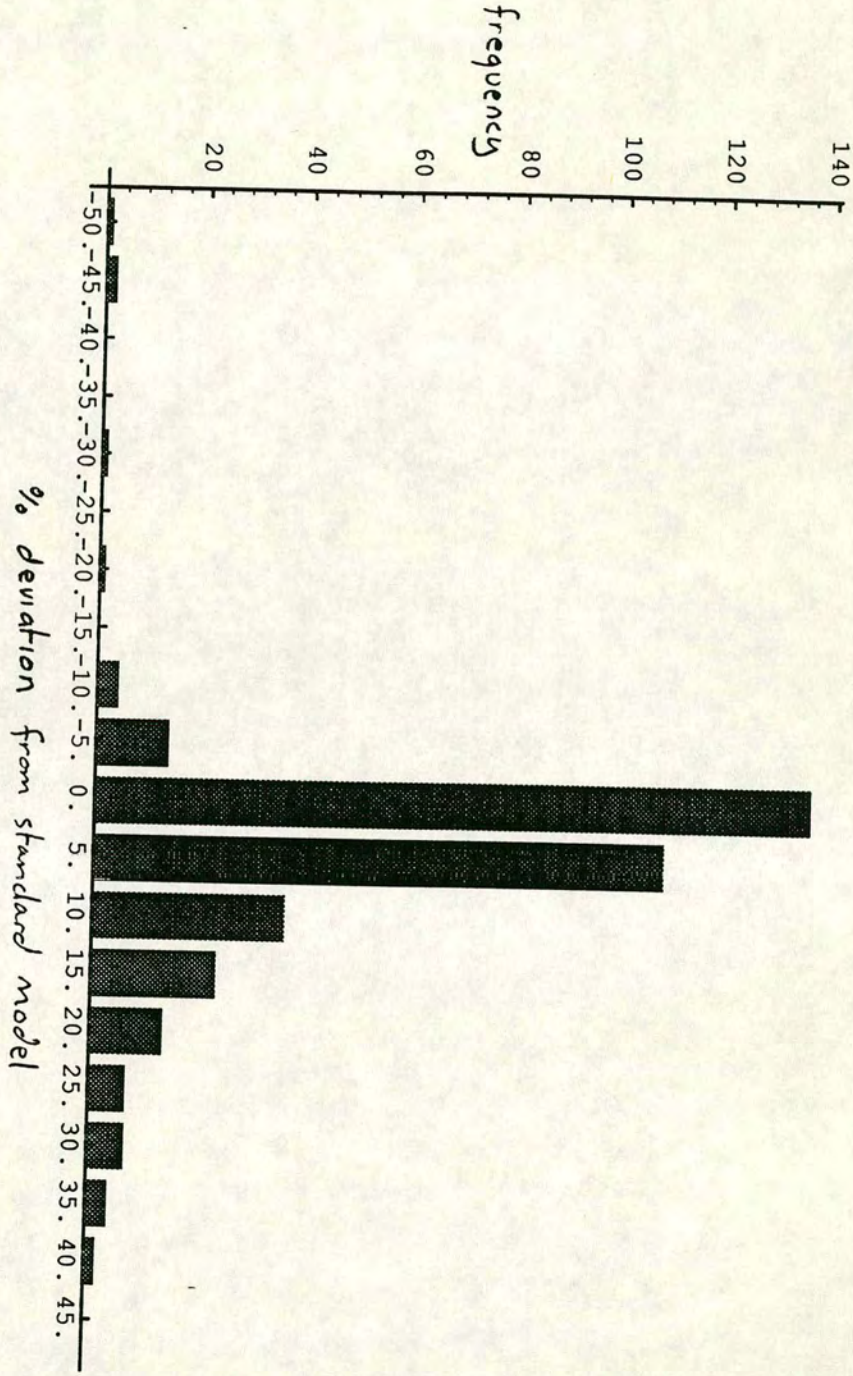

Fig 3.30. Sensitivity of the model to model formulation is shown here by the distribution of deviations of the simplified model's output from the original model's. Some of the high deviation results are a cosequence of the failure of the original model not being repeated by the simplified version.

Approaching optimum arrangements always involved inclining the branch and laterals so that a maximum amount of shoot length was held near to the horizontal, especially at the distal extremities. This, of course is contrary to the natural tendency of at least the first few orders of branch which are strongly phototropic. The phototropic incentive included in the model by the filter term F_3 had to be exaggerated greatly before the natural growth habit (branches held between 60° and 40° to the vertical) began to emerge in the model. If it is not assumed that the model is wrong in this respect, then it might be concluded that the young branches in the top of the crown are sacrificing profitability to achieve some other goal, perhaps at a whole tree level. However, it is argued in section 4.3.1 that photosynthesis is not especially affected by shoot orientation, particularly high in the crown, because the needles are operating close to, or above their saturation point for much of the time during photosynthesis. Thus, no cost in carbon assimilation is incurred by the phototropism.

Evidence was shown which indicates that a substantial range of branch efficiencies can be achieved, using the same total branch-wood mass, from varing the twelve design parameters used in the model. when all these parameters were varied simultaneously, branch efficiency and total shoot deflection were shown to co-vary linearly. This was thought not to be sufficient explanation for excessive shoot thickening, but some advantage in competitive shading of neighbouring plants might be gained from this behaviour.

Considerable effort was spent in providing a level of detail which in the end has proved unnecessary. Taper in shoots is of little significance for mechanical support when confined within reasonable limits (if it increased beyond some critical value, the model could no longer find a stable solution). A similar conclusion has been reached for the diameter changes at inter-link nodes and only small effects on distorted shape were observed from variations in rank and generation length and diameter ratios within the range of values which gave solutions.

Most particularly, modelling in detail the mechanical interaction between shoots in a branch has been shown to be unnecessary and even counter-productive. Advantage would be gained from considerably simplifying the mechanical behaviour simulation in the model described in this work.

chapter 4

DISCUSSION

• 4.1 The evidence for design principles in Sitka spruce branches

After measuring the geometric attributes of 125 individual branches taken from four different provenances and four age classes, a substantial data base of branch geometry for these trees has been collected. The data has been organised into an hierarchical classification so that each link within the network which describes the branch topology can be referenced and cross referenced with others sharing a topological feature (position in the branch). Using this resource, statistical analysis has been applied in a search for underlining geometric design principles, especially those which may be related to static loading: the distribution of stresses within the branch under static conditions.

• 4.1.1 topological design principle

One of the reasons given for choosing *Picea sitchensis* (Bong.(Carr.)) as the subject of this study was that its apparent regularity of topology would greatly simplify the relationships between form and function because of the repetition of form which results from growth expressed as a rigid reiteration. It follows that the first question which arose in the analysis of the branches was: how uniform is the geometry of Sitka spruce branches? The answer was that a uniform underlying topology is adhered to in branches of Sitka spruce so that the geometry can be represented as repeated expressions of a simple topological generating rule. Thus systems of link and shoot indexing could be used to classify the component parts of branches. An exception appeared: the interlateral shoots (those not growing from annual whorls) did not show a repeated relationship with the branch topology and these were not included in the classification of shoots in the analysis. Taking the main shoot axes, the topology of the measured branches conformed well to the mathematical description given by the Papentin form [Papentin, 1980]:

$$3n(ieee) \qquad n=1,2,3...$$

where n defines the order of the branch, *i* represents interior links (which end in another link) and e represents external links (which are terminal) (see fig. 2.5).

• 4.1.2 Genotypic differences in branch geometry

The four provenances: Cordova, Sitka Island, Skidegate and Northbend could not be statistically separated with confidence on the basis of single characters of branch geometry alone. However, when branch geometry characters were combined into optimum discrimination functions by canonical variates analysis, then all combinations of pairs of provenances could be separated, except for Cordova-Skidegate. Branch angles made the highest contribution to the Northbend-Cordova axis of discrimination whilst the Sitka-Skidegate axis was made up of a wide distribution of variates with no obvious groupings of variate type. The claim that the provenances were adequately separated by the analysis of these branches is made on a weak foundation, especially as no obvious pattern could be found in the latent vectors of the canonical variates analysis. This result is not a strong encouragement for breeders to embark on a program of selecting for improved branch design efficiency. However, there is room for hope, because the variates used in the analysis of tree differences were only the most gross combination of branch characters. This analysis could now be extended to include more variates from the data base, since not all have been used. When this is done, more significant differences between the branch designs might be revealed. If that becomes the case, then the data presented in this work will not, after all, be in contradiction of the general view supported by [Cannell,1974] and others: that different provenances give rise to significantly different branch characters.

• 4.1.3 Distribution of shoot lengths in the branch

Biomass is distributed among the shoot links of branches of *P. sitchensis* in a way that is closely related to their position in the branch topology. Material investment appears to be most closely related to the topological generation of shoots, establishing a hierarchy among shoots of the same topological rank which counts shoots of low topological generation as more important than those of high topological generation. This has the effect of distributing resources among shoots in a way which is highly biased in favour of those offering the greatest opportunities for extension into new space as opposed to those filling in space within the crown. The shoots offering the greatest opportunities for extension into new space are situated distally on the leader, or are their low generation laterals. It is possible to interpret these shoots as the 'pioneer' class of shoots which exhibit

something like the ' competitor behaviour' described by Grime [1977] in the context of partially autonomous shoots as members of a community within the branch [Sprugel & Hinckley, 1988]. Conversely the shoots which do not offer such opportunities are the more basepetally attached (older) and higher generation shoots whose function in filling space in the wake of the 'pioneers' suggests the term 'settlers' (by analogy) to describe the converse behaviour of 'stress tolerator' defined by Grime [1977]. In this context the stress tolerator will be a shoot adapted to a shaded light regime, exporting less photosynthate to the organism.

Priority is given to extension of the leader and the most distal of its laterals in each annual growth increment, while resources available for growth in shoots of increasingly high topological generation become so constrained that in the limit they cease to grow and subsequent laterals are entirely suppressed (self pruning). This pattern of resource allocation might be interpreted as being determined by the availability of light resources, but, one might speculate that it seems to in some way anticipate future light availability and the relative opportunities for shoots to exploit resources in the future.

- 4.1.4 Length - diameter allometry

Measurements revealed a linear correlation between total length and mean diameter which contrasts with the diameter-squared law for constant mechanical stress. Fresh weights of shoots bearing interlaterals are proportional to their length times mean diameter squared. These findings concur with those of Castéra and Morlier [1991]. Should this closeness to the geometric similarity model be surprising? During the ontogeny of a tree, its stem passes through the allometric relations predicted by, first geometric similarity and then, depending on the species, the elastic or stress similarity model [Niklas, 1992]. Thus, in this respect the young branches which were investigated in this study were behaving as 'saplings'; Bertram [1989] found the same phenomenon in a sugar maple tree. This behaviour could be a result of the trade off between mechanical requirements and the need to gain maximum length extension in the early years of development. On the other hand, it may merely be a reflection of the means by which secondary (thickening) growth follows primary growth: revealing a biological limit rather than a physical limit in branch form: part of the developmental constraints. Carefully designed experiments in which the light regime or other factors that may affect growth are manipulated would not necessarily help resolve this issue because it is not known to what extent the behaviour of geometric similarity, if it is a response to competing demands, is plastic as opposed to genetically inherited

and fixed. It would be necessary to develop an understanding of the detailed mechanism of development from the primary meristem tissues to lateral meristem (fascicular cambium) and secondary tissues in the growing shoot. This further raises the new question as to what extent the mechanical properties of the material of the shoot change over its ontogeny and possibly compensate for the seeming loss in rigidity of design which comes about from geometric similarity. A study of the elastic modulus at different growth stages of shoot and the biological limitations to the laying down of secondary tissues following the primary meristem is needed to answer these questions.

The relationship between the diameter of branch links and their length differs significantly among links classified by their topological position. The distribution of allometric relations was tested against two competing models: one based on a theory of hydraulic transport requirements (the pipe model), the other being based on the requirement of shoot axes to provide mechanical resistance to static loads. Static load resistance required link radius raised to the power 4 to be proportional to a load parameter ($W l_l^2 / E I_l$). This was shown to be true within 95% statistical confidence for the measured branches. On the other hand the pipe model required link radius squared to be proportional to total distal shoot length, but the measured branches did not conform to this model. Thus it is concluded that mechanical requirements dominate over hydraulic requirements in determining the diameters of branch elements (links).

• 4.1.5 Deflections of shoots under self-loading

One of the central questions of form and function was addressed by comparing measurements of self-loading deflections of branch shoots with their geometric design. The measurements were carried out with a simple apparatus which gave rise to uncertainties and experimental error often large enough to seriously compromise the data. These measurements are thought to be valuable, but would certainly be more so if a more robust and precise apparatus were constructed for deflection measurements. Most especially, an improved means of turning the branch through exactly 180° is required for improved accuracy, but more rigid clamping and more sensitive distance measurements would also be required for high quality measurements. The apparatus design shown in fig 4.1 uses optical means to make the measurements and this, it is expected, would offer a considerable improvement.

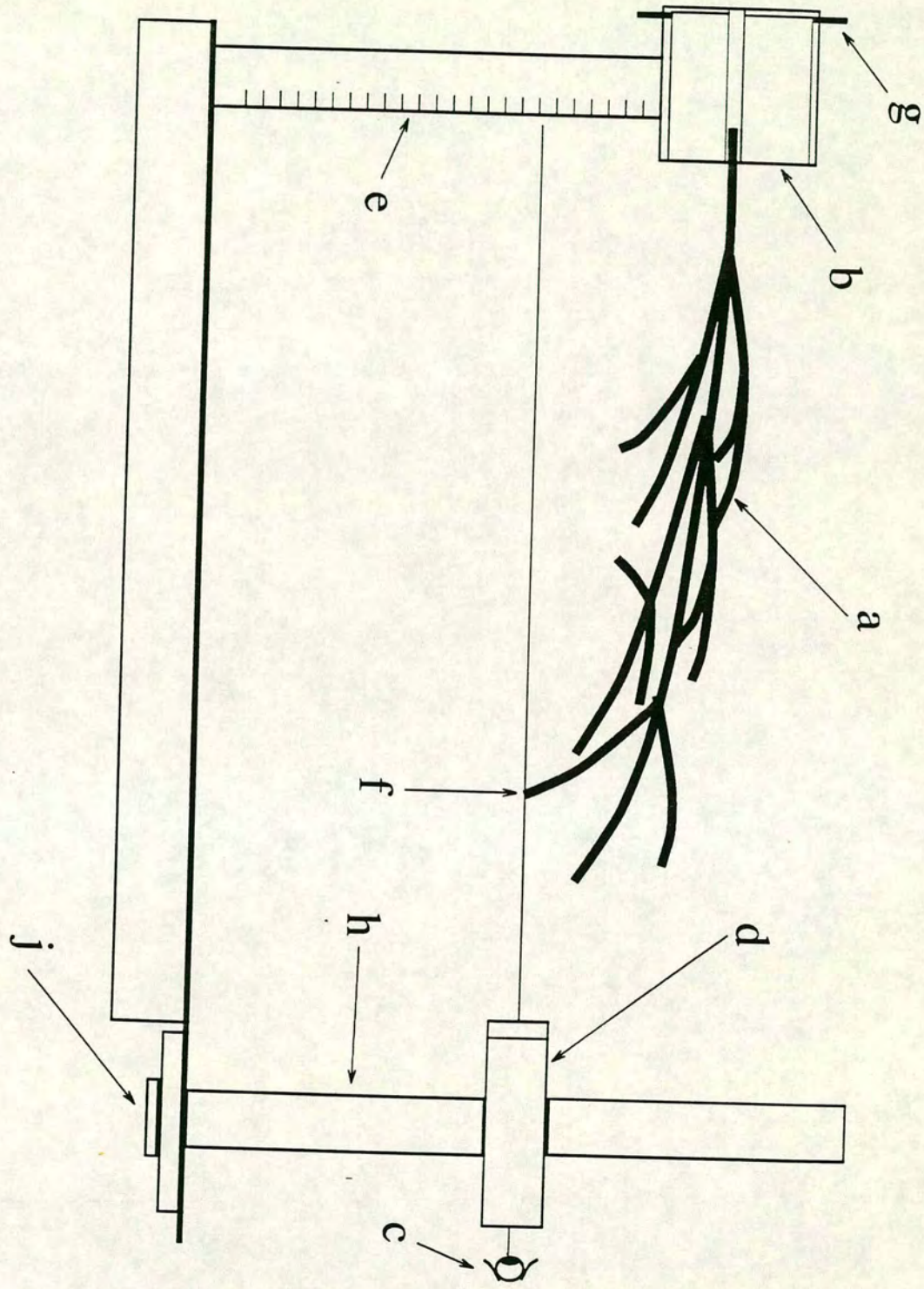

Fig 4.1 An apparatus to measure the deflection of shoot apicies as a result of their self-loading (weight). The whole intact branch (a) is inserted into the clamp (b) and the observer (c) moves the telescope (d) (focussed on the scale (e)) to see the shoot apex (f). The telescope can move verticaly on its support column (h) and in an arc centred on the clamp column by running it in a groove (j) set in the apparatus table. When one measurement is complete, the branch can be rotated through 180° in the clamp using the guides (g): the clamp consists of 2 concentric cylenders permiting the rotation.

Relative deflection was defined as the deflection of a shoot per unit length of path from the basal end of the branch to the apex of the shoot. This was found to be linearly related to deflection among all the shoots, thus shoots with apices further from the branch base were less rigid than those nearer. To interpret this result, it was noted that the fixed topology of the branches dictated that all paths from apex to base within a branch pass through the same number of links (equal to the branch order). Thus, the distribution of paths lengths is a reflection of the distribution of link lengths within the branch alone. Link length was correlated with shoot rank (the leader having the longest links), so it can be concluded that low rank shoots tend to be more rigid than high. Since the measurements were made on intact branches, the loading of lateral and interlateral shoots added to the stress on the high rank shoots. This finding then, indicates that shoots are less than proportionally stiffened for the extra load they bear.

Experiments carried out using the branch distortion model indicated that a substantial range of branch efficiencies can be achieved, using the same total branch-wood mass, from varying the twelve design parameters used in the model. when all these parameters were varied simultaneously, branch efficiency was shown to depend linearly on total shoot deflection. This was thought not to be sufficient explanation for excessive shoot thickening (observed by Morgan and Cannell [1988], but some advantage in competitive shading of neighbouring plants might be gained from this behaviour, never the less.

• 4.1.6 Relation between deflections and geometry

No clear relationship was found between measured shoot tip deflections under static load and the geometric branch characters. Some obscure relationship may exist in a multivariate sense, but no conclusion could be drawn about what that might be because it was so weakly expressed and because no phenomenological interpretation was found. At first sight this result may appear puzzling, since it seems to imply that the geometry has no influence on the shoot tip deflections and therefore on the distribution of strain in the branch under static load. It is, though, precisely because of the arrangement of matter in the branch that no pattern is observed in the shoot tip deflections. The distribution of secondary growth amongst the branch elements has equalised total shoot strains to the extent that systematic variation in the results has been lost beneath residual statistical variation in strain among the shoots. This result would be the conclusion of

assuming that load parameter is proportional to radius raised to the power 4 in all branch elements.

The cost of following an hydraulic design principle (the pipe model) for diameter control, in terms of mechanical efficiency was estimated. By designing a branch using the average of measured link lengths and the pipe theory model, it was possible to calculate diameters and load parameters for such a hypothetical branch. Following the pipe model resulted in an increase in mechanical strength with increasing rank of shoot over that of the mechanically oriented design. Using the most distal of the leader shoots as a bench mark for design, the pipe model branch was not mechanically compromised, but was materially inefficient, using more wood than appears to be necessary.

The detailed pattern of resource allocation among structural branch elements within the branch has been shown to be consistent with mechanical stability criteria and also to indicate the possibility of allocation on the basis of some other criterion differentiating shoot topological generations (for example potential light interception by the shoots).

• 4.2 Criticisms of the light interception / static load hypothesis

Chapter one made it clear that the hypothesis lying behind this work was necessarily limiting and the mathematical model of branch optimisation, and to some extent the treatment of branch measurements, were limited in scope as a result. The observed relationship between secondary growth and load bearing of shoots was complex and contained much detailed information, some of which is not simple to explain. This fact indicates that a widening of perspective would be appropriate for further progress. Several factors additional to light interception and static loading may influence branch design. These are discussed in this section and a brief suggestion of how they might be taken into account in the branch model is made in section 4.3.

- 4.2.1 The argument for dynamic forces.

The analysis of mechanical forces underlying the modelling work presented in chapter three was founded on the assumption that static load bearing due to weight represented the primary mechanical force acting on the structure. However, it is known that forces due to wind loading can be an order of magnitude greater than the weight loading of gravity in tree branches [King, 1986]. Gravity acts in a constant direction on the tree branch, so that responses to the stresses which it causes within the structure can be built up over time as the structure grows, thus leading naturally to a form reflecting these stresses. If such a process were taking place in branch growth, it would be expected to show as a pattern in shoot thickening which matches, in some way, the pattern of expected stresses. At a very simple level, given a steady force field acting uniformly in one direction, the growing shoots would be expected to develop anisotropically as described in fig 4.2. Occasionally, shoots are encountered which show some cross sectional anisotropy, perhaps bearing reaction wood, particularly at their base, thickening it only in the direction aligned with gravitational forces - i.e. vertically. However, almost all branch shoots deviate very little indeed from a circular cross section.

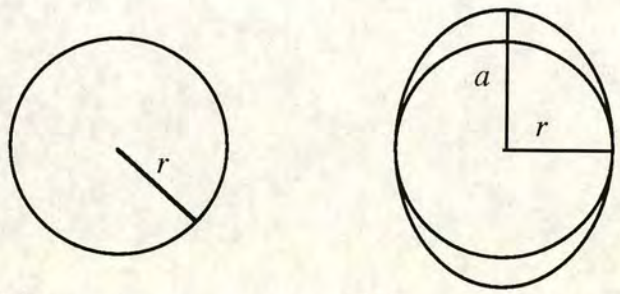

Fig 4.2. A circular cross-section shoot (a) is subjected to a static load in the vertical directiion only. To make efficient use of material, the growth response should lead to the eliptical cross section shown in (b).

The bending stiffness of a beam in a given direction is the product of the elastic modulus E and the second moment of area I. If a beam is bent with curvature K (reciprocal of radius of bending curvature), a stress σ is experienced by a unit area dA of material of the beam, at a distance from the neutral axis ζ such that

$$\sigma = K E \zeta \tag{4.1}$$

if the material is behaving elastically (if stress/strain $=E$). The local turning moment acting on dA about the neutral axis is $F\zeta$ where $F = \sigma dA$, so substituting for F, the local moment is

$$dM = E \zeta^2 K \, dA \tag{4.2}$$

The total bending moment is the sum of all these infinitesimal moments over the total cross-section area

$$M = \int_{-r}^{r} E \zeta^2 \, K \, dA = EK \int_{-r}^{r} \zeta^2 dA \tag{4.3}$$

Where r is the distance to the outer surface of the beam from the neutral axis. The integral $\zeta^2 dA$ over $\pm r$ is the second moment of area of cross section of the beam about the neutral axis I.

Clearly, the ratio of stiffness to cross-section area can be increased by elongating the cross section in the direction ζ perpendicular to the neutral axis: a circle becomes an ellipse with the long axis aligned with the bending moment. In general a beam of cross section described in dimensions x parallel with the neutral axis and y perpendicular to it (in the direction of ζ) has a second moment of area which goes as xy^3.

If a circular beam of cross-section radius r required to become two times stiffer, with a minimum addition of material , it would become an ellipse with a long axis length a perpendicular to the neutral axis (fig. 4.2(b)), with

$$2\frac{\pi r^4}{4} = \frac{\pi a^3 r}{4} \tag{4.4}$$

giving $a = 2^{1/3} r \approx 1.26r$ so that the cross-section area would increase by a factor of approximately 1.26. If the beam were to achieve a doubling of stiffness whilst maintaining a circular cross-section, it would need to increase r by $2^{1/4}$ times and

this would result in an increase in cross-section area by a factor of $2^{1/2}$ (approximately 1.41). Clearly development in the x direction adds less to the second moment of area and consequently little to bending stiffness in the y direction and so results in a reduction of the efficiency of the structure. In a world where static forces dominate, tree branch shoots may reasonably be expected to take on an elliptical cross-section, but this is not what is observed in the overwhelming majority of cases.

Wind force loading differs from gravitational loading in two vital respects. First, it is dynamic in magnitude, so that it may reach magnitudes far greater than average, also, it is capable of exciting complex dynamic behaviour in the branch including amplification due to resonance [Baker & Bell, 1992]. Second, it is dynamic in its direction of action, and this in combination with a complex response from the structure, distributes about the mean the direction of forces acting on different parts of the structure. The distribution of force directions may approach uniform randomness. Given this, dynamic wind loading seems a better explanation for the cross-sectional symmetry of branch shoots. Because wind force loading is likely to peak to much greater amplitude than background static forces due to gravity, it is likely to exert a larger selection pressure on the structure. Thus the evolutionary process of design by natural selection would tend to result in tree branch geometries adapted to wind forces and not gravitational self loading.

Wind drag exerts a distributed load on a shoot proportional to the area of material (shoot and foliage) perpendicular to the direction of wind velocity [Mayhead, 1973], so that the moment exerted at the shoot base is

$$M \propto \int_0^L A_p \, dl \tag{4.5}$$

where A_p is the area perpendicular to the wind and L is the length of the shoot.

This has interesting consequences for the allometry of shoots. For example, if the stiffness of the shoots were small (either their diameters or elastic modulus small), then shoots would deflect greatly when subject to wind forces and would tend to align with the direction of the wind vector, thus reducing the wind loading force. As the deflection of shoots increase, the strain in their tissues increases and may reach the breaking strain resulting in failure. However, as the diameter of shoots is reduced, the strain in the tissues declines in proportion for a given radius of curvature because strain is proportional to Kd. This suggests a different strategy

for branch geometric design: low investment costs result from small diameters of shoots which have a low stiffness and therefore deflect easily with wind loading and so quickly reduce the magnitude of the wind loading and so reduce the risk of mechanical failure. The low investment cost would compensate for the loss in exposure of foliage to light resulting from the more pendulous branches of this type of design. It is possible that such trees as cedar and birch follow some design principle of this sort. Following this argument, the stiff branches found in Sitka spruce are at a disadvantage in the presence of wind loading.

It has been suggested by Mattheck [1991 (private communication.)] that the pattern of shoot thickening in Sitka spruce branches, which gives some shoots (those of lower topological generation) greater thickening than the requirement for static loading due to gravity, could be explained by dynamic wind loading. It is possible that the shoots furthest from the branch base are most exposed to wind loading and therefore require more stiffening: this could partly account for shoot thicknesses being correlated with their generation.

• 4.2.2 Respiration losses in shoots

Respiration incurs losses of carbon due to the metabolic processes in growth and maintenance of living tissues. Since these tissues are found in the outer layers of shoots and the shoot tip (terminal meristem), maintenance respiration losses in shoots are proportional to their surface area, so these losses rise in proportion to diameter times length. Growth respiration losses in any one growth season will also be proportional to surface area, but taken accumulatively over the lifetime of the shoot, they are proportional to the mass of material in the shoot. Similarly, material investment costs are proportional to the mass of material in the shoot, so rise in proportion to diameter squared times length. Thus the ratio of maintenance respiration loss to material investment costs is inversely proportional to shoot diameter, but growth respiration losses are proportional to material investment. Since growth respiration losses are linearly related to material investment, they have been included in the model by association with shoot mass.

Maintenance losses were not included in the model because they were expected to be insignificant in comparison with material investment and growth losses in shoots (although this is certainly not the case in other organs). Dark respiration, which includes growth and maintenance, was measured in shoots of Sitka spruce (including foliage) by Ludlow and Jarvis [1972] as being typically 6% of maximum net photosynthesis in field conditions. This value is highly temperature

dependent and changes with shoot age, but other than in exceptional circumstances, would not exceed about 10% of net photosynthesis [Jones, 1986]. From measurements made in this work, the ratio of dry mass of foliage to living material in the shoot axis is typically of the order of 10 in shoots under 4 years old. Thus it would be expected that maintenance of shoot axis material accounts for only around 1% of net photosynthesis. This quantity will increase with shoot age as foliage becomes less efficient and as the diameter of the shoot axis increases, but would probably remain very small in comparison with total investment and growth cost.

• 4.2.3 Including the branch's transport function (hydraulic modelling)

In chapter 1, the hydraulic transport function of branches was given mention, but this has not been included as a design criterion in the analysis presented in this work. The justification for neglecting it was that used by Morgan and Cannell [1988] when they assumed that mechanical constraints were more rigorous for distal shoots than hydraulic function constraints. They believed that the smallest cross-section area required for mechanical support has sufficient hydraulic conductivity to supply the foliage with water and noted the existence of totally pendulous lateral branches on some trees as evidence for this.

If the above assumption were incorrect, it might be appropriate to model shoot diameters according to the principle of the 'pipe model' which predicts cross-section area of shoot axes proportional to the total distal foliage area [Shinozaki, 1964]. This and the mechanical design principle may compete for prevalence in the tree shoots as they do in the scientific literature. Although measurements made in this work provide good evidence for the prevalence of the mechanical design principle, the hydraulic constraints should be given further consideration.

Niklas [1986] has considered both mechanical and hydraulic design principles in tandem. Niklas argued that as well as branching geometry influencing bending moments and light interception, it can also affect the flow of substances through branches and this may become a further design criterion in branch geometry. If this were the case, then the three major features of branch design : mechanical, light interception and hydraulic conduction might be integrated. Theories relating the resistance to fluid flow in branched conduits and branching angles are based on fairly high Reynolds number flow so that the flow is dominated by inertial forces. In contrast flow in plant tracheids is dominated by viscous forces.

However, the discovery of 'hydraulic constrictions' [Zimmermann, 1978] at branch junctions, which may serve to localise the formation of embolisms when the plant is subject to water stress, shows that conduction may be sensitive to branching angle at crucial points in the vascular network.

On this basis, Niklas constructed model trees with axes (links) labelled in a way which encoded the sequence of dominant to subordinate paths taken in a route from the base to any apex of the tree. fig 4.3 shows an order four Sitka spruce branch labelled in the same way: axes marked 0 are dominant (lower branching angle) whilst those marked 1 are subordinate (higher branching angle). This leads to an alternative model of branch design based on the assumption that material flows through the branch from base to apices following a path of least resistance.

This view may be countered by pointing out that flow is frequently in the basepetal direction, but a possible interpretation of this model is that a diffusion gradient of some growth regulator emanating from the dominant 0-internode apices (meristems) is set up within the network. However it is still true that acropetal flow of water is necessary to maintain photosynthesis and terminal axes may compete in demand for this water, or the architecture of the branch may be arranged so that in times of severe water stress, the less important sub-branches would be sacrificed by catastrophic embolism as suggested by Zimmermann [1978]. What is meant by 'most important' here may not simply be a matter of greatest material investment, but also depend on the net relative net export of the sub-branch to the whole organism, which would in turn be a function of light interception and age. Thus dominant paths leading to shoots which are exporting relatively higher net gain would be paths of least resistance at shoot junctions.

Following this model, an order four branch can be constructed in which the lengths and diameters of links are determined by the number of dominant (0) axes passed through when tracing back to the branch base from each particular axis. Such an arrangement is shown in fig 4.4 where diameters are set at junctions in the ratio 4:5 between 1-axes and 0- axes (compare with branch designs shown in figs. 2.10 and 2.15) As table 4.1 shows, this reproduces a generation dependent geometry.

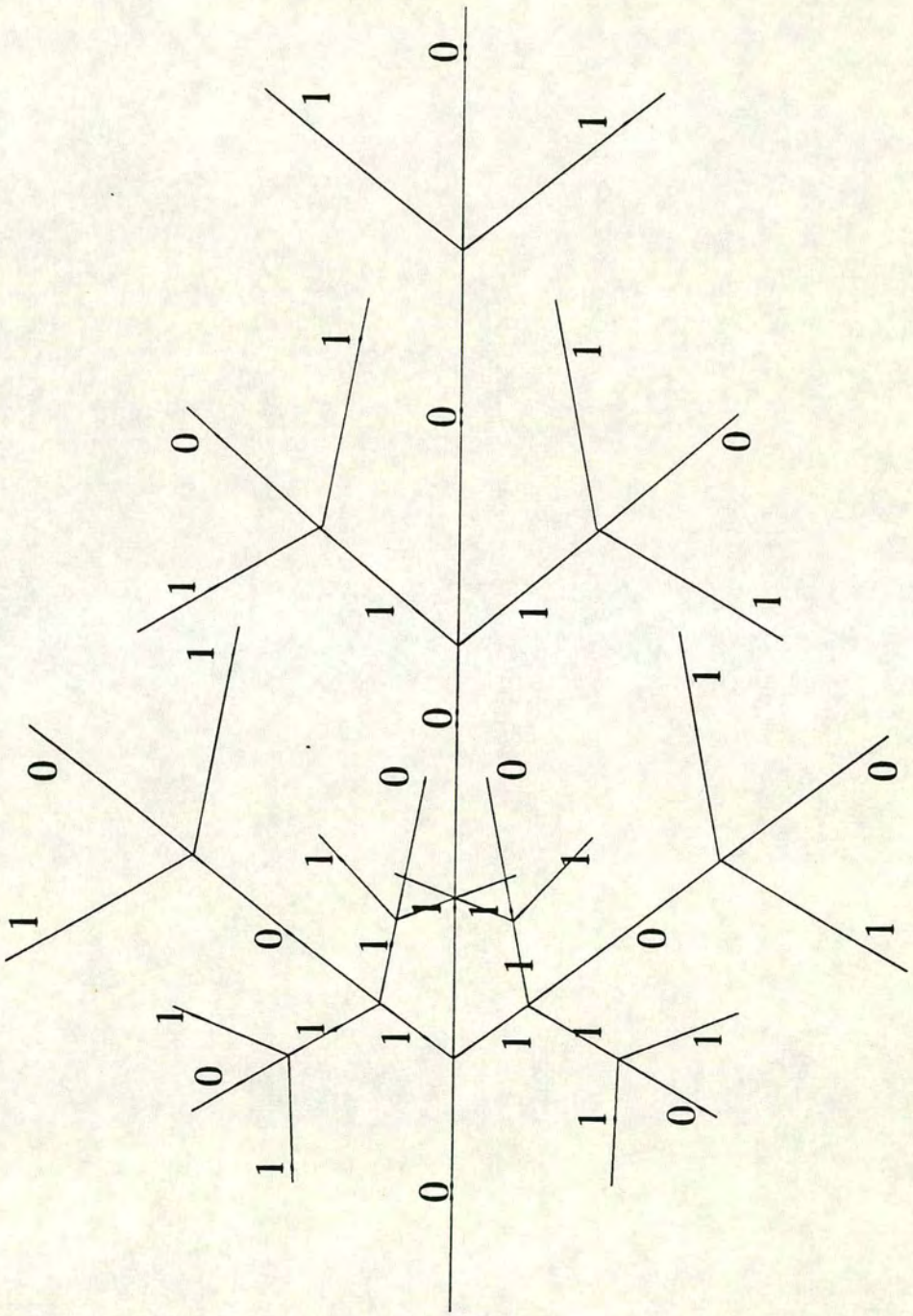

Fig 4.3. The binary labelling system suggested by Niklas [1986], applied to the Sitka spruce topology. At each junction, the link which continues in the same direction is assigned the binary value 0, whilst the other two are assigned 1. The shoot apicies are thus each labeled with an m bit word, where m is the branch order.

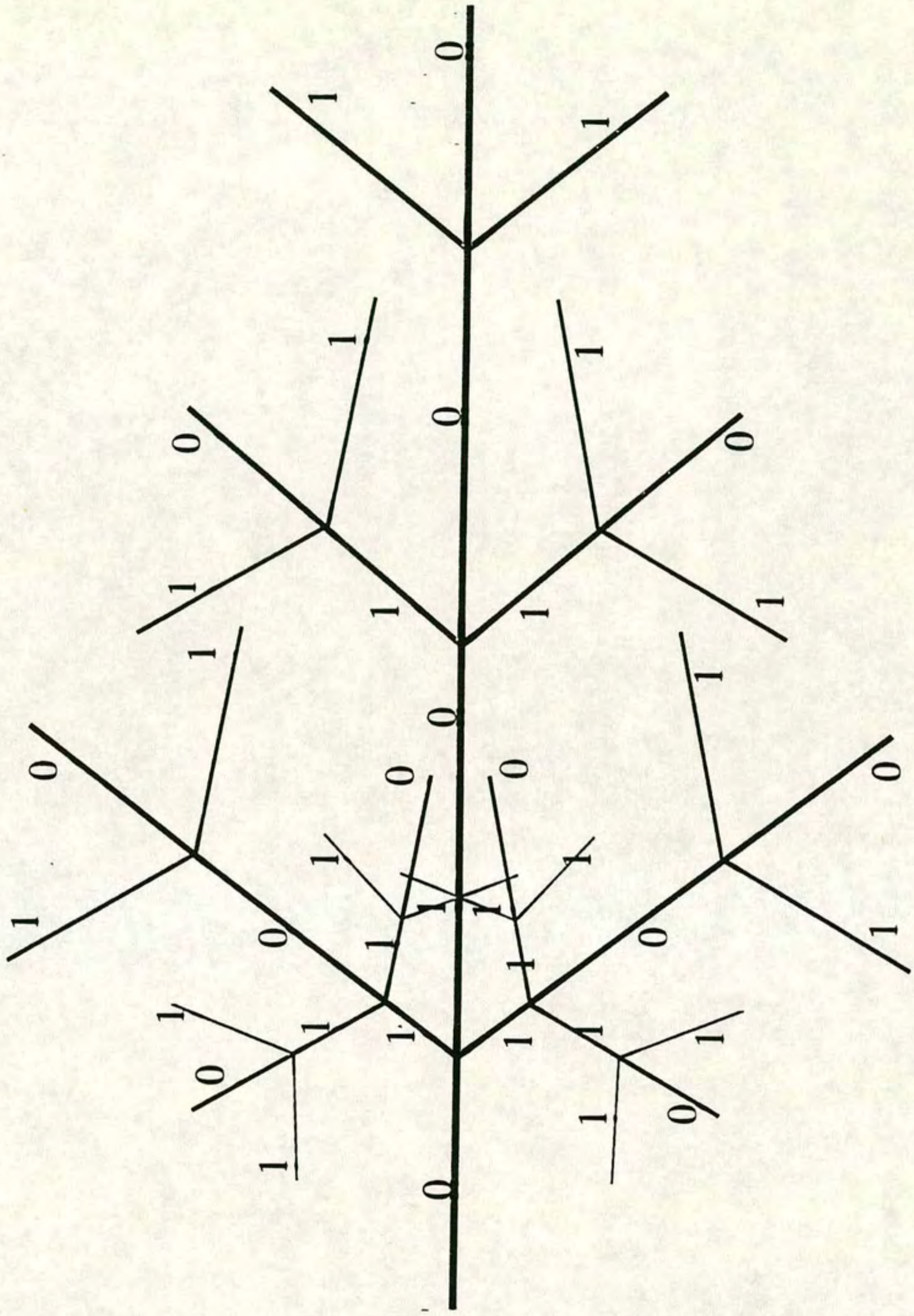

Fig 4.4. An order 4 branch with link diameters determined by the sequence of dominant / subordinate shoots on the path between the branch base and the link in question. At each junction, diameters of subordinates are reduced in the proportion 4/5 to the dominant. This gives rise to a model of link dimeters based on Zimmermann's theory of hydraulic constrictions [1978] which may select less valuable shoots for sacrifice during accute water stress.

shoot	path	path rank	generation	rank	rel. diameter
1	0000	1	1	1	1.0
2	0001	2	2	4	0.8
3	0010	2	2	3	0.8
4	0011	3	3	4	0.64
5	0100	2	2	2	0.8
6	0101	3	3	4	0.8
7	0110	3	3	3	0.64
8	0111	4	4	4	0.51

Table 4.1: relative diameter of shoot axes according to Niklas's model based on dominance expressed through the hydraulic architecture of branches

Shoot apices are labelled as in fig 4.3. The path is a binary sequence of links from the branch base to a shoot apex. The number of 0-ranking links in the path gives the path rank which is then compared to the generation and rank of the shoot as defined in section 2.1.3. In this model, the diameters of shoots depend on the path rank because at nodes, lateral (1) diameter to leader (0) diameter is in the ratio d1/d0 which, by way of an example is 4/5 here.

- 4.2.4 Taking risk into account.

The paradigm lying behind the concept of optimisation of form to achieve the highest photosynthetic return for the minimum investment of material resources is fundamentally an economic one. The optimal plant according to this economic analogy is one that allocates resources so as to maximise biomass accumulation. This view rests on the assumption that maximising biomass accumulation confers a higher fitness to the plant and will therefore be preferentially selected over evolutionary time. This view has already been criticised in chapter one for relying on too narrow (and anthropocentric) a criterion for fitness, but if the discussion is restricted to one of how best can tree branches be 'engineered' to achieve maximum biomass accumulation in the tree, then it may be valid. In classical economic theory, the risks of investment and loss of gains to competitors are not taken into account, although later developments have included risk as a factor.

For the growing tree, risk must be an inherent factor of resource allocation. Investment in foliage and shoot extension to achieve higher photosynthetic yield

quickly, runs the longer term risks of a) loss due to mechanical failure of shoots resulting from a declining margin of safety, b) loss due to embolism in a time of high water stress because of the additional water demand of photosynthetically active organs or c) loss due to herbivory of less well protected tissues. On the other hand an over cautious strategy which invests heavily in safety, not only leads to a less efficient system, but runs the risk that resources in the future will be unobtainable because a neighbouring plant in competition with a higher resource acquisition rate has taken them first. Thus a fuller description of resource allocation economics demands that the risks of tissue and resource access loss be incorporated explicitly into the model. Any sensitivity to risk in natural tree branch design, would, of course, have to come from natural selection since the growing plant can not respond to potential factors, only actual ones. For example a branch can not grow in anticipation of a wind storm occurring with a mean frequency of once every ten years. It can only either survive or fail in that storm and be thus selected. If the loss causes a loss in fitness to the tree which carries over to its breeding success, then an adequate margin of safety to survive the storm will be incorporated by natural selection in the progeny of affected trees.

4.3 Further developments of the branch model

4.3.1 Improved light interception modelling

The model showed a relatively high sensitivity to light incidence angle. This suggests that the way in which the light regime of the branch is defined is very important. Sensitivity analysis is of crucial importance to research using mathematical models because it reveals areas where expansion and increased sophistication may be profitable and conversely where simplifications can be made. The analysis carried out in this work suggests that an improvement in the representation of light interception and in the description of the light environment of a branch would prove profitable.

The model presented in chapter 3 has some modest provision for extending the description of incoming light by including an arbitrary number of rays. These can represent any angle of incidence from 0 to 180° and can be weighted according to any filter function to represent the intensity varying with incidence angle. In addition, a distinction between sun and shade shoots (which perform differently from one an other in different light regimes) could be made simply by suitably weighting the contribution made by sun shoots to net photosynthesis.

Two important developments are proposed to improve the light interception modelling. The first relates to the fact that the model so far only deals with the unit projected area *Ap/A*, but this alone can not be used to represent the crucial factor - net photosynthetic yield. This is because the photosynthetic rate is not a linear function of photon flux density (light intensity) for foliage. Thus the variation of *Ap/A* based on Norman and Jarvis's investigation [1976] is not sufficient to describe the relative benefit of different branch designs, but must be combined with a function relating the net photosynthesis to light intercepted and to the angle of incidence of the radiation.

Such relations for coniferous foliage have been investigated experimentally and by theoretical modelling by Oker-Blom et al. [1983] and in Sitka spruce specifically by Leverenz and Jarvis [1979]. Furthermore, Leverenz and Jarvis [1980] demonstrated that a leaf on a plant which has most of its foliage shaded will have a different capacity to photosynthesise than will a leaf which has grown at identical photon flux densities, but on a plant on which most of the foliage is not shaded. Thus the photosynthetic efficiency of foliage, of shoots and of branches depends on the light flux falling on the whole tree as well as the local intensity and direction of illumination. Carter and Smith [1985] studied the influence of shoot structure on net photosynthesis of conifer shoots under field conditions. They found that the 'silhouette leaf area to total leaf area ratio - STAR' was less in sun shoots (which had more needles per unit length) than shade shoots. Needle mutual shading and an increased inclination of needles towards the vertical accounted for the reduced STAR of sun shoots. However, relatively low light saturation levels in the foliage meant that despite the mutual shading and disadvantageous foliage inclination, photosynthesis per unit leaf area was no less than in optimally displayed foliage. Thus, in the field conditions studied by Carter and Smith, the effect of branch geometry on the orientation of sun shoots would have little impact on their net photosynthesis. What is more, photosynthesis (measured by photosynthetic CO_2 flux density per unit leaf area) was shown to be almost insensitive to photosynthetically active photon flux density above 100 $\mu mol.m^{-2}s^{-1}$ in shade shoots. Therefore unless shading is very great (e.g. low in the crown), the performance of both kinds of shoot will not be greatly influenced by shoot orientation. The very low saturation points of needles in Sitka spruce observed by Leverenz and Jarvis [1979] rather supports the view that under natural lighting conditions near the top of the crown, net photosynthesis of shoots would be relatively insensitive to shoot orientation. On this basis, it would be legitimate to modify the light interception model used in this work by relating net

photosynthesis directly to leaf area rather than through projected area (or silhouette area).

The second development suggested relates to the modelling of shading from other shoots within the branch and from other branches. The geometric treatment of shading in the model given in chapter three is very crude indeed, although, to some extent the arguments given above concerning shoot orientation also apply to shading. However, especially when obstructions to incoming light are close to foliage, their effect on photon flux density can be large. Between branch shading is a matter of tree geometry at a scale higher than that considered in the main part of this work. Within branch mutual shading of shoots, however is strongly influenced by branch geometry and could be incorporated into the model.

Because in this model, the spatial distribution of shoots and therefore foliage are known explicitly, the effect of shading from over-topping branches and from self shading within the branch can be calculated exactly. Whitehead et al. [1990] gave an expression for the probability p of a light beam passing through a tree crown, when the actual foliage distribution is known, by dividing the space into a grid of voxels

$$p = \exp\left\{-k \sum_{i=1}^{n} d_i \, s_i\right\} \qquad (4.6)$$

where k represents the fraction of leaf area that is projected onto the plane normal to the beam (=Ap/A in the notation used previously) and d_i and s_i are the leaf area density and light path length within the ith voxel and n is the number of voxels the light beam passes through to reach the ith. Over all solar angles, the total probability of penetration to the *kth* voxel is given by

$$P_k = \int_{-\pi/2}^{\pi/2} \int_{-\pi/2}^{\pi/2} p(\theta,\varphi) \sin(\theta) \cos(\theta) \sin(\varphi) \cos(\varphi) \quad d\theta \, d\varphi \qquad (4.7)$$

where θ is the solar zenith angle and φ is the azimuth. Any distribution of leaf area density can be represented by the voxels which could be arranged in a Cartesian grid containing the branch. Taking each voxel containing a portion of the branch, P_k could be calculated to give a total light availability to that portion. This result could feed directly into a classification of shoot productivity within the branch.

Finally, because the foliage of Sitka spruce is arranged along the shoot in a spiral which is formed before shoot extension, the number of new needles for each year's growth increment is pre-determined. The foliage, being of limited size and shape is constrained to occupy a cylinder centred on the shoot axis with radius approximately equal to the sum of shoot radius and needle length. The density of foliage along the shoot is thus set by the length of shoot extension made in the annual growth increment (density around the shoot is set by shoot diameter). Variation of foliage density with shoot length has not been accounted for in this work because foliage has been considered as a constant number of needles per unit length of shoot. One consequence of this assumption is that gains in foliage efficiency due to reduced mutual shading of needles as foliage density decreases are not included with the advantages of increasing shoot length, but this is not expected to be an important omission in most cases. More seriously, the extension of a shoot to reach higher light flux will not yield as great an increase in light interception from a fixed number of needles as given the assumption of constant needle density: fewer needles would be exposed to the higher light levels. This may have resulted in a significant error in the estimation of the relationship between light regime and optimum length extension. Thus an improved light interception model should replace the constant foliage per unit length assumption with one based on a pre-set number of needles distributed along the shoot length.

- 4.3.2 Improved geometric description

The limitations of the model were set out in section 3.1.2 and among them were mentioned those resulting from a simplification of the morphological description. This simplification was also used in the analysis of natural branches: it was described in section 2.1.2. Clearly, the model does not express a full description of branches most likely to be encountered in nature. However, this does not mean that weight and light intercepting surface has been erroneously ignored leading to incorrect calculations because the model branches, although simplified are self consistent. The laws governing the distribution of stresses in the branches and the light interception of their foliage apply to the simplified description as well as a fuller one. When the mass of branch material was measured in the analysis of real tree branches, the whole structure was measured - including interlaterals and additional whorl shoots. Thus relationships between lengths, diameters and weights of parts of the branch remain legitimate.

However, the comparison of model branches with the measured branches falls down, not only in the absolute magnitude of parameters, but also in the relations

between them. For example, the ratio of diameter of a basal link to the mass distal to it will depend on the properties of interlateral and additional whorl shoots. In turn the relation between this diameter and the length of the shoot, or link will be influenced by the mass which was left out from the model.

Thus, the most important additions to the model to improve comparisons between it and the measured material would come from allowing lateral whorls to include more than two laterals and from the inclusion of interlateral shoots. In practice, if the turning moments of daughter shoots do not strongly interact with the parent's deflection (as has been concluded), then these extra shoots could be represented as point loads and moments acting on the parent.

• 4.3.3 Extension to whole tree growth modelling

One possible aim which builds on the description of branch design and performance given in this work is to simulate tree growth. The simulation could take account of mechanical and light regime constraints using the branch design objective function as a driving force for setting the parameter values. This could be arranged to maximise, say stem wood production. A model of this type has previously been described by Ford et. al. [1990], though with a simpler branch description and without lateral turning moments being included. It would be sensible to move on to tree growth modelling once the simplifications to the model described here are made (see section 3.7.2).

One factor which must always be remembered when considering the effectiveness of branches in real trees is that they are not stationary, permanent structures, but a result of a continuing growth process. As primary growth is carried out in a series of pulses of activity during which reiteration of shape extends the branch and increases its complexity, growth can be represented as the transition between successive branch orders : one for each year. Thus, the change in objective functions through time can be predicted and the quantity of wood mass increase from secondary growth needed to maintain a certain condition such as an optimum foliage-to-branch mass-ratio can be measured. These growth considerations may provide insights into the constraints made by growth behaviour on design strategy. Unfortunately, The model has not worked sufficiently satisfactorily to carry out that experiment. As an objective for the future, the branch growth model based on carbon economics which is shown in fig. 4.5 could be developed. This system would have the advantage of offering a model of growth which both dynamically accounts for carbon and finds the maximum possible growth or export potential

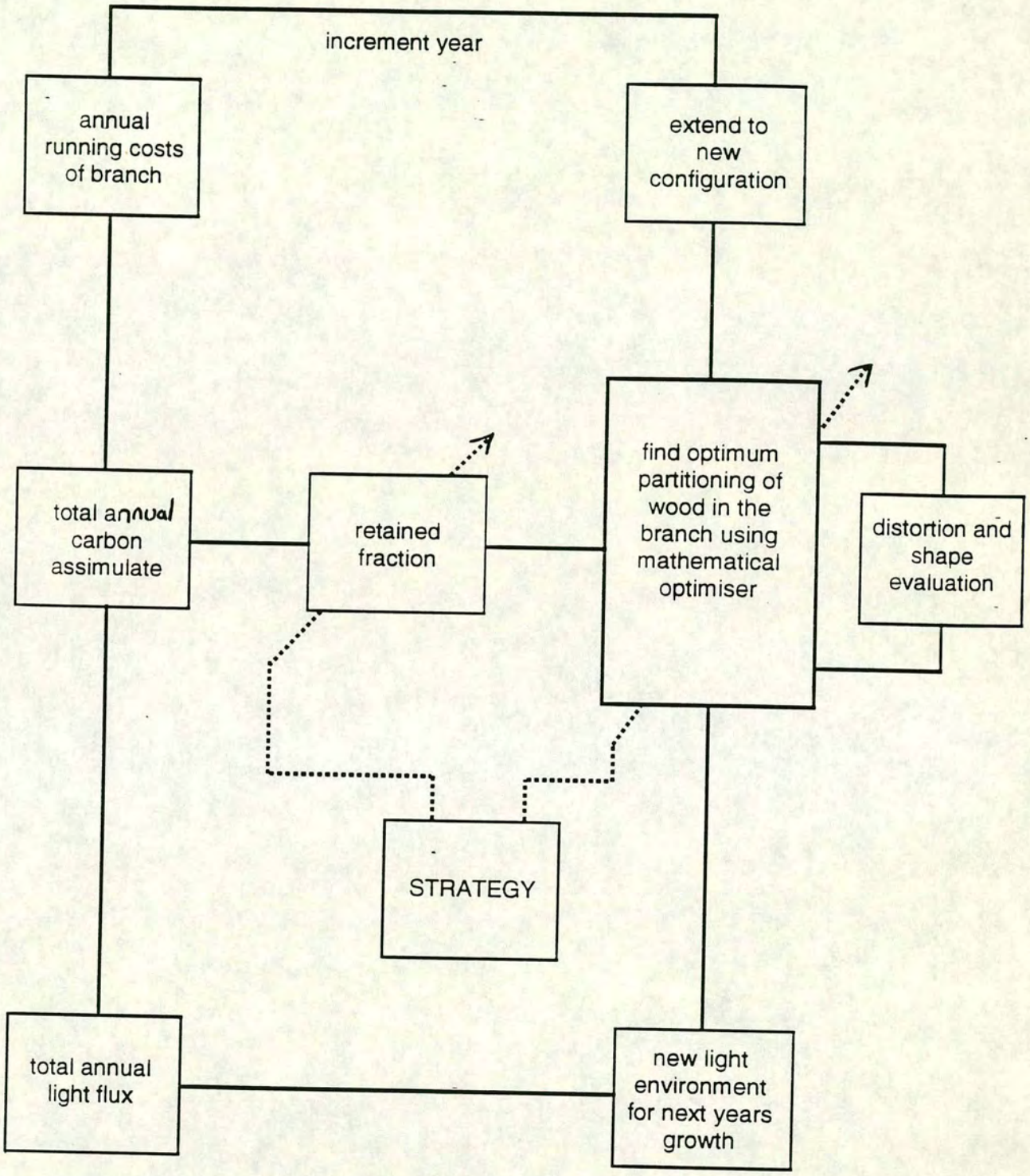

Fig 4.5. Proposal for a branch growth model based on carbon budgeting and dynamic optimisation. The growth in each year is dependent on the net product of the previous year and is distributed among existing links and the creation of new links according to the principles of optimal design. The geometry of the previous years branch sets a geometric constraint for the growth.

from dynamic optimisation during the simulated growth process. In other words, carbon allocation at each stage in the model of growth can be directed towards optimum growth or export of photosynthate.

- 4.3.4 Inclusion of a hydraulic model

Section 4.2.2 reintroduced the hydraulic transport function of branches and argued that it might have an important role in branch design. Niklas [1986] suggested a way in which mechanical, light interception and hydraulic functions can be integrated into one model for predicting optimal design. This can not be achieved simply by the inclusion of the pipe model, since this and mechanical optimisation give rise to conflicting design principles. A feedback mechanism was proposed instead, which relates both the hydraulic requirement and the growth potential of a shoot to its light interception. The relative vigour of shoots within the branch is determined by their relative light interception. Diameters among shoots would diverge according to the annual increments due to each of them according to light interception and therefore hydraulic need and growth ability. This model is a dynamic one with shoot diameters being calculated by the history of successive annual increments in length and diameter. If a loss in light interception resulted from large deflection of the shoot because it was failing to meet the full demand of mechanical support, then it would loose rank in the branch and grow less vigorously. This sets a limit to the ratio of diameter to length growth in order to maintain the dominance of leader shoots which achieve the greatest light interception and therefore growth rate. Thus the mechanical constraints act to quantify the minimum allocation of resources to diameter growth for a given length extension. The further development of the model in this work along these lines is likely to provide useful insights into the relationships between mechanical, hydraulic and light interception influences on branch growth.

- 4.3.5 extension of the model to include dynamic forces

In section 4.2.1, it was made plane that a more realistic description of the mechanical requirements of branches would need a description of the effect of wind loading on the system. This would have to include an analysis of the dynamic behaviour of the branch system as it responds to dynamic (changing) forces : the transfer function, or impulse response of the branch system would have to be calculated. The appropriate theory to describe the dynamic behaviour of a single shoot (perhaps with some minor modification) is available in the literature (e.g. Baker & Bell, 1992), but the connection of the shoots in a hierarchical network and

the consequent interactions of moment, shear force and angle of attachment among the shoots would pose a major challenge to computation. The technique developed in this work and described in section 3.3.5 and Appendix 2.2 which is intended to deal with the inter-shoot interactions should serve as a good basis from which to build a computational method that will solve this problem. It is further possible that consideration of shear forces alone would not be adequate for a description of the dynamic behaviour of interconnected shoots and torsional forces would have to be taken into account. Suffice to say that the development of the mechanical model of a tree branch from static to dynamic would involve a very considerable increase in computational complexity.

- 4.3.6 extension of the model to include other species

The model and to a lesser extent, the empirical analysis of branches has been closely related to the basic topological form of Sitka spruce branches described earlier. This sets a constraint for the extension of these techniques to other species. However, most, if not all species of spruce share a common branch topology and the extension of the methods described here to other spruce species would be a simple matter. Among conifers, repeated rigid rules of morphogenesis are most common and topological descriptions which can be used in the same way as in this work would not be difficult to find. This is the case for a number of angiosperms too, though many show considerably more stochastic development. Observation of other tree species quickly reveals the fact that there are a wide variety of working solutions to the basic problem of matching form to function in tree branches. The possibility of different strategies being followed by species might be studied by comparison of species with different branch forms. For example the birches grow with distal shoots having a much lower diameter to length ratio than do the spruces or many other trees. This does not necessarily mean that they more frequently fail mechanically due to wind loading, since they are considerably more flexible than the shoots of Sitka spruce, having a minimum radius of curvature before failure at least an order of magnitude less (see the discussion in section 4.2.1).

The advantage of selection for more efficient branch designs might be much greater in species with a smaller light extinction coefficient or smaller specific leaf area index (see section 1.2.1). If the methods developed in this work were adapted to such species then they are likely to provide a useful tool to guide any breeding program for more efficient branches by providing a goal and the theoretical constraints to its achievement. The application of the principles used in this work

have already proved useful in developing an understanding of the evolution of plant form and function Niklas [1992]. They could also prove useful in comparison of strategies or forms among species occupying contrasting ecological niches to gain a deeper understanding of the ecological significance of plant architecture [e.g. Küppers, 1989].

• 4.3.7 Widening the optimisation goal

The failure of the optimisation simulation in attempting to reproduce recognisable tree branch design may be attributed to the narrowness of the optimisation goal.

The observed geometry of tree branches is the evolutionary consequence of two principle requirements made by the plant: the interception of light and the transport of materials. These requirements of the plant are subject to physical constraints which at least limit the range of possible form. The mathematics of light geometry, the mechanics of structures subject to physical forces (both static and dynamic) and the hydraulics of viscous transport set these limits. In addition, the display of reproductive structures must be accommodated by the branch geometry. It is all together possible that these constraining physical laws act to produce conflicting optimisation demands on the structure.

In chapter three it was shown that even with one simple optimisation criterion, with constraints limited to a single static mechanical force and a very simple description of light regime, geometrical parameters were driven in opposite directions by the physical constraints. It was not obvious how to define an appropriate weighting (expressing relative importance) to simulate the natural competition between these requirements. For example, simply combining the optimisation goals of maximising light interception and minimising material costs in a ratio led to the domination of mechanical constraints and predictions of optimal form which were unlike those observed in real Sitka spruce branches: laterals were reduced to an insignificant size during optimisation and vertical branch angles were reduced in opposition to the phototropic response.

It is likely that the evolution of branch geometry is in large part the result of reconciling conflicting design requirements. Given this, it has been concluded [Niklas, 1986] that there is no single optimal design. Instead, there are numerous optimising solutions whose probabilities of survival depend on the particular environment occupied by the plant. Thus the relative importance or weighting of optimisation goals varies from case to case depending on the environmental

circumstances. An attempt to widen the optimisation goal further to include the demand for transport of materials within the branch would increase the dispersion of potential optimising solutions and add a further dimension to the function expressing the relative importance of the design requirements.

The problems by no means stop there when considering a more realistic optimisation: the environmental circumstances which act to 'select' a particular solution may themselves be subject to temporal variation. Perhaps more significantly, the tree branch (and the tree itself) changes in geometry as it grows, so that different circumstances apply at different points in the development of the structure. Furthermore, the physical geometry arrived at, at any given time, sets a strong constraint on the geometry which can be achieved by further change. In short, the ontogeny of the tree sets an important constraint in optimisation.

The comments made above are not intended to be an argument against widening the optimisation goal, since it is likely that the narrow definition of it used in this work is one of the factors which has led to a disappointing simulation result. However, the added complexity sets tight requirements for the further development of the idea of simulated optimisation of form.

Probably the most crucial change in approach necessary for widening the optimisation goal would be to take account of the ontogeny of branches. This would be achieved simply by restricting the variable geometric parameters to the diameters of links and the lengths and angles of only the current year's growth, leaving the other parameters fixed. This gives an entirely different perspective on design - one which reflects the real design problem far more closely. An optimisation of say an order three branch would then require first an order 1, then an order two branch to be constructed according to optimisation goals and the order three branch would be developed from the existing order two geometry. A fixed total mass of material could be made available and the problem would become one of optimal allocation of carbon.

• 4.3.8 Including risk in the resource economics

A cost-benefit model incorporating risk sensitive discount rates has been suggested by Lerdau [1992] for the improvement of plant resource allocation models. This offers a reasonably accessible means of incorporating risk into the model presented in this work. If such a development were carried out, it may provide valuable new insights with a direct bearing on the problem of shoot length to diameter ratios and the way they depend on shoot rank and generation.

• 4.4 The implications of this work

• 4.4.1 Implications for understanding branch form and function.

Measurements of branches from Sitka spruce trees and the theoretical modelling of branch form were intended to develop an understanding of the relation between branch form and function in terms of static mechanical loading and light interception geometry. This definition of branch function described only a limited set of the total function of branches as discussed in section 4.2 above. In chapter 2 it was concluded that the measured branch form did not obviously reflect the function as it is defined here and as a result one of two conclusions must be drawn. First, it is possible that the limited definition of function excluded an important component which if included would account for the observed branch form. Second, the underlying assumption that natural processes have led to an optimised form may be incorrect and the observed form may simply be an arbitrary selection from an infinite variety of permissible solutions matching form to function. It may be, in this case, that form is primarily dictated by genetic constraints which have been inherited over evolutionary time and that natural selection has not acted strongly on branch design to force optimisation. If the simulation of branch optimisation developed in chapter three had proved more successful in describing the branch morphology space over which branch performance varied, the question as to which of these conclusions to take might have been resolved. There was, though, no firm conclusion to be drawn from the simulation exercise other than that it was failing to adequately model the relationship between form and function. To address the problem with empirical studies would necessitate an inter species investigation of branch allometry so that widely contrasting designs could be compared and a pattern sought which might

reveal at least the underlying boundary to possible solutions to the problem of form and function.

The shoots within branches simultaneously provide mechanical support and transport of materials. The tree compensates for the increased mechanical and hydraulic demand from the growth of foliage and the need for extension to achieve higher light capture by augmenting shoot diameters through the activity of lateral cambium (secondary growth). Each new layer of secondary xylem functions for a year or more, primarily as a transport tissue. This function is gradually replaced as the vascular cambium expands in girth to accommodate new layers of secondary xylem. Over the years, each layer of wood is progressively internalised as the cambium advances outwards and its role becomes primarily mechanical. The question remains as to whether the stimulation of secondary growth develops from the initially dominant demand for the transport function, or from an anticipated demand for the mechanical function some time in the future. Efforts to separate these two responses by observing form in Sitka spruce tree branches have been made difficult because they are complimentary. However, to find that secondary growth is distributed in a way which can more easily be explained by a hydraulic argument than a static load bearing one (see section 4.2.3) suggests that the hydraulic architecture may still influence secondary growth after the point at which Morgan and Cannell [1988] noted 'the smallest cross-section area required for mechanical support has sufficient hydraulic conductivity to supply the foliage with water'. They assumed that because the hydraulic function was no longer limiting, that its influence would not be seen in branch form. Under optimal design this might be the case, but there is evidence from chapter two to suggest that even so, hydraulic architecture is still echoed in the design. In the discussion of chapter two, it was suggested that the expression of shoot autonomy might result in this pattern being observed. Only by contrasting widely differing forms such as vines which have relatively small mechanical needs and swamp plants which have relatively small hydraulic needs might this question be resolved further. Taken as a population the shoots which were measured conformed to a geometrically similar allometric model which suggested that the young branches (none older than four years) were expressing a 'sapling-like' growth habit where shoot extension takes precedence over mechanical safety.

- 4.4.2 Implications for yield improvement.

Only subtle differences were found in the design of branches among the four provanences measured. Not enough replications of genotypes were measured to draw conclusions at that genetic level, but again, it seems likely that only relatively small repeatable differences in branch geometry exist. The range of opportunities to make improvements in branch design by means of a breeding program are therefore likely to be limited in Sitka spruce. However, these findings may well give an incomplete impression of the true range of branch design within the species because all the trees measured were grown in the same plot, i.e. under the same environmental conditions. There may be considerable plasticity of form in response to environmental conditions which would not be revealed by the study carried out here. If this were the case it would be of interest to breeders aiming to maximise the efficiency of Sitka spruce as wood crop plants.

The importance of the geometric design of branches to harvest yield comes from two influences: the effect of geometry on light interception and so potential net photosynthetic yield and the effect of the efficiency of construction in terms of the total mass of carbon used to support and maintain the structure. Light interception in a Sitka spruce canopy changes with canopy age, but is extremely high, so the expected gain from improvement in this species can not be great, but the application of the concepts and, perhaps, the techniques in this work to other species might prove very useful in aiming for higher branch efficiency. It seems likely that with the model simplified in the way suggested in section 3.7.2 and after including an improved light interception model as suggested in section 4.3.2 , a valuable tool for studying branch efficiency will be available.

chapter 5

CONCLUSIONS

All structures, whether natural, engineered, inert or living are necessarily limited by having to exist within the laws of physics. When these structures are required to carry out some purpose (function) then their design must be appropriate to that purpose: form is related to function. When the function is expressed in general terms, it is likely that a wide variety of forms can satisfy the function. When the structure is a part of a system which competes with rival systems for the same resources and there is a process for the adaptation of form and for the preferential selection of more efficient forms through time, then a gradual movement towards an optimally efficient form-function relation can be expected. Within the developmental constraints of evolutionary history, this is what was expected of tree branches in this thesis. The study set up the hypothesis that branches are shaped so as to maximise total photosynthetically active radiation interception per unit of assimilate expended in branch material. This hypothesis discounted the significance of the fluid transport and sexual functions of branches and regarded developmental constraints only in so far as the underlying topology of the branch geometry was taken to be invariant: a property of the species. Thus, the central hypothesis was that branch form, within the topological constraint, was a result of optimising the display of foliage to sunlight using a minimum of structural support material.

If the hypothesis were true, then one result which would follow is that the diameters of branch elements could all be in predicted by the mechanical loads which they cary. In seeking to test this hypothesis, four discoveries were made: 1) Lengths of branch elements were distributed in relation to the topology of the branches, being greater for low topological generation elements, especially those distally placed (more externally growing shoots). 2) Branch elements follow a geometrically similar allometry (diameter proportional to length) in which the proportionality constant depends on the topological position of the branch element in such a way as to give a greater margin of safety in mechanical design to the more externally growing shoots. 3) An allocation model based on the mechanical design of shoots with respect to gravitational load was more successful in explaining the distribution of shoot allometry than one based on the hydraulic design pipe model. 4) Hydraulic design according to

the pipe model did not compromise mechanical design in terms of relative margins of mechanical safety, but rather re-enforced the pattern of distribution of secondary growth which favoured the more vigorous branch elements.

The observations summarised above were felt to lead to the following conclusions. 1) That the mechanical design of branches with respect to gravitational loading is an important factor of branch form. 2) That the relative mechanical strength of branch elements is related to their topological position which is a reflection of their light interception potential and therefore their importance to the tree: margins of safety are greater where the tree looses more from failure. 3) That the hypothetical function 'light interception per unit material investment', probably does not fully reflect the true biological function which includes hydraulic support for the foliage and that the assumption that form can respond exactly to function is likely to be an over- simplification in the presence of ontogenic and genetic constraints.

To aid the understanding of the relationship between form and function in Sitka spruce branches, a mathematical model was built which simulated the complex interactions in the static loading of a set of connected cantilever beams exhibiting large deflections. This model was integrated with a crude light interception model which calculated the total silhouette area of the branch from various incident light angles. Branch efficiency was defined as the total silhouette area per unit matter invested in the branch structure. This was calculated for a variety of computer generated branch designs. Multivariate stochastic sensitivity analysis showed that the vertical component of branch angle was the most important determinant of branch efficiency from among 15 design variables which include rules for the apportioning of matter among branch elements. Branch design was subject to a numerical optimisation procedure, maximising the silhouette area per unit branch mass. The optimisation procedure revealed serious weaknesses in the model which resulted in computation errors when branches expressed large deformations. Efforts made to solve this problem were not successful during the course of the work presented here. Consequently, no predictions of optimal branch form have been made. However, sensitivity analysis of the mechanical and light interception model revealed that considerable simplifications could be made to the model and further considerations of the model's weaknesses have led to suggestions for improved light interception modelling. A suggestion has been made for a new dynamic carbon budget growth model based on form-function optimisation with these changes in place.

The study of complex ramiform structures and of optimisation principles in biology are both rapidly developing fields aided by advances in computer technology. The work presented here has combined aspects of both in a way which has broken new ground in the numerical treatment of complex systems. The aim of this work was ambitious and novel applications of techniques were sometimes necessary to surmount the problems encountered. It has finished with, perhaps more questions than answers, but, has demonstrated many of the possible techniques (multivariate statistical, iterative programming and numerical optimisation) which could be brought to bear in a future study. The conclusions about branch form and function - the design principles followed by branches - are more a stimulus to further study than the last word on the matter. The complexity and uncertainty of interactions and the natural variability of biological material made firm conclusions very difficult to derive. This work provides further and stronger evidence for the multiple goal, multiple function model of tree branches and points to new directions of research to resolve questions of form and function: which of the functions, under which circumstances, dominates the demands of design and to what extent are branches optimal in design.

Finally, it seems appropriate to quote from the end of Niklas's text on Biomechanics [1992]:

'*Debates in biology, unlike those in the pure physical sciences, are rarely canonically resolved. There is no equation for adaptation, nor are there any currently known formulas to adequately assess the prevalence of adaptive versus non-adaptive evolution in plants. But plants have evolved through a corridor in time and space defined in large part by the physical environment, one that is dominated by the laws of physics and chemistry and interpretable in terms of biomechanics.*'

Appendix

Appendix 1.1 - List of tree clone types used for the measurement of branches

CLONE		CORDOVA				SITKA				SKIDGATE				NORTHBEND			
			1		2		1		2		1		2		1		2
1	1	20	47		57	25	65		116	23				11	74		103
	2		48		58		66		117						75		102
	3		1	+	15		17	+	18		25		26		39	+	101
	4		2		16		122		123						40		129
			[1]		[8]		[9]		[23]		[13]		[27]		[20]		[28]
2	1	27	49		53	5	67		125	7	59		133	3	76		(78)106
	2		50		54		68		126		60		134		77		(79)105
	3		3	+	9		19		20		27	+	29		41	+	104
	4		4		10						28		30		42		43
			[2]		[5]		[10]		[24]		[14]		[15]		[21]		[22]
3	1	29	55		138	8	69		114	6	61		111	6	140		109
	2		56		139		70		141		62		135		80		108
	3		5	+	13		21	+	22		31	+	33		81	+	107
	4		6		14		120		124		32		34		(82)130		131
			[3]		[7]		[11]		[25]		[16]		[17]		[29]		[30]
4	1	21	2			14	71		127	18	63		136				
	2						72		128		64		137				
	3		7				23	+	24		35	+	37				
	4		8				118		119		36		38				
			[4]				[12]		[26]		[18]		[19]				
5	1	11	51														
	2																
	3		11														
	4		12	[6]													

Order of branches

Numbers in italics are actual genotype specifications.
Numbers in square brackets are tree numbers
Pairs of trees used in the analysis are indicated by '+'

Appendix 1.2 Summary of raw data from branch measurements.

SUMMARY OF DATA FOR BRANCHES ARRANGED BY ORDER

ORDER 1

Variable	N	Mean	Std Dev	Minimum	Maximum
WEIGHT	24	21.8083333	11.3015165	5.8000000	51.9000000
LENGTH	24	322.0833333	88.3657993	130.0000000	480.0000000
AGE COEF	N.A.	---------	---------	---------	---------
DEFLECT	13	0.0844615	0.0759853	0.0050000	0.2710000
TAPER	24	1.3999583	1.1555951	0.1400000	6.0200000
VERT ANG	22	73.8636364	11.5399738	45.0000000	90.0000000

Variable	N	Mean	Std Dev	Minimum	Maximum
WEIGHT	24	78.4375000	30.6706603	32.5000000	164.5000000
LENGTH	24	982.5000000	198.9155381	670.0000000	1460.00
AGE COEF	24	-0.0534583	0.3263054	-0.8420000	0.3750000
DEFLECT	14	0.1150714	0.0612843	0.0010000	0.2490000
TAPER	24	1.2768750	0.2331376	0.9330000	1.7990000
VERT ANG	22	61.3636364	13.0184684	45.0000000	80.0000000

Variable	N	Mean	Std Dev	Minimum	Maximum
WEIGHT	24	145.4916667	59.1289888	35.2000000	276.0000000
LENGTH	24	1705.79	477.9288631	725.0000000	2740.00
AGE COEF	24	0.1382083	0.1074701	-0.0550000	0.3600000
DEFLECT	21	0.2722381	0.4005399	0.0490000	1.5020000
TAPER	24	2.8764167	1.5252532	1.1680000	9.1290000
VERT ANG	24	50.8333333	16.1290089	30.0000000	90.0000000

Variable	N	Mean	Std Dev	Minimum	Maximum
WEIGHT	24	339.8666667	195.1440486	115.3000000	820.0000000
LENGTH	24	3266.83	880.8136390	1870.00	4970.00
AGE COEF	24	0.2031250	0.1463279	-0.0650000	0.4650000
DEFLECT	16	0.3461875	0.2797561	0.0350000	1.1590000
TAPER	24	3.9241250	2.9772905	0.3910000	11.9080000
VERT ANG	24	58.9583333	±8.7650905	25.0000000	90.0000000

SUMMARY OF LINK DATA BY BRANCH ORDER

ORDER 1 BRANCHES

Variable	N	Mean	Std Dev	Minimum	Maximum
LENGTH	22	319.0909091	90.8116361	130.0000000	480.0000000
WEIGHT	22	27.2844091	22.5201795	6.4430000	114.4590000
DIAMETER	22	6.3759091	1.6599818	3.7500000	9.7500000
TAPER	22	1.4229091	1.2020201	0.1400000	6.0200000
DJUMP	0	.	.	.	.

ORDER 2 BRANCHES

Variable	N	Mean	Std Dev	Minimum	Maximum
LENGTH	88	248.0681818	104.3959963	100.0000000	510.0000000
WEIGHT	88	27.1657955	40.0958678	1.5040000	264.9030000
DIAMETER	88	5.4946591	2.8823011	1.3800000	14.5000000
TAPER	88	1.4918864	0.9578552	0	5.5560000
DJUMP	22	0.9772727	1.2317938	-1.0000000	3.2500000

ORDER 3 BRANCHES

Variable	N	Mean	Std Dev	Minimum	Maximum
LENGTH	348	140.6522989	91.3221319	0	550.0000000
WEIGHT	348	11.3608621	21.1108421	0	134.1970000
DIAMETER	348	3.4362644	2.7351027	0	13.7500000
TAPER	348	4.0903190	26.9273779	-15.8730000	500.0000000
DJUMP	108	0.7504630	0.9065054	-5.0000000	3.0000000

ORDER 4 BRANCHES

Variable	N	Mean	Std Dev	Minimum	Maximum
LENGTH	753	110.7702523	87.1741902	0	500.0000000
WEIGHT	754	9.5841406	28.6606970	0	375.0000000
DIAMETER	754	2.6406499	2.9493924	0	20.7500000
TAPER	754	2.3170743	3.1499055	-7.5440000	33.3330000
DJUMP	313	0.6781150	0.6668852	-0.5000000	4.5000000

SUMMARY OF SHOOT DATA BY BRANCH ORDER AND SHOOT

ORDER 1 BRANCHES

Variable	N	Mean	Std Dev	Minimum	Maximum
DFL	13	29.6538462	26.1090538	1.5000000	83.5000000
DFLL	13	0.0844538	0.0758971	0.0045000	0.2708000
SW	24	21.8083333	11.3015165	5.8000000	51.9000000
SL	24	322.0833333	88.3657993	130.0000000	480.0000000
TAPER	24	6.4375000	1.6113558	3.7500000	9.7500000
AGE	24	0	0	0	0
AJR	24	1.3999583	1.1555951	0.1400000	6.0200000
LLRO	24	0	0	0	0

ORDER 2 BRANCHES

SHOOT 1

Variable	N	Mean	Std Dev	Minimum	Maximum
DFL	14	94.2500000	59.9197380	20.0000000	262.5000000
DFLL	14	0.1352857	0.0608040	0.0323000	0.2823000
SW	24	69.9125000	27.9523090	26.5000000	141.5000000
SL	24	656.6666667	136.1478310	440.0000000	980.0000000
TAPER	24	7.6484583	1.5896098	4.5000000	11.6250000
AGE	24	0.1406667	0.1598643	-0.1330000	0.4190000
AJR	24	1.2768750	0.2331376	0.9330000	1.7990000
LLRO	24	1.2620833	0.5303329	0	2.1720000

SHOOT 2

Variable	N	Mean	Std Dev	Minimum	Maximum
DFL	14	54.8000000	42.7880285	-7.5000000	170.0000000
DFLL	14	0.1049214	0.0621292	-0.0142000	0.2317000
SW	24	4.2750000	2.8953111	0.5000000	11.5000000
SL	24	162.9166667	35.6893806	110.0000000	240.0000000
TAPER	24	3.3099583	0.9380224	1.9380000	6.0000000
AGE	0	.	.	.	.
AJR	0	.	.	.	.
LLRO	24	0	0	0	0

ORDER 3 BRANCHES

SHOOT 1

Variable	N	Mean	Std Dev	Minimum	Maximum
DFL	21	110.2380952	45.4209806	45.0000000	215.0000000
DFLL	21	0.1330476	0.0548418	0.0556000	0.2654000
SW	25	114.1880000	50.5442572	25.7000000	223.0000000
SL	25	822.8000000	143.7089072	560.0000000	1320.00
TAPER	25	7.3203600	1.3620590	4.7500000	9.8830000
AGE	25	0.2544800	0.2766201	-0.8450000	0.6000000
AJR	25	1.2000800	0.4542721	-0.6500000	1.8950000
LLRO	25	1.8704800	0.8008413	0	3.8300000

SHOOT 2

Variable	N	Mean	Std Dev	Minimum	Maximum
DFL	21	82.1809524	41.9994955	27.5000000	181.3000000
DFLL	21	0.1160905	0.0612448	0.0504000	0.2627000
SW	25	4.4960000	1.1734848	2.4000000	7.5000000
SL	25	157.2000000	24.2418371	110.0000000	215.0000000
TAPER	25	3.0575600	0.5269341	2.1880000	4.1880000
AGE	0	.	.	.	.
AJR	0	.	.	.	.
LLRO	25	0	0	0	0

SHOOT 4

Variable	N	Mean	Std Dev	Minimum	Maximum
DFL	21	59.4523810	25.8177772	20.0000000	145.0000000
DFLL	21	0.1253381	0.0602549	0.0574000	0.3387000
SW	25	7.2320000	3.9041346	1.4000000	16.0000000
SL	25	231.9200000	58.4074553	105.0000000	325.0000000
TAPER	25	2.7564400	0.6748878	1.2810000	3.6880000
AGE	25	0.1757600	0.1367371	-0.0690000	0.5330000
AJR	25	4.0990400	2.9470173	1.3010000	13.3900000
LLRO	25	0.1705200	0.2586864	0	0.8600000

SHOOT 6

Variable	N	Mean	Std Dev	Minimum	Maximum
DFL	19	79.5736842	130.7603696	13.1000000	510.1000000
DFLL	20	0.3596950	0.7703477	0.0387000	3.1249000
SW	25	1.2400000	1.0766460	0	5.5000000
SL	25	55.3120000	29.5168782	0	95.0000000
TAPER	25	1.3150000	0.7520931	0	3.4380000
AGE	0	.	.	.	.
AJR	0	.	.	.	.
LLRO	25	0	0	0	0

ORDER 4 BRANCHES

SHOOT 1

Variable	N	Mean	Std Dev	Minimum	Maximum
DFL	16	175.1875000	124.8149130	20.0000000	587.5000000
DFLL	16	0.1597625	0.0761531	0.0225000	0.3193000
SW	25	233.2600000	152.0061923	44.6000000	683.0000000
SL	25	1057.40	207.2192880	725.0000000	1840.00
TAPER	25	8.0776800	1.6314275	5.4690000	12.7500000
AGE	25	0.3627200	0.1607424	0	0.7460000
AJR	25	1.2376000	0.3957320	0.8100000	2.7590000
LLRO	25	3.0097600	0.8937376	1.0640000	4.8150000

SHOOT 2

Variable	N	Mean	Std Dev	Minimum	Maximum
DFL	16	176.5312500	142.5559853	28.8000000	559.5000000
DFLL	16	0.1711375	0.1258637	0.0254000	0.5802000
SW	25	7.4760000	3.8817178	3.0000000	17.3000000
SL	25	151.2000000	25.6693722	115.0000000	205.0000000
TAPER	25	2.8250800	0.6812466	1.1880000	3.8750000
AGE	0	.	.	.	.
AJR	0	.	.	.	.
LLRO	25	0	0	0	0

SHOOT 4

Variable	N	Mean	Std Dev	Minimum	Maximum
DFL	16	119.3125000	81.9783051	25.0000000	402.5000000
DFLL	16	0.1478250	0.0692324	0.0278000	0.3027000
SW	25	16.1280000	8.0575803	4.0000000	30.3000000
SL	25	270.2000000	56.9261217	160.0000000	400.0000000
TAPER	25	2.9504000	1.0549048	1.8750000	7.1630000
AGE	25	0.2098800	0.1672330	0	0.5880000
AJR	25	3.0549600	2.4217309	-1.1370000	10.2830000
LLRO	25	0.2951600	0.4569516	0	1.9980000

SHOOT 6

Variable	N	Mean	Std Dev	Minimum	Maximum
DFL	16	99.3937500	73.7335335	38.8000000	352.5000000
DFLL	16	0.1677375	0.0930280	0.0521000	0.4217000
SW	25	16.0800000	10.0687636	3.1000000	39.4000000
SL	25	319.7000000	111.1641054	130.0000000	595.0000000
TAPER	25	2.4098800	0.9119515	1.0000000	4.9170000
AGE	25	0.2867200	0.2376202	-0.0790000	0.7660000
AJR	25	4.3092800	3.8218937	1.3610000	19.1480000
LLRO	25	0.2618400	0.4667822	0	1.9210000

SHOOT 8

Variable	N	Mean	Std Dev	Minimum	Maximum
DFL	16	164.1562500	154.3276945	16.3000000	563.9000000
DFLL	16	0.2263625	0.2358565	0.0194000	0.9095000
SW	25	1.9400000	1.6680827	0	5.9000000
SL	25	53.3000000	36.5983265	0	115.0000000
TAPER	25	0.9426400	0.6379680	0	2.0630000
AGE	0	.	.	.	.
AJR	0	.	.	.	.
LLRO	25	0.000200000	0.0010000	0	0.0050000

SHOOT 12

Variable	N	Mean	Std Dev	Minimum	Maximum
DFL	7	314.6714286	192.4606775	43.1000000	573.3000000
DFLL	7	0.5496714	0.3655042	0.0584000	1.0780000
SW	20	1.1600000	1.2491681	0	3.6000000
SL	20	0	0	0	0
TAPER	20	0.5860500	0.5751313	0	1.5000000
AGE	0	.	.	.	.
AJR	0	.	.	.	.
LLRO	20	0	0	0	0

SHOOT 16

Variable	N	Mean	Std Dev	Minimum	Maximum
DFL	15	132.7800000	171.8729522	16.3000000	515.8000000
DFLL	15	0.2898800	0.4930780	0.0260000	1.6602000
SW	24	2.6833333	1.9291058	0	6.4000000
SL	24	0	0	0	0
TAPER	24	0.8387083	0.5758017	0	2.0630000
AGE	24	0.1184167	0.1850184	0	0.6150000
AJR	24	3.9812917	3.9064279	0	11.4290000
LLRO	24	0	0	0	0

SUMMARY OF LINK DATA BY BRANCH ORDER AND LINK GROWTH YEAR

ORDER 1 BRANCHES

YEAR 4

Variable	N	Mean	Std Dev	Minimum	Maximum
LENGTH	22	319.0909091	90.8116361	130.0000000	480.0000000
WEIGHT	22	27.2844091	22.5201795	6.4430000	114.4590000
DIAMETER	22	6.3759091	1.6599818	3.7500000	9.7500000
TAPER	22	1.4229091	1.2020201	0.1400000	6.0200000
DJUMP	0	.	.	.	.

ORDER 2 BRANCHES

YEAR 3

Variable	N	Mean	Std Dev	Minimum	Maximum
LENGTH	22	328.6363636	96.6237403	180.0000000	500.0000000
WEIGHT	22	72.2972727	58.0682593	15.5000000	264.9030000
DIAMETER	22	9.4550000	2.2110841	5.2500000	14.5000000
TAPER	22	1.0415455	0.3793158	0.2480000	1.9400000
DJUMP	22	0.9772727	1.2317938	-1.0000000	3.2500000

YEAR 4

Variable	N	Mean	Std Dev	Minimum	Maximum
LENGTH	66	221.2121212	92.9601263	100.0000000	510.0000000
WEIGHT	66	12.1219697	11.9679412	1.5040000	71.8110000
DIAMETER	66	4.1745455	1.5690607	1.3800000	8.7500000
TAPER	66	1.6420000	1.0440369	0	5.5560000
DJUMP	0	.	.	.	.

ORDER 3 BRANCHES

YEAR 2

Variable	N	Mean	Std Dev	Minimum	Maximum
LENGTH	27	235.5555556	49.4845223	160.0000000	330.0000000
WEIGHT	27	61.3427778	33.7653600	5.5240000	134.1970000
DIAMETER	27	10.1296296	2.2790543	3.5000000	13.7500000
TAPER	27	0.9307037	0.7339724	-1.7860000	2.8570000
DJUMP	27	0.9907407	1.4452866	-5.0000000	3.0000000

YEAR 3

Variable	N	Mean	Std Dev	Minimum	Maximum
LENGTH	81	193.3086420	94.6419096	13.0000000	550.0000000
WEIGHT	81	17.6092099	20.8231634	0	88.0000000
DIAMETER	81	4.6379012	2.0635974	1.7500000	10.3800000
TAPER	81	1.7870370	1.7393706	0	13.9860000
DJUMP	81	0.6703704	0.6278822	-1.0000000	2.7500000

YEAR 4

Variable	N	Mean	Std Dev	Minimum	Maximum
LENGTH	239	112.0878661	78.0777235	0	440.0000000
WEIGHT	239	3.6275272	4.7432997	0	29.2490000
DIAMETER	239	2.2757322	1.4070027	0	8.7500000
TAPER	239	5.2395523	32.4312648	-15.8730000	500.0000000
DJUMP	0	.	.	.	.

ORDER 4 BRANCHES

YEAR 1

Variable	N	Mean	Std Dev	Minimum	Maximum
LENGTH	26	259.8076923	74.6254751	120.0000000	490.0000000
WEIGHT	26	108.9108846	80.5604659	27.5000000	375.0000000
DIAMETER	26	12.5919231	2.8369068	8.6300000	20.7500000
TAPER	26	0.8001154	0.4513247	0	1.4880000
DJUMP	26	1.0576923	0.8009610	-0.2500000	3.0000000

YEAR 2

Variable	N	Mean	Std Dev	Minimum	Maximum
LENGTH	77	180.1298701	82.6453028	0	440.0000000
WEIGHT	77	26.2980649	37.8387664	0	189.0000000
DIAMETER	77	5.5801299	3.1477701	0	13.7500000
TAPER	77	1.2647013	1.2464313	0	7.4070000
DJUMP	77	0.6493506	0.6555177	-0.5000000	3.7500000

YEAR 3

Variable	N	Mean	Std Dev	Minimum	Maximum
LENGTH	224	124.5982143	82.6946363	0	500.0000000
WEIGHT	225	6.6991067	13.1693002	0	100.0000000
DIAMETER	225	2.6588000	2.0031292	0	10.5000000
TAPER	225	2.3845778	2.7883538	-0.6170000	20.0000000
DJUMP	210	0.6416667	0.6413686	-0.5000000	4.5000000

YEAR 4

Variable	N	Mean	Std Dev	Minimum	Maximum
LENGTH	426	81.8661972	71.6977541	0	410.0000000
WEIGHT	426	2.0246690	3.2139874	0	24.6670000
DIAMETER	426	1.4923944	1.4515202	0	14.2500000
TAPER	426	2.5642230	3.5758321	-7.5440000	33.3330000
DJUMP	0	.	.	.	.

Appendix 1.3 Correlations among branch geometry characters.

LINKS OF ORDER 1 BRANCHES

1	1.0000				
2	0.7436	1.0000			
3	0.6894	0.8561	1.0000		
4	-0.5498	-0.3919	-0.3659	1.0000	
	1	2	3	4	

LINKS OF ORDER 2 BRANCHES

1	1.0000				
2	0.8089	1.0000			
3	0.7545	0.9239	1.0000		
4	-0.2267	-0.3271	-0.4315	1.0000	
5	0.0477	0.1737	0.3431	-0.6076	1.0000
	1	2	3	4	5

LINKS OF ORDER 3 BRANCHES

1	1.0000				
2	0.8293	1.0000			
3	0.6864	0.9442	1.0000		
4	-0.5106	-0.4150	-0.3915	1.0000	
5	0.3198	0.4346	0.4312	-0.0712	1.0000
	1	2	3	4	5

LINKS OF ORDER 4 BRANCHES

1	1.0000				
2	0.9145	1.0000			
3	0.8389	0.9703	1.0000		
4	-0.2986	-0.2853	-0.3059	1.0000	
5	0.3665	0.3798	0.3593	-0.1413	1.0000
	1	2	3	4	5

LINKS OF ALL BRANCHES POOLED

1	1.0000				
2	0.9042	1.0000			
3	0.8249	0.9680	1.0000		
4	-0.3382	-0.3191	-0.3329	1.0000	
5	0.3267	0.3735	0.3686	-0.1277	1.0000
	1	2	3	4	5

1 length
2 fresh weight
3 mean diameter
4 taper
5 diameter jump
(distal end)

SHOOTS OF ORDER 1 BRANCHES

1	1.0000					
2	0.9072	1.0000				
3	0.5230	0.2151	1.0000			
4	0.3642	-0.0065	0.8698	1.0000		
5	0.3349	0.1284	0.8430	0.6970	1.0000	
6	-0.2622	-0.1412	-0.4689	-0.6039	-0.6093	1.0000
	1	2	3	4	5	6

SHOOTS OF ORDER 2 BRANCHES

1	1.0000							
2	0.9194	1.0000						
3	0.7129	0.4081	1.0000					
4	0.7698	0.5081	0.9286	1.0000				
5	0.4950	0.1479	0.8962	0.8099	1.0000			
6	-0.0260	-0.1239	0.0810	0.1232	0.1341	1.0000		
7	-0.2584	-0.1008	-0.4586	-0.5000	-0.5998	-0.1467	1.0000	
8	0.3379	0.4954	0.0435	0.0765	-0.2189	-0.6340	0.1926	1.0000
	1	2	3	4	5	6	7	8

SHOOTS OF ORDER 3 BRANCHES

1	1.0000							
2	0.7641	1.0000						
3	0.6025	0.0426	1.0000					
4	0.6114	0.0321	0.9800	1.0000				
5	0.5771	0.0307	0.9813	0.9587	1.0000			
6	0.1447	0.0327	0.2218	0.1997	0.1851	1.0000		
7	-0.5409	-0.1165	-0.7871	-0.7812	-0.8046	0.1910	1.0000	
8	0.5515	0.0513	0.8917	0.8684	0.8498	0.2433	-0.6887	1.0000
	1	2	3	4	5	6	7	8

SHOOTS OF ORDER 4 BRANCHES

1	1.0000							
2	0.7473	1.0000						
3	0.2714	-0.1452	1.0000					
4	0.3159	-0.1111	0.9738	1.0000				
5	0.3200	-0.1410	0.9543	0.9586	1.0000			
6	-0.0731	-0.2171	0.3391	0.3667	0.3177	1.0000		
7	0.0361	0.3970	-0.3632	-0.3568	-0.4192	-0.2697	1.0000	
8	0.2681	-0.0945	0.8999	0.9145	0.8597	0.2773	-0.3454	1.0000
	1	2	3	4	5	6	7	8

Appendix 1.4 Canonical variates analysis of branch geometry in genotype classifications.

***** Canonical variate analysis *****

*** Latent Roots ***

1	2	3
3.102	2.454	1.244

*** Percentage variation ***

1	2	3
45.62	36.09	18.30

*** Trace ***

6.799

*** Latent Vectors (Loadings) ***

	1	2	3	
1	-0.310	-0.161	-5.791	Dl1
2	-3.715	-2.237	-5.032	Dl2
3	-4.171	4.581	2.342	Dl3
4	0.774	-0.769	-1.217	Dw1
5	1.909	3.767	2.390	Dw2
6	1.970	-2.634	-3.511	Dw3
7	-3.869	1.707	3.425	th0
8	-1.902	2.834	-2.661	Dth1
9	-4.231	-1.018	-2.771	Dth2
10	-2.106	1.623	0.208	Dth3

*** Canonical Variate Means ***

PROVENANCE		CANONICAL VARIATE SCORE		
		1	2	3
CORDOVA	1	1.392	-0.613	1.464
SITKA	2	0.831	2.233	-0.551
SKIDEGATE	3	0.507	-1.677	-1.258
NORTHBEND	4	-2.730	0.056	0.345

*** Inter-group distances ***

1	0.000			
2	3.532	0.000		
3	3.053	3.987	0.000	
4	4.323	4.269	4.006	0.000
	1	2	3	4

Appendix 1.5 Correlations among shoot variates within order 3 and 4 branches.

deflections in order 3 branches

shoot type				
1	1.0000			
2	0.8626	1.0000		
4	0.7448	0.8320	1.0000	
6	0.2232	0.2144	0.3385	1.0000
	1	2	4	6

relative deflections in order 3 branches

shoot type				
1	1.0000			
2	0.8847	1.0000		
4	0.8053	0.8078	1.0000	
6	-0.3077	-0.1230	0.0738	1.0000
	1	2	4	6

fresh weight in order 3 branches

shoot type				
1	1.0000			
2	0.7389	1.0000		
4	0.6585	0.7131	1.0000	
6	0.1441	0.2802	0.2964	1.0000
	1	2	4	6

length in order 3 branches

shoot type				
1	1.0000			
2	0.7927	1.0000		
4	0.5892	0.6863	1.0000	
6	0.3974	0.4252	0.6785	1.0000
	1	2	4	6

deflections in order 4 branches

shoot type						
1	1.0000					
2	0.5605	1.0000				
4	0.8907	0.6427	1.0000			
6	0.8403	0.6453	0.9670	1.0000		
8	0.5331	0.4958	0.4035	0.3310	1.0000	
16	-0.3350	-0.2169	-0.1241	-0.1277	0.0549	1.0000
	1	2	4	6	8	16

relative deflections in order 4 branches

1	1.0000					
2	0.2571	1.0000				
4	0.4740	0.3869	1.0000			
6	0.1445	0.3512	0.9197	1.0000		
8	0.5713	0.3684	0.3193	0.1187	1.0000	
16	-0.3854	-0.0243	0.3623	0.5615	0.1312	1.0000
	1	2	4	6	8	16

fresh weight in order 4 branches

shoot type						
1	1.0000					
2	0.5290	1.0000				
4	0.6001	0.6973	1.0000			
6	0.7415	0.7332	0.8216	1.0000		
8	0.2623	0.8560	0.6978	0.6144	1.0000	
16	-0.1421	0.2088	0.1190	0.2683	0.3642	1.0000
	1	2	4	6	8	16

length in order 4 branches

shoot type						
1	1.0000					
2	0.6018	1.0000				
4	0.6443	0.6068	1.0000			
6	0.7412	0.4072	0.8434	1.0000		
8	0.0145	-0.1093	0.2111	0.2998	1.0000	
16	-0.0367	0.0320	0.2173	0.3332	0.3275	1.0000
	1	2	4	6	8	16

Appendix 1.6 Canonical variates analysis of shoot variates classified by rank and generation.

```
**********************************************************************

1)          ORDER 3 BRANCHES - SAME RANK DIFFERENT GENERATION

***  Latent Roots  ***

            1
        5.187

***  Latent Vectors (Loadings)  ***

                    1
          1      -0.1603        deflection (PC1 score)
          2      -0.1265        fresh weight (g)
          3      -0.0381        length (mm)
          4      -0.3210        average diameter (mm)

***  Canonical Variate Means  ***

                    1
          1      -2.139
          2       2.364

***  Adjustment terms  ***

                    1
          1      -5.465

***  Inter-group distances  ***

   1      0.000
   2      4.504        0.000
             1            2

**********************************************************************

2)          ORDER 3 BRANCHES - SAME GENERATION DIFFERENT RANK

***  Latent Roots  ***

            1
        1.712

***  Latent Vectors (Loadings)  ***

                    1
          1      -0.2209          deflection (PC1 score)
          2       0.0517          fresh weight (g)
          3      -0.0312          length (mm)
          4       1.2478          average diameter (mm)

***  Canonical Variate Means  ***

                    1
          1       1.293
          2      -1.293

***  Adjustment terms  ***

                    1
          1      -2.184


***  Inter-group distances  ***

   1      0.0000
   2      2.5859       0.0000
             1            2
```

****

3) ORDER 4 BRANCHES - SAME RANK DIFFERENT GENERATION
RANK = 1

*** Latent Roots ***

1
3.208

*** Latent Vectors (Loadings) ***

	1	
1	0.1511	deflection (PC1 score)
2	-0.0219	fresh weight (g)
3	0.0181	length (mm)
4	0.8846	average diameter (mm)

*** Canonical Variate Means ***

	1
1	2.120
2	-1.475

*** Adjustment terms ***

	1
1	3.133

*** Inter-group distances ***

1	0.000	
2	3.594	0.000
	1	2

****

4) ORDER 4 BRANCHES - SAME RANK DIFFERENT GENERATION
RANK = 2

*** Latent Roots ***

1
16.67

*** Latent Vectors (Loadings) ***

	1	
1	0.1071	deflection (PC1 score)
2	0.1623	fresh weight (g)
3	-0.0415	length (mm)
4	0.5348	average diameter (mm)

*** Canonical Variate Means ***

	1
1	-3.889
2	4.148

*** Adjustment terms ***

	1
1	-3.038

*** Inter-group distances ***

1	0.000	
2	8.038	0.000
	1	2

****

5) ORDER 4 BRANCHES - SAME GENERATION DIFFERENT RANK
GENERATION = 1

*** Latent Roots ***

1	2
2.692	0.042

*** Percentage variation ***

1	2
98.47	1.53

*** Trace ***

2.734

*** Latent Vectors (Loadings) ***

	1	2	
1	0.1112	0.7764	deflection (PC1 score)
2	0.0620	-0.0286	fresh weight (g)
3	-0.0233	0.0003	length (mm)
4	1.2155	-0.7540	average diameter (mm)

*** Canonical Variate Means ***

	1	2
1	2.0066	0.1358
2	-0.0590	-0.2843
3	-1.9476	0.1485

*** Adjustment terms ***

	1	2
1	-1.409	-2.512

*** Inter-group distances ***

1	0.000		
2	2.108	0.000	
3	3.954	1.938	0.000
	1	2	3

****

6) ORDER 4 BRANCHES - SAME GENERATION DIFFERENT RANK
GENERATION = 2

*** Latent Roots ***

1
0.1952

*** Latent Vectors (Loadings) ***

	1	
1	0.2616	deflection (PC1 score)
2	-0.5283	fresh weight (g)
3	0.0000	length (mm)
4	1.3772	average diameter (mm)

*** Canonical Variate Means ***

	1
1	0.6319
2	-0.2949

*** Adjustment terms ***

	1
1	0.3299

*** Inter-group distances ***

1	0.0000	
2	0.9268	0.0000
	1	2

****

SUMMARY OF CVA ON SHOOTS

test	loadings diam	dfl	weight	length	distance
1 order 3 rank=1	-.32	-.16	-.13	-.04	4.5
2 order 3 gen=2	1.25	-.22	.05	-.03	2.6
3 order 4 rank=1	.88	.15	-.02	.02	3.6
4 order 4 gen=1	1.22	.11	.06	-.02	2.1, 4.0, 1.9
5 order 4 rank=2	.53	.11	.16	-.04	8.0
6 order 4 gen=2	1.38	.26	-.53	.00	.93

Appendix 2

The branch stress simulation program in more detail.

• A2.1 The theoretical basis for strain calculations.

Consider a beam consisting of isotropic, linearly elastic material. Let the beam be subject to a stress which bends it with curvature K (radius of curvature $R = K^{-1}$) in pure flexural strain. There is an axis within the beam where the strain $\varepsilon = 0$, which is the neutral axis. Distance measured perpendicular to the neutral axis is denoted $\pm \zeta$, using the neutral axis as the origin. The strain can be written in terms of K and ζ thus:

$$\begin{aligned} \varepsilon &= (l - l_0) / l_0 \\ &= (2\pi (R \pm \zeta)/2\pi R) - 1 \\ &= \pm K\zeta \end{aligned} \qquad \text{(A2.1)}$$

For any linearly elastic material stressed to below its elastic limit,

$$E = \sigma/\varepsilon \qquad \text{(A2.2)}$$

Where E is the elastic modulus and σ is the stress at the same point ε is measured. Thus,

$$\sigma = \pm K E \zeta \qquad \text{(A2.3)}$$

The local turning moment acting on an element of cross-section dA about the neutral axis is $F\zeta A$, where $F = \sigma A$, so substituting for F, the local moment is

$$dM = E \zeta^2 K \, dA \qquad \text{(A2.4)}$$

The total bending moment is the sum of all these infinitesimal moments over the total cross-section area

$$M = \int_{-r}^{r} E\,\varsigma^2\,K\,dA = EK\int_{-r}^{r}\varsigma^2 dA \qquad \text{(A2.5)}$$

Where r is the distance to the outer surface of the beam from the neutral axis. The integral $\zeta^2 dA$ over $\pm r$ is the second moment of area of cross section of the beam about the neutral axis I.

Thus,

$$M = KEI \qquad \text{(A2.6)}$$

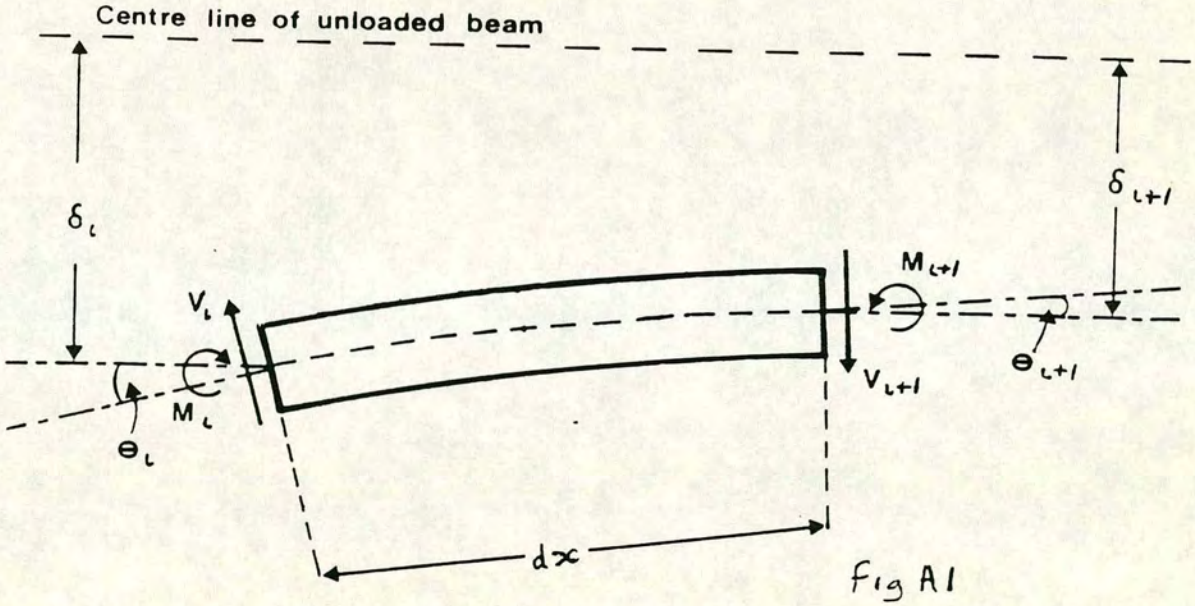

fig A1

Referring to fig. A1 (reproduced from Morgan and Cannell [1987]), consider a small element of length dx in a horizontally held beam a distance x from the origin where the vertical displacement (deflection) is δ. The angle the stressed beam's axis makes to the horizontal at x is given approximately as

$$\theta \approx d\delta / dx \qquad \text{(A2.7)}$$

and assuming that the curvature is small,

$$K \approx d^2\delta / dx^2 \qquad \text{(A2.8)}$$

(the exact equation for K is given in Niklas [1992] on page 133.)

Adopting the sign convention where positive curvature is in the opposite direction to the bending moment (following Morgan and Cannell [1987]), the bending moment at position x is thus given by

$$M_x = -EI\frac{d^2\delta}{dx^2} \tag{A2.9}$$

By definition, the shear at x is given by

$$V_x = \frac{dM_x}{dx} = -EI\frac{d^3\delta}{dx^3} \tag{A2.10}$$

and the distributed load at x is

$$p_x = -\frac{dV_x}{dx} = EI\frac{d^4\delta}{dx^4} \tag{A2.11}$$

Successive integration four times of equation A2.11 yields the following relations :

$$\begin{aligned} EI\,(d^3\delta / dx^3) &= \int p\,dx + C_1 \\ EI\,(d^2\delta / dx^2) &= \iint p\,dxdx + C_1x + C_2 \\ EI\,(d\delta / dx) &= \iiint p\,dxdxdx + C_1x^2/2 + C_2x + C_3 \\ EI\ \ \delta &= \iiint\int p\,dxdxdxdx + C_1x^3/6 + C_2x^2/2 + C_3x + C_4 \end{aligned} \tag{A2.12}$$

The integration constants $C_1 ... C_4$ are found from applying the boundary conditions to give:

$$
\begin{aligned}
V_n &= F_1 + V_{n+1} \\
M_n &= F_2 - V_{n+1} l + M_{n+1} \\
\theta_n &= -F_3 - \frac{V_{n+1} l^2}{2EI} + \frac{M_{n+1} l}{EI} + \theta_{n+1} \\
\delta_n &= -F_4 + \frac{V_{n+1} l^3}{6EI} + \frac{M_{n+1} l^2}{2EI} + \theta_{n+1} l + \delta_{n+1}
\end{aligned}
\qquad \text{(A2.13)}
$$

Where the load functions F_1 ... F_4 are a combination of the evaluated integrals (for distributed load) and point loads and moments, added to represent the effect of laterals (P is a point load at a and Q is a point moment at b) as follows:

$$
\begin{aligned}
F_1 &= -\int_0^{-l} p\, dx + P = pl + P \\
F_2 &= -\int_0^{-l}\int_0^{-l} p\, dxdx - Pa + Q = \frac{-pl^2}{2} - Pa + Q \\
F_3 &= -\int_0^{-l}\int_0^{-l}\int_0^{-l} p\, dxdxdx + \frac{Pa^2}{2EI} - \frac{Qb}{EI} = \frac{pl^3}{6EI} + \frac{Pa^2}{2EI} - \frac{Qb}{EI} \\
F_4 &= -\int_0^{-l}\int_0^{-l}\int_0^{-l}\int_0^{-l} p\, dxdxdxdx - \frac{Pa^3}{6EI} + \frac{Qb^2}{2EI} = \frac{-pl^4}{24EI} - \frac{Pa^3}{6EI} + \frac{Qb^2}{2EI}
\end{aligned}
\qquad \text{(A2.14)}
$$

In the transport matrix method the shoot (cantilever) is regarded as a series of short untapered segments (elements), each carrying a small increment to the total deflection resulting from the gravitational stress, building up into a large deflection at the free end due to a progressive change in angle. Each segment is a cantilever in its own right and is described by its mean diameter d_i from which is given the second moment of area of cross-section I_i The element has a length a_i, mass p_i and stiffness (modulus of elasticity) E_i. The angle its axis in stressed equilibrium makes with the axis of the shoot in the absence of stress is denoted θ_i. In addition to the distributed mass of the elememt, a point load P_i and moment Q_i may be applied at a position on the element to represent the attachment of lateral shoots here. At each end of the element, the shear force V_i, bending moment M_i, angle to the vertical θ_i and deflection δ_i (relative to the axis of the undistorted shoot) are matched to the neighbouring elements values for these terms in an input-output relation. The input-output relation states that the terms on the distal side of the *nth* element are equal to the terms on the proximal side of the *n+1th* element. This links all the elements in the shoot by a chain of equations which are calculated in turn as a transport matrix calculation. The equations are those given in A2.13.

These simultaneous equations are written in linear algebra matrix form as

$$\Psi in_i = \underline{T}_{i,\, i+1} \cdot \underline{\Psi} out_i \qquad \text{(A2.15)}$$

to represent the relations (A2.13) for the *i*th segment where $\underline{T}_{i,i+1}$ represents the transport matrix from the *i*th to the *i*+1th element. The output of the *i*th element ($\underline{\Psi} out_i$)is the input to the $(i+1)$th element ($\underline{\Psi} in_{i+1}$), so the a sequence of contiguous elements can be related in a chain of equations by successive evaluation thus :

$$\underline{\Psi} in_1 = \underline{T}_{1,2} \underline{\Psi} out_1 \quad = (\underline{T}_{1,2} \underline{T}_{2,3}\,) \underline{\Psi} out_2$$

$$= (\underline{T}_{1,2} \underline{T}_{2,3} \cdots\cdots \underline{T}_{N-1,N}) \underline{\Psi} out_{N-1} \qquad \text{(A2.16)}$$

The transport matrix method calculation therefore consists of a series of matrix multiplications.

• A2.2 A detailed account of the branch stress simulation program.

The input variables driving the tree branch stress simulation program are issued to the main program by an external procedure to maximise the flexibility of the program. The first procedure of the main program 'SETUP1' is responsible for setting all the geometric and other parameter values (such as those defining the light environment and the calculation accuracy). 'SETUP1' also sets the number of elements (*nel*) used to represent each different rank of shoot according to the relation:

$$nel = (order - rank + 1) \times 12 \qquad \text{(A2.17)}$$

(recall that rank=1 for the highest and rank=order for the lowest ranking shoots).

The geometric parameters and driving variables are used in the procedure 'DIMS' to calculate the initial geometry of the branch, setting initial lengths angles and diameters before particular values reflecting shoot rank, generation and age are made (i.e. at this stage shoots of the same rank are treated equal).

The topology of the branch is generated by the procedures 'SETUP2' (which sets index labels for shoots and links and defines their rank and generation) and 'FOD' (which creates a record of the order of the sequence in which calculations should be carried out in the stress simulation phase of the program (the 'fixed order of differences' sequence - see below for further explantion)). 'SETUP2' calculates a serial number for all the daughter laterals of each parent shoot and attaches the label of the mother to the daughter index so that a 'family tree' is constructed which expresses the connectivity within the branch.

fig. A2.1 shows an order 5 branch in which the shoots are labelled according to the binary codes which are used as shoot labels. Starting with the first generation main branch as 0000, its daughters (generation 2 shoots) form the sequence 1000, 0100, 0010, 0001 labeling shoots of rank 2, 3, 4, 5 respectively. Taking shoot 1000, its third generation daughters are 1100, 1010, 1001. A shoots label is made up from adding the binary label of its parent to the code representing its rank. Thus, for

example, the third generation daughters of 0100 are 0110 and 0101. This method uniquely labels all the shoots for any order of branch.

In order to maximise program flexibility, all the sequence numbering and labelling is calculated from numerical relations derived from the branch topology, rather than storing them as tables. This adds to the complexity of the program (the procedure 'LAT-ID' calculates several indexing systems for links and shoots which are used at various stages in the stress simulation of branches). The indexes calculated are (a) shoot rank, (b) shoot generation, (c) shoot daughter number (laterals of the one generation are ordered in rank acropetally along their parent), (d) shoot mother number (the identification label of the parent shoot) and the link number (links are ordered 1,2,3... acropetally along the shoot).

The geometry of each rank of shoot is next calculated by the procedure 'DIMS'. In this procedue the shoots are divided into the length elements used in the transport matrix calculation of strain and the calculation of light interception, later in the simulation. The length and average diameter of each element in the shoot is calculated for the given shoot rank and the elements are numbered acropetally and those bearing lateral shoots are identified. The distances between elements with lateral attachments give the link lengths making up the shoot. These link lengths are then modified in relation to the link number to represent the ageing effect of growth in which growth in length (annual growth increments) changes from year to year so that the interlateral spacings are a function of the ranks of the laterals they separate. An ageing parameter is defined which acts to change lengths in linearly with link number.

The FOD sequence controls the program flow in calculations of strain among connected shoots in the branch. Pairs of shoots are ordered in a set sequence to be input to a function which calculates strain for the two shoots concerned. The function's output on each iteration is compared to the previous value to assess the change in branch shape after each use of the function. Depending on the outcome of this comparison, a pre-determined feedback path may be taken to recalculate the strain distribution within part of the branch : this is brought about by a return of pogram flow to an earlier stage in the FOD sequence.

The need for this sequence arrises from the complex mutial dependance interactions between geometry and strain among the interconected shoots of the branch. If calculations of shoot strain are not made in the correct order, these interactions make convergence towards a whole branch solution far less likely. The sequence

and its associated feed-back parameters define an efficient order for taking shoots into the calculation which minimises errors in intermendiate stages of the calculation that result from incomplete accounting for the shoot interactions. The rules defining the fixed order, feed back paths and feedback parameters are constructed to minimise interaction effects at intermediate stages in the calculation, i.e. when the branch is only partially described.

The fixed order sequence of shoot pairs depends on the topology of the branch (depending on branch order and the occurence of missing shoots), so it is calculated for each simulation. The interaction minimising sequence was found initially through logical deduction which resulted in two rival strategies : top down (in which the highest rank parent shoots with highest generation daughter laterals are calculated first) and bottom-up (in which the lowest rank shoots are calculated first). The superior strategy was chosen from trials where it was found that the top down strategy consistently outperformed the bottom-up strategy by allowing convergence towards a whole branch solution in fewer iterations. The model program now incorporates the top-down sequence generating algorithm only (procedure 'FOFM') The rules are calculated as follows:

The mothers are

0	2^1	2^2	2^2+2^1	2^3	2^3+2^1	2^3+2^2	$2^3+2^2+2^1$
0	2	4	6	8	10	12	14

and their paired daughters are

$D = M + 2^k$ where $k = 1, 2, \ldots lm2$. and $lm2$ is the lowest multiple of 2 of M shown in the binary notation for M. The sequence parameters are listed in table A2.1.

J	*M*	*D*	*lm2*	*k*	FB	*Q* or θ
1	0000	0001	4	0	-	-
2	0000	0010	4	1	1	$\theta 2$
3	0000	0100	4	2	2	$\theta 3$
4	0000	1000	4	3	3	$\theta 5$
5	0010	0011	1	0	2	$Q3$
6	0100	0101	2	0	3	$Q5$
7	0100	0110	2	1	6	$\theta 6$
8	0110	0111	1	0	7	$Q7$
9	1000	1001	3	0	4	$Q9$
10	1000	1010	3	1	9	$\theta 10$
11	1000	1100	3	2	10	$\theta 11$
12	1010	1011	1	0	10	$Q11$
13	1100	1101	2	0	11	$Q13$
14	1100	1110	2	1	13	$\theta 14$
15	1110	1111	1	0	14	$\theta 15$

Table A2.2

J is the sequence number, M the binary label for the mother and D for the daughter. lm2 is the lowest multiple of 2 in m or the least significant bit equal to 1. k is is a counter, incremented for each J where m is unchanged, when M changes in the sequence, k returns to 0.

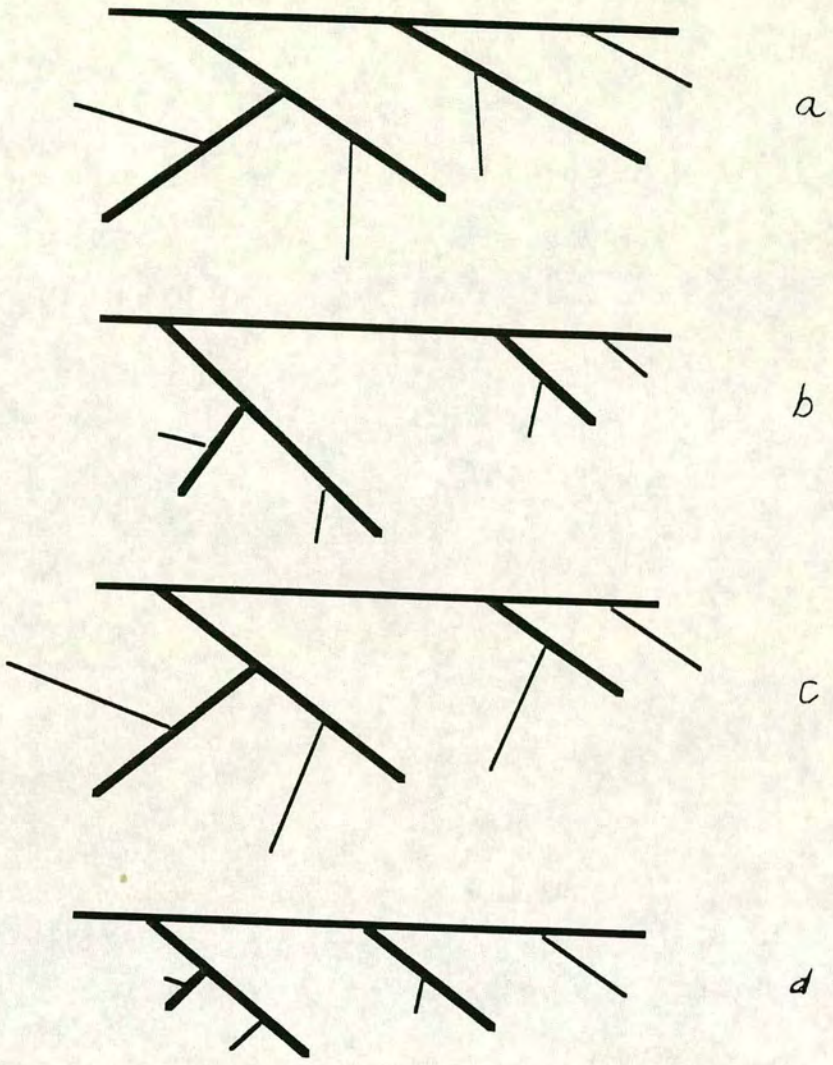

Fig A2.2 The geometric variables controlling branch shape in the model can produce a very wide variety of branch shapes, the illustrations here help to illustrate their impact. (a) dlg =1, dlr > 1; (b) dlg =1, dlr <1; (c) dlg >1, dlr =1; (d) dlg <1, dlr =1; (e) φ <45°; (f) φ =90°; (g) θ_0<90°,θ_i=0; (h) θ_0<90°,θ_i>0; (i) a <1; (j) a>1. In addition to these variables, there are those which operate on the diameters of links.

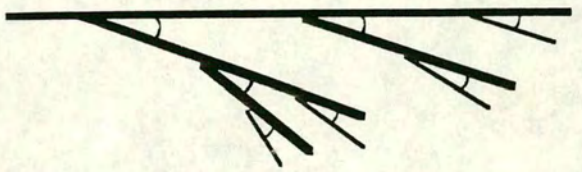

e

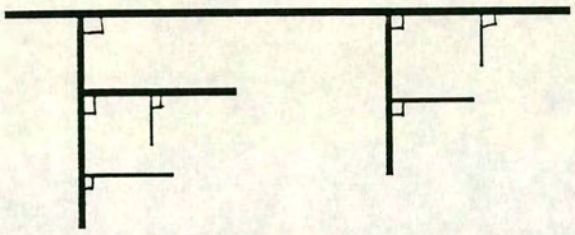

f

g

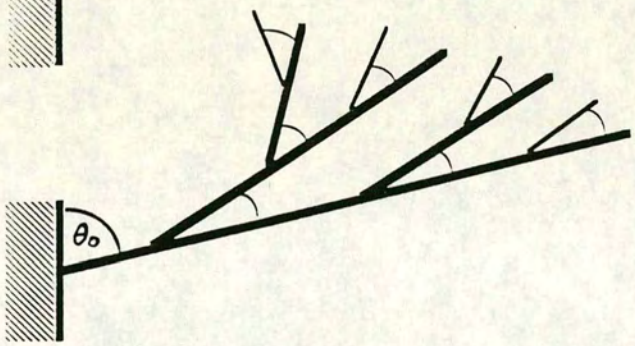

h

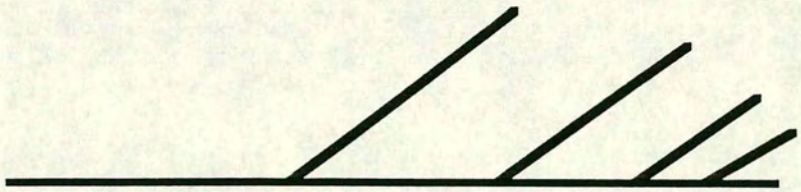

i

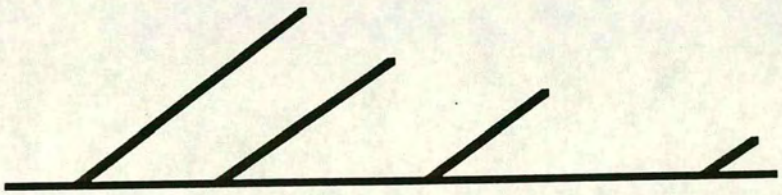

j

The initial values of the angles of emergence of laterals in the vertical plane (θ_0) and the horizontal plane (ϕ) are calculated and placed in a global array by procedure 'SETUP3'. To do this, SETUP3 must first find, for each shoot in turn, which is its parent : this information is useful in many other parts of the program as well and so goes into the global memory. The sequence of parents of each shoot is found, counting back shoot generations to the leader. Θ and Φ - vertical and horizontal plane shoot orientation angles relative to the global coordinates (in which Q of the leader = θ and Θ of the leader = 0) are found by summing the angles of the parants in the sequence. Θ and Φ are defined with respect to a coodinate system local to the branch, but the strain calculations need the angles defined in a cordinate system which is independent of the branch's orientation. Every mother-daughter pair of shoots is put through the procedure ADJUST-ANG to carry out the angle transformation during strain calculation.

Adjustments to the link lengths and diameters according to branch growth aging and differences in allocation among shoots of different topological generation (on top of differences according to shoot rank) are made next.

ADJUST_L takes the shoot lengths and applies the age factor scaling: the *ith* link in the shoot is scaled according to

$$l' = l \{ a (n/2 - i) + 1 \} \quad \text{if } n \text{ is odd}$$

$$\text{and} \qquad l' = 1 \{ a (n/2 - i) + a/2 + 1 \} \quad \text{if } n \text{ is even} \tag{A2.18}$$

where a is the age parameter, n is the number of links in the shoot and l is the original link length. This is then re-scaled to ensure that

$$\Sigma\, n\, l' = nl \tag{A2.19}$$

so that the total shoot length remains unchanged. The scaling requires fine tuning to correct for errors in the shoot's length arrising from its description as an integer number of elements.

Whole shoot lengths are related to rank by the rank-length coefficient (*dlr*) as follows

$l'' = l' \{ dlr\text{-}1 \}$ where r is the shoot's rank (A2.20)

and to their generation by the generation-length coefficient (*dlg*) according to

$l''' = l'' \{ dlg\text{-}1 \}$ where g is the shoot's generation. (A2.21)

In exactly the same way, the mean diameters of the the shoots are modified for their rank and generation using the procedure 'ADJUST-D' which calculates a new diameter for every element in the shoot using the rank-diameter coeficient (*ddr*) and the generation-diameter coeficient (*ddg*). There are also abrupt changes in diameter moving from one link to the next (i.e. from one growth year to the next along the shoot). These are calculated by the procedure ADJUST-D according to the relation:

$$r' = C\, r\,. \tag{A2.22}$$

where C is a consatant.

With the diameters and lengths for all the elements of all the shoots known, the weights and second moments of area of the elements can be calculated. This is done by procedure 'WEIGHTS' using a set of species specific values provided by a procedure called 'SPECIES' which selects appropriate mass of foliage, wood density and Young's modulus for the species, with values taken from Morgan and Cannell [1987]. The total branchwood mass and total foliage mass are calculated separately by summing the masses calculated for each shoot type (of each rank and topological generation), multiplied by the number of shoots of each type in the branch in a particular order. The particular order of summation is necessary because stress calculations require a knoledge of shoot weight including all laterals (the whole system of shoots connected to the shoot in question), so that each sub-branch which can be described within the branch must have a weight calculated. The identification of all the sub-branch systems and the appropriate summation is carried out by the procedure 'WEIGHTS-2' This calculation enables shoot total weights and their associated bending moments as a point loads and moments to be applied to their parent shoots.

A2.2.2 The Stress simulation Phase

Calculation of stress in shoots is carried out for pairs of one lateral type and its parant at a time (making use of symmetry, only one lateral of each whorl is considered in the calculations: the others are regarded as identical). Thus if there are three lateral types on a parent shoot, there are three separate shoot pairings in which the stress distribution is evaluated. The initialisation phase of the model has calculated a fixed order sequence for taking these shoot pairs for calculating the stresses in the whole branch. This sequence, together with the sensitivity criteria (to trgger , or not, a feedback in the calculation) and the feedback destinations (the shoot pair requiring re-calculation if feedback is triggered) are followed by the outer loop of the stress simulation phase.

The stress calculation problem is broken down into a set of mother/daughter shoot interactions. These are arranged in a sequence for the calculation flow to follow, but with each interaction, a test is carried out to establish whether a significant perterbation has occurred in the previously calculated pair where the daughter was the shoot which is now the mother : if so, the flow is fed back to that pair. The interaction between a mother and daughter pair is found by itteratively calculating the distortion of each of them in turn using the constantly updated information about initial angle and moment, until the changes in estimate solutions are small. The calculation of distortion of each shoot uses a transport matrix method described previously.

The outer-most loop takes pairs of shoots through the 'fixed order and difference sequence, applying the feedback tests and rules which were described in section A2.2.1. In this loop, the whole branch is subjected to sucessive trial strain distribution functions (successive approximations), iterating until the turning moments through the branch are within a threshold of equilibrium. The input arguments for each application of the stress distribution calculation are provided by a globally defined array holding the FOD sequence parameters. This array is indexed by a sequence number J . If a feedback path is followed, it is J which is changed to identify the new arguments to the function. Alongside these arguments, for each J, there is a flag which dictates which of bending moment values or vertical angle values (Q or θ), is tested against a threshold value before a feedback is carried. After each application of the stress distribution calculation, a test of either the change in Q or the change in θ from its last calculated value is made. If this change is greater than the threshold value AC, then the feedback path is taken, otherwise J is incremented and this sequence is continued until $J = 2(ORD\text{-}1)$. The value AC is calculated in the function 'ACC' and depends on the number of feedbacks made before in the calculation and the path taken in the stress distribution

calculation. If the program shows signs of following an endless loop around feedback paths, ACC will increase AC so that the criterion for feedback becomes less likely. This facillity was added to the program to increse the chance of convergence to a stable solution after observing the behaviour of the feed-back loops many times.

The calculation of stress distribution between a paraent/lateral pair of shoots is caried out in the procedure 'BRANCH' which is the next hierarchical level beneath the stress simulation loop described above. BRANCH is provided with indexes from which it accesses all the current data which describes the geometry of the particular parent/lateral (mother/daughter) pair. A loop within BRANCH alternately calls for the calculation of single shoot strain and stress for the mother and the daughter shoots. This calculation is carried outt in the procedure 'STEM'. I BRANCH, a loop is followed which iteratively finds the point of equilibrium between the turning moments applied between the mother and daughter shoots. Whenever the mother is recalculated, the deflection at its tip (last element) is recorded as dfl and this is compared to whatever value was previously calculated. This deflection is a function of the bending moment Q_k exerted by the daughter at the point where it is attached to the mother, but that moment depends on the angle of attachment θ_k, which in turn depends on the deflection of the mother : this is where a mutual interaction between shoot characters affects the calculation. The interaction between the mother and daughter is found from repeated calculations, driven in the direction which causes the changes in dfl to become smaller on each repetition. When $(dfl_k\text{-}dfl_{k-1})$ is less than a fixed percentage of dfl (the accuaracy threshold), the solution is considered found. Once this has been achieved, the difference between the very first dfl (dfl_1) and the last to be calculated (dfl_K) is found together with the counterparts representing the change in moment and deflection angle ($Q_1\text{-}Q_K$) and $(\theta_1\text{-}\theta_K)$. These differences are used to calculate the finite differential

$$(dfl_1\text{-}dfl_K) / (\lambda_1\text{-}\lambda_K) \qquad \text{(A2.23)}$$

where λ = either Q or θ .

The value of this finite differential, which represents the rate of change of tip deflection (a measure of shoot stress) is weighted by a constant ACO which fixes the accuracy of comparisons in the stress simulation loop. These differentials are the values AC (referred to above) which are used as a threshold for feedback criteria in the outer loop of the simulation program. These diferentials represent a weighted measure of change in either Q or θ due to recalculation of bending with updated

data for the shoots. The weighting *ACO* is a measure of the relative importance of the change in terms of its effect on the final deflection profile of the mother branch : if deflection is little changed by a large change in *Q*, then the weighting is small and the test for feedback is correspondingly insensitive. This form of 'dynamic' testing in which the thresholds are variable and depend on the 'history' of calculation is useful in minimising the number of iterations carried out in the calculation. However, the calculation can enter endless loops, still where it, constantly returns through the same feedback path due to a localised instability in the interactions between deflection angles and turning moments. For this reason, the accuracy constant *ACO* used to scale the differentials is made variable too. A record is kept of the number of times a particular point *J* in the sequence of mother/daughter pairs in the outer loop of the program has been returned to and the scaling is increased in proportion, thus making the stringency of the feedback test less. With these adjustable tests and the flow paths defined, there is little chance of the calculation becoming trapped in an endless loop or a 'blind alley'. The cost of this strategy is an increased probability of error propagation and consequently a danger of misleading results. The simulation can compensate even for unrealistic stress distributions and present results which are merely an artefact of the calculation method. This is likely behaviour when the limits of the stress calculation are exceeded. Unfortunately there are few guidelines as to what the limits of computation might be, so the results should always be approached with thoughtful criticism: this is not always practical, especially when a large number of simulations are required to, for example, calculate a Hessian matrix for the branch design objective function. This is the source of the unsermounted difficulties encountered in branch design optimisation.

After each application of STEM the angles defining the shape of the shoot are returned to the global coordinate space by passing them through the angle transformation procedure 'ADJUST_ANG'.

The procedure STEM is composed of a loop and decision making process from which internal procedures are called on each pass of the loop. For a single shoot, this procedure finds the relaxed, distorted shape which the shoot takes up given the point loads and moments applied by its laterals along its length. The forces and moments along the length of the shoot must be balanced and this entails finding values for the end conditions : the force and moment applied to each end of the shoot. However the moment applied to the base is unknown, although at the tip it must be zero, so the base moment which gives a resultant tip moment equal to zero must be found. The calculation of the distorted profile of a shoot when a given set of loads and moments are applied to the base end is modelled as a function of the

moment at the base end of the shoot M_{base} to give the moment at the tip end M_{tip} thus:

$$f(M_{base}) = M_{tip} \tag{A2.24}$$

This function f is repeatedly applied with different values of M_{base} to find the solution (where $M_{tip} = 0$) by using a successive division algorithm, which searches for the presence of a solution within an ever decreasing region (i.e. by successive divisions of the search region). The procedure followed is the bisection algorithm [Press et al., 1986] As a precursor to the bisection algorithm, a region bounding a sign change in M_{tip} must be found to locate the solution within known bounds. The solution containing bounds are found by the procedure 'BRAC' which extends the range of the bounds repeatedly until there is a sign difference in M_{tip} between them, so guaranteeing the existence of a solution within the range difined by the bounds. When found, this range is passed on to procedure 'BISECT' which divides the range in two and tests both halves to see which now contains the zero. It divides the part containing the solution again and repeats the test, on and on for a set number of cycles to achieve a set accuracy. The mid point of the last range is then taken as the base moment which, when applied to the given shoot, results in a moment at the tip which is approximately zero.

Both procedures BRAC and BISECT use multiple applications of the procedure 'MATRIX' which calculates $f(M_{tip})$. MATRIX is an implementation of the transport matrix method for calculating large deflections of cantilevers appropriate to tree branches [Morgan & Cannell 1987] (see A2.1). MATRIX calculates the deflected profile d_i (deflection of each element i in the shoot) and the bending angles θ_i of the distorted shoot as well as the moment at the tip for a given bending moment at the base of the shoot. The procedure ' MATRIX' is a copy of the main program describbed by Morgan and Cannell [1987] with the data entry and mass calculations (and some other ancillary functions) removed. MATRIX makes calls to the function 'FIVE_1' to perform the matrix multiplications required for transport matrix calculations in the same way as the Morgan and Cannell program does (except that in the implementation described here, there is a variable number of shoot elements and laterals may be attached to any and any number of these elements).

Calculation errors were reconised when the model was run (see section 3.4.3) for which modifications have been built into this part of the program. It is possible that the function $f(M_{tip})$ fails to model the distortion of the shoot correctly due to errors propergating and amplifying through the transport matrix. This behaviour results in

a great error in estimated M_{tip} (perhaps orders of magnitude out), which cause both the bracketing and the bisection routines to act on the basis of wrong information. The result of this is that these two algorithms loose their direction and the whole calculation spins off out of control. Following unsuccessful work to remedy the problem occuring with the calculation of $f(M_{tip})$, modifications to the bracketing and bisection algorithms were carried out to reduce their sensitivity to errors. A flag is set if the bending angle increases beyond π radians or rises too rapidly, or if the deflection exceeds the elememt length (all three conditions being symptomatic of transport matrix error propagation). If such errors persist after several attempts at finding a stable bracketing range, the bracket and bisect algorithm is abandoned in favour of a much less efficient, but perhaps more robust method: the same as that used in the program described by Morgan and Cannel [1987] to do the same job. If this procedure also fails to find a stable bracket, flags are set which signal to the branch level procedure 'BRANCH' that the calculation could not be completed and an incomplete result is returned in which the shoot is represented in an undistorted state. If this occurs, the accuracy constant *ACO* incresed to reduce the accuracy on the next attempt at calculating this shoot's distortion. If the shoot continues to fail, a failure message is sent back to the main program.

For each use of the procedure MATRIX, FIVE_1 is used N times (the number of elements representing the shoot). MATRIX is used by 'BRAC' a minimum of 2 times, but, possibly as many as 6 times to find the range enclosing the solution where moment at the shoot's tip is zero. BISECT then uses MATRIX 10 times to find the solution to an accuracy of1 part in 2^{10} (1024). STEM2 is used alternately on the mother and the daughter shoots in procedure BOUGH and there might be between 4 and eight cycles within BOUGH to find an equilibrium between the mother and the daughter. For an order M branch there are $2(M\text{-}1)$ mother/daughter pairs and so the minimum number of times BOUGH is used, (i.e. when there are no feedbacks), will be $2(M\text{-}1)$. However, with feedback loops activated, this number can escalate to many times that value: the exact number being impractical to predict, it is prevented from becoming too large by a progressive reduction in the accuracy of the calculation when a particular feedback loop is repeatedly activated. In all, the minimum number of matrix multiplications involved in the whole program are as follows :

minimum number of 5*5 matrix multiplications

for order:	1	2	3	4
	N	$24N$	$96N$	$288N$

Efforts to reduce the number of multiplications in each calculation of objective function have been made (see section 3.7.2), but these result in the total number more nearly approaching the minimum quoted above. Typically, the model program as it has been described here will use 2 to 5 times the minimum number of matrix multiplications.

- A2.3 Using the Hessian matrix in the neighbourhood of an optimum

The Hessian matrix has already been used to describe some general properties of the estimated objective function which are important to optimisation. Optimisation algorithms using higher derivatives of the objective function depend on being able to approximate the Hessian as a constant. The theoretical reasoning is as follows.

In a neighbourhood around a general point x^* in objective space, the objective function can be approximated by a quadratic hyperplane.
Let

$$F(\underline{x}) = \underline{a}^T\underline{x} + {}^1/_2\, \underline{x}^T\underline{\boldsymbol{G}}\,\underline{x} \qquad \text{(A2.25)}$$

The matrix of constants $\underline{\boldsymbol{G}}$ is the Hessian of $F(\underline{x})$ because it is all that remains in the second derivative of $F(\underline{x})$ (a property of a quadratic). (The Hessian matrix is the set of all partial second derivatives of the function F).

Following Gill et al. [1981], if $\underline{x}$ is changed by a small amount from $\underline{x}^*$ to $\underline{x}^*+a\underline{v}$, where a is a small constant and $\underline{p}$ is a unit vector giving the direction, then

$$F(x^*+ \alpha\underline{v}) = F(x^*) + {}^1/_2\, \alpha^2\, \underline{v}^T\underline{\boldsymbol{G}}\,\underline{p} \qquad \text{(A2.26)}$$

If the eigenvectors of $\underline{\boldsymbol{G}}$ are u_j and the eigenvalues β_j (j=1...n), i.e.

$$\underline{\boldsymbol{G}}\,\underline{u} = \beta\,\underline{u} \qquad \text{(A2.27)}$$

then, if F moves along the direction $\underline{u}_j$ from x*

$$F(x^*+ \alpha\underline{p}) = F(\underline{x}^*) + \alpha^2\, \beta_j \qquad \text{(A2.28)}$$

What this means is that if we move along u_j, $F(\underline{x})$ increases if a_j is positive and decreases if it is negative. Taking all the eigenvectors at once, it is easy to see that $F(x)$ increases in all directions from x^* if the Hessian $\underline{\boldsymbol{G}}$ is positive definite.

Hence the local optimum point is where the Hessian is positive definite.
Furthermore, in the neighbourhood of a minimum (it is normal to construct optimisation as a minimisation problem in practice), the most negative eigenvalues

are associated with the steepest multivariate descent directions - this property of the eigensystem is the basis of the optimisation algorithms used in this work.

REFERENCES

Acton, F.S. (1970) . Numerical Methods that Work. Harper & Row, New York.

Aono, M. & Tosiyasu, L.K. (1984). Botanical tree image generation. *I.E.E.E. Computer Graphics and Applications*, **27,** 10-34.

Baker, C.J. & Bell, H.J. (1992). The aerodynamics of urban trees. *Journal of Wind Engineering and Industrial Aerodynamics*, **44,** 2655-2666.

Bassow, S.L. & Ford, E.D. (1990). A process based model of carbon translocation in trees: an exploration of the branch autonomy theory. *Silva Carelica*, **15,** 77-87.

Bertram, J.E.A. (1989). Size-dependent differential scaling in branches: the mechanical design of trees revisited. *Trees*, **4,** 241-253.

Borchert, R. & Honda, H. (1984). Contol of development in the bifurcating branch system of *Tabebuia rosea* : a computer simulation. *Botanical Gazette*, **145,** 184-195.

Brazier, J.D. (1987). Mans use of Sitka spruce. *Proceedings of the Royal Botanical Society of Edinburgh*, **93(B),** 213-221.

Brent, R.P. (1973) . Algorithms for Minimisation without Derivatives. Prentice-Hall, Englewood Cliffs, New Jersey.

Burley, J. (1964). Genetic variation in *Picea sitchensis* (Bong.) Carr. *Commonwealth Forestry Review*, **43,** 47-59.

Cahalan, C.M. (1981). Provenance and clonal variation in growth, branching and phenology in *Picea sitchensis* and *Pinus contorta. Silvae Genetica*, **30,** 40-46.

Cannell, M.G.R. (1974). Production of branches and foliage by young trees of *Pinus contorta* and *Picea sitchensis*: provenance differences and their simulation. *Journal of Applied Ecology*, **11,** 1091-1115.

Cannell, M.G.R., Sheppard, R.L.J., Ford, E.D. & Wilson, R.H.F. (1983). Clonal differences in dry matter distribution, wood specific gravity, and foliage "efficiency" in *Picea sitchensis* and *Pinus contorta. Silvae Genetica*, **32,** 195-202.

Cannell, M.G.R. & Morgan, J. (1987). Young's modulus of sections of living branches and tree trunks. *Tree Physiology*, **3,** 355-364.

Cannell, M.G.R. (1987). Photosynthesis, foliage development and productivity of Sitka spruce. *Proceedings of the Royal Society of Edinburgh*, **93B,** 61-73.

Cannell, M.G.R., Morgan, J. & Murray, M.B. (1988). Diameters and dry weights of tree shoots: effects of Young's modulus, taper, deflection and angle. *Tree Physiology*, **4,** 219-231.

Cannell, M.G.R. (1989). Physiological basis of wood production: a review. *Scandinavian Journal of Forest Research*, **4,** 459-490.

Cannell, M. & Morgan, J. (1990). Theoretical study of variables affecting the expot of assimilates from branches of Picea. *tree Physiology*, **6,** 257-266.

Carter, G.A. & Smith, W.K. (1985). Influence of shoot structure on light interception and photosynthesis in conifers. *Plant Physiology*, **79,** 1038-1043.

Castéra, P. & Morlier, V. (1991). Growth Patterns and bending mechanics of branches. *Trees*, **5,** 232-238.

Chandler, J.W. (1989). Effects of mineral nutrient supply on needle growth and photosynthesis in Sitka spruce (*Picea sitchensis* Bong. (Carr.)). **PhD**, Edinburgh

Chochrane, L.A. & Ford, E.D. (1978). Growth of a Sitka spruce plantation: analysis and stochastic description of the development of the branching structure. *Journal of Applied Ecology*, **15,** 227-244.

Dean, T.J. & Long, J.N. (1986). Validity of constant-stress and elastic-instability principles of stem formation in *Pinus contorta* and *Trifolium pratense*. *Annals of Botany*, **58,** 833-840.

Digby, P.G.N. & Kempton, R.A. (1987). Multivariate Analysis of Ecological Communities. Chapman & Hall, London.

Elston, D.A. (1992). Sensitivity analysis in the presence of correlated parameter estimates. *Ecological Modelling*, **64,** 11-22.

Fisher, J.B. & Honda, H. (1977). Computer simulation of branching pattern and geometry in *Terminalia* (Combretacae), a tropical tree. *Botanical Gazette*, **138,** 337-384.

Fisher, J.B. & Honda, H. (1979). Branch geometry and effective leaf area: a study of *Terminalia* branching pattern. I Theoretical trees. II Survey of real trees. *Americal Journal of Botany*, **66**, I: 633-644,II: 645-655.

Fisher, J.B. (1983). Branching patterns and angles in trees in: "On the economy of plant form and function", Ed: T. Givnish. Cambridge University Press, Cambridge, London, New York

Fisher, J.B. (1985). Branching patterns and angles in trees. in: "On the economy of Plant form and Function", 493-523. Ed: T. J. Givnish. Cambridge University Press, Cambridge, London, New York

Fletcher, A.M. & Faulkner, R. (1972). A plan for the improvement of Sitka spruce by selection and breading. *Forestry Commission Research and Development Paper*, **85,** 31pp.

Ford, E.D. & Ford, R. (1990). A model for branch growth in the *Pinaceae*: structure and basic eqations. *Journal of Theortical Biology*, **146,** 1-13.

Ford, E.D., Avery, A. & Ford, R. (1990). Simulation of branch growth in the *Pinaceae*: Interactions of morphology, phenology, foliage productivity, and the requirement for structural support, on the export of carbon. *Journal of Theortical Biology*, **146,** 15-36.

Ford, E.D. (1992). The control of tree structure and productivity through the interaction of morphological development and physiological process. *International Journal of Plant Science*, **153,** S147-S162.

Genstat_5_Committee (1988). Genstat 5 Reference Manual. Clarendon Press, Oxford.

Gilgarcia, J., Gimenodominguez, M. & Murilloferroll, N.L. (1992). The arterial pattern and fractal dimension of the dog kidney. *Histology and Histopathology*, **7,** 563-574.

Gill, P.E., Murray, W. & Wright, M.H. (1981). Practical Optimisation. Academic Press, London.

Gravelius, H. (1914). Flusskunde. Goschen, Berlin.

Grime, J.P. (1977). Evidence for the existence of three primary strategies in plants and its relevance to ecological and evolutionary theory. *Americal Naturalist*, **111,** 1169-1194.

Hallé, F. & Olderman, R.A.A. (1970). Essai sur l'architecture et la dynamiques de croissance des abres tropicaux. Masson, Paris.

Hallé, F., Olderman, R.A.A. & Tomlinson, P.B. (1978). Tropical trees and forests: an architectural analysis. Springer-Verlag, Berlin.

Honda, H. (1971). Description of the form of the tree like body: effects of branching angle and the branch length on the shape of the tree-like body. *Journal of Theoretical Biology*, **31,** 331-338.

Honda, H. & Fisher, J.B. (1978). Tree branch angle: maximising effective leaf area. *Science*, **199,** 888-890.

Honda, H., Tomlinson, P.B. & Fisher, J.B. (1981). Computer simulation of branch interaction and regulaton by unequal flow rates in botanical trees. *American Journal of Botany*, **68,** 569-585.

Horn, H.S. (1971). The adaptive geometry of trees. Princeton University Press, Princeton.

Horsfield, K., Dart, G., Olson, D.E., Filley, G.F. & Cumming, G. (1971). Models of the human bronchial tree. *Journal of Applied Physiology*, **31,** 207-217.

Horton, R.E. (1945). Erosional development of streams and their drainage basins: hydrophysical approach to quatitative morphology. *Bulliten of the Geological Society of America*, **56,** 257-370.

Jeffers, J.N.R. (1967). Two case studies in the application of principal component analysis. *Applied Statistics*, **12,** 225-236.

Jeffers, J.N.R. (1988). Practitioner's handbook on the modelling of dynamic change in ecosystems. Scientific Committee on Problems in the Environment,

Katz, M.J. & George, E.B. (1985). Fractals and the analysis of growth paths. *Bulletin of Mathematical Biology*, **47,** 273-286.

King, D.A. (1986). Tree form, height growth, and susceptability to wind damage in *Acer saccharam. Ecology*, **67,** 980-990.

King, D. & Loucks, O.L. (1987). The theory of tree bole and branch form. *Radiation and Environmental Biophysics*, **15,** 141-165.

Küppers, M. (1989). Ecological significance of above ground architectural patterns in woody plants: A question of cost-benefit relationships. *Trends in Ecology and Evolution*, **4,** 375-379.

LaBarbera, M. (1986). The evolution and ecology of body size in: "Patterns and Processes in the History of Life", 69-98. Ed: D. M. Raup Jablonski, D. Springer-Verlag, Berlin, Heidelburg

Larcher, W. (1983). Physiological Plant Ecology. Springer-Verlag, Berlin, New York, Tokyo.

Lefèvre, J. (1983). Teleonomical optimisation of a fractal model of the pulmonary arterial bed. *Journal of Theoretical Biology*, **102,** 225-248.

Lerdau, M. (1992). Future discounts and resource allocation in plants. *Functional Ecology*, **6,** 371-375.

Leverenz, J.W. & Jarvis, P.G. (1979). Photosynthesis in Sitka spruce (*Picea sitchensis* (Bong.) Carr.), VIII. the effects of light flux density and direction on rates of net photosynthesis of needles. *Journal of Applied Ecology*, **16,** 919-923.

Leverenz, J.W. & Jarvis, P.G. (1980). Photosynthesis in Sitka spruce (*Picea sitchensis* (Bong.) Carr.), IX. The relative contribution made by needles at various positions on the shoot. *Journal of Applied Ecology*, **17,** 59-68.

Lindenmayer, A. (1982). Developmental algorithms: lineage versus interactive control mechanisms in: "Developmental Order: Its Origin and Regulation", 219-245. Ed: A. R. Liss. New York

Lindenmeyer, A. (1968). Mathematical models for cellular interactions in development, II: Simple and branching filaments with two-sided inputs. *Journal of Theoretical Biology*, **18,** 300-315.

Lowe, A.J. (1987). Sitka spruce silviculture in Scottish forests. *Proceedings of the Royal Botanical Society of Edinburgh*, **93(B),** 93-106.

Ludlow, M.M. & Jarvis, P.G. (1971). Photosynthesis in Sitka spruce (*Picea sitchensis* (Bong.) Carr.). I General characteristics. *Journal of Applied Ecology*, **8,** 925-953.

MacDonald, N. (1983). Trees and Networks in Biological Models. John Wiley and Sons, Chichester.

Malcolm, D.C. (1987). Some ecological aspects of Sitka spruce. *Proceedings of the Royal Botanical Society of Edinburgh*, **93(B),** 85-92.

Margolis, H.A., Gagnon, R.R., Pothier, D. & Pineau, M. (1988). The adjustment of growth,, sapwood area, and sapwood saturated permeability in balsalm fir after different intesities of pruning. *Canadian Journal of Forest Research*, **18,** 723-727.

Mattheck, C. & Burkhardt, S. 1989. Computer aided shape optimisation based on biological growth.

Mattheck, C. (1990). Design and growth rules for biological structures and their application to engineering. *Fatigue and Fracture Engineering and Material Structures*, **13,** 535-550.

Mattheck, C. (1990). Why they grow, how they grow: the mechanics of trees. *Arboricultural Journal*, **14,** 1-14.

Mayhead, G. (1973). Some drag coefficients for British forest trees derived from wind tunnel studies. *Agricultural Meteorology*, **12,** 123-130.

McMahon, T.A. (1975). The mechanical design of trees. *Scientific American*, **233,** 92-102.

McMahon, T.A. & Kronauer, R.E. (1976). Tree structures: deducing the principle of mechanical design. *Journal of Theoretical Bioogy*, **59,** 433-466.

McNamee, J.E. (1991). Fractal perspectives in pulmonary physiology. *Journal of Applied Physiology*, **7,** 1-8.

Meyer, D.G., Schoorl, D., Butler, D.G. & Kelly, A.M. (1991). Efficiency and fractal behaviour of optimisation methods on multiple-optima surfaces. *Journal of Agricultural Systems*, **36,** 315-328.

Milne, R. (1991). Dynamics of swaying *Picea sitchensis. Tree Physiology*, **9,** 383-399.

Morgan, J. & Cannell, M.G.R. (1988). Support costs of different branch designs: effects of position, number, angle and deflection of laterals. *Tree Physiology*, **4,** 303-313.

Morgan, J. & Cannell, M.G.R. (1988). Structural analysis of tree trunks and branches: tapered cantilever beams subject to large deflections under complex loading. *Tree Physiology*, **3,** 365-374.

NAG (1977). Minimizing or maximising a function. *NAGLIB version 15*, Oxford University.

Niklas, K.J. (1982). Computer simulations of early land plant branching morphologies: canalisation of patterns during evolution? *Paleobiology*, **8,** 196-210.

Niklas, K.J. & O'Rourke, T.D. (1982). Growth patterns of plants that maximise vertical growth and minimise internal stresss. *American Journal of Botany*, **69,** 1367-1374.

Niklas, K.J. & Kerchner, V. (1984). Mechanical and photosynthetic constraints on the evolution of plant shape. *Paleobiology*, **10,** 79-101.

Niklas, K.J. (1986). Computer simulations of branching patterns and their implications on the evolution of plants. *Lectures on Mathematics in the Life Sciences*, **18,** 1-50.

Niklas, K.J. (1990). Biomechanics of *Psilotum nudum* and some early Paleozoic vascular sporophytes. *American Journal of Botany*, **77,** 590-606.

Niklas, K.J. (1992) . Plant Biomechanics. University of Chicargo Press, Chicargo, London.

Norman, J.M. & Jarvis, P.G. (1974). Photosynthesis in Sitka spruce (*Picea sitchensis* (Bong.) Carr.), III. Measurement of canopy structure and interception of radiation. *Journal of Applied Ecology*, **11,** 375-398.

Norman, J.M. & Jarvis, P.G. (1975). Photosynthesis in Sitka spruce (*Picea sitchensis* (Bong.) Carr.), IV. Radiation penetration theory and a test case. *Journal of Applied Ecology*, **12,** 839-878.

Oker-Blom, P., Kellomäki, S. & Smolander, H. (1983). Photosynthesis of a scots pine shoot: the effect of shoot inclination on the photosynthetic response of a shoot subject to direct rdiation. *Agricultural Meteorology*, **29,** 191-206.

Oker-Blom, P., Tapani, L. & Smolander, H. (1992). Photosynthesis of a Scots pine shoot: a comparison of two models of shoot photosynthesis in direct and diffuse radiation. *Tree Physiology*, **10,** 111-125.

Papentin, F. (1980). On order and complexity. *Journal of Theoretical Biology*, **87,** 421-456.

Powell, M.J.D. (1964). An efficient method for finding the minimum of a function of several varables without calculating the derivative. *Computer Journal*, **7,** 155-162.

Press, W.H., Flannery, B.P., Teukolsky, S.A. & Vetterling, W.T. (1986) . Numerical Recipes. The Art of Scientific Computing. Cambridge University Press, Cambridge, New York, Sidney.

Renshaw, E. (1985). Computer simulation of Sitka spruce: spatial branching models for canopy growth and root structure. *I.M.A. Journal of Mathematics Applied in Medicine and Biology*, **2,** 183-200.

Richter, H. (1973). Frictional potential losses and total water potential in plants: a reevaluation. *Journal of experimental Botany*, **24,** 983-994.

Rosen, R. (1967) . Optimality Principles in Biology. Butterworths, London.

Seim, E. & Saether, B.E. (1983). On rethinking allometry: which regression model to use? *Journal of Theoretical Biology*, **104,** 161-168.

Shinozaki, K.K., Hozumi, Y.K. & Kiara, T. (1964). A quantitative analysis of plant form-the pipe model theory. I Basic analysis. *Japanese Journal of Ecology*, **14,** 97-105.

Shlotzhauer, S. & Ramon, C. (1987) . SAS system for Elementary Statistical Analysis. SAS Institute Inc., Cary,NC,USA.,

Sprugel, D.G. & Hinckley, T.M. (1988) . The branch autonomy theory in: "Response of Trees to Air Pollution: The Role of Branch Studies", 1-19. Ed: W. E. Winner and L. B. Phelps. U.S. Environmental Preotection Agency, Corvallis, Oregon

Stevens, M.D. & Unsworth, M.H. (1979). The angular distribution and interception of diffuse solar radiation below overcast skies. *Quarterly Journal of the Royal Meterological Society*, **105,** 593-602.

Strahler, A.N. (1952). Hypsometric (area-altitude) analysis of erosional topography. *Bulliten of the Geological Society of America*, **63,** 1117-1142.

Tomlinson, P.B. (1983). Tree Architecture. *American Scientist*, **71,** 141-149.

Tuma, J.J. (1969). Theory and problems of structural analysis. McGraw-Hill, New York.

Tyree, M.T. & Sperry, J.S. (1988). Do woody plants operate near the point of catastrophic xylem dysfunction caused by dynamic water stress? Answers from a model. *Plant Physiology*, **88,** 574-580.

Wang, Y. (1989). Crown structure, radiation absorbtion, photosynthesis and transpiration. **PhD**, Edinburgh

Wang, Y.P. & Jarvis, P.G. (1990). Effect of incident beam and diffuse radiation on P.A.R. absorption, photosynthesis and transpiration of Sitka spruce - a simulation study. *Silva Carelica*, **15,** 167-180.

Waring, R.H., Schroeder, P.E. & Owen, R. (1982). Application of the pipe model theory to predict canopy leaf area. *Canadian Journal of Forest Research*, **12,** 556-560.

Watson, M.A. & Casper, B.B. (1984). Morphogenic constraints on patterns of carbon distribution in plants. *Annual Review of Ecological Systems*, **15,** 223-258.

West, P.W., Jackett, D.R. & Sykes, S.J. (1989). Stress in, and shape of, tree stems in forest monoculture. *Journal of Theoretical Biology*, **140,** 327-343.

Whitehead, D., Edwards, W.R.N. & Jarvis, P.G. (1984). Conducting sapwood area, foliage area and permiablity in mature trees of *Picea sitchensis* and *Pinus contorta. Canadian Journal of Forest Research*, **14,** 940-947.

Whitehead, D., Grace, J.C. & Godfrey, M.J.S. (1990). Architectural distribution of foliage in individual *Pinus radiata* D.Don. crowns and the effect of clumping on radiation. *Tree Physiology*, **7,** 135-155.

Wilson, B.F. (1987). Tree branches as populations of twigs. *Canadian Journal of Botany*, **67,** 434-442.

Wolfram, S. (1991). Mathematica - A system for Doing Mathematics by Computer. Addison-Wesley, Redwood City, California.

Zamir, M. (1976). Optimality principles in arterial branching. *Journal of Theoretical Biology*, **62,** 227-251.

Zimmermann, M.H. (1978). Hydraulic architecture of some diffuse-porous trees. *Canadian Journal of Botany*, **56,** 2286-2295.

Zimmermann, M.H. (1983). Xylem structure and the ascent of sap. Springer-Verlag, Berlin.